Muscle coordination and musculoskeletal disorders - Investigation of Achilles tendinopathy

Marion Crouzier

UNIVERSITE BRETAGNE LOIRE
EDUCATION
LANGAGES, INTERACTIONS
COGNITION, CLINIQUE

UNIVERSITÉ DE NANTES

THESE DE DOCTORAT DE

L'UNIVERSITE DE NANTES
Comue Université Bretagne Loire

ECOLE DOCTORALE N° 603
Education, Langages, Interaction, Cognition, Clinique
Spécialité : *STAPS*

Par
Marion CROUZIER

Muscle coordination and musculoskeletal disorders
Investigation of Achilles tendinopathy

Coordination musculaire et pathologies musculo-squelettiques
Etude de la tendinopathie d'Achille

Thèse présentée et soutenue à Nantes, le 1er juillet 2020
Unité de recherche : EA 4334 « Motricité, Interactions, Performance »

Rapporteurs avant soutenance :

Dylan MORRISSEY	Professeur, Queen Mary University of London (Royaume-Uni)
Nicola MAFFIULETTI	Chercheur, Schulthess Clinic (Suisse)

Composition du Jury :

Président :	Antoine NORDEZ	Professeur des Universités, Université de Nantes (France)
Examinateurs :	Dylan MORRISSEY	Professeur, Queen Mary University of London (Royaume-Uni)
	Nicola MAFFIULETTI	Chercheur, Schulthess Clinic (Suisse)
	Taylor DICK	Enseignante-chercheuse, The University of Queensland (Australie)
Dir. de thèse :	François HUG	Professeur des Universités, Université de Nantes (France)
Co-dir de thèse :	Lilian LACOURPAILLE	Maitre de conférences, Université de Nantes (France)

Invitée :

Co-dir de thèse :	Kylie TUCKER	Enseignante-chercheuse, The University of Queensland (Australie)

Where to begin, when it is time to write the ending…

He may not remember this, but being a wise supervisor, François once told me: "*a PhD is a roller coaster, do not worry when you are at the bottom*". For this journey, I had three supervisors, who did an amazing job in making sure I always came out back on top. Besides, I could rely on some people who made sure the view was always nice, and who kept the sky blue (which is no small feat in Nantes). In these few pages I will try to express my gratitude to everyone who, from near or far, contributed to keep me healthy and happy.

PREFACE

Nantes has a nice University and I am glad this is where I conducted my PhD. At the Sport Sciences department, the **"Motricité, Interactions, Performance" laboratory** is warm and welcoming, and it has been a great pleasure to be part of it over the last couple of years. I sincerely thank the academic world for the opportunity they gave me. Besides supporting my livelihood and time in the lab, I very much enjoyed that, every once in a while, the scholarship could pay for a beer.

For a year I had the opportunity to experience research at the **University of Queensland**, a university that was somewhat different than the University of Nantes, and perhaps even nicer because of the frequently mown lawn. It has been a pleasure to spend time at the **"Pain and Motor Control" laboratory**. I thank the University of Queensland, cockatoos, and bush turkeys, for having me and treating me well.

I express sincere gratitude to **Prof. Dylan Morrissey** and **Dr. Nicola Maffiuletti** for accepting to review this work. It is a great honour to have your expert opinion on the content of this work, and I am looking forward to reading your feedback. I also want to express my gratitude to **Dr. Taylor Dick** for her great suggestions and comments on the last study of this work, and for accepting to be part of the reviewing committee.

I extend my gratitude to **Prof. Antoine Nordez**, firstly for accepting to be the president of the reviewing committee, secondly for having served as an external member of my supervising PhD committee, thirdly for the close race with Sylvain for greatest office-colleague.

I also would like to thank **Dr. Gaël Guilhem** for serving as an external member of my supervising PhD committee all along the way.

This PhD work has been supervised by the *crème de la crème*. My greatest thanks are addressed to (in alphabetic order) **Prof. François Hug**, **Dr. Kylie Tucker** and **Dr. Lilian Lacrouapille**. I am not able to give you the recognition you deserve in these few lines. François, Kylie, Lilian, you rock! I owe you tremendous gratitude for your work and your time, your patience, your support, and the transfer of your passion. From the bottom of my heart, thank you.

Once, a participant told **François** and me how good *his* English was compared to *mine*. Since that day, I knew François had no weaknesses. I have done some statistics on the delay in François's feedback and I usually received comments on average in the following 42 ± 12 hours, with 0.32 ± 0.23 comments per minute within documents. I am almost not sure you are a human being anymore. I guess, with such a passion for science and a thirst for knowledge, it is normal for you to be the tremendous researcher you are. It has been a great pleasure to work with you François. Now I will stop here, because you taught me not to overextend myself. I have been quite bad at learning this, as evidenced by the already 8 lines in this paragraph… I am super glad I had you, as otherwise my PhD may have last a hundred years.

Kylie, I have received a warm welcome from you. It felt like I was welcomed with open arms by Australia through your kindness. I will always remember the first time I came to your home to work on this bunch of data, and we ended up spending the night close to the fire, drinking bubbles. It was a good representation of your talent for combining work with "life deliciousness". I thank you for the scientific values you shared with me, and to have inspired me to do further research when you were supervising my Master thesis. I like how you approach research, and also how you approach life. I thank you for your confidence, your generosity, and for giving me the greatest English teachers I have ever had in **Annika** and **Nienke**.

What I admire the most in **Lilian** is the joy he brings with him, for no apparent reason. Oops, je reprends. Ce que j'admire chez Lilian, c'est la joie qu'il transporte sans vraiment de raison. Le travail avec toi, c'était toujours dans la joie et la bonne humeur. Je te remercie d'avoir été là, particulièrement pendant la première année, que ce soit pour me montrer comment on allume le Contrex, ou me faire croire que tu peux utiliser Matlab… Plus sérieusement, ton expertise et ton aide aux prémices de cette thèse ont été précieuses. Merci pour ton temps, merci pour ta disponibilité, merci pour les bons moments de collecte de données de Méchadrive. J'en garde un souvenir si drôle. Merci d'avoir emmené les participants jusqu'à l'IRM, les samedis, à 7h, le matin. Et merci d'avoir rappelé ceux qui par mégarde avaient oublié de se réveiller car ils étaient allés se coucher… trop tôt. Je suis fière d'être ta première étudiante de thèse, et j'espère bien que tu l'écriras en gras dans ton CV.

Je passe maintenant à la partie immergée de l'iceberg.

Brisbane,

Brisbane has been my home for a while, and I must say that what I enjoyed the most in Australia was not the food (huge joke), it was not the life-style, it was not the sea or the weather, it was the sweet people. I thank **Cambridge's, Ryan's** and **Harriett's houses**, with a special mention for the pasta chef **Joey**. **Marielle**, **Izzy**, thank you for all the good moments we shared. A special acknowledgment goes to this very special friend, who came from far away, probably purposely for me: **Simon**, it was a joy to have you around in Brisbane, I have seen you grow, from begging for a job to the serving of cocktails without pouring them onto customers. I thank you, and **Clara**, for the time we shared, with an honourable mention for Arcadia. When the key words are heat and sun, how could we know we would end up in the middle of nowhere, dying of cold with muddy shoes on. As our dear Uncle **Sam** would say… we milked it! Thank you for these magical moments, dear friends.

Nantes,

J'ai rencontré dans le Grand Ouest de très belles personnes, qui ont participé activement à l'engouement que j'avais pour cette thèse. Un merci spécial à **Ploplo**, pour avoir si bien porté le comptoir de la Ribouldingue, quand il avait résisté au *Santos*. Et une mention spéciale pour **Val**, que ce soit pour entourlouper Matlab ou pour partager des canons, ta présence ces années fût un petit bonheur. Merci à mes physios favoris **Ricard et Guitou**, d'avoir joué un peu aux Nerfs avec moi. Merci **Feige** d'aimer si fort la coinche et de venir nous voir régulièrement, qu'on soit dans l'hémisphère nord ou sud. Merci à **Mehdi, Iris et Maxime, Alison et Eric**.

Merci aux petits nouveaux, qui prennent le relai quand tout s'essouffle : **Raphaël, Grégoire, Julien, Marine, Jean, Emilie**, vous méritez tous votre CAP pâtisserie. Et notre tout juste arrivé **Jeroen**, pour qui *ce sera tout*, merci aussi. Merci aux plus anciens de la boutique, **Marc, Christophe, Thibault, Jacques**… Merci **Véro**, secrétaire incroyable, pour ta disponibilité et ton énergie. **Amiral Guevel**, j'ai toujours pensé que tu conduisais très bien le bien STAPS mais, je dois dire que c'est la conduite du voilier qui m'a le plus plu. Merci pour les week-ends en mer. Et puis, il y avait ce collègue, qui faisait beaucoup de bruit dans mon bureau, mais bon, paraît que c'était bien l'plus heureux… **Sylvain**, merci pour ta bonne humeur du quotidien qui a égayé plus d'une de mes journées. Merci **Julie**, déjà pour aimer tendrement la clairette, et puis pour tout le reste, comme par exemple ~~ta maitrise du ras-el-hanout~~ les petits plats que tu nous as souvent préparé avec amour. A tous les deux, merci pour votre amitié. Enfin, **Thom**, permets-moi ici de te remercier bien sincèrement pour (1) le puits de savoir que tu es concernant le *Anas Platyrhynchos*, plus connu sous le nom de « canard colvert », c'est un plaisir de les compter sur les bords de l'Erdre avec toi ; (2) le modèle de discrétion que tu incarnes pour nous tous, comme le démontre ta coupe de cheveux ; (3) tes talents d'éducateur félin, même si Simon continue de miauler à toute heure ; (4) tous ces bons petits plats qui m'engraissent, même s'il faudrait que tu y apportes un peu plus de gourmandise ; (5) l'amourette que nous vivons, même si la seule liberté que j'ai eu c'est la verticalité de la bibliothèque.

A mes chers parents, je dédicace ce travail qu'ils ne liront jamais. Papa, quand j'ai débarqué sans prévenir ce mercredi après-midi avec pour seule mission la construction de *la boite* et une demi-journée de temps, tu ne connaissais pas les enjeux de la tâche. Et pourtant, cette œuvre d'art conditionnait la faisabilité de ma dernière étude de thèse, et constitue aujourd'hui l'apogée de mon travail. Alors, merci. J'ai fait une illustration, au cas où Maman et toi, vous auriez oublié comment ça s'était passé:

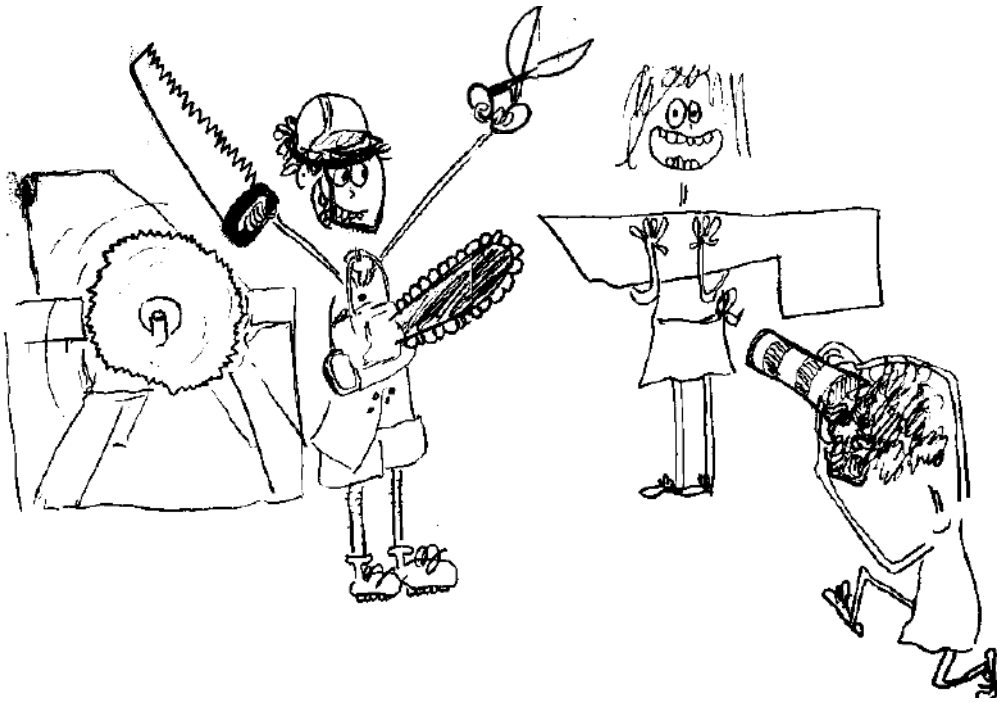

J'aimerais ici envoyer une belle pensée à mes **Papis**, vos Papas qui sont tous les deux partis pendant ma thèse, parce que dans ce travail il y a 25 % de chacun d'eux. J'ai oublié de les remercier des incroyables parents qu'ils m'avaient donnés. **Maman**, **Papa**, merci de votre soutien. Merci à mes frères et sœur, et tout particulièrement à **Jehanne**. Parce que ma jeune sœur est l'une des choses les plus précieuses que j'ai dans la vie (avec mes chats). Merci pour la complicité des années passées.

Je remercie plus largement **mes amis, de Nantes, de Lyon, et d'ailleurs**, pour tout ce qu'il y avait autour de la thèse. Je souhaite ici faire une mention spéciale à la rue de Strasbourg, et au soutien quotidien que j'y trouvais. Vous ne l'avez peut-être pas vu mais, vous avez été ces petites étoiles qui font que même dans les moments les plus sombres, il y a toujours de la lumière. C'est feu **Simon du 3 de Strasbourg**, qui m'avait dit tantôt que « c'est quand on l'a perdu qu'on découvre la valeur de ce qu'on avait ». Ces mots font de toi un grand homme Simon (1m76), puisque toi et moi mieux que personne nous connaissons la qualité de vie générée par le partage d'un toit avec **Romane** et **O'main A'vou'é**. A vous, ainsi qu'à tous les autres **colocataires** de mon passé, merci. Afin qu'aucun d'eux ne se sente oublié ici, je précise que cette dernière phrase comprend, entre autres, une variété de différents **Simons** qui sont au nombre de quatre.

Et pour finir, j'ai deux vieilles copines que je voudrais mentionner ici, car je leur dois beaucoup. Pourvu que dans dix ans, on décachette ces enveloppes remplies de tant de secrets, puisque **Cha** ne les aura pas perdues, j'en serai bien heureuse. Les filles, merci d'être de si bonnes copines, et merci de m'avoir apporté du rire, du soutien, mais surtout du rire, mais quand même du soutien, tout au long de la thèse. Dans ce travail, je n'ai fait qu'essayer de comprendre les petits bonhommes à l'intérieur de nous, qui tirent sur les ficelles. **Pol** rappelle-toi, c'est une histoire qui est née sur le pont du Coteau il y a bien des années...

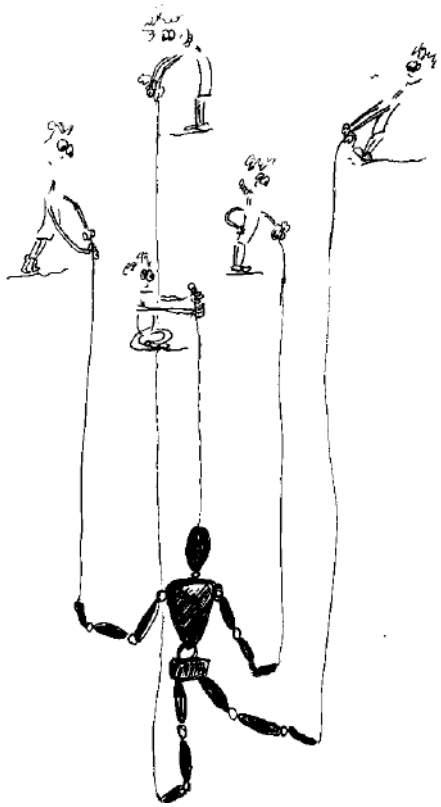

A Brad

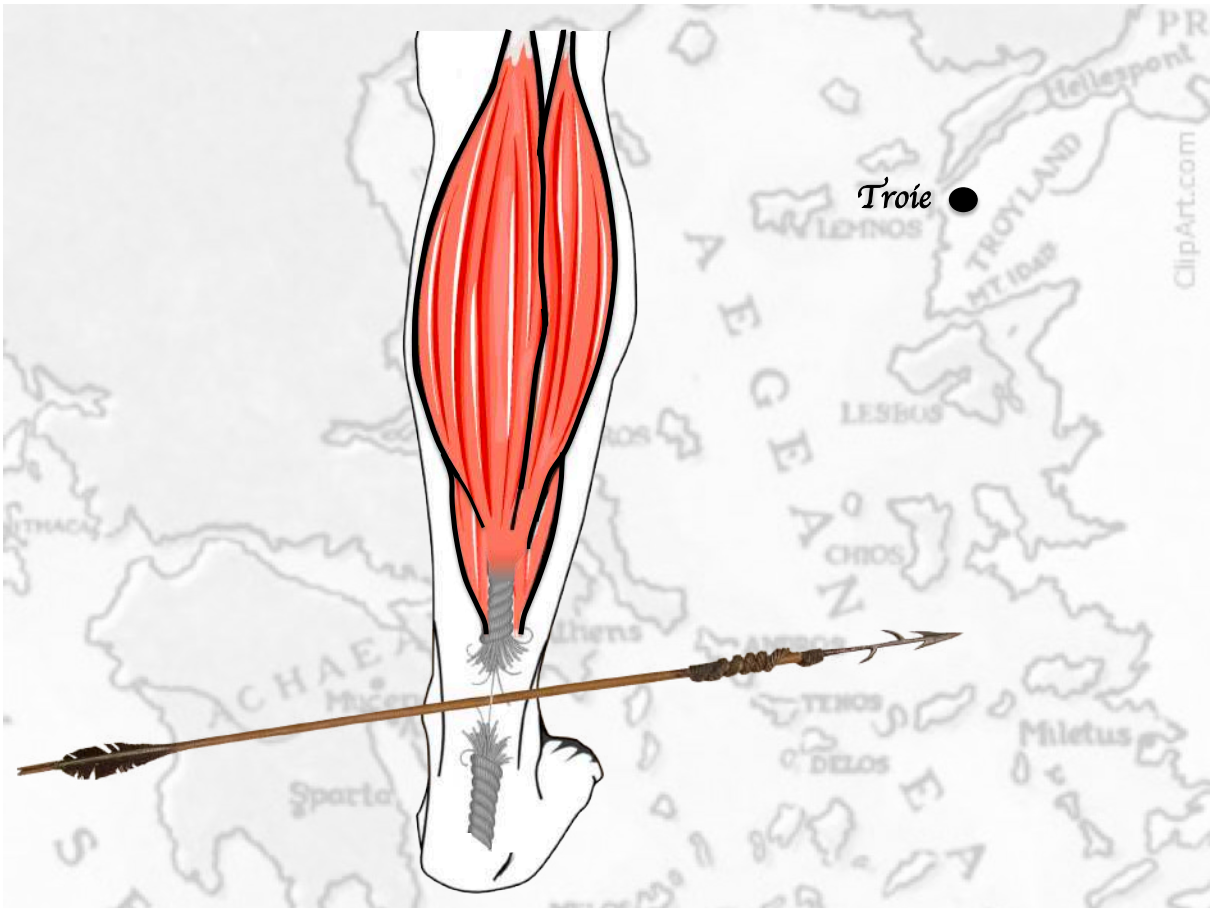

Ma thèse en 180 secondes
https://www.youtube.com/watch?v=sFouafRUQU8&t=1s

PUBLICATIONS AND CONFERENCE PRESENTATIONS

Published peer-reviewed articles related to this thesis

Crouzier, M., Hug, F., Dorel, S., Deschamps, T., Tucker, K., Lacourpaille, L. (2018). Do individual differences in the distribution of activation between synergist muscles reflect individual strategies? *Experimental Brain Research*, 223 (7) : 625 – 635.

Crouzier, M., Lacourpaille, L., Nordez, A., Tucker, K., Hug, F. (2018). Neuromechanical coupling in the human *triceps surae* and its consequence on individual force-sharing strategies. *Journal of Experimental Biology*, 221 (pt21).

Crouzier, M., Tucker, K., Lacourpaille, L., Doguet, V., Fayet, G., Dauty, M., Hug, F (2018). Force-sharing within the *triceps surae*: an Achilles heel in Achilles tendinopathy. *Medicine & Science in Sports & Exercise*, 52 (5) : 1236.

Conference presentations related to this thesis

Crouzier, M., Lacourpaille, L., Nordez, A., Tucker, K., Hug, F. (2018). Neuromechanical coupling within the human *triceps surae* and its consequences on individual force-sharing strategies. *XXII International Society of Electrophysiology and Kinesiology (ISEK)*. June 2018, Dublin, Ireland.

Crouzier, M., Lacourpaille, L., Tucker, K., Hug, F. (2018). Force-sharing within the synergist muscles of the human *triceps surae*. *Clinical and Public Health Postgradutate Symposium*. October 2018, Brisbane, Australia.

Crouzier, M., Lacourpaille, L., Tucker, K., Hug, F. (2018). Force-sharing within the synergist muscles of the human *triceps surae*. *XXVII International Society of Biomechanics*. August 2019, Calgary, Canada.

Other articles currently submitted

Thomare, J., Lacourpaille, L., McNair, P., **Crouzier, M.**, Ellis, R., Nordez, A. A gel pad designed to measure muscle volume using 3D freehand ultrasound. *Journal of Ultrasound in Medicine* (submitted).

ABSTRACT

The Achilles tendon is made of three *subtendons* that each arises from a different head of the *triceps surae*, i.e. *gastrocnemius medialis, gastrocnemius lateralis,* and *soleus*. In this anatomical conformation, it was hypothesized that non-optimal distribution of load and/or the amount of sliding between subtendons would contribute to the development of Achilles tendinopathy. Moreover, there is evidence that the non-uniform distribution of load or strain within the Achilles tendon is partly determined by the distribution of force among the heads of the *triceps surae*. The overall aim of this thesis was to provide a deeper understanding of the role of muscle coordination (i.e. the distribution of force among muscles) on the development of Achilles tendinopathy. Because *in vivo* measurement of muscle force is not feasible in humans, we used an experimental design where combined neurophysiological (muscle activation) and biomechanical measures (muscle volume and architecture) were used to estimate individual muscle forces. Three studies were conducted to (*i*) provide insight into the distribution of activation and the distribution of force among the three heads of the *triceps surae* in pain-free populations and (*ii*) compare muscle coordination between people with Achilles tendinopathy and controls. Results from this doctoral research were threefold. First, the distribution of normalised electromyography amplitude among *triceps surae* is robust between days and varies greatly between individuals. Similarly, the distribution of muscle force among *triceps surae* demonstrates large inter-individual variability during isometric submaximal tasks. Second, among *gastrocnemii*, there is a significant positive correlation between the distribution of physiological cross-sectional area and the distribution of activation during submaximal isometric plantarflexion tasks. Third, muscle coordination among the *triceps surae* differs in people with Achilles tendinopathy compared with controls, with the *gastrocnemius lateralis* contributing significantly less to total *triceps surae* force in people with Achilles tendinopathy. Whether this altered strategy is a cause or a consequence of Achilles tendinopathy should be further explored.

Key-words

Electromyography, Physiological cross-sectional area, Muscle force,
Tricep surae, Achilles tendon

LIST OF ABBREVIATIONS

CSA	Cross-Sectional Area
CV	Coefficient of Variation
EMG	Electromyography
GM	*Gastrocnemius medialis*
GL	*Gastrocnemius lateralis*
ICC	Intraclass correlation coefficient
MRI	Magnetic Resonance Imaging
MVC	Maximum Voluntary Contraction
PCSA	Physiological Cross-Sectional Area
SOL	*Soleus*
TS	*Triceps surae*
VL	*Vastus lateralis*
VM	*Vastus medialis*

TABLE OF CONTENT

GENERAL INTRODUCTION

Figure 1: eccentric loading of Achilles tendon with knee straight (top) and knee bent (bottom). *From Alfredson et al. (1998).*

"This started 1995. Myself I was a recreational runner, who gradually started to get midportion Achilles tendon pain" (Alfredson, 2010). Håkan Alfredson is an orthopaedic surgeon. He asked his colleague to operate him on his Achilles tendon but the colleague refused. At the hospital, they could not have Alfredson on sick leave. As a result of this decision, Alfredson, disappointed and angry, followed the conservative treatment method. He gave a try to the eccentric training as described by Stanish (1986), and after a few weeks of painful training, his Achilles tendon gradually started to improve. This was the impetus for Alfredson's research on eccentric training as a treatment model for Achilles tendinopathy. When Alfredson and colleagues (1998) conducted a prospective study to investigate eccentric calf training for Achilles tendinopathy treatment, they described a protocol with two knee positions (Figure 1), including a knee bent position that aimed to "*maximize the activation of the soleus muscle*". It was therefore thought that the distribution of activation, or force-generating capacity, among the three heads of the *triceps surae* was somehow related to recovery.

In the field of physiotherapy and rehabilitation sciences, it is a long-held belief that alterations in neuromuscular control may be involved in the development or persistence of musculoskeletal disorders. In other words, specific patterns of magnitude and/or timing of muscle activations are thought to relate to the development of some pathologies. For example, at the shoulder – a joint easily subjected to instability – several muscles (e.g. *posterior deltoid, trapezius, biceps brachii,* rotator cuff) create a stable base of support for the gleno-humeral joint to function. An inadequate neuromuscular control is thought to lead to gleno-humeral joint maltracking, and joint dysfunction (Davies and Dickoff-Hoffman, 1993). At the knee, each head of the *quadriceps* muscle has a different mechanical effect on the patella. An altered neuromuscular control is thought to generate abnormal patella tracking, and patellofemoral pain (Grabiner et al., 1994). Achilles tendinopathy is no exception to this rationale. It has been proposed that the distribution of activation among the heads of the *triceps surae* would impact the distribution of load within the Achilles tendon (Wyndow et al., 2010).

As muscles attach to bones via tendons, muscle forces impact non-muscular structures (e.g. joint, bones, tendons). Using electromyography, differences in the timing and/or the amplitude of muscle activation has been observed between populations with and without musculoskeletal disorders [e.g. for shoulder instability (Barden et al., 2005; Rajaratnam et al., 2013); patellofemoral pain (Cowan et al., 2001; Karst and Willet, 1995); and Achilles tendinopathy (Masood et al., 2014b)]. However, because there are inconsistent findings in the literature, there is no clear consensus on the role of activation strategies in the development of these disorders. For example, when comparing people with and without patellofemoral pain, some studies report differences in the balance of activation between *vastus medialis* and *vastus lateralis* muscles (Owings and Grabiner, 2002; Powers et al., 1996), but other studies do not (Boucher et al., 2005; Laprade et al., 1998). These discrepancies may originate from the methodological approaches used in the literature. Indeed, muscle activation assessed using electromyography cannot be used to infer the mechanical constraints imposed on the non-muscular structures. Theoretically, it is the distribution of muscle ***force***, rather than the distribution of muscle ***activation*** that impact the non-muscular structures. Although muscle activation is the first requirement for a muscle to produce force, other parameters such as muscle size and architecture, specific tension, dynamic properties, inherently contribute to the

force output. *In vivo* measurement of tendon or muscle force in humans is not feasible, as current methods are extremely invasive (e.g. Komi, 1990). Currently, individual muscle forces can, at best be, estimated using biomechanical models. This constitutes the most prominent limitation to our understanding of the role of muscle coordination, defined as the distribution of muscle force, in the development or persistence of musculoskeletal disorders.

This thesis focused on Achilles tendinopathy. The overall aim was to provide a deeper understanding of the link between *triceps surae* coordination and the presence of Achilles tendinopathy. We used an approach that combines neurophysiological (muscle activation) and biomechanical measures (muscle volume and architecture) to investigate muscle coordination among the synergists of the *triceps surae*.

This document contains four main sections. The first provides a literature review on (*i*) individual muscle force and muscle coordination; (*ii*) the *triceps surae* group and its relation to the Achilles tendon; and (*iii*) the Achilles tendinopathy. The second section of this thesis describes the overall experimental methods used for three research studies. The third section includes the three published research studies that were included as part of my PhD. The fourth section provides a general discussion about the implications of my studies, and future directions for work in this field.

LITTERATURE REVIEW

Part 1

Individual muscle force and coordination

1. Neuromuscular and biomechanical determinants of muscle force

Force production by the skeletal muscles depends on several factors. First, active force production requires activation of muscle by the nervous system. Second, many biomechanical factors and dynamic muscle properties influence the amount of muscle force produced and transferred to the tendons. This section describes the factors involved in force production for a single muscle, and the methods used to assess them.

1.1. Activation of muscle by the nervous system to produce force

1.1.1. Motor unit description and function

A motor unit is composed of one motor neuron and all the muscle fibres it innervates. The activation signal sent from the nervous system to the muscle arises from motor neurons in the spinal cord or the brain stem. When synaptic input sufficiently depolarizes the membrane potential of a motor neuron to reach its recruitment threshold, an action potential is generated within this motor neuron. The action potential then propagates along the motor axon, toward the neuromuscular junction. Acetylcholine is released at the neuromuscular junction, and activates receptors on muscle fibres, which initiate the generation of an action potential that propagates along each of the muscle fibres within the motor unit (Hall, 2004). Due to the secure synaptic connection between the axon of the motor neuron and the muscle fibres innervated, one neural action potential that is generated within a motor neuron typically results in several hundred muscle fibre action potentials (Dideriksen et al., 2011; Enoka and Duchateau, 2015; Enoka and Duchateau, 2019; Martinez-Valdes et al., 2018). The nervous system controls force production by varying the number of motor neurons that are recruited, and the rate at which they discharge action potentials (Enoka and Duchateau, 2019; Mogk et al., 2009; Mota et al., 2019; Wiegel et al., 2019). The sum of all the motor unit action potentials forms the **neural drive** to the muscle while the sum of all muscle fibres action potentials forms the **muscle activation** (Enoka and Duchateau, 2015).

The number of motor units per muscle (the motor unit pool) varies greatly between muscles. For example, in humans, motor unit pools were estimated to comprise 445 motor units for *tibialis anterior*, 579 motor units for GM, 315 motor units for *brachioradialis* and 119 motor units for *first dorsal interosseous* (Feinstein et al., 1955). The number of muscle fibres innervated per motor neuron (the innervation number) also varies greatly depending on the muscle. For example, a study performed on cadavers showed that, each motor neuron innervates on average 562 muscle fibres in *tibialis anterior*, 1934 muscle fibres in GM, 410 muscle fibres in *brachioradialis* and 340 muscle fibres in *first dorsal interosseous* (Feinstein et al., 1955). These features (number of motor neurons and number of muscle fibres) are specific to each muscle, and can lead to differences between muscle force productions. Importantly, when considering a **single muscle**, the innervation number also varies greatly between its own motor units, from a few tens to several hundred (Enoka and Duchateau, 2019). For example, in the *first dorsal interosseous* of humans, the innervation number varies between 22 to 1550, depending on the motor unit (Figure 2; Enoka and Fuglevand, 2001). As a result, the relationship between the number of motor neuron action potentials and the number of muscle fibre action potentials is not linear among a single muscle (Enoka and Duchateau, 2015; Enoka and Fuglevand, 2001). Because the peak force of a motor unit depends mainly on its innervation number (Enoka and Duchateau, 2019; Heckman and Enoka, 2012), the number of muscle fibre action potentials (muscle activation) is theoretically a more precise indicator of muscle force than the number of motor neuron action potentials (neural drive). This is the reason why the studies presented in this thesis considered muscle activation (albeit estimated indirectly) rather than neural drive to estimate muscle force.

In addition, within a motor unit pool, the motor unit size varies with fibre type and contractile properties (Figure 2). Motor unit types range from slow to fast type motor units. Slow type motor units produce low-force and are fatigue-resistant. Fast type motor units produce high-force and are less fatigue-resistant. Slow type motor units are smaller (they innervate a lower number of slow twitch muscle fibres), whereas fast type motor units are larger (they innervate a higher number of fast twitch muscle fibres; Hall, 2004). Functionally, smaller (and weaker) motor units are recruited earlier during a contraction, i.e. at lower intensities, as they present a lower recruitment threshold (Enoka and Duchateau, 2019). Similarly, larger motor units are recruited later, at higher task intensity. This is known as the *size principle* (Henneman, 1957). This orderly recruitment has been questioned in some contexts [e.g. during fast movement

(Desmedt and Godaux, 1977), or in the presence of pain (Tucker et al., 2009)]. However, it was supported for progressive increased isometric voluntary contraction in humans (Milner Brown et al., 1973).

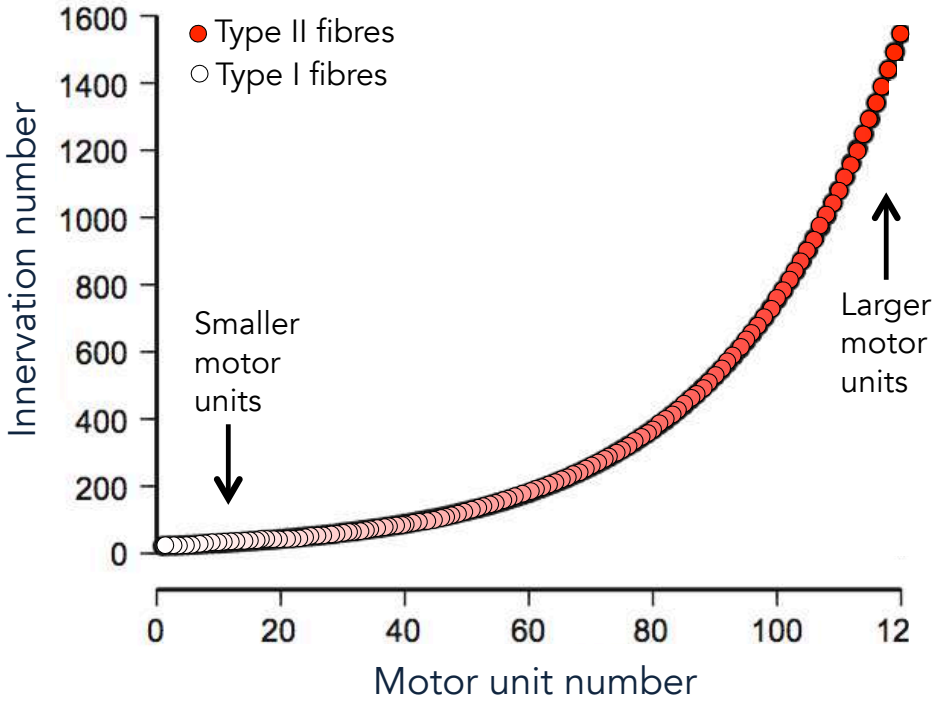

Figure 2. Distribution of innervation number for the 120 motor units of the *first dorsal interosseous* muscle. *Each motor unit innervates between 22 and 1550 muscle fibres (x axis). Motor unit organization shows a skewed distribution of various properties: small motor units and large motor units innervate slow (type I) and fast (type II) muscle fibres, respectively. From Enoka and Duchateau (2019).*

1.1.2. The electromyography technique

Action potentials generated in the muscle fibres are conducted in both directions from the neuromuscular junction towards the ends of muscle fibres, until they meet tendons. The technique of electromyography (EMG) measures the electrical manifestation of the neuromuscular activation associated with a contracting muscle (Basmajian and De Luca, 1985). In the bipolar configuration, the muscle fibre action potentials are recorded as the signal difference between the two electrodes (Merletti et al., 2001). EMG can be collected with electrodes within the muscle (intra-muscular EMG) or placed on the skin above a muscle

(surface EMG; Figure 3). Intra-muscular EMG records action potentials much closer to the source (muscle fibres). However, it is an invasive and selective technique that provides information about the activation of a relatively small part of the muscle (i.e. typically < 10 motor units per muscle on GM and GL; Heroux et al., 2014). As this technique is not used within the studies conducted in this doctoral research, it is not discussed in further detail. Surface EMG is non-invasive, and can provide information about the activation of a larger proportion of muscle. Surface EMG recordings may be made from a variety of electrode configurations that range from single, and bipolar, to grid electrodes (described in more detail in Section 1.1.3). Irrespective of electrode type, surface EMG signals are affected by multiple non-physiological factors (Farina et al., 2004a). The limitations associated with surface EMG are also described in Section 1.1.3.

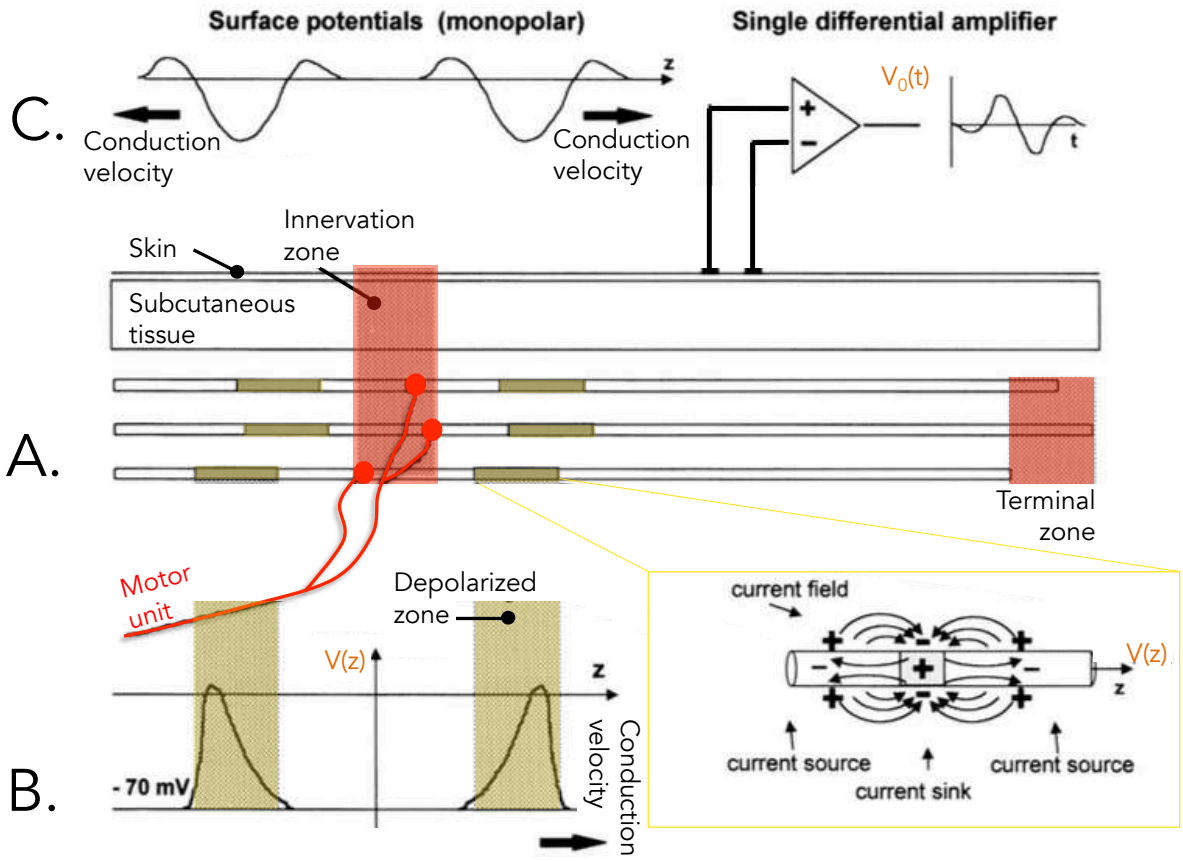

Figure 3. Schematic diagram of the surface electromyography (EMG) generation mechanism. *Panel A: an example of motor unit made of three fibres is provided. Panel B: each muscle fibre action potential travels from the neuromuscular junction to the tendons and causes membrane voltage V(z). Panel C: the muscle fibre action potentials add up to generates the signal $V_0(t)$ at the output of the amplifier when propagating underneath the detection electrodes. From Merletti et al. (2001).*

EMG can provide information on either **neural drive** (sum of motor unit action potentials) or **muscle activation** (sum of muscle fibres action potentials), depending on recording technique and type of analysis (Figure 4). Briefly, the study of neural drive requires the separation of the action potentials of individual motor units contained in the recorded EMG signal, a technique known as decomposition. This methodology enables each detected action potential to be associated, with appropriate clustering methods, to a specific motor unit (Farina et al., 2016). The neural drive to the muscle corresponds to the sum of the discharge events of the activated motor units, expressed in pulses per second (Farina et al., 2010; Farina et al., 2014). Because in this thesis muscle force was estimated from (in part) the measure of muscle activation, neural drive will be no further described, as it is beyond the scope of this thesis.

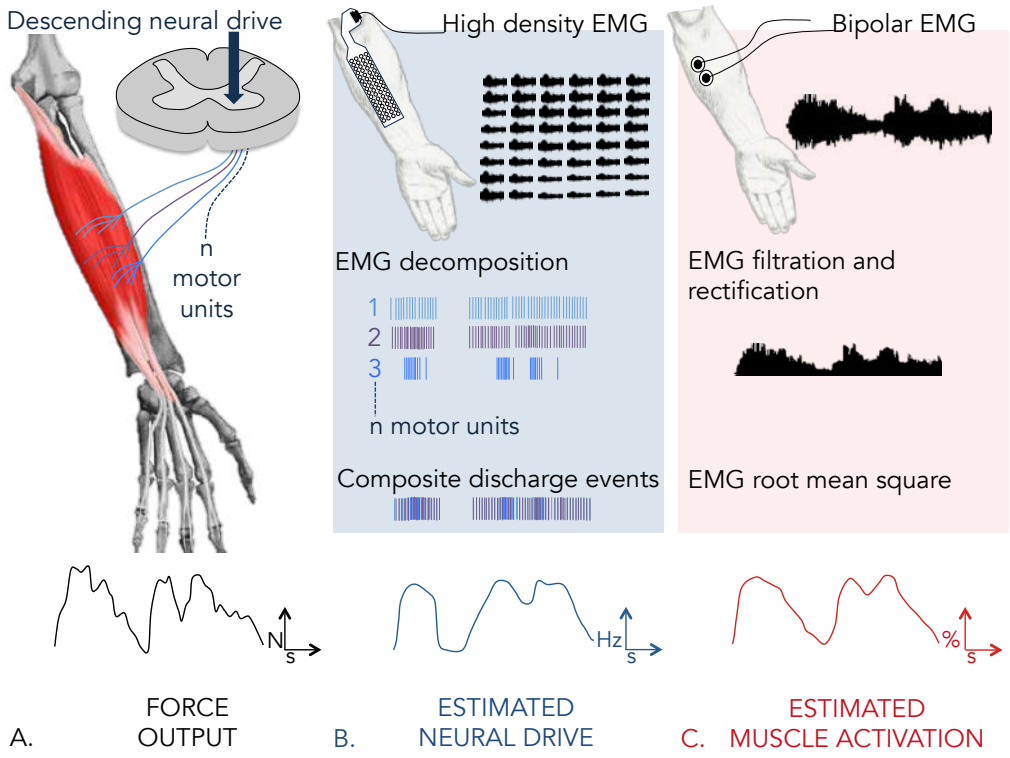

Figure 4. Neural drive and muscle activation. *Muscles receive neural drive from their motor neuron pools. The number and firing rate of activated motor neurons regulate muscle force. Panel A: representation of three (out of n) motor neurons innervating the muscle. Their electrical activity can be collected with high density electromyography (EMG, panel B) and bipolar electrodes (panel C). Panel B: high-density EMG and decomposition technique to measure motor unit action potentials. The frequency of the composite discharge events of the active motor units can provide an estimation of the neural drive. Panel C: bipolar surface EMG to measure muscle fibre action potentials. This gives an estimation of the muscle activation.*

1.1.3. Estimation of muscle activation

The study of muscle activation requires a measure of muscle fibre action potentials. The surface EMG signal is modelled as a linear, spatial and temporal summation of the muscle fibre action potentials detected by the electrodes. Thus, the amplitude of the EMG signal is considered to provide a good representation of muscle activation. However, several non-physiological and physiological factors affect surface EMG signal (Farina et al., 2004a; Merletti et al., 2001). Non-physiological factors comprise of anatomical factors (e.g. thickness of the subcutaneous layer), detection system (e.g. inter-electrode distance), geometrical (e.g. muscle fibre shortening), and physical factors (e.g. crosstalk). Physiological factors comprise fibre membrane properties (e.g. conduction velocity) and the number of motor units recruited (Farina et al., 2004a). To be correctly interpreted, EMG collection requires methodological considerations. In this section, two factors that can confound the ability for an EMG signal to accurately represent muscle activation are discussed: amplitude cancellation and crosstalk.

Amplitude cancellation refers to the overlapping of positive and negative phases of motor unit action potentials in the bipolar configuration of electrodes (Farina et al., 2004a). Signal cancellation is due to different conduction velocity between fibres and different discharge times (i.e. not synchronous muscle fibre action potentials). To estimate the error that is due to signal cancellation, Keenan et al. (2005) ran a model were the signal was rectified before being summed, and compared to a normal EMG measure (where signal is summed before being rectified; Figure 5, panel A). Amplitude cancellation generated a loss of up to 62 % of the amplitude of the signal at maximal contraction intensity (Keenan et al., 2005). The effect of amplitude cancellation on our ability to use EMG as an estimate of muscle activation, can be greatly diminished (less than 5 %) by normalising the EMG signal with respect to an isometric maximal voluntary contraction (Keenan et al., 2005).

Crosstalk is defined as a contamination of the EMG signal by a nearby muscle's electrical activity (Farina et al., 2002). The amount of crosstalk is influenced by parameters such as electrode location, inter-electrode distance, muscle size, distance source-electrode, or thickness of the subcutaneous layer (Farina et al., 2002). Crosstalk can be reduced with a double differential electrode configuration (van Vugt and van Dijk, 2001) associated with a

low skin-electrode impedance (Mesin et al., 2009). Figure 5 (panel B) depicts the contamination of *tibialis anterior* EMG signal by *peroneus longus* activation during gait. This study showed that the activation of the *tibialis anterior* exhibited an extra burst of activity for electrodes closer to the *peroneus longus* (Campanini et al., 2007). This extra burst likely originated from *peroneus longus*. Even if there is no methodology to quantify and avoid crosstalk, in bipolar configuration, proper electrode localisation limits crosstalk. Indeed, in the aforementioned study, an index of crosstalk was calculated as the ratio between the area of the entire normalised envelope and the area of the normalised envelope outside the expected activation phase of *tibialis anterior* (Campanini et al., 2007). This index indicated that the amount of crosstalk between *tibialis anterior* and *peroneus longus* depended on electrode location. The European project for standards of "*surface EMG for non-invasive assessment of muscle"* (SENIAM recommendations) describe placement electrode for each muscle of the human body, with respect to the longitudinal fibre direction and halfway between the distal motor endplate and the distal tendon (Hermens et al., 2000). Usually, electrode positions are described considering anatomical landmarks. As example, electrode location for SOL is *"at 2/3 of the line between the medial condyle of the femur to the medial malleolus"*. To overcome the potential that anatomical individual variations introduce error in placement of electrodes, ultrasonography can be used to identify muscle borders so that electrode location is adjusted to be at the centre of the muscle belly, away from the neighbouring muscles.

Even in the presence of these methodological factors, surface EMG remains the most common technique used to provide insight into muscle activation (De Luca, 1968; De Luca, 1979; Merletti et al., 2001). Indeed, surface EMG constitutes a relevant tool to evaluate activation of individual muscles among a group of synergists, and thus quantify their respective contribution to the total activation (Hug, 2011).

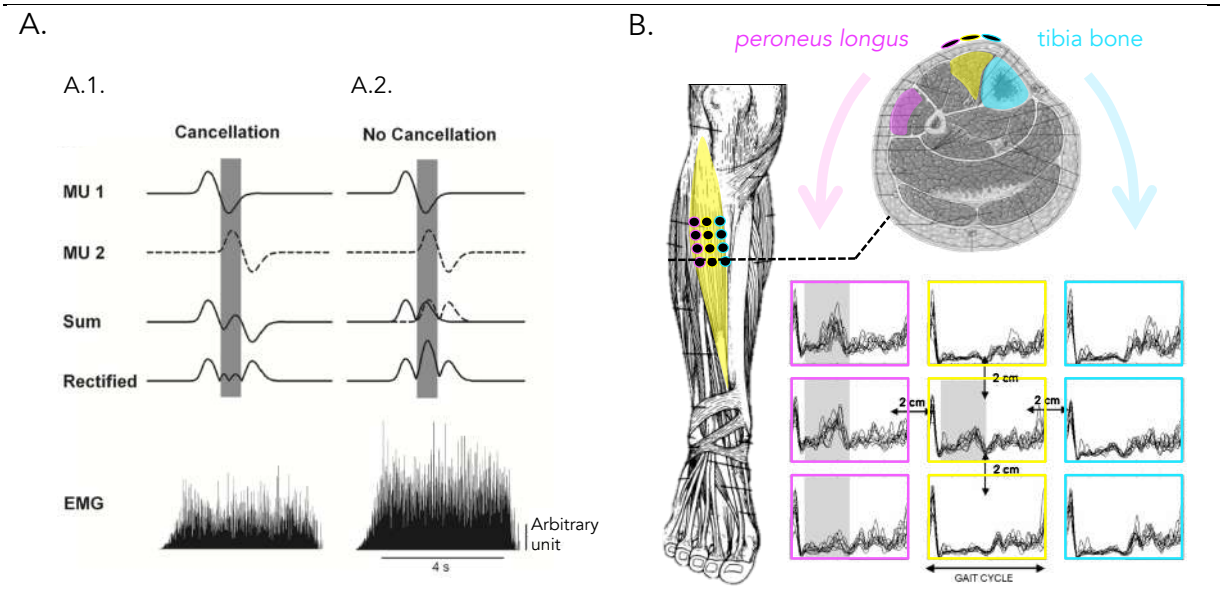

Figure 5. Drawbacks of surface electromyography (EMG) technique. *Panel A: illustration of signal amplitude cancellation. Impact on muscle EMG when two motor unit potentials were summed and then rectified (A.1), or rectified and then summed (A.2). From Keenan et al. (2005). Panel B: illustration of crosstalk due to anatomical proximal regions [i.e. nearness of tibialis anterior (yellow) and the peroneus longus (pink)]. On EMG envelope, grey stripes outline the activity of the peroneus longus, recorded on electrodes regarding tibialis anterior (pink and yellow) due to crosstalk. Adapted from Baldry and Thompson (2005); Campanini et al. (2007); Iannotti and Parker (2013).*

1.1.4. Distribution of activation between individual muscles

It has been often assumed that activation is equally distributed over (some) synergist muscles. Thus, the activation of only one muscle is often measured among a muscle group. Consistent with this, biomechanical models often consider homogeneous activation of muscles based on uniform activation levels (e.g., Lemay et al., 2007). Take, for example, an isometric knee extension at 20 % of maximal voluntary contraction (MVC). If we consider that all muscles are activated equally, this would mean that the 4 heads of the *quadriceps* muscles [i.e. *vastus lateralis* (VL), *vastus medialis* (VM), *vastus intermedius* and *rectus femoris*] would all be activated at 20 % of their maximal activation. However, some studies have demonstrated that it is not the case in the *quadriceps* group (Hug et al., 2015a). Similarly, activation is not equally distributed among hamstrings (Avrillon et al., 2018) or *triceps surae* muscles (Lacourpaille et al., 2017; Masood et al., 2014a) during isometric submaximal contractions.

To more accurately determine the relative activation of individual muscles within a group, the activation of a single muscle over the activation of all the muscles that compose the muscle group (i.e. ratio) may be considered. For example, the normalised activation of GM, divided by the summed activation of the GM + GL + SOL (i.e. GM/TS ratio) can be used to indicate the relative activation of GM among the muscles of the *triceps surae*. Using this approach, Lacourpaille et al. (2017) found that the activation ratios of GM/TS, GL/TS and SOL/TS were 39 ± 7, 20 ± 6 and 41 ± 7 % respectively, during an isometric contraction at 20 % of MVC (Figure 6). This means that the GL was significantly less activated than the GM and SOL during this task.

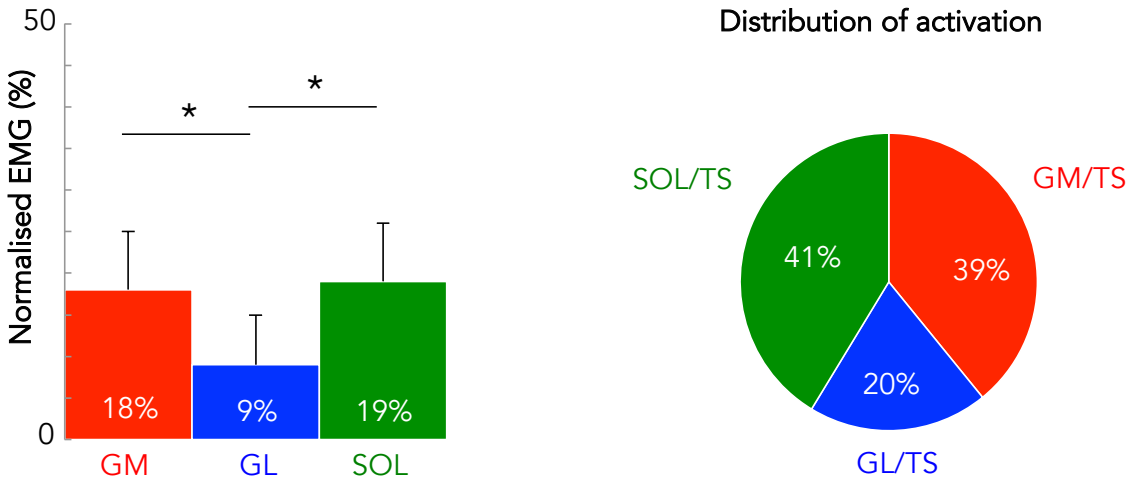

Figure 6. Between-muscle differences in muscle activation. *Gastrocnemius medialis (GM), gastrocnemius lateralis (GL) and soleus (SOL) activation during submaximal isometric contraction performed at 20 % of maximal voluntary contraction (left) and their proportion among the group (right). EMG, electromyography; TS, triceps surae. *, p<0.05. Adapted from Lacourpaille et al. (2017).*

In addition to the between-muscle differences, large differences between individuals exist in the way they activate synergist muscles. For example, between-individual differences have been described for the distribution of activation among *gastrocnemii*, which is calculated as GM activation divided by the summed activation of GM + GL (GM/Gas). Ahn et al. (2011) observed that during gait, seven out of ten participants activated their GM more than their GL (GM/Gas activation ratio: 74 ± 6 %), while the other three participants activated their GM and GL nearly equally (GM/gastroncemii activation ratio: 57 + 6%; Ahn et al., 2011). Inter-individual variability of activation strategies assessed using EMG has been observed during a wide variety of tasks, from multi-joint tasks [e.g. gait (Ahn et al., 2011; Ivanenko et al., 2002;

Winter and Yack, 1987); and pedalling (De Marchis et al., 2013; Hug et al., 2010)] to simple isometric single-joint tasks in different muscle groups [e.g. plantarflexion (Lacourpaille et al., 2017; Masood et al., 2014a) and knee extension (Hug et al., 2015a)].

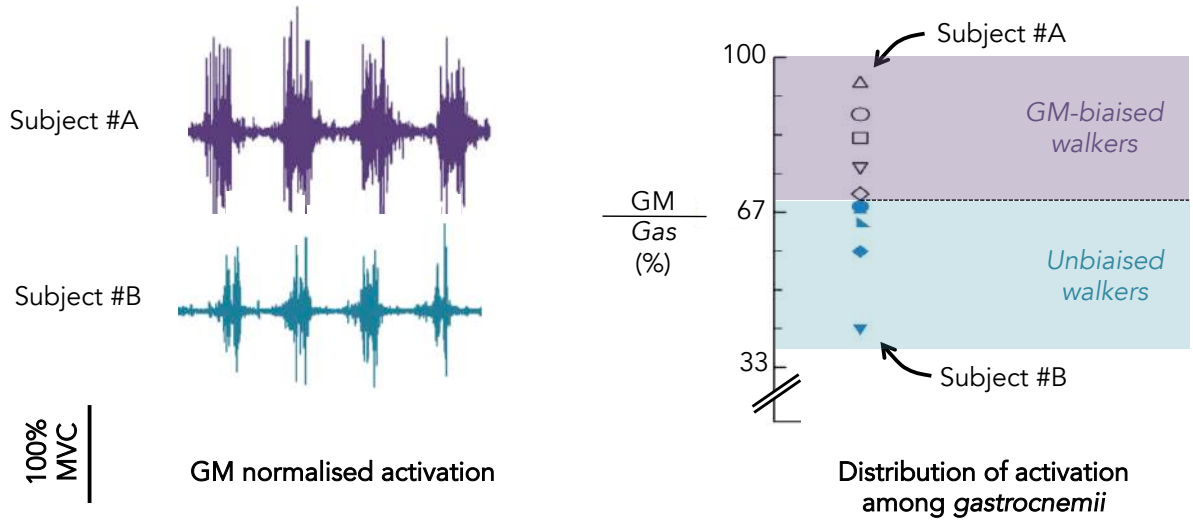

Figure 7. Between-individual differences in muscle activation. *Gastrocnemius medialis (GM) normalised activation for two individuals during 4 cycles of gait (left) and ratio of GM/Gas activation (right). The graph shows a large spread of participants (ratios ranging from ~ 48 % to ~ 92 %). Subjects A and B presented low and high GM activation respectively (and could be the lowest and highest dot in population distribution). Adapted from Ahn et al. (2011).*

Whether these individual differences in the distribution of activation among synergist muscles translate to individual differences in muscle coordination strategies is unclear. Muscle coordination is defined here as the **distribution of force among synergist muscles**. The force produced by a muscle depends on its activation, but also on several biomechanical factors such as its physiological cross-sectional area (PCSA), specific tension, force–length and force–velocity relationships (Zajac, 1989). It is unclear whether an imbalance of muscle activation is compensated by biomechanical factors. To better understand the control of muscle force, we need to consider the interplay between muscle activation and muscle biomechanical factors.

1.2. Biomechanical factors that contribute to muscle force production

1.2.1. Maximal isometric force

Theoretically, the maximal amount of muscle force F_{max} that can be produced during an isometric contraction depends on the muscle PCSA and its specific tension (Close, 1972):

$$F_{max} = PCSA \times Specific\ Tension$$

Equation (1)

With F_{max} in Newtons, specific tension in $N.cm^{-2}$, and PCSA in cm^2.

1.2.1.a. Physiological cross-sectional area

The PCSA (cm^2) is the averaged area of the muscle cross-section perpendicular to its fibers. It is commonly calculated by dividing volume (cm^3) by fascicle length (cm; Haxton, 1944). When a muscle is pennated, the axis of shortening of fibres is different from the axis of shortening of the whole muscle (Figure 8). The functional PCSA accounts for the projection of fibres force along the muscle-tendon unit, i.e. the longitudinal component of the force (Haxton, 1944; Narici et al., 2016). The formula to calculate the functional PCSA is as follows:

$$PCSA_{functional} = Volume \times Fascicle\ length^{-1} \times \cos(Pennation\ Angle)$$

Equation (2)

With functional PCSA in cm^2, volume in cm^3, fascicle length in cm and pennation angle in degrees. Regardless of the consideration of the pennation angle, muscle PCSA is considered as a strong indicator of its maximal force-generating capacity (Enoka and Duchateau, 2019). Experimental studies performed on 10 guinea pig muscles, all from the hindlimb, and with varying architecture, demonstrated a strong positive relationship between muscle functional PCSA and maximal muscle force *in vitro* (i.e. muscle tetanic tension), as depicted on Figure 9 (Powell et al., 1984). In humans, PCSA correlates to maximal voluntary force [r ranging from 0.52 to 0.95] in different muscle groups [e.g. knee extensors (Massey et al., 2015), or elbow flexors (Marchetta et al., 2012)]. In humans, volumetric features of different muscles vary greatly. For example, muscle volume ranges from approximately 19 cm^3 (*flexor digitorum*

longus) to 849 cm^3 (*gluteus maximus*; Handsfield et al., 2014). Moreover, skeletal muscle architecture (fascicle length and pennation angle) varies widely from fusiform to pennated muscles (Figure 8; Lieber and Friden, 2000). For a given muscle volume, the shorter are the fibres, the higher is the PCSA. Fascicle lengths in human skeletal muscles range widely, for example, fibres of the *first dorsal interosseous* are ~ 2 cm (Infantolino and Challis, 2010) while fibres of *semi-tendinosus* or VL are > 10 cm (Avrillon et al., 2018; Blazevich et al., 2006). This generates very high PCSA for muscles that combine high volume and short fascicle length. For example, the large volume of SOL (490 cm^3 *in vivo*; Fukunaga, 1992) and its short fascicle length (3 to 4 cm; Agur et al., 2003) results in SOL having the largest PCSA of any human lower limb muscle (490 divided by 3 equals 163 cm^2; Bolsterlee et al., 2018; Ward et al., 2008).

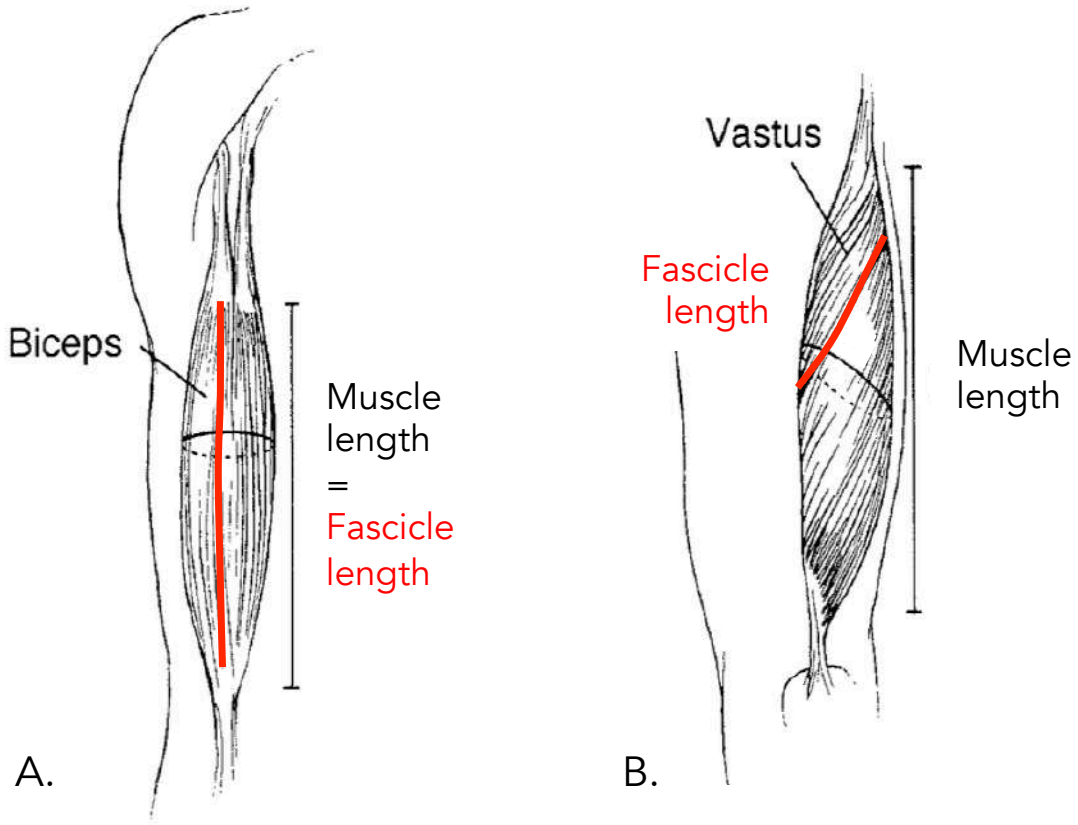

Figure 8. Illustration of the different types of skeletal muscle architecture. *Panel A: fibres can be parallel to the muscle force-generating axis (longitudinal or fusiform muscle, e.g. biceps brachii, right arm). Panel B: fibres can run at an angle relative to the muscle force-generating axis (pennated muscle, e.g. VL, left leg). From Lieber and Friden (2000).*

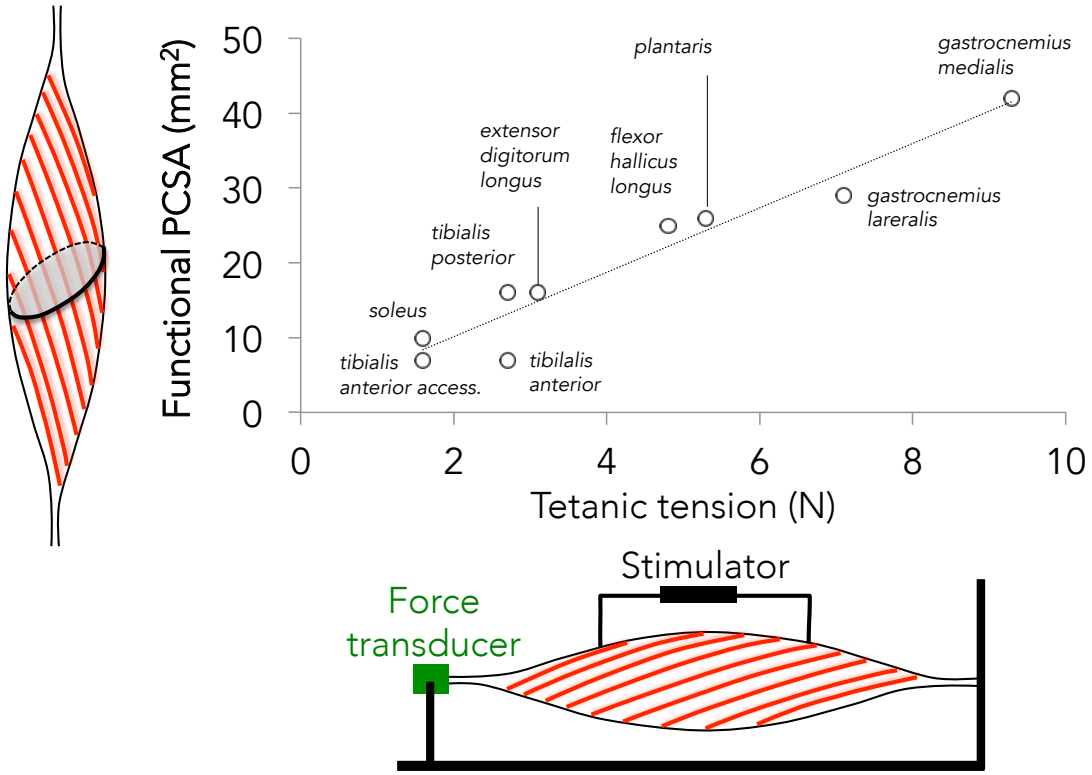

Figure 9. Relationship between muscle physiological cross-sectional area (PCSA) and maximal force *in vitro* on guinea pig muscles. *The measured maximal forces were evoked by electrical stimulation of the muscle nerves at stimulus rates that elicited tetanic force. Muscle functional PCSAs were calculated from muscle mass, density, pennation angle, and fascicle length. The graph shows a strong positive correlation (r = 0.98). Adapted from Powell et al. (1984).*

Muscle architecture is a primary determinant of muscle function (Gans and Gaunt, 1991). Longer-fibered muscles favour contractions that produce large movements, but are limited in the force that can be produced; whereas short-fibered muscles (i.e. with higher pennation angle) produce larger forces but are limited in the range of length change that can be produced (Biewener, 2016). The between-muscle differences in architecture in the human body have important functional consequences. For example, Biewener (2016) has suggested that proximal muscles (generally long-fibered) modulate the majority of limb work; whereas distal muscles (generally short-fibered) favour force generation. Alternatively, Lieber and Friden (2000) proposed that antigravity extensors such as *triceps surae* or *quadriceps* (which have relatively high pennation angles, large PCSAs, and short fibers) are more designed toward

force production. In contrast, the flexors such as hamstrings (which have relatively long fibers and intermediate PCSAs) are more designed for high excursions in the lower limb.

Investigation of volume. The investigation of muscle PCSA requires both volumetric and architectural measurements. In the literature, human muscle volumes have been obtained either from cadaveric measurements (Engstrom et al., 1991; Ward et al., 2008; Woodley and Mercer, 2005), or from *in vivo* imaging techniques (Barber et al., 2009; Engstrom et al., 1991; Handsfield et al., 2014). Magnetic resonance imaging (MRI) segmentation is the gold-standard technique for obtaining *in vivo* muscular volume measurements (Figure 10; Mitsiopoulos et al., 1998). To reconstruct muscle volume from MRI scans, the muscle area is segmented on a series of transversal images. MRI produces images with high contrast between tissues of different molecular properties. However, MRI is relatively expensive, and it can be difficult to access. The procedure also requires relatively long acquisition times, while the participants lays, without motion, within a relatively enclosed space. There are multiple contraindications for the use of MRI (e.g. metallic foreign body, claustrophobia). Taken together, it is reasonable to consider alternatives to MRI for the estimation of muscle volumes.

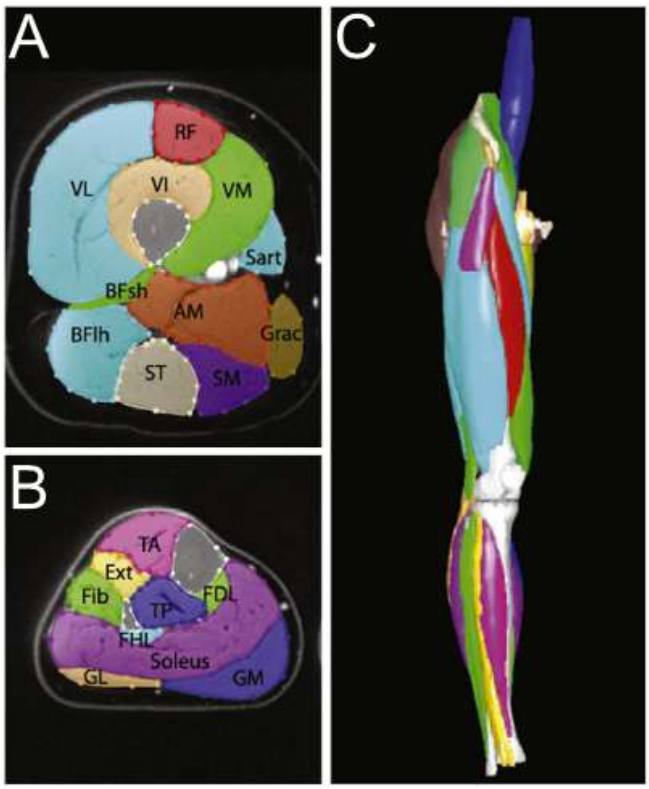

Figure 10. Three D-reconstruction of the leg from magnetic resonance imaging (MRI) scans. *Muscles and bones were segmented in transversal images in each thigh cross-sections (A) and shank cross-sections (B). The reconstruction in 3D is shown in an anterior view (C). From Handsfield et al. (2014).*

Recently, an alternative ultrasound-based technique called "freehand 3D ultrasound" has been developed. Freehand 3D ultrasound uses conventional B-mode images that are collected sequentially along the length of the tissue of interest while the position and orientation of the image is recorded so that images can be stacked together to generate a 3D volume (Figure 11; Lichtwark, 2017). This methodology requires both ultrasound and a 3D motion capture system. The trajectory of the ultrasound probe is tracked by the 3D motion capture system as the operator moves the probe across the limb. It has been shown that freehand 3D ultrasound is valid [intraclass correlation coefficient (ICC) > 0.99 and coefficient of variation (CV) = 1.1 %; compared to MRI] and reliable (ICC > 0.99) to measure *in vivo* GM muscle volume (Barber et al., 2009).

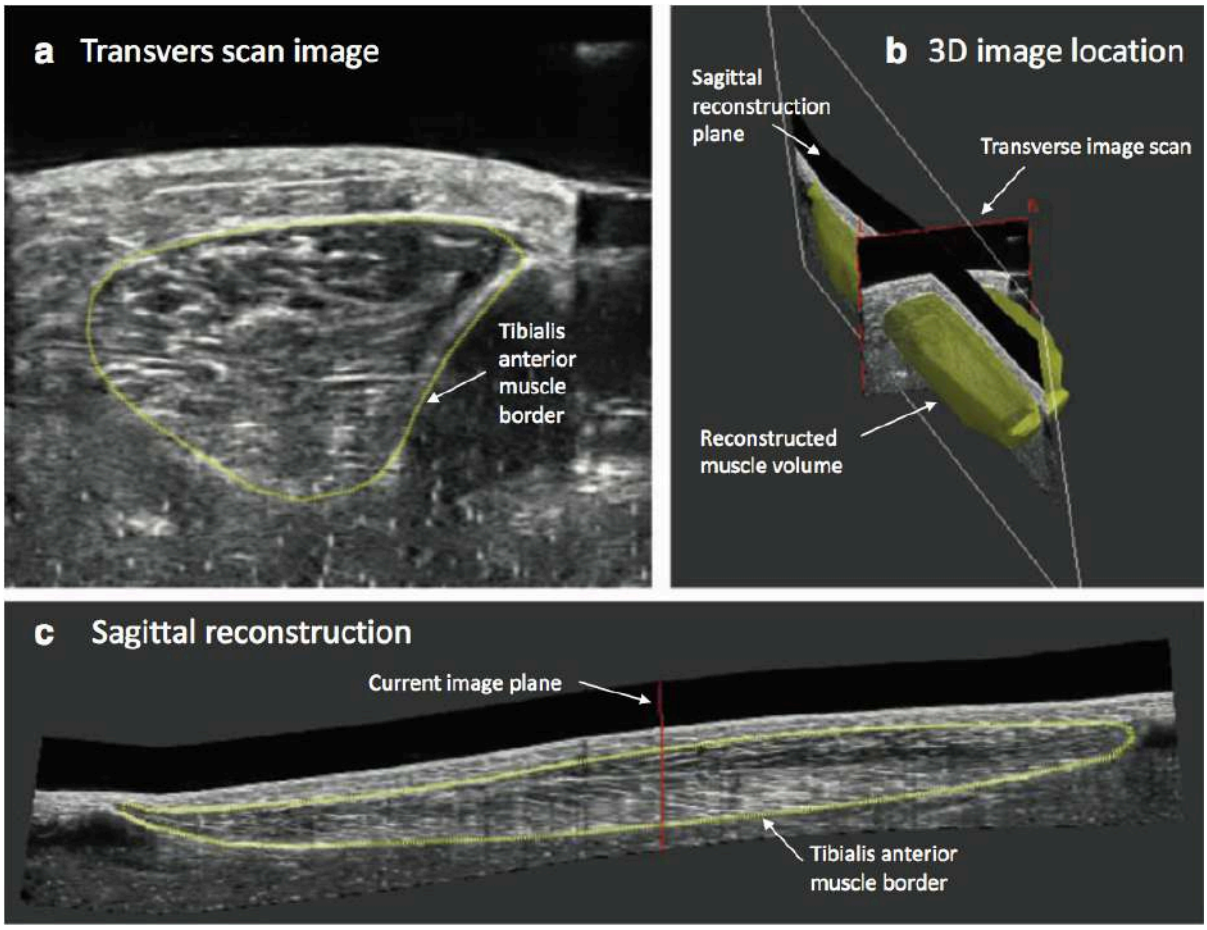

Figure 11. Conventional use of freehand 3D ultrasound. *Panel A: transverse scan of the tibialis anterior muscle. Panel B: position of transverse scan relative to muscle and a 3D reconstruction of the muscle volume. Panel C: sagittal plane reconstruction of the muscle. From Lichtwark (2017).*

Investigation of fascicle length and pennation angle. The most widely used method for obtaining non-invasive *in vivo* human muscle fascicle length and pennation angle is ultrasonography. Specifically, the probe is placed on the skin longitudinally to the fascicles orientation so that fascicles lie in the image plane as much as possible (Bolsterlee et al., 2016). Pennation angle is classically calculated as the angle between the fascicles and the superficial aponeurosis, deep aponeurosis, or both. Fascicle length is usually measured as the distance between the two aponeuroses following the chosen fascicle path. Even though ultrasound captures 2D images of fascicles that have a 3D shape, this technique is reliable and accurate for both fascicle length and pennation angle measurement in human investigation, when conducted on large limb muscles in a relaxed state (Kwah et al., 2013). In this latter review article, the 42 studies included showed an ICC ≥ 0.62 (fascicle length) and ≥ 0.51 (pennation angle) for between-sessions reliability; and an ICC ≥ 0.77 (fascicle length) and ≥ 0.88 (pennation angle) for validity (Kwah et al., 2013). Sometimes, the probe width (classically ~ 5 cm) is shorter than muscle fibre length [e.g. ~ 8 cm for VL with hip and knee extended (Noorkoiv et al., 2010)]. In such cases, fascicle path is linearly extrapolated to estimate fascicle length (Ando et al., 2017). To address this limitation, some research teams used two probes in series (Heroux et al., 2016). Also, an extended field of view (or panoramic) mode has been developed on numerous ultrasound scanners, which overcomes this limitation as well. This technology works in much the same way as the *panoramic mode* on smartphone stitches together multiple photos to make one longer image, with the final saved image having content that was outside the field of view of the original image. Scanning from the origin to the attachment of the muscle with a continuous ultrasound scan creates an image where long and curved fascicles can be seen (Figure 12, panel A.2). This technique has shown *excellent* reliability (ICC > 0.97) and validity when compared to traditional B-mode ultrasound images (Bland-altman analysis showed a bias within the 95 % limits of agreement) for the *extensor carpi ulnaris* muscle (Adkins et al., 2017). Most recently, fascicle length has also been estimated using anatomically constrained diffusion tensor images tractography, which is based on MRI. Diffusion tensor image tractography enables the detection of unique fibres (called fibre tracts) within the imaged region (Figure 12, panel B). During the processing of images, anatomical constraints are identified, which allows accurate identification of fibre tract termination points. Diffusion tensor image tractography produced reliable fascicle length data in the *triceps surae* muscle (ICC = 0.81; Bolsterlee et al., 2019). Moreover, diffusion tensor image tractography provides information about a high number of

fascicles, and allows for whole-muscle architecture estimation (e.g., 2450 fibers for GM; Bolsterlee et al., 2019). This contrasts significantly with the capability of ultrasound, which is used to identify only a small number of fascicles (typically no more than 10 per muscle). However, as discussed above, MRI is expensive, can be difficult to access, requires long acquisition times, and there are several contraindications. Although it provides high quality data, it is not currently in wide used.

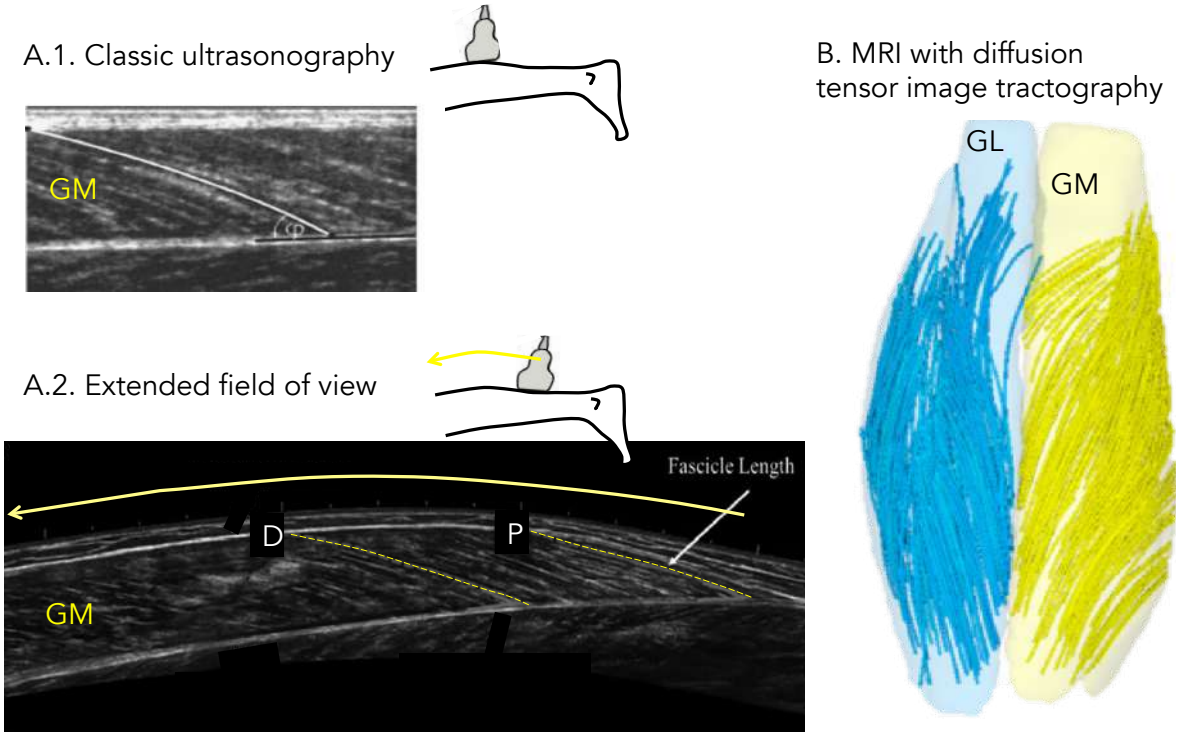

Figure 12. The different techniques to measure fascicle length, example of *gastrocnemius medialis* (GM). *Panel A.1: classic B-mode ultrasound image of GM, from Maganaris (2003). Panel A.2: panoramic image of GM, from Simpson et al. (2016). Panel B: GM (yellow) and gastrocnemius lateralis (GL, blue) fascicles reconstruction from magnetic resonance imaging (MRI) with diffusion tensor image tractography, from Bolsterlee et al. (2019). D, distal; P, proximal,*

1.2.1.b. Specific tension

Specific tension quantifies the peak of force per unit of area (e.g. expressed in $N.cm^{-2}$). At the level of individual fibre, specific tension has been calculated as the peak isometric tension divided by the cross-sectional area of an isolated fibre (reviewed in Bottinelli and Reggiani,

2000). At the level of muscles, specific tension has been estimated as the maximal muscle force divided by the muscle PCSA (e.g. Erskine et al., 2009).

Specific tension of fibres. Human muscles are composed of different fibre types that are divided into types I, I/IIa, IIa, IIa/IIx and IIx (Bottinelli et al., 1999). For simplicity, this section describes fibre properties with only slow (type I) and fast (type II) fibres. The specific tension of isolated single fibres has been largely investigated *in vitro,* from peak isometric tension and cross-sectional area of an isolated fibre. Histochemical classification of fibre type is conducted by identification of myosin ATPase or myosin heavy chain isoform composition (Bottinelli and Reggiani, 2000; Enoka and Duchateau, 2019). The specific tension developed by human muscle fibres *in vitro* in highly variable, i.e. differences between the weakest and the strongest fibres are very large (more than 10-fold; Bottinelli and Reggiani, 2000). Reported specific tensions range from 2.3 $N.cm^{-2}$ (Harridge et al., 1998) to 36.5 $N.cm^{-2}$ (Fink et al., 1990). Such large variability is thought to be little dependent on fibre type, and rather explained by experimental conditions (reviewed in Bottinelli and Reggiani, 2000). Indeed, specific tension of slow type fibres has been shown to be mostly (Bottinelli et al., 1996; Burke and Tsairis, 1973; Parente et al., 2008; Widrick et al., 2002) but not always (Erskine et al., 2011; Trappe et al., 2000) lower than specific tension of fast type fibres. On average, for human skinned and freeze-dried muscle fibres, values of 12 $N.cm^{-2}$ and 18 $N.cm^{-2}$ were reported for slow and fast fibre types respectively (Fitts et al., 1989; Larsson and Moss, 1993; Stienen et al., 1996).

Specific tension of individual muscle. Specific tension at the muscle level is estimated from maximal muscle force and muscle PCSA. Of note, the presence of extra volume occupied by non-contractile material at the muscle level may bias this calculation (Maganaris et al., 2001). Fat infiltration, collagen, water, capillaries, and potentially other structures increase muscle cross-sectional area (CSA) but not force-generating capacity. When measured *ex vivo* in guinea pig, muscle specific tension has led to an average value of 22.5 $N.cm^{-2}$ (Figure 13, panel A). In this protocol, muscle specific tension was calculated as tetanic force, evoked by electrical stimulation, divided by the muscle PCSA. Interestingly, among the 10 muscles investigated (including GM and GL), all had similar specific tension values (22.5 $N.cm^{-2}$), except for SOL, which was significantly lower (15.7 $N.cm^{-2}$). Importantly, it is not possible to directly compare data from animals with human muscles due to the vast dissimilarities in

anatomy (Figure 13, panel B). In particular, the SOL in rodents is relatively small compared to other hind limb muscles in contrast with humans, where the SOL is one of the largest muscles in the body. Further, GM and *plantaris* masses in rodents are 4.2 and 2.5 times respectively higher than SOL. Despite the differences between animals and humans, the constant of 22.5 N.cm^{-2} is most typically used for mammalian muscles specific tension (Enoka and Duchateau, 2019). This value is higher than the specific tension at the level of fibres (i.e. 18 N.cm-2 for fast fibre type; Maganaris et al., 2001). Because of the non-contractile material present in the muscle, one may have expected specific tension in the muscle to be lower. This observation, non-explained, suggests that such data should be interpreted with caution.

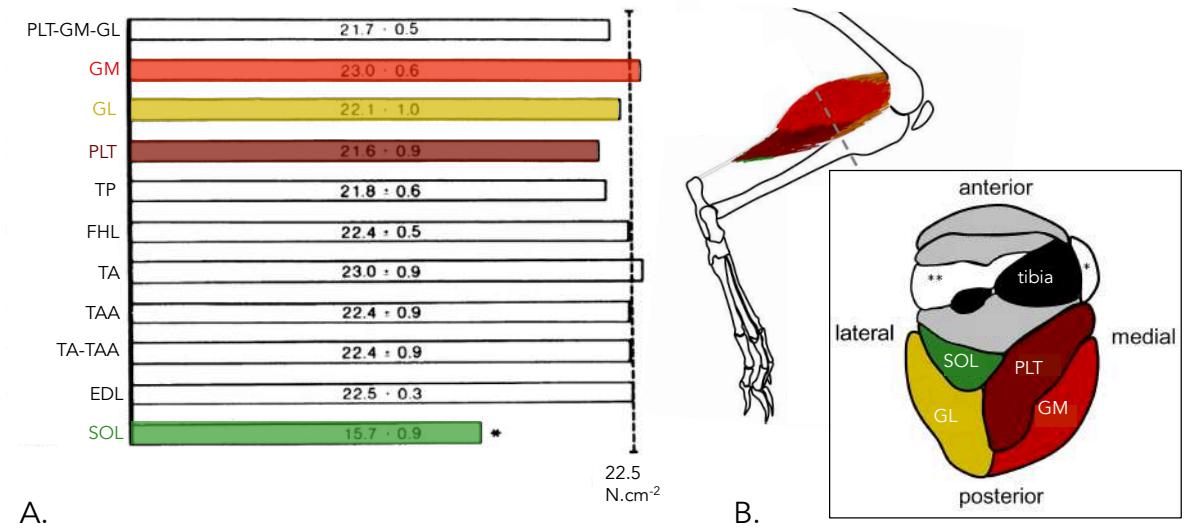

Figure 13. Investigation of individual muscles specific tension. *Panel A: histogram showing specific tension values of nine guinea pig muscles measured in situ. All muscles or muscle groups had specific tension values similar to 22.5 N.cm^{-2}, except of soleus (SOL), which was 32 % less. From Powell et al. (1984). Panel B: anatomy for rodents (example of rabbit). From Siebert et al. (2015). GM : gastrocnemius medialis, GL: gastrocnemius lateralis, PLT : plantaris, TP : tibialis posterior, FHL : flexor hallicus longus, TA : tibialis anterior, TAA : tibialis anterior accessorius, EDL : extensor digitorum longus.*

Specific tension of a muscle group. In humans, specific tension *in vivo* has been estimated in different muscle groups, as the maximal force (estimated from joint torque and moment-arms) divided by the sum of all muscles PCSA. This resulted in specific tensions of 30 N.cm^{-2} for the knee extensors (Erskine et al., 2009), 24 N.cm^{-2} for elbow flexors (Kawakami et al., 1994), 11 and 25 N.cm^{-2} for plantarflexors and dorsiflexors respectively (Fukunaga et al., 1996). The main limitation of such studies is that they can only estimate specific tension for a

muscle group and not for an individual muscle. This is because when force production is shared between several synergist muscles, there are no tools to measure individual muscle forces. This is particularly problematic as specific tension could vary between muscles, as supported by variability in fibre types across muscles (e.g. SOL vs *gastrocnemii*, Johnson et al., 1973). This has been somewhat overcome in studies that considered that one muscle was the single actuator (or main contributor) in some anatomical configuration (e.g. *triceps brachialis* for elbow extension). Using this approach, a specific tension of 15.5 $N.cm^{-2}$ was reported for *tibialis anterior* (main dorsiflexor; Maganaris et al., 2001), 14.5 $N.cm^{-2}$ for *triceps brachialis* (main elbow extensor; Kawakami et al., 1994), and 15.0 $N.cm^{-2}$ for SOL (main plantarflexor if knee flexed; Maganaris et al., 2001). One group has attempted to quantify individual muscle specific tensions on the *quadriceps* group (Narici et al., 1992). Estimation of individual muscle forces were calculated by weighting total force according to each muscle PCSA proportions. This yielded specific tensions of 23.7, 27.9, 24.1 and 24.3 $N.cm^{-2}$ for VL, VM, *vastus intermedius* and *rectus femoris* respectively. Of note, implicit in these calculations was that individual muscle forces are distributed similarly to individual muscle PCSA's, which required some assumptions. For example, it assumes that 1) the force-length relationship of all knee extensor muscles have the same shape, i.e. all synergist muscles present similar relative fascicle excursions and the same optimal length, 2) all agonist muscles have a similar moment arm. These assumptions drastically limit the interpretation of such data. Overall, the absence of a non-invasive experimental technique to measure individual muscle force *in vivo* in humans limits our knowledge on individual muscle specific tension. The differences for specific tension between muscles and between individuals remain unclear. However, most importantly for the aims of this thesis, if some synergist muscles have different specific tension, it is unlikely that this would impact the force distribution, during **submaximal contractions, particularly at low intensities**. This is because for all muscles, slow type fibres are recruited preferentially at low forces (Henneman and Oslon, 1965; Henneman et al., 1965).

Muscle PCSA and specific tension directly contribute to maximal isometric force. However, for an isometric contraction when muscle length is not optimal, or during a dynamic movement, PCSA and specific tension are not the only biomechanical factors that influence force output. Dynamic muscle properties in relation to muscle fibre length and velocity of contraction (fibre shortening) also impact force production.

1.2.2. Force-length and force-velocity relationships

The cross-bridge theory states that contraction and force production in muscles is caused by the cyclic interaction of cross-bridges between actin (thin) and myosin (thick) filaments (Huxley, 1957). The cross-bridge theory captures well many experimental properties of muscles (Herzog, 2017). First, the **force-length relationship** is well explained by the increase and decrease number of cross-bridges between actin and myosin filaments, as sarcomere lengths go beyond and over those at which maximal active force can be produced. Note that later refinements of the cross-bridge theory were made by including a spring element, the titin, a cytoskeletal protein connecting the myosin filaments to the Z line (Herzog, 2017). However, this theory does not fall within the scope of the thesis, as its implications mainly concern dynamic contractions. Second, the cross-bridge theory is also consistent with the **force-velocity relationship**. The rate of change in sarcomere length impact the level of interaction between thin and thick filaments and thus in the force produced (Enoka and Duchateau, 2019). The following section describes the influence of force-length and force-velocity relationships on force production at the whole muscle level.

1.2.2.a. Muscle force-length relationship

At the muscle level, the force-length relationship is defined as the relationship between the maximum active steady-state isometric force of a muscle and its entire muscle tendon unit length. As muscle tendon unit length depends on joint angle, researchers often rely on the moment-angle relationship of muscles. This has the great advantage of facilitating investigation, as joint torques and angles can be accurately measured with dynamometers, while muscle length cannot (Herzog, 2017). Experimentally, data collection consists of recording the maximal isometric joint moment at different joint angles (Sale et al., 1982). The relationship between joint moment and joint angle often presents a typical bell-shape: there is an optimal angle, at which the torque is the highest (Figure 14). Ascending and descending limbs of the curve show that below and above this angle, joint torque capacity is lower. For example, in Figure 14 (panel A), the moment-angle relationship of elbow flexors demonstrates that the optimal joint angle was 90° of elbow flexion (Enoka and Duchateau, 2019). Of note, because joint angle is conditioned by anatomical constraints, the length at which the isometric torque capacity is maximal may lie outside of physiological range for

some muscles (Buchanan, 1995). For example, it was argued that *gastrocnemii* muscle are limited to the ascending portion of their force-length relationship *in vivo* (Maganaris, 2003). Indeed, the moment-angle relationship measured for plantarflexors was mainly ascendant (Figure 14, panel B). This is because plantarflexors reach their optimal angle (15° of dorsiflexion; Sale et al., 1982) as plantarflexion gets close to the maximal physiological angle for dorsiflexion (~ 20°). Hence, there is no more physiological range where plantarflexion torque capacity would reduce (the descending part of the relationship), which would happen over 20° of dorsiflexion.

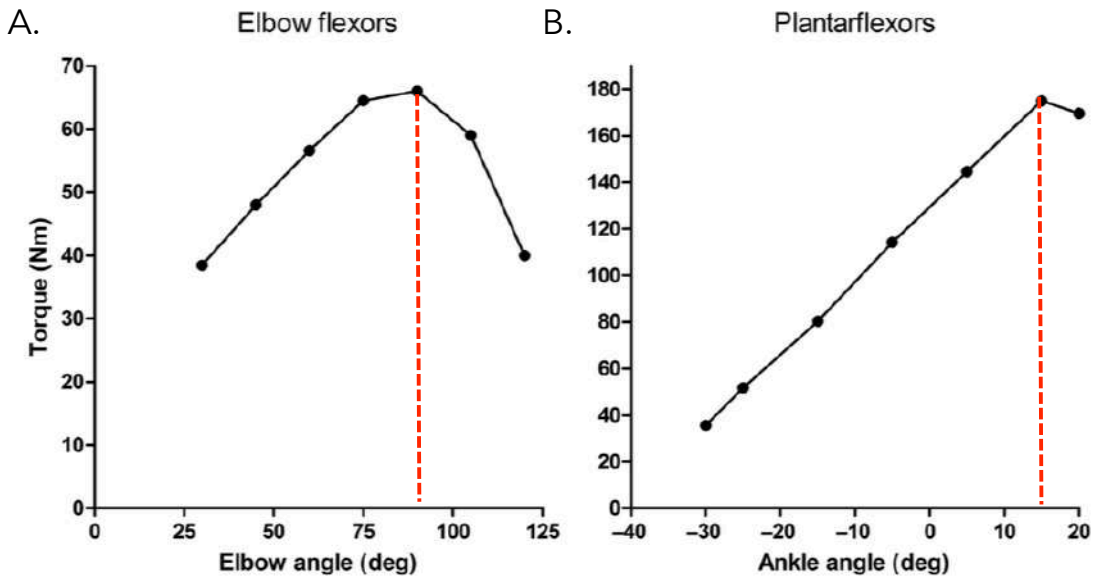

Figure 14. Relationship between maximal isometric torque and joint angle. *Panel A: elbow flexors, from Pertuzon (1972). Panel B: plantarflexors, from Sale et al. (1982). Peak torque occurs at 90° for the elbow flexors, and at 15° of dorsiflexion for plantarflexors (regardless of the knee angle). From Enoka and Duchateau (2019).*

In the absence of a tool to directly measure individual muscle force, we cannot determine individual muscle force-length relationship. However, some studies have aimed to estimate the force-length relationship of individual human muscles. For example, muscle fascicle length change was measured during maximal isometric contractions that were elicited from muscle specific electrical stimulation, and the resulting tendon force was estimated from dynamometry and moment arm data, for the GM (Hoffman et al., 2012) and SOL (Maganaris, 2001). These studies reported an optimal ankle angle at approximately 15° of dorsiflexion for the SOL (Maganaris, 2001) and 19° of dorsiflexion for the GM (Hoffman et al., 2012). When

the aim is to compare synergist muscles forces, placing the two muscles at a similar length relative to their optimal length would limit the influence of force-length properties on the difference of force between the two muscles. Although it limits the comparison to just this joint angle, which is not physiologically relevant, it is the first step to investigate muscle force-sharing.

1.2.2.b. Muscle force-velocity relationship

The force-velocity relationship is defined as the relationship between the peak force a muscle can produce and the velocity at which it operates. Muscle tendon unit lengthening and shortening depends on joint angular speed, and researchers often rely on the moment-angular speed relationship of muscles. Experimentally, data collection consists of recording peak torque of maximal voluntary isokinetic contractions at different speeds (de Brito Fontana et al., 2014). The relationship between peak moment and joint angular speed is inversed: as the velocity increases, the peak force the muscle can produce reduces; and vice-versa (Wilkie, 1950). For example, plantarflexors torque was 72 $N.m^{-1}$ at 25 $°.s^{-1}$; it was 6 $N.m^{-1}$ at 264 $°.s^{-1}$ (Wickiewicz et al., 1984).

Similar to the investigation of muscle force-length relationship, the absence of a non-invasive experimental technique to measure individual muscle force limits our knowledge on individual muscle force-velocity properties. When the aim is to compare force from two synergist muscles, isometric contraction appears as a way to limit differences (for this factor) between the two muscles force production. Indeed, an isometric contraction greatly reduces the impact of the parameter linked to dynamic motion (force-velocity relationship) on force, for the two muscles. While it is acknowledged that the outcomes from such isometric studies cannot be inferred to dynamic contractions, it is an important first step.

In the human body, several muscles coordinate to achieve the vast majority of movements. Importantly, coordination occurs at multiple levels of the motor control hierarchy: between limbs, between joints and between individual muscles (Diedrichsen et al., 2010). In this work, we were interested in the distribution of force between individual muscles. **Muscle coordination is defined here as the force distribution, or the force-sharing, among a group of muscles.**

2. Force-sharing among a group of synergist muscles

2.1. The general distribution problem

2.1.1. Muscle redundancy

The human body has a much larger number of muscles (~ 630) than it has degrees of freedom (244; Prilutsky and Zatsiorsky, 2002). For example, the activity of 10 muscles influences the forces applied about the knee (*biceps femoris*, *tensor fascia latae*, *quadriceps, sartorius, gracilis, semi-tendinosus, semi-membranosus, popliteus*, GM, GL; Figure 15), while the knee has six degrees of freedom (flexion / extension, abduction / adduction, internal / external rotation). Moreover, muscles may span more than one single joint and may produce movements in several degrees of freedom. Due to this redundancy, numerous combinations of muscle forces can generate the same joint torques (Prilutsky and Zatsiorsky, 2002). In other words, several muscle coordination strategies can lead to a similar motor outcome.

2.1.2. Force distribution at a joint

The problem of calculating the force within the anatomic structures at a joint can be thought of as the "distribution problem". At a joint, the force (F) created is composed of the sum of force from each different structures affecting the joint: muscles, ligaments and bones contact (Crowninshield and Brand, 1981; Herzog, 1996). The contributions of ligaments and bony contacts to joint force are often assumed to be small and are therefore ignored. This reduces the equation to the muscle component only (Herzog, 1996):

$$F^0 = \sum_{i=1}^{m} (f_i)$$

Equation (3)

Where F is the force at the joint centre, ^{0} designates the joint centre, m the number of muscles and f_i the force of the ith muscle (Figure 15). Contributions from ligaments and bony contacts to joint torque are also assumed negligible. Hence, the joint moment is equal to (Herzog, 1996):

$$M^0 = \sum_{i=1}^{m} (f_i \times r_i)$$

Equation (4)

Where M is the moment at the joint centre, ^{0} designates the joint centre, m the number of muscles, f_i and r_i the force and moment arm of the ith muscle respectively. Equations 3 and 4 represent the general distribution problem. When solving the distribution problem, the purpose is to determine the forces from individual muscles from the resultant joint torque.

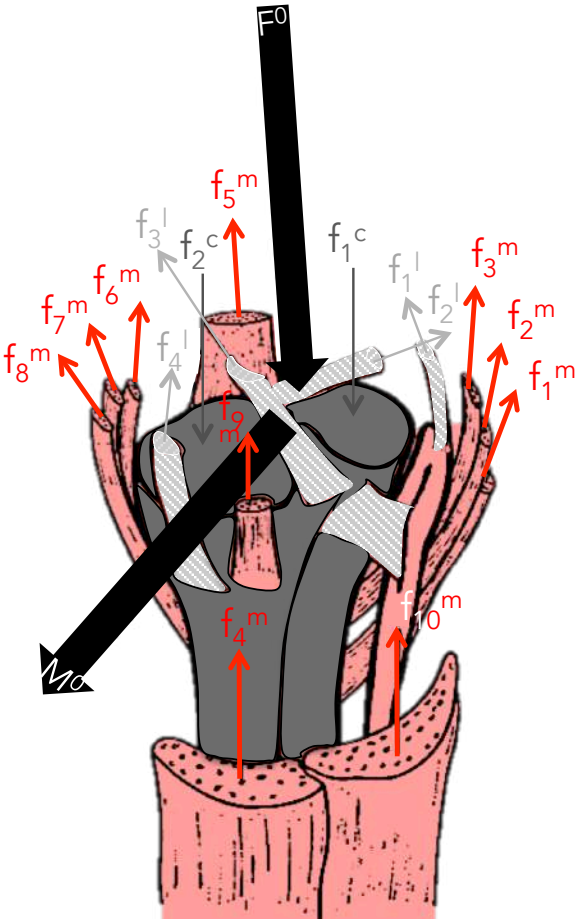

Figure 15. Structures carrying force about the knee (see from the posterior aspect). *F^0 if the force at the knee center. Each f_i^m represents the ith force for the muscle m. M^0 if the moment at the knee center. Each f_i^l represents the ith force for the ligament l. Each f_i^c represents the ith force for the bony contact c. From Crowninshield and Brand (1981).*

The distribution problem hence relates to the understanding of how the central nervous system selects muscle coordination strategies among all possibilities (Bernstein, 1967). In humans, the number of muscles crossing a joint typically exceeds three [as explained above, for example 10 muscles control the knee joint (Figure 15; Herzog, 1996)]. Equation 4 contains m unknown muscle forces (f_i), and represents a mathematically indeterminate system, i.e. the system contains more unknowns than equations. Mathematically indeterminate systems generally have an infinite number of solutions, which is why the distribution problem has often led to the conclusion that there are infinite numbers of force-sharing strategies that can lead to similar motor outcomes. Although it is well known that muscle redundancy grants the nervous system many options to perform a task, the "infinity" of such options has been debated.

2.1.3. Set of possible coordination strategies

Kutch and Valero-Cuevas (2011) raised the question whether muscles are "equally redundant". They studied the necessity of each muscle by analysing the static transmission from muscle force to endpoint output, across different force directions and magnitudes. To this end, they resected cadaver arms at the mid-forearm level and identified the proximal tendons of all seven muscles controlling the index finger (i.e. *flexor digitorum profundus, flexor digitorum superficialis, extensor indicis, extensor digitorum communis, first lumbricals, first forsal interosseous* and *first palmar interosseous*). They glued each tendon to nylon cords attached to motors. With this protocol, they could experimentally measure the fingertip forces resulting from known tensions in all seven tendons. Kutch and Valero-Cuevas (2011) found that the loss of one muscle often compromises force production, with clear differences among muscles in relative importance to force production. For example, on average for varying fingertip forces, *first palmar interosseous* muscle is the most necessary muscle (its loss resulted in ~ 90 % of force deficit) while the *first lumbrical* muscle is the least necessary (its loss resulted in a ~ 30 % force deficit). Moreover, Kutch and Valero-Cuevas (2011) quantified the proportion of muscles that are "truly necessary" or more "optional" in the set of all possible forces (i.e. the "feasible force set") that can be achieved in the sagittal plane (i.e. finger flexion-extension) with the seven involved muscles. They found that only 8 % of the area was free from any necessary muscles. Hence, the rest of the feasible force set area (92 %) required *at least* one particular muscle. In another model of a simulated human

leg with 14 muscle groups, 84 % of the feasible force set area (sagittal plane) required at least one particular muscle. This demonstrated that mechanical task constraints also influence whether a muscle is necessary for a particular force, hence reduce the number of solutions to the distribution problem.

The feasible coordination patterns are not only bounded by mechanical constraints but also by the biomechanical and neurophysiological properties of muscles. Muscle biomechanical properties include volumetric and architectural features. Neurophysiological properties refer to muscle activation. First, the maximal force a muscle can produce is bound by its biomechanical factors (i.e. the ones that determine its maximal generating-force capacity). Second, the force a muscle produces depends on the muscle activation. We know that each muscle in a group of synergists receives some specific neural drive and some drive that is shared with other muscles in the group (Laine et al., 2015). For example, during isometric contractions, VL and VM share the majority of the drive they receive (> 60% of the input; Laine et al., 2015; Negro et al., 2016). If the activation of two muscles is difficult to dissociate, this potentially reduces the number of options for coordination. Interestingly, the common input between synergist muscles vary greatly depending on the group considered. For example, experiments from our group led to the conclusion that the two *gastrocnemii* muscles share no (or minimal) common synaptic input (Hug et al., unpublished observations). The ability to diasssociate the activation of these muscles theoretically leads to a larger number of force-sharing strategies. Furthermore, it is possible that biomechanical factors and neural factors of a muscle are related in some contexts. Some models (further described in Part 1, Section 2.2.2) proposed that among a group of synergists, muscles presenting the highest PCSA would produce the highest force (Crowninshield and Brand, 1981). This would mean that (*i*) muscle activation does not compensate for different PCSAs between muscles and they each receive balanced activation (for example, as case 1 in Figure 16), or that (*ii*) the muscle with the highest PCSA generates the highest activation (i.e. there is a neuro-mechanical coupling which further increase the imbalance of force, as case 3 in Figure 16). However, other hypotheses are possible: (*iii*) activation compensates for imbalance of PCSA (i.e. there is an inverse neuro-mechanical coupling, which results in equal force production between synergists; case 2, Figure 16), or (*iiii*) there is no specific relationship between activation and PCSA (not shown in the Figure 16). Some experimental evidence supports the existence of a neuro-mechanical coupling. For example, a positive correlation between the

ratio of muscle activation and the ratio of PCSA in two mono-articular synergist muscles of the thigh (VL and VM) was found during submaximal isometric contractions (Hug et al., 2015a). The muscle with the higher force-generating capacity generated greater activation. This link identified during isometric contractions between biomechanical and neuromuscular factors inherently reduce the number of coordination options. Of note, it could be different in other scenarios (i.e. dynamic contractions).

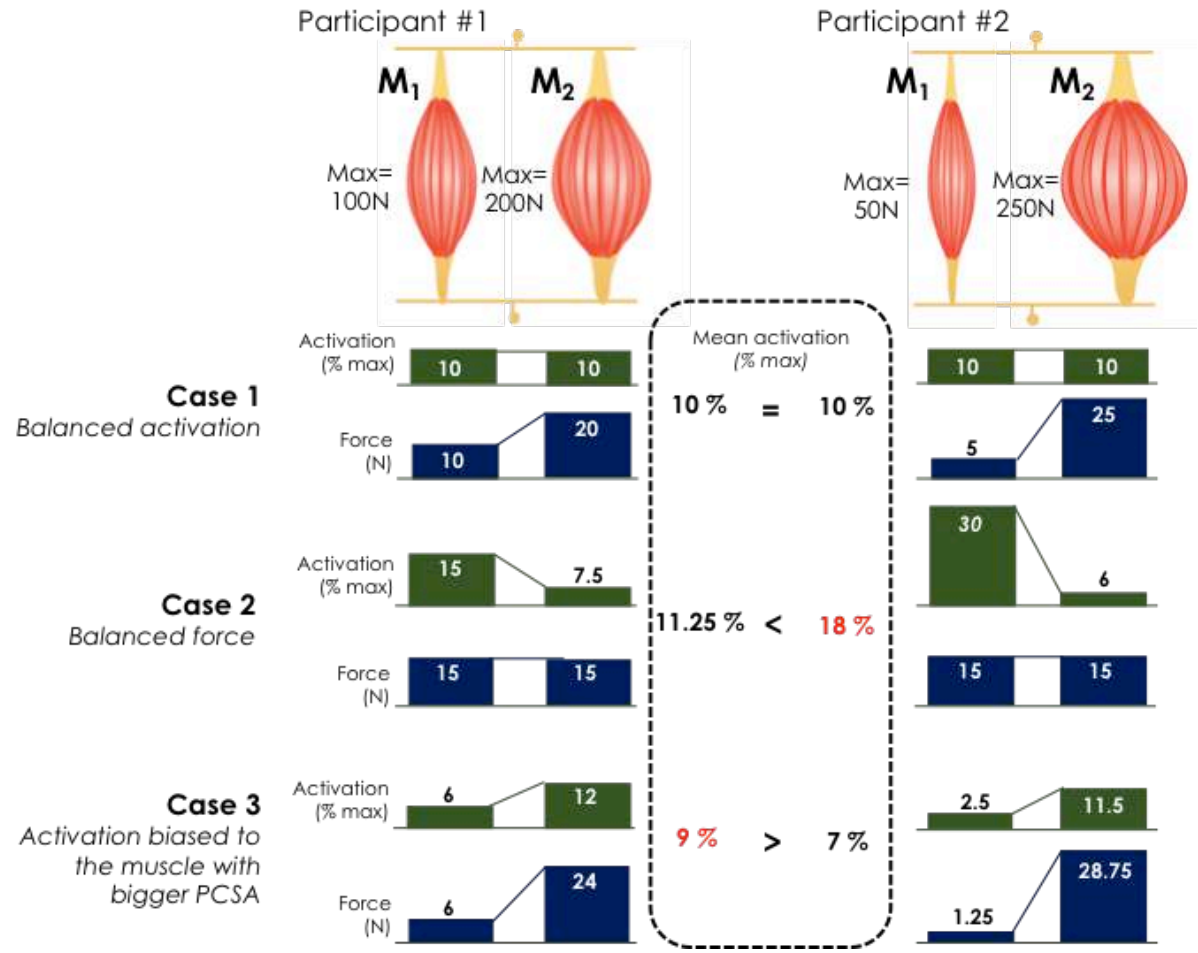

Figure 16. Scenarios of the coupling (or not) between muscle force-generating capacity (PCSA) and muscle activation, and their consequences on force distribution. *M1 and M2 are two hypothetical synergist muscles. Case 1: activation is equally shared between synergist muscles, no matter their PCSA. Case 2: force is equally shared between synergist muscles, hence activation compensate for between-muscle differences in PCSA. Case 3: the muscle with the highest PCSA receives the highest activation. The absence of a specific coupling between activation and PCSA (a fourth solution) is not represented on the figure.*

Even though the investigation of force-sharing strategies requires the knowledge of individual muscle force, there is no non-invasive technique to measure muscle force. Dynamometers provide information on joint torque only, i.e. the resultant of all muscle-combined forces. Individual muscle forces can be estimated using biomechanical models or measured experimentally using invasive procedures.

2.2. Investigation of muscle force-sharing

2.2.1. Experimental measures

The experimental measure of individual muscle force *in vivo* requires the insertion of a force-gauge (Komi, 1990) or optic fibres (Finni et al., 2000) within the tendon to record the pulling forces from the muscle(s). Tendon sensors produce reliable results (Ginn et al., 1993) but present some limitations (Hahs and Stiles, 1989; Ravary et al., 2004). First, their use requires surgery in order to implant the device, and it is unknown to what extent the invasive surgery generates motor adaptation due to pain and/or healing reactions. Second, once inserted, it is challenging to ensure accurate calibration is maintained. For experiments performed on animal models, it is recommended to perform the calibration *in vitro* by a post-mortem procedure in the site and anatomical structure that has been instrumented *in vivo* (Ravary et al., 2004). This raises questions regarding the validity of tendon sensors measurements in human experimentations, where calibration is done indirectly, using inverse dynamics calculations (Komi, 1990). Finally, when tendons from different muscles are merged such as in the human Achilles tendon, it is not possible to isolate individual muscle forces.

Using tendon sensors, a few studies have been conducted in humans Achilles tendon (Finni et al., 1998; Komi, 1990), patellar tendon (Finni et al., 2000), flexor finger tendons (Dennerlein et al., 1998; Schuind et al., 1992), and shoulder muscle (Bull et al., 2005). In the Achilles tendon, Komi (1990) used tendon buckle transducers (Figure 17) and reported peak force of 9 kN during running. This was the first evidence for the Achilles tendon to carry forces of ~ 12.5 times the body weight during such activities (considering all limitations with such measures). Later, the same research team (Finni et al., 1998) used optic fibre force transducers through the Achilles tendon and reported high inter-individual variations in the peak force during walking (ranging from 0.8 to 2.4 kN). Overall, these procedures are not conducted in humans anymore because of ethical limits.

Figure 17. X-ray side view showing the buckle transducer around the Achilles tendon. *Human in vivo investigation. From Komi (1990).*

Tendon sensors have been extensively used on animals to investigate force-sharing between synergist muscles (for review, see Herzog, 2000; Ravary et al., 2004). For example, in cats, it has been demonstrated that the force-sharing between GM and SOL depends on the task. Large SOL forces and zero GM forces were produced during still standing; while large GM forces and no SOL forces were produced during a high-frequency paw shake (Herzog, 1998).

In mallard ducks, GM and GL have distinct tendons that run separately for approximately 15-18 mm before joining to form a common tendon (Biewener and Corning, 2001). Taking advantage of this anatomical arrangement, a study assessed the distribution of force between the two *gastrocnemii* (Figure 18). The GL contributed to 67 % of the total force during swimming (GL and GM produced 10 and 5 N, respectively). During terrestrial locomotion, GL contributed to 59 % of the total force (GL and GM produced 20 and 14 N respectively; Biewener and Corning, 2001).

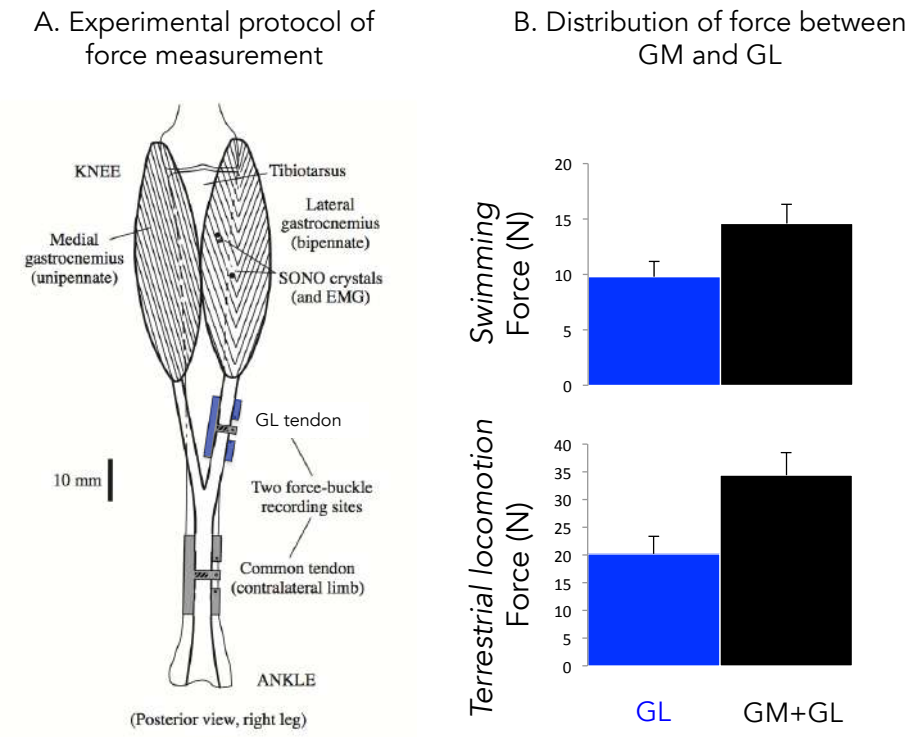

Figure 18. *Gastrocnemius medialis* (GM) and *gastrocnemius lateralis* (GL) contribution during swimming and terrestrial locomotion in mallard duck. *Panel A: anatomy of the mallard hindlimb, illustrating the sites where tendon buckle force transducers were implanted. Panel B: force distribution between GM and GL during swimming and terrestrial locomotion. From Biewener and Corning (2001).*

Except from tendon sensors, we have no **direct** experimental tool to measure muscle force. The **non-direct** method of EMG has been extensively used to estimate individual muscle forces experimentally in humans (Basmajian and De Luca, 1985). However, the nature of the relationship between EMG and muscle force is affected by many factors (Hug et al., 2015a). During submaximal contractions, muscle activation combined with others factors (e.g. PCSA,

force-length and force-velocity relationships) modulate the force produced. Other **indirect** tools, based on the velocity of acoustic wave propagation (shear wave elastography), have been proposed as a possible solution to estimate individual muscle (Hug et al., 2015b) or tendon forces (Martin et al., 2018a). Shear wave elastography relies on the idea that the stiffness of a muscle is linearly related to muscle force, and that the shear modulus (measured with shear wave elastography) is linearly related to the elastic properties of the tissue. Using the *equine superficial digital flexor* tendon, the velocity of an ultrasonic wave was found to increase with the force applied to the tendon, even in the presence of skin overlying the tendon (Martin et al., 2018a). On muscle tissue, it was shown that shear modulus and active force are linearly related ($r^2 > 0.86$; Ates et al., 2018). However, changes in shear modulus can presently be only expressed as corresponding *changes* in force, without the possibility of giving an absolute value for the force. In other words, this technology can only assess variation of muscle (or tendon) force. From there, comparison between muscles is not possible. The absence of non-invasive tools limits our understanding of muscle force-sharing in humans. An alternative approach is to use biomechanical models.

2.2.2. Biomechanical models

Optimization models based on physiological considerations. A common approach to solving for individual muscle forces during movement has been mathematical optimization. Optimization relies on the fact that human (or animal) movements obey some "law of optimal control" (Herzog, 1996). It requires the assumption that the central nervous system selects muscles for a given activity according to some criterion: the objective function. For example, Crowninshield and Brand (1981) considered that for prolonged activities such as gait, muscle coordination aims at minimizing the sum of muscular stresses:

$$\sum_{i=1}^{N} \left(\frac{F_i}{PCSA_i} \right)^3$$

Equation (5)

Their model was the first to consider each muscle PCSA, i.e. the physiological significance of the system to optimize motor control. Here, to minimize muscular stresses, relatively more force is allocated to muscles that have a large maximum force capacity (large PCSA). Dul et al. (1984) proposed an objective function for individual muscle force prediction that attempted to maximise endurance, hence minimize fatigue. For a given force level, a muscle

with relatively more slow-twitch fibres has a greater endurance time and is thus more fatigue-resistant. In their minimum-fatigue criterion model, both PCSA and fibre-type were considered. Their objective function was the first to require input about the fibre-type composition of the studied muscles. Herzog (1987) proposed an optimization algorithm with an objective function that contained the force length velocity properties of the muscles of interest, but was confronted to a main problem of feasibility (i.e. force length and force velocity relationships for most muscles cannot be known). Another approach to estimate individual muscle forces involved initial sets of muscles activations that are fed into the model (reviewed in Erdemir et al., 2007). These EMG-driven models present the benefit of implicitly accounting for specific individual activation patterns (Lloyd and Besier, 2003), and accounting for time-varying muscle activation patterns (throughout a gait cycle, for example).

Hill-type model. A lot of models used in the biomechanical field are derived from Hill-type model that is free from optimization, hence does not require any assumption. They predict muscle force from different factors (Zajac, 1989): its maximum force capacity, its pennation angle, its activation, its instantaneous length and its instantaneous rate of change in length. This model usually relies on collecting experimental participant-specific data (e.g. muscle activation, PCSA, fascicle length and fascicle velocity, pennation angle), which are combined with information from the literature (e.g. specific tension, shape of force-length and force-velocity relationships) to estimate muscle force. The force (F_m) the muscle exerts has been expressed with the following equation (Zajac, 1989):

$$F_m = F_{max} \times \cos(\beta) \times \left[Act_{(t)} \times F_{a,L(t)} \times F_{a,V\,(t)} + F_{p,L\,(t)}\right]$$

Equation (6)

Here, F_{max} (the maximal isometric force-generating capacity of the muscle) depends on muscle PCSA and specific tension, and the cosine of pennation angle (β) represents the projection of fascicle force onto the tendon axis. $Act_{(t)}$ (muscle activation), $F_{a,L\,(t)}$ and $F_{p,L\,(t)}$ (respective active and passive force-length relationships) and $F_{p,L\,(t)}$ (force-velocity relationships) are time-dependent *(t)*, as variables which influence the instantaneous muscle force.

2.2.3. Approach of the current work

Knowing that (*i*) the omission of some biomechanical factors, e.g. force-velocity relationship, is thought to explain in parts the errors observed in some models (Herzog & Leonard 1991), and that (*ii*) the experimental investigation of some factors is not feasible in humans *in vivo*, we proposed to simplify the approach for individual muscle forces estimation, so that unknown factors would play minimal roles. The expression of force prediction with Hill-type model, attractive because of computational simplicity, is limited by the impossibility to experimentally determine three parameters *in vivo* and in humans: specific tension (hence F_{max}), force-length and force-velocity relationships. As such, we chose an experimental design where the force produced by each muscle is not dependent on velocity (e.g. isometric contractions). Moreover, during submaximal isometric contractions, the impact of different specific tensions between muscles is reduced due to the size principle of orderly recruitment of fibres (Henneman and Oslon, 1965; Henneman et al., 1965). Finally, we chose joint angles in order to place all muscles on a similar portion of their force-length relationship, to limit the impact of different muscle lengths (relative to their optimal length) on force-sharing (see previous Section 1.2.2.a in Part 1). In such conditions, a simplified approach of Hill-type model can be used, i.e. combined data of muscle activation and architecture (volume, fascicle length, pennation angle) would give great indication of the isometric submaximal force each muscle produces, and in turn, on force distribution among the synergist muscles.

Individual muscle force and coordination

– Summary –

The human body has a much larger number of muscles than it has degrees of freedom. Due to this muscle redundancy, numerous muscle coordination strategies can generate the same joint torques. **Muscle coordination is defined here as the distribution of force among muscles.** Although the set of possible coordination strategies is large, it is restricted by mechanical constraints of the task (i.e. force direction and magnitude). Additionally, mechanical and neurophysiological constraints of each muscle, such as muscle architecture and activation, reduce the set of possible solutions. Finally, the interaction of these properties between the muscles involved for a task (e.g. their common drive, a neuro-mechanical coupling) also contributes to reduce the possible strategies to produce a joint torque. The knowledge on muscle coordination mainly relies on the use of musculoskeletal models, since *in vivo* measurement of muscle force in humans is not feasible. **Hill-type models** can be used to estimate force of a single muscle from its maximum force capacity, its pennation angle, its activation, its instantaneous length and instantaneous rate of change in length. This model usually relies on collecting experimental participant-specific data (e.g. muscle activation, pennation angle), which are combined with information from the literature (e.g. shape of force-length relationship) to estimate muscle force. In order to limit the impact of the parameters that cannot be determined experimentally, we chose an experimental design where a simplified approach of the Hill-type model may be applied. Performing **isometric contractions** reduces the impact of force-velocities relationships of the different muscles. At a **submaximal intensity**, the impact of specific tension is limited, as we can assume slow type fibres to be preferentially recruited in all muscles, according to the orderly recruitment principle. If the muscles considered are on the **same portion of their force-length relationships**, we can assume that the difference of force production between muscles is minimally affected by difference in length relative to their optimal length. In these conditions, the difference of force between muscles contributing to the task primarily depends on their activation, PCSA, and pennation angle.

Part 2

The *triceps surae* and Achilles tendon

1. The *triceps surae* muscle group: three individual heads

1.1. Descriptive anatomy and morphology

The *triceps surae* is composed of three muscles: GM, GL, and SOL, which occupy the posterior compartment of the leg. GM and GL originate from the medial and lateral femoral condyles respectively (Figure 19; Standring et al., 2008). Their muscle bellies join each other's approximately at distal third along the length of the tibia and become the proximal portion of the Achilles tendon. SOL is situated immediately deep to *gastrocnemii*. It arises from two origins on the fibula and tibia (Figure 19; Dalmau-Pastor et al., 2014). The distal SOL tendon merge with the tendons arising from *gastrocnemii*, and they all insert on the calcaneus.

GM and GL are classically described as unipennate muscles, although some also describe GL as bipennate (surface and deep parts; Johnson et al., 1973). The human SOL has a more complex architecture. It is compartmentalized in a unipennate posterior part which is wrapped around a radially bipennate anterior part (Hodgson et al., 2006). An intramuscular aponeurosis creates the anterior and posterior parts of the SOL. This muscle is also separated in medial and lateral parts by the median septum, creating four distinct sub-compartments (Bolsterlee et al., 2018). SOL goes distally and joins the tendinous portion of the *gastrocnemii* ≈ 6 cm above the *calcaneus* (Pekala et al., 2017). *Triceps surae* muscles (i.e. GM, GL and SOL) have different functions, due to their different proximal insertions, with GM and GL being bi-articular muscles (both plantar flexors and knee flexors). Although GM, GL and SOL share the similar function of plantarflexors, they present very different architectural and composition features.

Of note, the *plantaris* muscle, which exists in ~ 80 to 93 % of the population has been very occasionally considered as part of the *triceps surae* (e.g. Spina, 2007). *Plantaris* origin is superior to the lateral condyle of the femur, its muscle belly is short (from 5 to 10 cm), and it has a long distal tendon (from 25 to 35 cm; Dalmau-Pastor et al., 2014; Olewnik et al., 2017;

Spina, 2007). Although the literature on *plantaris* is scarce, it is known to insert distally on the calcaneus medially to the Achilles tendon, either independent or in association with Achilles tendon (Spina, 2007). Because plantaris muscle is a small and vestigial muscle (Spina, 2007), and because far more frequently, the *triceps surae* is considered to include GM, GL and SOL only (e.g. Albracht et al., 2008), *plantaris* muscle is not considered further in this work.

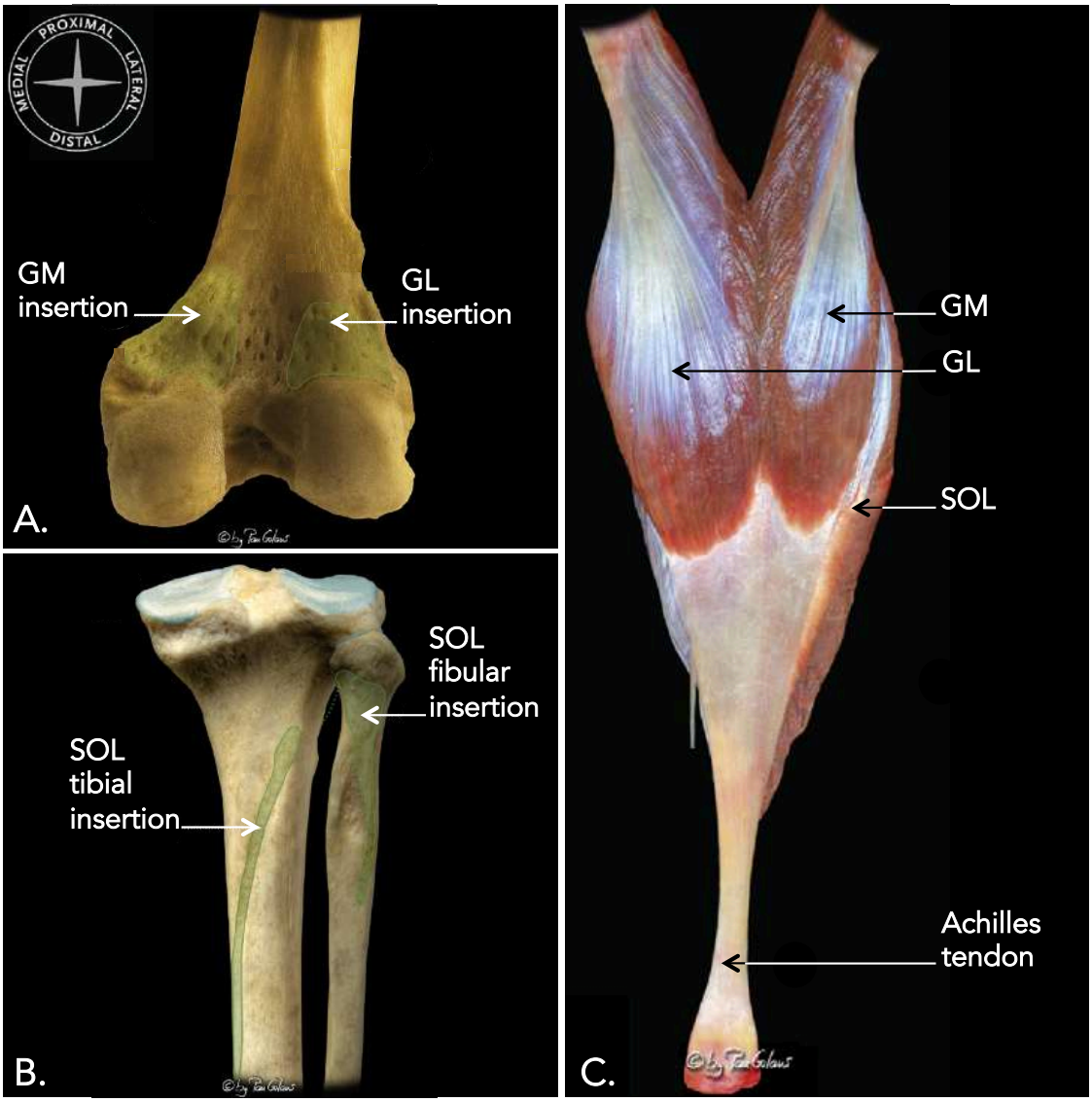

Figure 19. Human leg dissections. *Panel A: posterior view of the femoral distal epiphysis showing the bony prominences and insertional areas of gastrocnemii (marked in green). Panel B: posterior view of the proximal half of tibia and fibula bones. Fibular and tibial proximal insertions of the soleus (SOL) muscle are shown in green. Panel C: posterior view of the triceps surae muscle group. GM, gastrocnemius medialis; GL, gastrocnemius lateralis. From Dalmau-Pastor et al. (2014).*

1.2. Architectural features and typology

Volume, architecture and PCSA. The three heads of the *triceps surae* exhibit large architectural differences. The SOL exhibits the largest volume, followed by GM and GL (Table 1). Also, large differences in fascicle length exist between these muscles. When the knee is extended, the ankle is at 90° (i.e. foot perpendicular to the shank), and the muscles are not active, GL and GM fascicles are longer than SOL fascicles (Table 1). In the same position and condition, SOL and GM exhibit similar pennation angles, while GL pennation angle is relatively smaller than both SOL and GM pennation angles (Table 1). Taken together, these features lead to large variation of functional PCSA between muscles, with SOL exhibiting the largest PCSA (~ 131 cm^2), followed by GM (~ 51 cm^2) and GL (24 cm2; Table 1; Albracht et al., 2008).

Muscle typology. *Triceps surae* fibre-type composition for human has been investigated in cadavers (Edgerton et al., 1975; Johnson et al., 1973). Both *gastrocnemii* exhibit ~ 50 % of slow-twitch fibres, while SOL exhibits 88 % of slow-twitch fibres. These data were reported for six young cadavers (range 18 - 30 years; Johnson et al., 1973). With biopsies on young individuals (range 20 – 41 years old; several studies with on average ten participants, Table 1), slow fibre type percentage was approximately 50 % for GM, 54 % for GL and 76 % for SOL (Table 1). Of note, variability between individual is large. For example, slow fibre type percentage range from 45 to 82 % for GL, and from 64 to 100 % for SOL (Gollnick et al., 1974).

There is a large heterogeneity of structural and composition features among the three heads of the *triceps surae*. This may lead to large differences in their force-generating capacities and/or force distribution during voluntary contractions. This is important as the three distal tendons of GM, GL and SOL muscles merge together to create the Achilles tendon.

Table 1. Review of architectural characteristics and composition of the three heads of the *triceps surae*. *All data were measured in vivo on healthy subjects. For the fascicle length and pennation angle, measurements were performed at rest with the knee angle at 180° (extended) and the ankle angle at 90° (foot perpendicular to the shank).* [$] *estimated from graphically presented data within the research paper; * range;* [€] *standard deviation not indicated. GM, gastrocnemius medialis; GL, gastrocnemius lateralis; SOL, soleus.*

	GM	GL	SOL	Reference
Volume *(cm^3)*	252 ± 65	137 ± 50	449 ± 194	Bolsterlee et al. (2019)
	-	-	362 ± 59	Bolsterlee et al. (2018)
	274 ± 75	-	-	Barber et al. (2009)
	285 ± 45	146 ± 23	477 ± 66	Albracht et al. (2008)
	247 ± 17	130 ± 7	430 ± 12	Kinugasa et al. (2005)
	244 ± 33	141 ± 28	489 ± 65	Fukunaga (1992)
Fascicle length *(cm)*	-	-	3.7 ± 0.8	Bolsterlee et al. (2018)
	4.8 ± 0.7	-	4.1 ± 1.0	Stenroth et al. (2012)
	5.7 ± 0.7	6.6 ± 0.7	3.9 ± 0.9	Albracht et al. (2008)
	5.7 ± 0.9	-	4.2 ± 1.0	Cronin et al. (2008)
	5.4 $^{\$}$	7.3 $^{\$}$	4.6 $^{\$}$	Arampatzis et al. (2007)
	-	5.5 ± 1.1	-	Morse et al. (2005)
	5.5 ± 0.3	-	-	Muramatsu et al. (2002)
	4.4 ± 0.9	4.2 ± 0.7	3.0 ± 1.1	Martin et al. (2001)
	5.2 ± 0.7	5.6 ± 0.8	3.8 ± 0.4	Kawakami et al. (1998)
	5.1 ± 0.4	-	-	Narici et al. (1996)
Pennation angle *(°)*	-	-	26 ± 3	Bolsterlee et al. (2018)
	25 ± 4	-	20 ± 5	Stenroth et al. (2012)
	27 ± 8	-	23 ± 4	Cronin et al. (2008)
	-	18 ± 4	-	Morse et al. (2005)
	22 ± 3	14 ± 2	25 ± 3	Morse et al. (2004)
	19 ± 4	16 ± 3	24 ± 6	Martin et al. (2001)
	24 ± 2	13 ± 1	21 ± 3	Kawakami et al. (1998)
	17 ± 3	-	-	Narici et al. (1996)
PCSA *(cm^2)*	-	-	102 ± 19	Bolsterlee et al. (2018)
	51 ± 10	24 ± 5	131 ± 31	Albracht et al. (2008)
	-	32 ± 6	-	Morse et al. (2005)
	49 ± 6	26 ± 5	128 ± 26	Morse et al. (2004)
	47 ± 6	-	-	Narici et al. (1996)
Slow type fibres proportion *(%)*	-	-	74 $^{€}$	Luden et al. (2008)
	-	-	78 ± 17	Harridge et al. (1996)
	50 ± 20	-	-	Moss (1992)
	-	54 ± 16	-	Rice et al. (1988)
	-	54 ± 3	71 ± 5	Secher et al. (1982)
	-	49 ± 3	-	Green et al. (1981)
	-	60 [45-82]*	81 [64-100]*	Gollnick et al. (1974)

2. The Achilles tendon: three subtendons

2.1. Descriptive anatomy

The Achilles tendon connects the *triceps surae* muscle to the calcaneus. It consists of two structurally distinct parts: (*i*) the proximal Achilles tendon originates at the *gastrocnemii* myotendinous junctions which runs contiguous with SOL; (*ii*) the free (or distal) Achilles tendon continues from the SOL myotendinous junction to its insertion on the calcaneus (Figure 20; Farris et al., 2013). At the lower margins of the *gastrocnemii* muscles (i.e. proximal attachment), the Achilles tendon is flat and wide in the transverse plan. The Achilles tendon becomes oval near its distal insertion. The Achilles tendon is the biggest and the strongest tendon in the human body (Pang and Ying, 2006). Its thickness and cross-sectional area at the level of the medial malleolus are respectively 5 mm and 57 mm^2 (Pang and Ying, 2006). At the level of the insertion on the calcaneus, they are respectively 6.4 mm and 112 mm^2 (Pekala et al., 2017). The length of the Achilles tendon ranges from ~ 6 cm for the free tendon (Farris et al., 2013; Obst et al., 2016; Pekala et al., 2017), until up to 26 cm when considering the proximal part (Doral et al., 2010; Morrison et al., 2015).

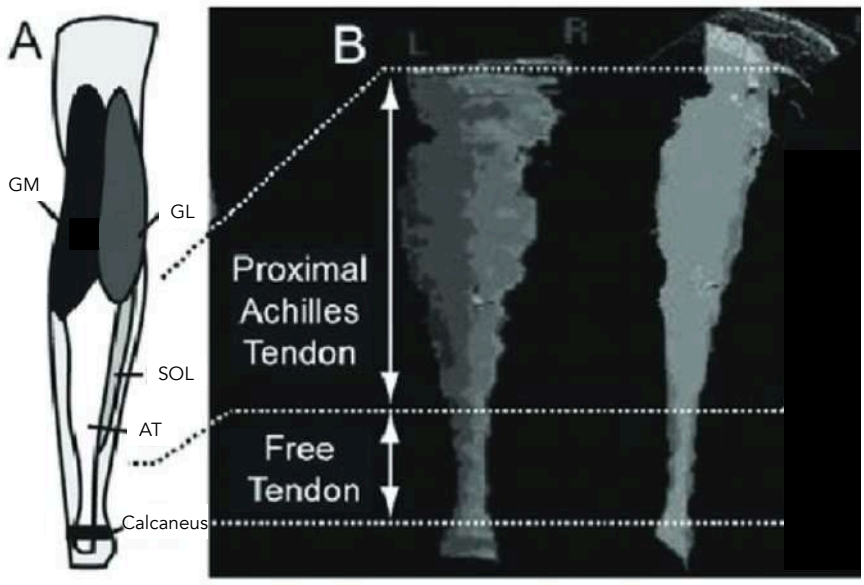

Figure 20. Anatomy of the Achilles tendon. *Panel A: posterior view of a leg. Panel B: two views of a reconstructed Achilles tendon using 3D ultrasonography. The proximal Achilles tendon starts below gastrocnemii myotendinous junctions. The distal Achilles tendon (or free Achilles tendon) starts below SOL (soleus) myotendinous junction. GM, gastrocnemius medialis; GL, gastrocnemius lateralis; AT, Achilles tendon. From Farris et al. (2013).*

The Achilles tendon is a *"multi-muscle tendon"* (Handsfield et al., 2016), as it consists of fibres arising from multiple muscles. GM, GL and SOL create three individualised "subparts" within the Achilles tendon. These three subparts have been termed differently throughout the years (e.g. fibers, fascicle, fascicle bundles). Due to the inconsistencies that existed in terminology, Handsfield et al. (2016) published a nomenclature guideline for tendon hierarchy. According to their work, the present thesis uses the term **subtendon** (Figure 21).

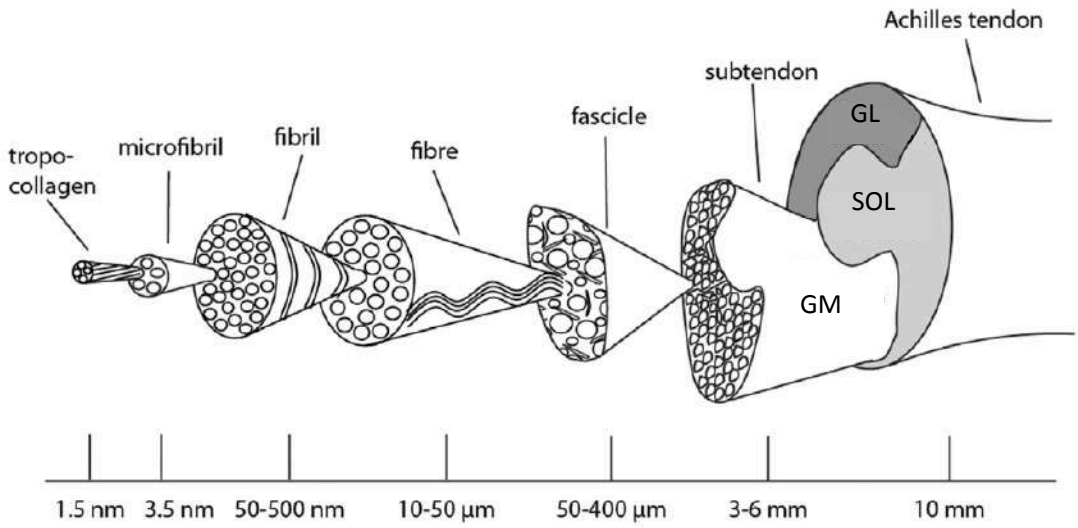

Figure 21. Proposed depiction and nomenclature for Achilles tendon hierarchy. *GM, gastrocnemius medialis; GL, gastrocnemius lateralis; SOL, soleus. From Handsfield et al. (2016).*

GM, GL and SOL subtendons were described first by Parsons in 1894, with examples presented from various mammals. From these animal models it was demonstrated that the subtendons are fused, but can be separated with little difficulty (Parsons, 1894). On human cadavers, it is possible to dissect the three subtendons from the myotendinous junctions to the distal insertion onto the calcaneus (Pékala et al., 2016). Once dissected, differences in subtendon features have been investigated [e.g. width, CSA]. For example, GM, GL and SOL subtendons CSA are 27, 44 and 27 mm^2 respectively, at the superior border of the insertion into the calcaneus (Pékala et al., 2016). This showed the largest proportion for GL subtendon (i.e. 44 % of the overall Achilles tendon CSA at this level). Subtendons also differ in their lengths, which can be assessed *in vivo* using ultrasound. With the knee extended and the ankle at 90°, GM subtendon is slightly shorter than GL subtendon [~ 20 and 22 cm for GM and GL, respectively (Morrison et al., 2015; Obst et al., 2016; Wolfram et al., 2020), whereas SOL

subtendon length is considerably shorter (6 cm) (Farris et al., 2013; Obst et al., 2016; Pekala et al., 2017)]. Overall, the three subtendons present clear differences in their shapes, which is likely to impact Achilles tendon deformations. Importantly, the elliptical "rope-like" structure of the Achilles tendon, i.e. the tendon twist (Farris et al., 2013) may influence its behaviour.

2.2. The twist of the Achilles tendon

Gross anatomical studies provide evidence that the Achilles tendon is a twisted structure (Cummins and Anson, 1946; Edama et al., 2015; Szaro et al., 2009; Van Gils et al., 1996). Specifically, the tendon twists among itself from proximal to distal, counter-clockwise in the right leg, and clockwise in the left leg (Cummins and Anson, 1946; Edama et al., 2015; Pekala et al., 2017). Most commonly, at the distal Achilles tendon insertion, the anterior part of the Achilles tendon's surface is formed by the GL subtendon, the posterior part is formed by the GM subtendon, and the medial part is formed by the SOL subtendon (Pekala et al., 2017). However, the variability between individuals is large, with three main subgroups, from low twist (Type I) to extreme twist (Type 3; Figure 22). Type I is the most common [48 % (Pekala et al., 2017), 84 % (Edama et al., 2015), 52 % (Cummins and Anson, 1946)]. Of note, a twist is also observed at the level of each subtendon. The course of fibre bundles revealed that GL and SOL are also twisted among themselves, especially within the Type III Achilles tendon. GM fascicles ran relatively parallel to each other in all classifications (Edama et al., 2015). In other words, the more twisted the global Achilles structure (Type III), the more twisted of GL and SOL subtendons.

The role of the Achilles tendon twist is not clear. Of note, it is not possible to quantify the degree of Achilles tendon twist *in vivo* with the current imaging techniques. A hypothesis defends that the "rope-like" structure regulates tendon stress and strain (Bojsen-Moller and Magnusson, 2019). In this way, biomechanical models predict a more equal distribution of stress among subtendons if the tendon is twisted rather than straight (Shim et al., 2018). Some authors have hypothesized that the degree of Achilles twist may be important in the development of Achilles tendon pathologies, if stress and strain are not optimally distributed among subtendons (Edama et al., 2015; Pekala et al., 2017). Whilst the Achilles tendon twist potentially affects stress and strain distribution within the tendon, other factors such as subtendon biomechanical properties will affect stress distribution.

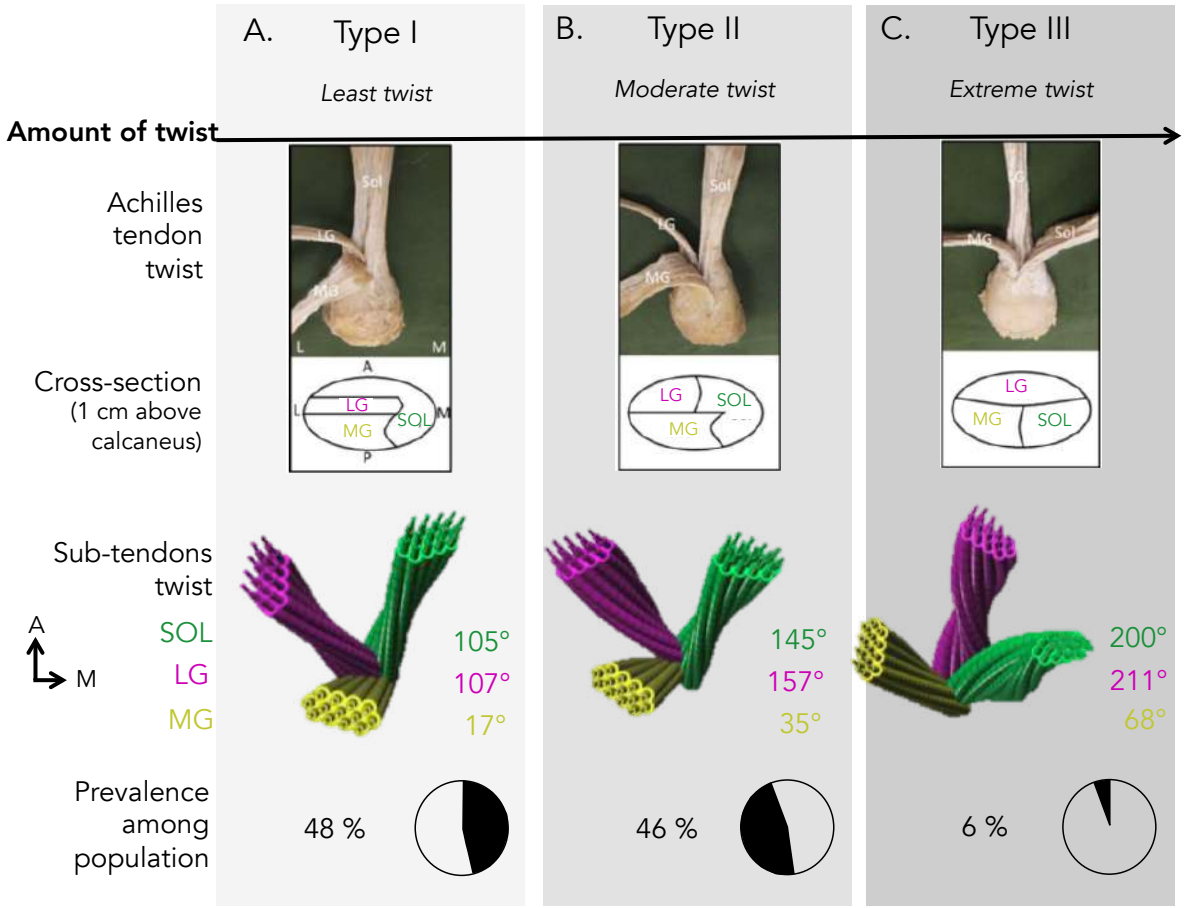

Figure 22. The different subgroups of Achilles tendon twist. *Panel A: type I, panel B: type II, Panel C: type III. Top pictures represent postero-superior view of human dissections and their cross-sections, from left legs. From Edama et al. (2015). Subtendon reconstructed models were made from cadaver dissections, from Pékala et al. (2016). Prevalence values were extracted from Pékala et al. (2016). A, anterior; L, lateral; M, medial; P, posterior; GM, gastrocnemius medialis; GL, gastrocnemius lateralis; SOL, soleus.*

2.3. Mechanical behaviour of the Achilles tendon

Tendon load can be quantified by tendon stress and tendon strain. Stress and strain are estimated from the combination of joint torque measurement, tendon elongation and tendon dimension data (Seynnes et al., 2015).

2.3.1. Achilles tendon stress

Tendon stress ($N.cm^{-2}$) is the force that exist within the tendon structure at a specific cross-section, and is calculated as the tendon force (N) divided by the tendon cross-sectional area (cm^2; Lieber, 2002). As the dimensions of a tendon are not necessarily uniform along its length, particularly within the Achilles tendon (as described above), the stress will vary along tendon length. The Achilles tendon is able to withstand very high loads. The *triceps surae* itself is responsible for ~ 70 to 80 % of the plantarflexion torque (Arndt et al., 1998; Murray et al., 1977; Sale et al., 1982), which can equal tendon loads up to 9 kN (when running; Komi, 1990). Considering Achilles tendon CSA of 0.80 cm^2 at the level of the midportion (Pekala et al., 2017), a force of 9 kN generates an Achilles tendon stress of 11.3 $kN.cm^{-2}$.

Subtendons stress. Currently, there is no non-invasive method to measure either individual subtendons CSA, or tendon force. Thus, it is not possible to measure the stress of each Achilles subtendon. However, the specific contribution of *gastrocnemii* muscles (GM + GL) to Achilles tendon force has been estimated. The anatomical configuration of the *triceps surae* provides the opportunity to alter length of *gastrocnemii* by modification of the knee angle while assuming constant SOL length in plantarflexion (Arndt et al., 1998). This way, Arndt et al. (1998) measured a force discrepancy of 967 N between knee almost extended (170°) and knee flexed (90°), for maximal isometric contraction. Considering that CSA of *gastrocnemii* subtendons is half of the Achilles tendon CSA (92 / 2 = 46 mm^2), this corresponded to a tendon stress discrepancy of 0.21 $N.cm^{-2}$. This study required strong assumptions, but it was the first to give insight into the variation of stress that may exist between Achilles subtendons.

2.3.2. Achilles tendon strain

Tendon strain is a measure of mechanical tendon deformation. For example, a muscle contraction constitutes an external force that creates a local stress field between the muscle and the bone attachment, which then induces tendon strain (Bogaerts et al., 2016). Tendon strain is often calculated as the variation in the longitudinal tendon length (cm) divided by the initial tendon length, and expressed as a percentage (%) of length change. Global tendon strain can be estimated by measuring tendon length change using ultrasonography. Classical B-mode ultrasound can be used to quantify overall tendon elongation (Seynnes et al., 2015). Speckle tracking algorithms can be used to quantify localised tendon displacement (Zelik and

Franz, 2017). With the first technique (conventional B-mode ultrasonography), the measurement of tendon elongation is based on manual tracking of anatomical landmarks such as the myotendinous junction. As such, it is possible to track individual myotendinous junction displacement for GM, GL and SOL, and possible to measure individual Achilles subtendons elongations during contractions. It is also possible to measure their strains, if their initial respective lengths are known. With the second technique, (speckle tracking algorithms) subpixel are identified and their displacement estimated within the tendon. They have been developed to quantify local tendon displacement without the need for specific anatomical landmarks (Korstanje et al., 2010). It is not possible to identify the different subtendons within the Achilles tendon with speckle tracking, but the technique allows the measurement of local elongations within the tendon. With speckle tracking, several studies have shown non-uniform Achilles tendon deformations (further described in Part 2, Section 3.2.2).

Subtendon strain. It is important to mention that multiple studies have inferred "whole Achilles tendon" strain, while only GM and/or SOL myotendinous junction measurements have been tracked (Arya and Kulig, 2010; Child et al., 2010; Muraoka et al., 2004; Waugh et al., 2012). However, GM and SOL subtendons strains can be significantly different during similar task. For example, on average, SOL subtendon strain (~ 4.8 %) is higher than GM subtendon strain (~ 3 %) during low intensity isometric contractions [reviewed by Bogaerts et al. (2016)]. Fewer studies investigated GL myotendinous junction behaviour. Of these studies, Wolfram et al. (2020) reported greater GM (~ 7 %) than GL (~ 5 %) subtendon strain during an isometric contraction, but others report no differences between GM and GL subtendon strain (Farris et al., 2013; Obst et al., 2016). The reasons for the disparities between these results are unclear as similar task intensities were conducted at similar joint angles, however disparities may be due to the use of different measurement techniques [i.e. conventional B-mode ultrasound (Wolfram, 2017) vs. 3D ultrasound (Farris et al., 2013; Obst et al., 2016)].

Overall Achilles tendon constraints have been extensively studied but there remains much uncertainty on how stress is distributed on the overall Achilles tendon. If this load was distributed on 100 % or 50 % of the Achilles tendon CSA (e.g. uneven spread between subtendons), the stress each portion receives would change drastically. Our understanding of load distribution is limited by the absence of a tool to investigate each subtendon stress *in vivo*. Most importantly for this thesis, the GM, GL and SOL muscles behave independently.

As each connects to a different subtendon, it is likely that coordination among the three muscles impacts the Achilles subtendon deformation and strain, and is an important contributor of load distribution within the Achilles tendon.

3. Impact of muscle coordination on Achilles tendon behaviour

3.1. Spatial heterogeneity of Achilles tendon behaviour

As explained above, Achilles tendon is compartmentalized, with each subtendon behaving partially independently from each other. However, we lack an experimental approach to measure individual subtendon displacements within the free Achilles tendon *in vivo*. Thus, the evidence for heterogeneous subtendon behaviours in the free Achilles tendon is indirect. Two examples of indirect evidence for Achilles heterogeneous motions are described here. First, Lubricin is a glycoprotein known to play a role in fascicle sliding (Thorpe et al., 2016a) and expresses at locations within tendons that are subject to sliding motions and shear forces (Sun et al., 2006). The high concentration of Lubricin measured in the interfascicular matrix of the Achilles tendon (Sun et al., 2015) constitutes biochemical evidence for intratendinous sliding motions within the tendon. Second, using speckle tracking, some works have explored the displacement of the deep and superficial layers of the free Achilles tendon *in vivo* (Figure 23). During passive ankle motions from 15° of dorsiflexion to 20° of plantarflexion with knee extended, the superficial layer displaced less (9 mm) than the deep layer (11 mm; Arndt et al., 2012). Similar observations (i.e. superficial layer displaced less than deep layer) were found during eccentric contractions (Slane and Thelen, 2014), and during isometric contractions (further described below, in section 3.2.2; Clark and Franz, 2018; Clark and Franz, 2019). Overall, these observations suggest that the magnitude of displacement differs within the free Achilles tendon.

As mentioned above, GM, GL and SOL muscles have different architectural features (Albracht et al., 2008), related to different maximal force-generating capacities. It seems reasonable to assume that such a force imbalance is likely to have mechanical effect on subtendons displacement. In other words, if one muscle produces more force, its corresponding subtendon would move more than the others. This is true when considering that all subtendons have similar shapes and mechanical properties, and are fully independent. Even though subtendons mechanical properties may differ (Corben et al., 2017), and

transversal force transmission is known to exist within the muscle-tendon unit (Finni et al., 2017b; Maas and Sandercock, 2010), there is some evidence demonstrating that force distribution within the *triceps surae* and Achilles tendon stress distribution are related

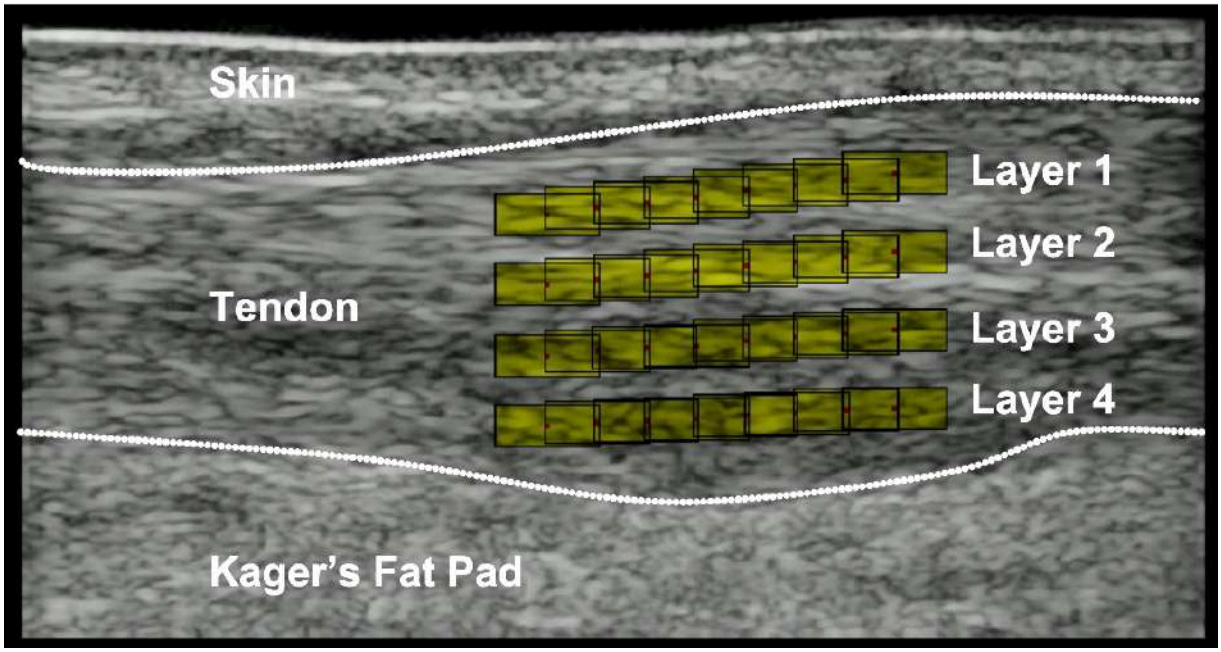

Figure 23. Example of an ultrasound image where individual kernels were identified and tracked within the Achilles tendon. *The layer 1 is the most superficial, the layer 4 is the deepest. It is not possible to know, from such image, which layer belongs to which subtendon. From Couppe et al. (2020).*

3.2. Relationship between force-sharing within the *triceps surae* and Achilles tendon behaviours

3.2.1. Cadavers and animal studies

On cadavers, Arndt et al. (1999) assessed the effect of different tensile force distributions among GM, GL and SOL muscles on the medial and lateral loading of the Achilles tendon. Specifically, they placed two strain-gauge-based transducers, in the medial and lateral parts of the Achilles tendon. They applied different tensile forces on muscles. They observed that if the GM muscle is tensed alone, it generated a higher load in the medial part (88 N) compared to the lateral part (36 N) of the Achilles tendon (+ 23 %). By contrast, tensing the two

gastrocnemii, or the three heads simultaneously always resulted in greater lateral tendon load (127 N in lateral vs. 48 N in medial when GM+GL are tensed; and 239 N in lateral vs. 156 N in medial when GM+GL+SOL are tensed). This work suggests that the force distribution among muscles affects the distribution of load within the Achilles tendon. Specifically, the lateral part of Achilles was more loaded for any combination of muscle tension. Of note, it is hard to draw straight conclusions from this work as a 4 mm longitudinal split was done through Achilles tendon in order to fix the medial and lateral force transducers. Also, the different subtendons were not identified, and the Achilles tendon twist further complicates the ability to interpret this data in a physiologically meaningful way.

In animal studies, accurate quantification of each subtendon displacements *in situ* is possible with knot sutures straight into the structures of interest (Finni et al., 2017a; Maas et al., 2020). Knots have been sutured in GL and SOL subtendons of rats, and GL and SOL muscles were stimulated individually using fine wires electrodes (Figure 24; Maas et al., 2020). Such studies showed that the distribution of force among muscles has an impact on the non-uniform displacements of the Achilles subtendons. At specific knee and ankle angles, stimulation of GL muscle alone generated GL subtendon displacement of 21 % greater than SOL subtendon; while stimulation of SOL muscle alone generated SOL subtendon displacement of 93 % greater than GL subtendon (Figure 24). It was clear that GL and SOL subtendons exerted some force on each other, but most of the force produced by each muscle was transmitted via its own subtendon (Maas et al., 2020). In other words, the distinct Achilles subtendons can move and deform differently, but they are not *fully* independent. This is potentially because the amplitude of subtendon displacement is also influenced by lateral force transmission, and by their respective mechanical properties (e.g. Finni et al., 2017a).

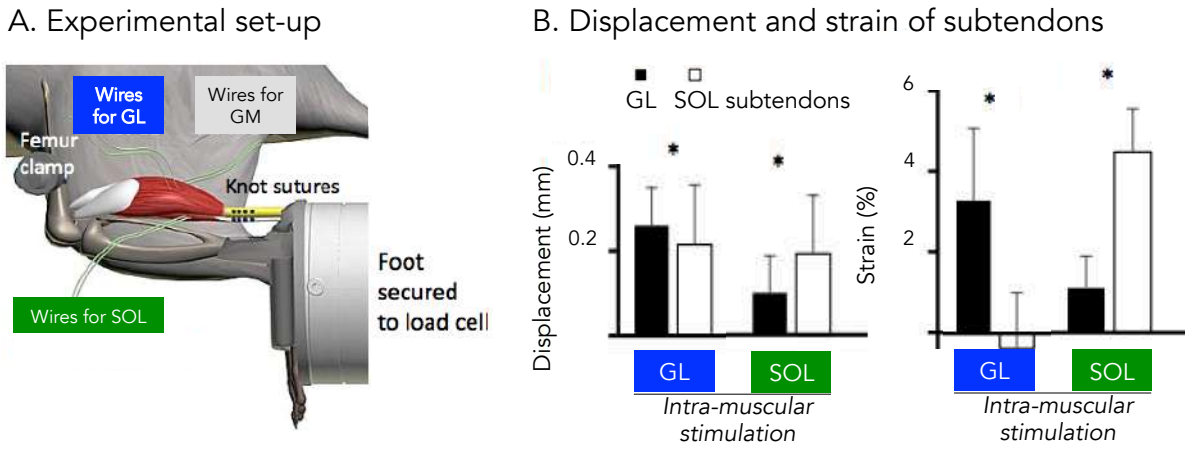

Figure 24. Investigation of Achilles subtendon displacement on rats. *Panel A: wire electrodes within gastrocnemius lateralis (GL) and soleus (SOL) muscle bellies were used for intra-muscular stimulation. Knots were sutured in GL and SOL subtendons. Blue and green colours indicate selective contraction of GL and SOL respectively. Panel B: effects on muscle stimulation condition on displacement and strain of GL and SOL subtendons. Data are presented for knee and ankle at 90°. * $p < 0.05$; ** $p < 0.01$. GM, gastrocnemius medialis; GL, gastrocnemius lateralis; SOL, soleus. From Maas et al. (2020).*

3.2.2. Investigations on humans Achilles tendon

In humans, speckle tracking was used to estimate displacements within Achilles tendon. Recently, it was shown that the deep Achilles tendon part displaced more (~ 3 mm) than the superficial part (~ 2 mm) during isometric contractions. This corresponded to a greater shortening of SOL muscle (~ 6 mm) than GM muscle (3 mm; Figure 25, panel A; Clark and Franz, 2018). As there is no experimental approach to identify subtendons, it was assumed that the deep and superficial tissue relate to SOL and GM subtendons, respectively. Under this assumption, these results suggest that *triceps surae* muscle dynamics govern partly the sliding between adjacent subtendons within the Achilles tendon. Of note, this is a strong assumption, as a large variability between individuals in Achilles tendon twist has been reported (see previous Section 2.2 in Part 2).

Using a computational model, Handsfield et al. (2017) evaluated the effect of twisting, sliding, calcaneal insertion and muscle force distribution on the mechanical behaviour of the Achilles tendon. The model suggested that the uniform distribution of load or strain within the

Achilles tendon is greatly determined by the distribution of force among the heads of the *triceps surae*. In their model, they tuned muscle forces according to data in the literature: peak forces for GM, GL and SOL were 423, 263 and 1157 N, respectively. This equated GM, GL and SOL contributions of 23, 14 and 63 %. They found that non-uniform displacements within the Achilles tendon resulted primarily from different muscle force distribution. Without the presence of the afore-mentioned force distribution (i.e. in the absence of any muscle force contribution), displacement non-uniformity was reduced by 85 %. This constitutes another evidence to consider that muscle force distribution substantially influences the heterogeneity of displacements in the Achilles tendon.

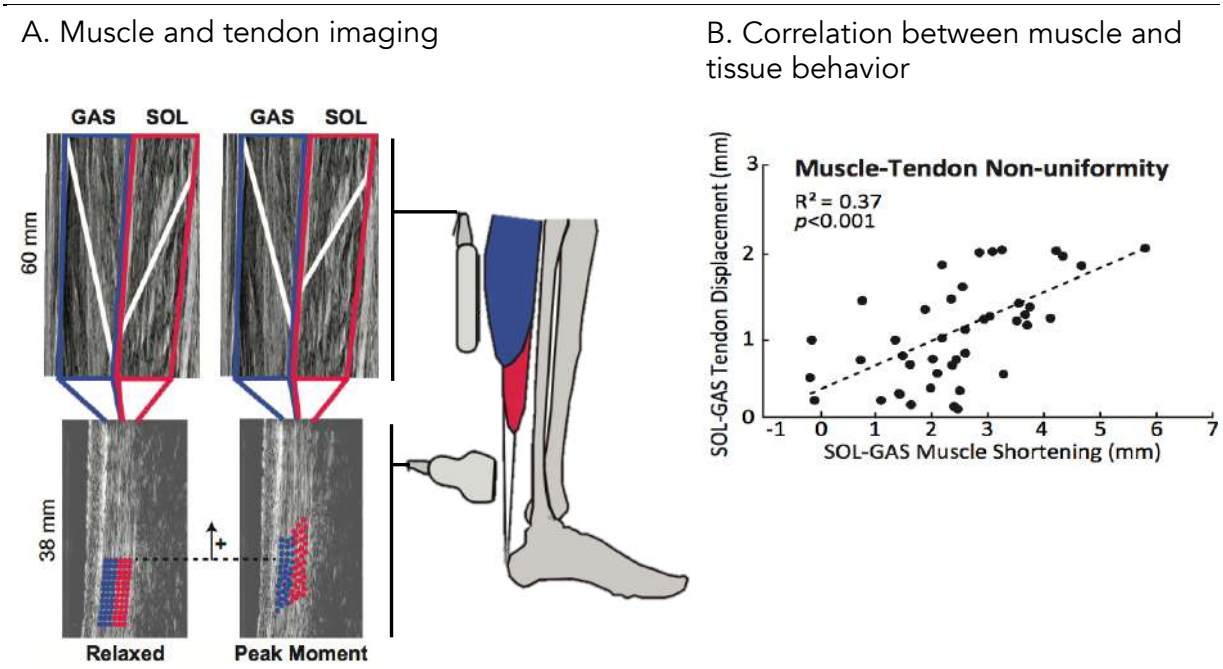

Figure 25. Imaging of *triceps surae* and Achilles tendon during isometric maximal voluntary contractions. *Panel A: muscle fascicle length (B-mode ultrasound) and localised displacements of superficial and deep tendon depths (with speckle tracking). Panel B: correlation between Achilles tissues displacement and muscles shortening. GAS, gastrocnemii; SOL, soleus. From Clark and Franz (2018).*

The *triceps surae* and Achilles tendon
– *Summary* –

GM, GL and SOL muscles present large differences in their features (e.g. architecture, fibre-type composition). These differences lead to an **imbalance of force-generating capacities**. The three distal tendons of GM, GL and SOL muscles merge to create the Achilles tendon, the biggest and strongest tendon in the human body. GM, GL and SOL subtendons exhibit **specific features** (e.g. length, CSA), **different behaviour** (e.g. strain), and are arranged in a **twisted configuration**, with large variations in the amount of twist between individuals. Even though there is no experimental approach to identify each subtendon within the free Achilles tendon *in vivo*, some works provided evidence of **non-uniform distribution of stress** and heterogeneous fascicle motions within the Achilles tendon. Animal experimentations demonstrated that the majority of force produced by GL or SOL was transmitted via their own subtendons respectively, but that the subtendons are not fully independent. Overall, there is evidence that **force distribution among GM, GL and SOL muscles** affects the distribution of load within the Achilles tendon.

Part 3

Achilles tendinopathy

1. Epidemiology and aetiology of Achilles tendinopathy

1.1. Definition and incidence of Achilles tendinopathy

Tendinopathy is a tendon disorder defined as localised pain during activities that load the tendon. As such, Achilles tendinopathy is associated with lower exercise tolerance, impaired function and reduced quality of life (Ceravolo et al., 2018; Cook and Purdam, 2008; Maffulli et al., 2004; Magnusson et al., 2010). Lifetime incidences are 5.9 % and 23.9 % for non-athletes and athletes respectively (Kujala et al., 2005). Moreover, among athletes, runners are most subjected to Achilles tendinopathy, with a life time incidence of 52 % for middle and long distance runners (Table 2; Kujala et al., 2005).

Table 2: epidemiological studies for Achilles tendinopathy occurrence among general and athletic population. *Extracted and modified from O'Neill (2016).*

	Population	Measure of occurrence		References
People who practice sport	Runners	57 %	Lifetime prevalence	O'Neill (2016)
	Athletes (distance runners)	52 %	Lifetime incidence	Kujala et al. (2005)
	Athletes mixed sports	24 %	Lifetime incidence	Kujala et al. (2005)
	Military recruit	7 %	Year incidence	Milgrom et al. (2003)
	Badminton players	17 %	Prevalence	Linde et al. (1996)
	Orienteers	12 %	Year incidence	Marti et al. (1988)
	Runners	2.1 %	Year incidence	Fahlström et al. (2002)
	Elite orienteers	14 %	Year incidence	Johansson (1986)
People who do not	General population	< 1 %	Year incidence	Albers et al. (2016)
	General population	< 1 %	Year incidence	de Jonge et al. (2011)
	Healthy non athletes	6 %	Lifetime incidence	Kujala et al. (2005)

1.2. Risk factors

The cause of Achilles tendinopathy is multifactorial. A large number of factors have been associated with risk of Achilles tendinopathy, with varying degrees of evidence for the association (Jarvinen et al., 2005; Maffulli et al., 2019; Maffulli et al., 2004; Maffulli et al., 2003; van der Vlist et al., 2019; Zhao et al., 2019). A Delphi study of active clinical researchers published in 2016, reached expert consensus on risk factors for Achilles tendinopathy (O'Neill et al., 2016). According to this study, intrinsic risk factors for Achilles tendinopathy are: previous lower limb tendinopathy, recent injury (any tissue), advancing age, gender, muscle power/strength and endurance, steroid exposure, reduced ankle dorsiflexion, weight, antibiotic treatment, foot pronation, obesity, foot alignment, diabetes. Of note, the involvement of *plantaris* muscle in Achilles tendinopathy development has been suggested for some people (Masci et al., 2016). Extrinsic risk factors for Achilles tendinopathy are: changes in loading (for example, return from off season), training errors (e.g. ramping up in training duration, frequency or intensity), footwear, training surface (O'Neill et al., 2016). The same study proposed a split in risk factors depending on patient profiles, i.e. whether individuals are sedentary or active (O'Neill et al., 2016). Active individuals may be more influenced by extrinsic factors such as load errors (for example, sudden increase in training level). Sedentary individuals may be more influenced by intrinsic factors. As the current work focused on the biomechanical aspect of overloading, conclusions of this work are more likely to concern the clinical group of active individuals.

An important aspect of risk factor analysis is to provide some direction in our understanding of aetiology of Achilles tendinopathy. Risk factors are characteristics of individuals, their environment and lifestyle that are associated with a higher probability to develop the pathology. However, risk factors do not *explain* pathogenesis and the mechanisms of Achilles tendinopathy development are still unclear.

1.3. Tendinopathy models

In the last years, we have used many different terminologies (e.g. tendinitis, tendinosis) to describe tendon pain, reflecting the evolution of our understanding of the pathology (Rees et al., 2014; Scott et al., 2015; Scott et al., 2019). Tendinopathy is the latest term recommended to describe tendon problems, because of its non-etiologic specificity (Khan et al., 2002;

Maffulli et al., 1998; Maffulli et al., 2003). It is known that the end-stage of tendinopathy is degenerative, but there is debate about how tendon changes from normal to degenerative (Cook and Screen, 2018). The exact role of inflammation is not clear, but there is growing evidence to support its presence at particular times of the disease progression (D'Addona et al., 2017; Dakin et al., 2018; Dean et al., 2016; Millar et al., 2017; Mosca et al., 2018). Other hypotheses argue for the role of direct mechanical tissue damage and cell driven tissue response (Cook and Screen, 2018). Different theories have been proposed to describe tendon pathogenesis [e.g. mechanical theory, cell matrix theory, over and under stimulation theory, inflammation theory, reviewed in (Ahmad et al., 2019)]. The most accepted theoretical model is the "continuum model" where excessive loading causes a loss of tissue homeostasis and triggers tendon pathology (Cook and Purdam, 2008; Cook et al., 2016). The first stage is "reactive" and is the primary cell response to excessive load. If the pathology persists because tendon loading is not adjusted, it leads to the "early disrepair", and then to the "degenerative" stage (Figure 26). *In vivo* human research confirmed a net degradation in collagen after loading (as further described in section 1.4 below, see Figure 28; Magnusson et al., 2010; Miller et al., 2005), supporting these mechanical models.

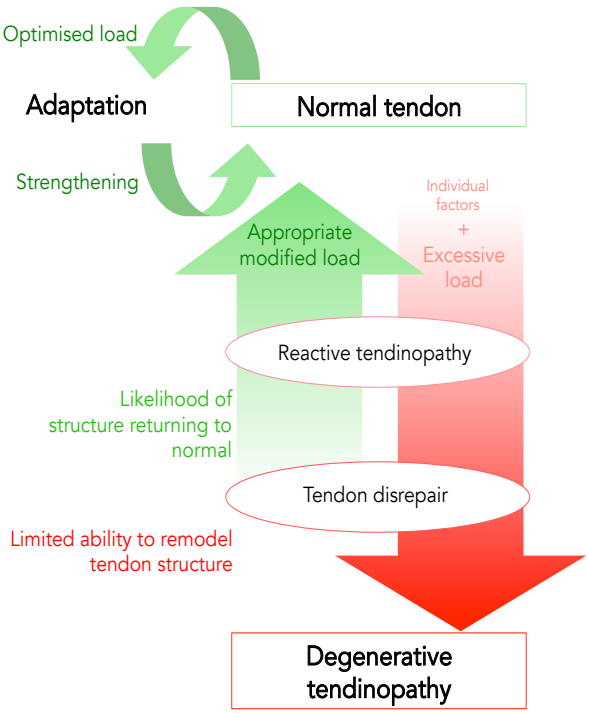

Figure 26. Continuum model of tendinopathy. *This model embraces the transition from normal to degenerative tendinopathy and highlights the potential for reversibility early in the continuum. Reversibility is unlikely in the degenerative late stage. From Cook and Purdam (2008); Cook et al. (2016).*

1.4. Response of the tendon to load in tendinopathy

Tendons are structures that respond to load (Lavagnino et al., 2015). When a tendon is loaded, the resident cells respond to the mechanical stimuli with tendon remodelling. This phenomenon, called mechanotransduction, is the conversion of the mechanical signal into a cellular response (Sharir and Zelzer, 2011). The cells that launch the response to load are situated in the interfascicular matrix. The interfascicular matrix contains a mixture of particular proteoglycans and glycoproteins (Thorpe et al., 2013). The collagenous fibers of tendons lay within the interfascicular matrix (Figure 27). Tendons are made of type I collagen (mainly) that provide the main tensile strength (Benjamin et al., 2008; Thorpe et al., 2016b; Thorpe and Screen, 2016). The tendon response to load engages a reaction balanced between degradation and production of collagen (Figure 28; Magnusson et al., 2010). Over the first 24 to 36h post exercise, there is a net loss of collagen. This is followed by a net synthesis 36 to 72h after exercise. Excessive loading triggers tendinopathy in the *continuum* theory. This causes a fail in balance between damage and repair, resulting in a net degradation of the matrix (Figure 28, panel B). Excessive loading can be due to repeated training with rest periods that are too short, or sudden increase in training load (i.e. combination of both volume and intensity).

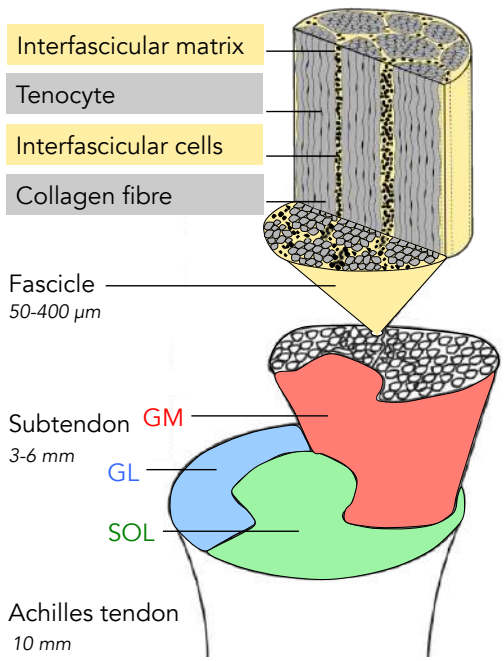

Figure 27. Schematic section of tendon histology. *Each Achilles subtendon is composed of several fascicles. Fascicles (diameter: 50-400 µm) are made of collagen fibres (diameter: 1-20 µm). The interfascicular matrix surrounds fascicles. GM, gastrocnemius medialis; GL, gastrocnemius lateralis; SOL, soleus. From Handsfield et al. (2016); Spiesz et al. (2015).*

In the case of the Achilles tendon, there is a compartmentalisation of three different subtendons. It is possible that GM, GL and SOL subtendons are exposed to different amounts of load, and in turn, that responses to load are different between subtendons. Non-uniform stress has frequently been described as an etiological factor in Achilles tendinopathy (Arndt et al., 1998).

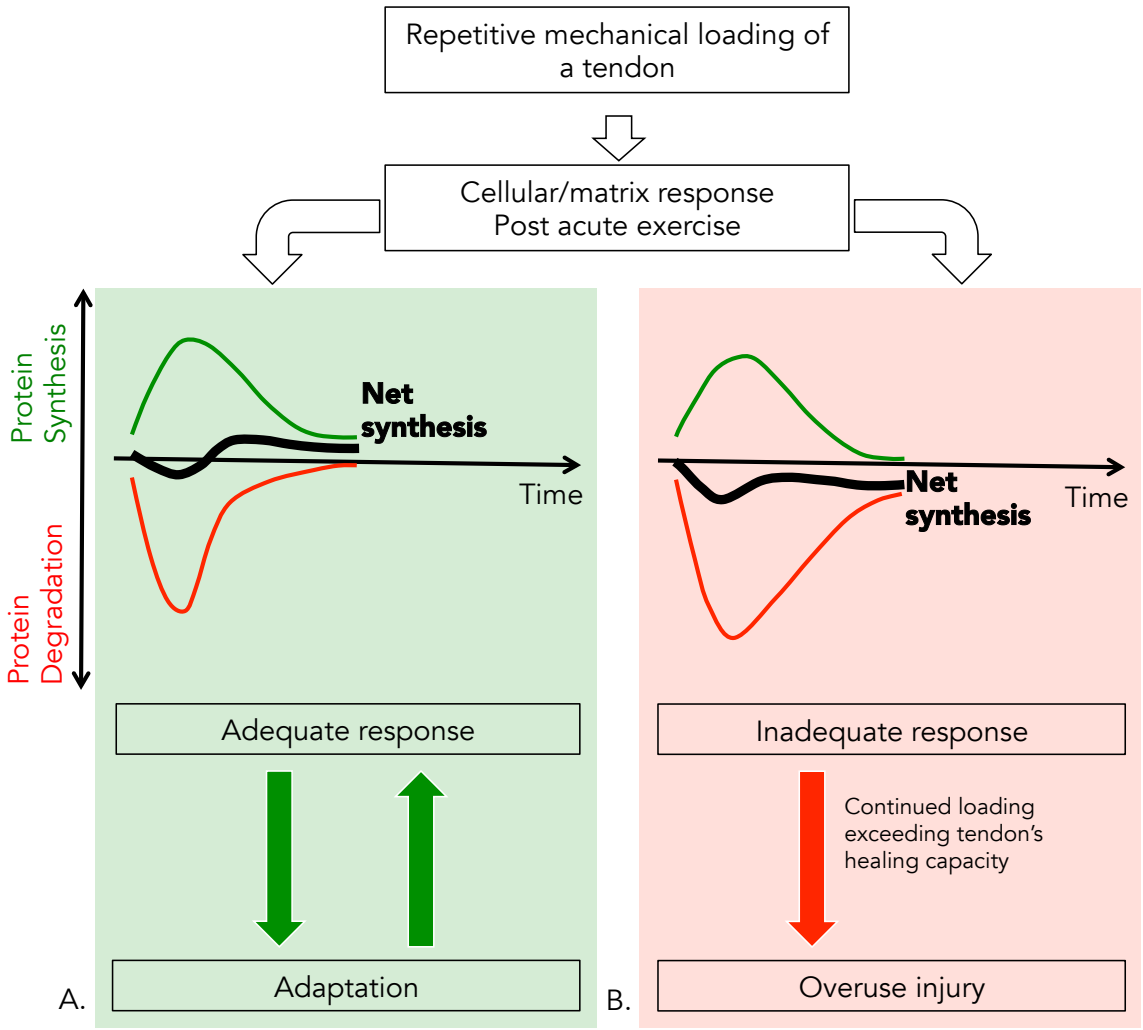

Figure 28. Tendon response to load post exercise. *Panel A: acute exercise is followed by an increase in both the synthesis and degradation of collagen. There is a positive net collagen synthesis in the long term (~ 36 to 72h). Panel B: possible explanation for pathogenesis of tendinopathy. Load is excessive, and the cellular and matrix responses are not sufficient to provide a positive net synthesis of collagen and proteins. Over time, tendon weakens, triggering tendinopathy. Adapted from Arnoczky et al. (2007); Magnusson et al. (2010).*

1.5. Anatomy and behaviour of the Achilles tendon

The anatomical compartmentalisation of the three subtendons creates the possibility for non-uniform load distribution. Depending on the force they are subjected to and their CSA, each subtendon could be subjected to a different stress. It was shown that both over-stimulation and under-stimulation of tendon cells reduce collagen synthesis (Arnoczky et al., 2007; Dideriksen et al., 2017). This underlines the importance of load distribution throughout a tendon cross-section. For a specific amount of *triceps surae* force, the sharing of stress between GM, GL and SOL subtendons potentially impacts each subtendon response and collagen synthesis. Take, for example, the hypothetical scenario where, GM, GL and SOL subtendons would each support a stress (force/CSA) of one third of the global stress. The amount of *triceps surae* force being fixed, an increase of stress in one subtendon (for example, GM subtendon supports half the stress) would ultimately result in the decrease in stress in the others (for example, SOL subtendon still supports one third, then GL supports one sixth). Both the over-stimulation of GM subtendon and the under-stimulation of GL subtendon would lead to a reduction of collagen synthesis. In other words, changes in force distribution would potentially have a doubled negative impact.

If GM, GL and SOL subtendons were subjected to different stresses, this could impact both the distribution of subtendons' strain, and the sliding motions between subtendons. This is because subtendon strains depend on the stress each subtendon is subjected to. However, each subtendon mechanical properties (e.g. stiffness) and their degree of interaction also impact subtendon strains. It is thought that shear forces between tendon fascicles lead to fascicles damage (Arndt et al., 1998). As explained previously, there is no experimental approach to investigate individual subtendon stress *in vivo*, but it is possible to investigate separate subtendon strains by tracking their respective myotendinous junction with ultrasonography. Individual subtendon strains have been described in healthy people during isometric submaximal contractions (described previously in Part 2, Section 2.3.2). Briefly, strain of SOL subtendon is higher than strain of *gastrocnemii* subtendons during isometric contractions ~ 50 and 70% of MVC (Farris et al., 2013; Obst et al., 2016), but non-consistent results are reported when comparing strains of GM and GL subtendons. To our knowledge, no studies have measured the three subtendons strains in populations with Achilles tendinopathy, but two studies measured GM subtendon strain during maximal isometric contractions (Arya and

Kulig, 2010; Child et al., 2010). They both reported a significantly higher strain for people with Achilles tendinopathy (5.1 %) than controls (4.4 %), while plantarflexion torques were similar between groups [data from Arya and Kulig (2010)]. Without information on GL and SOL subtendons, these results do not give insights into the difference in the distribution of tendon strain between populations. Using speckle tracking, a recent study measured differences of displacement between superficial and deep layers of the Achilles tendon in people with Achilles tendinopathy (Couppe et al., 2020). They reported that tendinopathic tendons presented lower displacements between layers, compared to the contralateral (asymptomatic) leg, during dynamic heel raise (Couppe et al., 2020). These data suggest that the presence of tendinopathy diminishes intratendinous sliding in the Achilles tendon. Yet, because subtendons cannot be distinguished on such images, it is not known if some (and which) subtendons displacements are more impacted.

Non-optimal distribution of load and/or the amount of sliding between subtendons have been hypothesized to contribute to the development of Achilles tendinopathy (Bojsen-Moller and Magnusson, 2015; Sun et al., 2015). Several works have suggested that the distribution of stress or strain within the Achilles tendon depends on the distribution of force among the heads of the *triceps surae* (see Part 2, Section 3). This suggests that the distribution of muscle force may be involved in the development of Achilles tendinopathy, as depicted on Figure 29 (Arndt et al., 2012; Bojsen-Moller and Magnusson, 2015; Hug and Tucker, 2017). To our knowledge, investigation of muscle force-sharing strategies in Achilles tendinopathy has never been conducted.

Although the pathology aetiology is unclear, many treatment options have been proposed. All treatments do not have similar success rate. There are high discrepancies between people in terms of response to treatment (Ceravolo et al., 2018), and heterogeneities in Achilles tendinopathy recovery are unexplained.

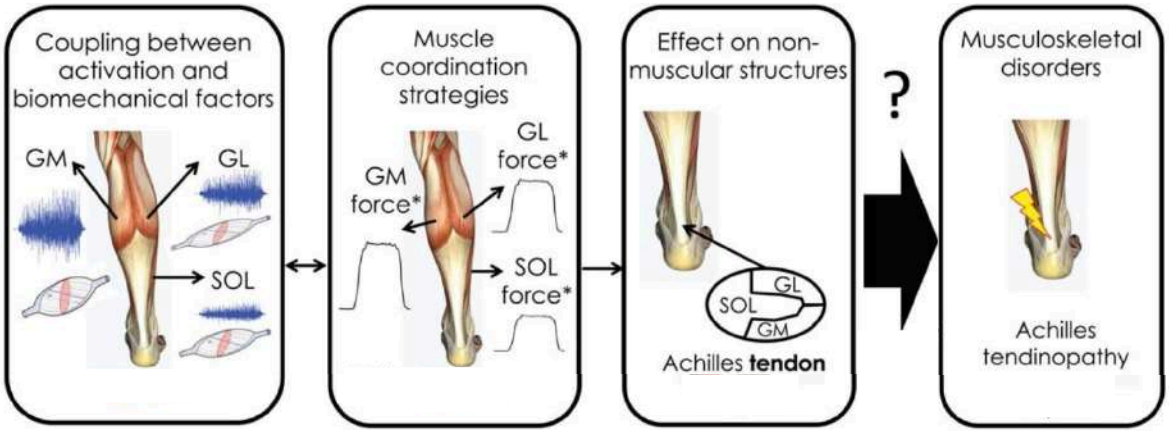

Figure 29. The pivotal role of particular *triceps surae* coordination strategies in the development of Achilles tendinopathy. *Gastrocnemius medialis (GM), gastrocnemius lateralis (GL) and soleus (SOL) each produce a certain amount of force. The distribution of force affects the distribution of Achilles tendon load, which could relate to Achilles tendinopathy. From Hug and Tucker (2017).*

2. Diagnosis and management of Achilles tendinopathy

2.1. Clinical evaluation and diagnosis

The diagnosis of Achilles tendinopathy is essentially clinical (Cardoso et al., 2019; Maffulli et al., 2019). The diagnosis usually involves subjective reported symptoms, palpation and clinical tests (Feilmeier, 2017; Hutchison et al., 2013). Achilles tendinopathy is classically sub-divided into two main categories, according to anatomical location. They include insertional (or enthesopathy) and non-insertional (or mid-portion) Achilles tendinopathy (Maffulli et al., 2019). The mid-portion Achilles tendinopathy describes symptoms from 2 to 6 cm above the *calcaneum* insertion, whereas Achilles enthesopathy classically denotes symptoms at the insertion on the calcaneus. Mid-portion Achilles tendinopathy seems to be the most frequent (66% of Achilles tendinopathy; Paavola et al., 2000).

Histological tendon impairments can happen independently of pain and dysfunction (Bley and Abid, 2015; Docking et al., 2015). There is a complex interplay between tendon structure, tendon function and pain (Cook et al., 2016; Rio et al., 2014). For example, 11 % to 46 % of people with asymptomatic Achilles tendons, present with abnormal tendon structure (such as thickening, hypo or hyperechogenicity) as identified with ultrasound (Kudron et al., 2019;

Lieberthal et al., 2019). For these reasons, diagnosis of Achilles tendinopathy is based on history and detailed clinical examination, and imaging is not recommended (Scott et al., 2013). Of note, tendon structural abnormalities on ultrasound images are predictive of future tendinopathy with a 3 to 4-fold increased risk (Docking et al., 2019; McAuliffe et al., 2017). This means that "*abnormal*" tendon structure may be regarded as a risk factor for tendinopathy (Cook and Purdam, 2008). When imaging a symptomatic tendon, three histological changes can be observed: tendon thickening, hypoechogenicity and/or neovascularization (Figure 30). These structural changes depend on the stage of tendinopathy. The increase of water content and proteoglycans generates the increase in tendon dimension (Docking et al., 2015). The loss of parallel-aligned fibres, leading to collagen fibrillar disorganisation, generates hypoechogenecity on ultrasound in a transversal view (Docking et al., 2015). Finally, the site of new vascularisation, which is visible on Doppler ultrasonography (Figure 30), usually correlates with the site of clinically determined pain (Divani et al., 2010).

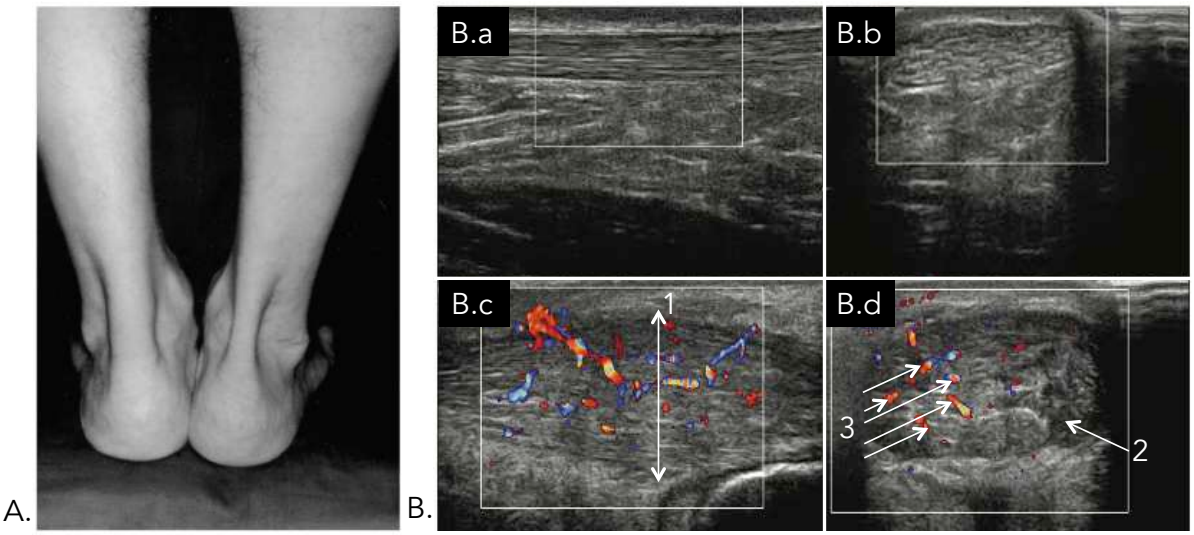

Figure 30. Achilles tendinopathy clinical aspect and ultrasound imaging. *Panel A: picture of patient's ankles from a posterior view. The left Achilles tendon presents a pronounced swelling. From Maffulli et al. (2004). Panel B: ultrasound image of Achilles tendons with color Doppler. Longitudinal (B.a) and transverse (B.b) images of an asymptomatic tendon. Tendon shows normal echo texture with no Doppler signal. Longitudinal (B.c) and transverse (B.d) images of a symptomatic Achilles tendon show significant thickening of the tendon (arrow 1), the presence of hypoechoic areas (arrow 2), and significant Doppler signal (arrows 3). From Docking et al. (2015).*

2.2. Conventional treatment, symptoms persistence and recovery

Conservative management, the first line of treatment for Achilles tendinopathies, has been well studied and described (Rowe et al., 2012). The most common modalities used are exercise-based treatment (load management), non-steroid anti-inflammatory drugs, injections and shock wave therapy (Egger and Berkowitz, 2017). Guidelines for conventional treatment have been summarized by the *Orthopaedic Section of the American Physical Therapy Association* (Martin et al., 2018b). Among the many interventions available, exercise-based programs (load management) have the strongest evidence of clinical effectiveness, and show the best long-term outcome for recovery (Ahmad et al., 2019; Martin et al., 2018b). Initially, exercise programs were mainly driven by protocols involving eccentric contraction models with well described dosage (e.g. 3 sets x 15 repetitions, 2 times daily for 12 weeks; Alfredson et al., 1998). Recently, the relevance of standalone eccentric treatment has been questioned, as it appeared that isometric or isokinetic contractions, heavy loads, heavy slow resistance, and others, could also improve pain and/or function for tendinopathy (Beyer et al., 2015; Murphy et al., 2018b; Rio et al., 2015). Additionally, current evidence supports the use of pain monitoring models to manage symptoms, instead of a single specific loading program (Sancho et al., 2019). This provides evidence that the amount of load applied on the tendon is highly important in the rehabilitation program.

To evaluate Achilles tendinopathy severity, the VISA-A (Victorian Institute of Sports Assessment for Achilles tendon) is the only questionnaire that has been validated (Murphy et al., 2018a; Robinson et al., 2001). The VISA-A consists of eight questions that measure the domains of pain, function in daily living and sporting activity, and gives a numerical result that is reliable (Robinson et al., 2001). Often, the assessment of Achilles tendinopathy recovery is inferred from the result of the VISA-A. However, the evaluation of recovery can also account for different criteria, such as symptoms or pain resolution alone, muscular strength, ankle range of motion, return to sport, or change of sport. Due to these heterogeneities and the fact that treatments delivered may differ between studies, proportions of patients recovering from Achilles tendinopathy must be interpreted cautiously. These numbers range widely. For example, a recent review mentioned long-term outcomes to be "poor" [with 24 to 45.5 % of unsuccessful conservative treatment (Maffulli et al., 2019)], or "excellent" [for 63 % of a cohort of 77 participants (Johannsen et al., 2018)]. In this last study (Johannsen et al., 2018), it is important to note that among the patients who were back to the

pre-injury activity level, approximately half of them had changed their sports. Given this, it is not possible to determine if the rehabilitation was successful *in a full return to sport*. When conservative treatment fails after 6 months, surgery is often considered (Maffulli et al., 2019), and is conducted in about 16 % of cases (Johannsen et al., 2018). Surgery is a procedure that involves some risks, and as such its legitimacy for the treatment of tendinopathy has been questioned recently (Millar et al., 2019).

More broadly, musculoskeletal pains are associated with lower health related quality of life scores (Taylor, 2005). For Achilles tendinopathy, symptoms can last for years (de Jonge et al., 2010). Sometimes, we manage to improve pain and symptoms, but often mild-pain remains (van der Plas et al., 2012). Persistent Achilles tendinopathy is associated with a significant psychosocial impact (Mc Auliffe et al., 2017). Some individuals describe profound impacts on their quality of life, in particular those who tie their identity and social activities to physical activity (Ceravolo et al., 2018).

Achilles tendinopathy
– *Summary* –

Tendinopathy is a disorder leading to pain during activities that load the tendon. As such, **Achilles tendinopathy** is associated with lower exercise tolerance, impaired function and reduced quality of life. Lifetime incidence of Achilles tendinopathy is 6 % and 24 % for non-athletes and athletes respectively, and **reaches 52 % for middle and long distance runners**. The amount of tendon load directly impacts tendon homeostasis, the capacity for the tendon to repair and adapt to mechanical constraint. In the anatomical configuration of the Achilles tendon, the three subtendons are compartmentalized, and there is still uncertainty on how force is distributed between the three subtendons. GM, GL and SOL subtendons could be exposed to different amount of load, hence differently affected by the overall load. **Non-optimal distribution** of load and/or the amount of **sliding motion between subtendons** have been hypothesized to contribute to the development of **Achilles tendinopathy**. Several works suggested that the non-uniform distribution of load or strain within the Achilles tendon is mainly determined by the **distribution of force among the heads of the *triceps surae***. Thus, distribution of muscle force might be involved in the development of Achilles tendinopathy, but this remains to be tested. The specific mechanical effect of *triceps surae* coordination could make some people more at risk of developing Achilles tendinopathy.

Aims and hypotheses

The overall aim of this thesis was to provide a deeper understanding of the role of muscle coordination on the development of Achilles tendinopathy. To this end, we used an approach that combines neurophysiological (muscle activation) and biomechanical measures (muscle volume and architecture) to estimate muscle coordination.

The **aim of the first study** was three-fold: (*i*) to test the between-day reliability of the distribution of activation between synergist muscles, (*ii*) to determine the robustness of these activation strategies between tasks, and (*iii*) to describe the inter-individual variability of activation strategies in a large sample size. To address these aims, we considered muscle activation strategies as the distribution of normalised EMG amplitude among synergist muscles within two muscle groups from the lower limb (*quadriceps* and *triceps surae* muscle groups). We tested the between-day reliability and described the activation strategies that were recorded during well-controlled isometric tasks, and then compared the activation strategies used during isometric tasks to those used during gait and submaximal pedalling. We hypothesized that activation strategies are (*i*) reliable between days, (*ii*) correlated between tasks, and (*iii*) highly variable between individuals.

The **aim of the second study** was to determine the relationship between the ratio of muscle activation measured during an isometric submaximal plantarflexion task and the ratio of muscle maximal force-generating capacity between the three heads of the *triceps surae*. The comparison of GM and GL provided insight into the distribution of activation for two muscles with similar actions (plantarflexors and knee extensors), and very different force-generating capacities. The comparison of SOL with *gastrocnemii* investigated the distribution of activation for muscles with different functions. We hypothesized that a positive correlation between GM/Gas activation and GM/Gas PCSA would exist, demonstrating a coupling between the distribution of activation and the distribution of force-generating capacity among *gastrocnemii*, but not for muscles with different functions (SOL and *gastrocnemii*). We further described the **inter-individual variability in force distribution** among the *triceps surae*, and hypothesized that variability between individual would be large.

The **aim of the third study** was to determine whether the distribution of force between the heads of the *triceps surae* differs in people with Achilles tendinopathy compared with controls. We further aimed to determine the effect of force distribution on GM, GL and SOL subtendon strain, within the Achilles tendon. Finally, we aimed to determine whether particular force-sharing strategies in people with Achilles tendinopathy were associated with recovery of symptoms over a six months follow-up period. We hypothesized that people with Achilles tendinopathy would exhibit a different force distribution between the heads of the *triceps surae* during submaximal isometric tasks.

MATERIAL AND METHODS

1. Summary of data collection and participants characteristics

All studies (#1, #2, #3) used dynamometry and surface EMG to investigate joint torque and muscle activation, respectively. Walking and cycling tasks have been investigated in study #1. For studies #2 and #3, the combination of architectural parameters, i.e. muscle volume, fascicle length and pennation angle, and surface EMG measurements was used to estimate an index of individual muscle force. In study #3, we also investigated Achilles subtendon displacement and strain using ultrasonography measures. All studies (#1, #2, #3) focused on the *triceps surae* muscle group. In addition, in study #1, the *quadriceps* muscle group was also investigated. Data from 147 participants (126 healthy and 21 with Achilles tendinopathy) are included across the three studies included in this thesis (Table 3). The local ethics committee approved the experimental procedures (Rennes Ouest V – CPP MIP-010) and all procedures adhered to the declaration of Helsinki.

2. Dynamometry measures and daily-living tasks

All studies (#1, #2, #3) required the measurement of ankle and knee joint torques. Participants were positioned on a dynamometer for these measures (Con-Trex, CMV AG, Dübendorf, Switzerland). In study #1, participants performed both isometric knee extension and plantarflexion tasks. For both tasks the hip was flexed at 80° (0° being hip fully extended). For knee extension task, the knee angle was set at 110° (180° being knee fully extended), and for plantarflexion tasks, the ankle was at 90° (i.e. foot perpendicular to the shank). In studies #2 and #3, participants only performed plantarflexion tasks, lying prone with their hip and knee fully extended, and the ankle angle set at 90°. This position was chosen to facilitate ultrasonography investigations planned for study #3. For studies #1 and #2, measurements were performed on the dominant side (the one used to kick a ball). For study #3, measurements were performed on the affected side for people with Achilles tendinopathy. In the control group, side was chosen in order to match with dominance of the tested side of their paired-Achilles tendinopathy participant.

Table 3. Characteristics of participants for the different studies, and data collected on the different protocols. *A total of 147 participants were included. The first two studies (#1 and #2) investigated muscle coordination in healthy population. Activation coordination strategies among quadriceps and triceps surae were investigated in study #1, force coordination strategies among triceps surae were investigated in study #2. Study #3 investigated force coordination strategies in people with Achilles tendinopathy. ♀: female, ♂: male.*

	Study #1	Study #2	Study #3
Participants number *First session* *Second session*	 85 62	 20 20	 42 -
Groups	All healthy	All healthy	21 AT & 21 healthy
Sex	30 ♀, 55 ♂	10 ♀, 10 ♂	6 ♀, 36 ♂
Age (years)	24 ± 5	26 ± 6	36 ± 8
Weight (kg)	67 ± 10	64 ± 12	72 ± 10
Height (cm)	175 ± 10	173 ± 11	177 ± 8
Data Collected	**Isometric tasks** Joint torque Muscle activation **Cycling** Muscle activation **Gait** Muscle activation	**Isometric tasks** Joint torque Muscle activation **Architecture** Muscle volume Fascicle length Pennation angle	**Isometric tasks** Joint torque Muscle activation **Architecture** Muscle volume Fascicle length Pennation angle **Tendon behaviour** Subtendons strain and elongation

2.1. Warm-up and familiarization with isometric tasks

Participants were first familiarized with the task(s) to be performed. This consisted of explanations of the required task, and then a series of submaximal isokinetic and isometric contractions. Then, participants performed a warm-up of approximately 20 isokinetic concentric contractions at 60 °.s^{-1}, with a progressive increase in contraction intensity. For isometric knee extensions, the torso was secured with two seatbelts and the shank was strapped to the dynamometer device. For plantarflexion tasks, foot immobilisation on the dynamometer was more challenging, due to the ankle joint conformation. To secure the foot,

we first applied a large rigid self-adhesive strap (6 cm wide), across the anterior surface of the ankle from one malleolus to the other, and the forefoot at the level of the toes. A piece of thin foam was then placed on the anterior surface of the foot/ankle, and a rigid band was strapped around the ankle and locked behind the pedal of the dynamometer, with a ratchet tensioner. The tightness was regulated depending on the participant's feedback in order to strap the ankle as securely as possible, without inducing any pain. Such precautions were taken in order to minimize ankle rotation during contractions, especially during MVC (Karamanidis et al., 2005). The small ankle joint rotation, which inevitably occurred was monitored and taken into account in the analysis (described in details in Section 5, below).

2.2. Maximal voluntary contraction

For between-muscle and between-participant comparisons, it was crucial to normalise the EMG values measured during the submaximal tasks to those measured during MVC. For this normalisation procedure to be correct, it is critical that participants activate their muscles fully during a MVC. In studies where indices of force were calculated (#2 and #3), the twitch interpolation technique was used to estimate the voluntary activation level of participants during their MVCs. A constant current stimulator (DS7AH; Digitimer, UK) delivered a doublet electrical stimulus (interstimulus interval: 10 ms; duration: 1 ms; amplitude: 400 V) to the tibial nerve during MVCs. For this stimulation, a self-adhesive cathode (50 mm diameter) was placed on the skin that lay directly over the tibial nerve, in the popliteal fossa, and the anode (80 x 130 mm) was placed on the skin over the anterior tibialis tuberosity. While the participants were at rest, the output current was increased incrementally (from 10 mA, with incremental steps of 10 mA) until a maximum plantarflexion twitch torque was reached despite an increase in current intensity. Then, an intensity of 120 % of this previous value was used for the rest of the protocol (Neyroud et al., 2014). The supramaximal doublet stimulus was delivered during the plateau of the MVC, and within 5 s in the subsequent rest period to elicit superimposed and resting twitches, respectively. Depending on the study, the design was slightly different, but participants performed between 4 (study #3) and 5 (study #2) MVCs, while two out of them were performed with the superimposed electrical electrostimulation. Participants were informed about the deliverance of the electrical stimulation prior each concerned contraction. Between each MVC, participants rested for approximately 120 s. The percentage of voluntary activation was measured from the torque signal according to the equation of Todd et al. (2004) for study #2:

$$Voluntary\ activation = \left(1 - \frac{Superimposed\ twitch}{Resting\ twitch}\right) \times 100$$

Equation (7)

For study #3, the percentage of voluntary activation was calculated as previously described by Strojnik and Komi (1998). With this approach, a correction factor is applied to account for the case where the superimposed twitch is delivered slightly after the maximal voluntary torque. The voluntary activation calculation follows the similar equation, except that the *Superimposed twitch* is calculated as:

$$Superimposed\ twitch = \frac{Superimposed\ twich \times Voluntary\ torque\ just\ before\ the\ superimposed\ doublet}{Maximal\ voluntary\ torque}$$

Equation (8)

2.3. Submaximal isometric contraction

Submaximal tasks were conducted using a visual feedback of the torque that displayed on a monitor in front of the participants. The submaximal tasks involved matching a target torque at either 20 % (study #2 and #3), 25 % (study #1) or 40 % (study #2 and #3) of MVC torque during short (about 8 s) isometric contractions, or ramped contractions from 0 to 70 % of MVC (study #2) during 10 s.

2.4. Walking and cycling

For study #1, participants walked on a treadmill (Cardiotread, Cardioline, Trento, Italy) at 0.83 $m.s^{-1}$. Participants walked barefoot and were given time to familiarize with the task (5 min at least). A force-sensitive resistor (FSR; FSR151AS) was taped under the heel of the dominant leg to detect foot contact, i.e. the onset of the stance phase. These signals were recorded on the same acquisition system as used for EMG, such that the foot pressure and the EMG data were synchronized.

The pedalling task was performed on an electronically braked cycloergometer (Excalibur Sport; Lode, Groningen, The Netherlands) equipped with standard cranks (170 mm) and clipless pedals. The saddle height was standardized to the height of the greater trochanter of each participant while they stood. Participants were instructed to maintain a seated position

throughout the task. After familiarization with the cycloergometer, participants were asked to pedal at 150 W at 80 rpm for 1 min. A Transistor–Transistor Logic pulse indicated the top dead center of the right pedal (highest position of the pedal) and was recorded on the EMG acquisition system, such that the crank position and the EMG data were synchronized.

3. Measure of muscle activation with surface electromyography

Myoelectrical activity was collected via surface EMG from VL, VM, and *rectus femoris* (study #1) and GM, GL, and SOL (studies #1, #2 and #3). As explained previously (see the literature review, Part 1, Section 1.1.2), surface EMG provides an estimation of *muscle* activation. Before applying the electrodes, the skin was shaved, and gently rubbed then cleaned with alcohol to minimize the skin-electrode impedance and facilitate electrode fixation. For study #1 and #2, a pair of surface Ag/AgCl electrodes (diameter of the recording area: 5 mm; Kendall Medi- Trace^{TM}, Canada) was attached to the skin with a ~ 20 mm inter-electrode distance (centre to centre). For study #3, wireless surface electrodes were attached to the skin with double-sided tape (Trigno Flex; Delsys, Boston, MA). For all studies (#1, #2, #3), electrode location was checked with a B-mode ultrasound (v11.0, Aixplorer, Supersonic Imagine, Aix-en-Provence, France) to ensure that the electrodes were positioned away from the borders of the neighbouring muscles and were aligned with fascicle direction. For *gastrocnemii*, the electrodes were placed on the middle line of the muscle belly, and two-thirds distal. For SOL, the electrode was placed below GL myotendinous junctions (studies #1 and #2). In study #3, an additional medial electrode for SOL was placed below GM myotendinous junction such that the two portions (medial and lateral) of the posterior parts of SOL were recorded. These electrode positions were selected to enable us to compare the medial and lateral parts of SOL activations during the tasks. They revealed no difference in activation level and data were averaged for all subsequent analyses.

For studies #1 and #2, EMG signals were pre-amplified close to the electrodes and digitized at 1000 Hz using an EMG amplifier unit (ME6000, Mega Electronics Ltd, Finland). For study #3, wireless electrodes were used, for which EMG signals were band-pass filtered (10–850 Hz) and digitized at a sampling rate of 2000 Hz (Trigno; Delsys). In all studies (#1, #2 and #3), EMG data were recorded on the same acquisition system that was used for the torque signal (Labchart V8; ADInstruments). The EMG amplitude measured during submaximal tasks was normalised to that measured during the MVCs. Throughout this work, we

calculated ratios of activation to quantify the distribution of activation among muscle groups. Ratios were calculated as the normalised activation of one muscle divided by the summed activations of the muscles involved (i.e. VL, VM, and *rectus femoris* for *quadriceps* - GM, GL and SOL for *triceps surae*). Because we were also interested in *vastii* and *gastrocnemii* distribution, the activation ratios of VL over *vastii* (VL/*Vastii*) and GM over *gastrocnemii* (GM/Gas) were also calculated.

4. Muscle volume and architecture

The volume and architecture of GM, GL and SOL muscles were investigated in studies #2 and #3 and used to estimate an index of force. Fascicle length and pennation angle (muscle architecture) were quantified with panoramic ultrasound for GM and GL and with classic ultrasound B-mode images for SOL. Muscle volume was estimated using either MRI (study #2) or 3D ultrasound (study #3).

4.1. Estimation of muscle architecture with ultrasonography

For fascicle length and pennation angle measurements, participants were placed in the same position as for experimental tasks, i.e. lying prone, hip and knee fully extended, and the ankle maintained at 90°. The panoramic mode was used with an ultrasound scanner (Aixplorer v11.0, Supersonic Imagine, France) coupled with a 50 mm linear probe (4–15 MHz; SuperLinear 15-4, Vermon, Tours, France).

Fascicles of *gastrocnemii* are too long to be captured fully in the classical probe width. As explained in the literature review (Part 1, Section 1.2.1), the advantage of the extended field of view over classical measurements from one B-mode image is that it does not require extrapolating the non-visible part of the fascicle, thus providing a more accurate estimation of muscle fascicle length (Noorkoiv et al., 2010). To verify the accuracy of the *in-built* panoramic mode, we performed a pilot study on a bovine sample of muscle (approximately 30×10×5cm). Four needles were inserted through the meat sample. The needle extremities remained visible outside the meat, and a retro-reflective marker (diameter: 10 mm) was attached to each needle extremity (a total of eight markers). The inter-needle distances were determined using an optoelectronic motion capture system composed of four cameras (Flex 13, Optitrack, Natural Point, USA). The inter-needle distances (from midline to midline) were 4.32, 4.85 and 6.75 cm; and the straight distance between first and fourth needle was 15.16

cm. Three US panoramic scans were performed; the reliability of the inter-needle distance measured during these three trials was *excellent* (for all distances, CV < 1.3 %). The three trials were averaged, and then compared to the distances measured using the motion capture system, to test the accuracy of the measurement. The absolute error percentage was lower than 2.2 %. For the acquisitions on participants of studies #2 and #3, the proximal and distal insertions and the medial and lateral borders of the GM and GL were located using B-mode ultrasound. A line was drawn on the skin at the middle of the muscle belly from the distal to the proximal insertion following the fascicle path. The ultrasound probe was then placed on the line and oriented within the plane of the fascicles. The scan consisted of moving the probe along this line with minimal pressure applied to the skin, to minimize compression of the muscle. Two (study #2) to three (study #3) reconstructed panoramic images were recorded per *gastrocnemii* (Figure 31).

For SOL, classical ultrasound B-mode images were wide enough to capture entire fascicles (Figure 31). To assess fascicle length and pennation angle, the ultrasound probe was placed slightly below the GL myotendinous junction (study #2) or below both GL and GM myotendinous junctions (study #3). Probe locations were chosen so that fascicles were clearly visible. The study #3 hence assessed the two posterior parts of SOL (medial and lateral) individually and revealed no difference in fascicle length and pennation angle. This is in line with a recent study investigating the 3D architecture of the whole SOL muscle, which reported no difference in fascicle length and pennation angle between the medial and lateral compartments (Bolsterlee et al., 2018). Of note, Bolsterlee et al. (2018) also reported no difference of fascicle length between the posterior and anterior compartments, but the pennation angle was larger in the posterior than the anterior compartments (+ 12° in average).

For each ultrasound image, we aimed to measure three fascicles (proximal, mid distance and distal) leading to a total of up to six (study #2) to nine (study #3) fascicles per muscle. As some fascicles exhibited a small curvature, we used a segmented line with a spline fit to model the fascicles. Data of study #2 were analysed with ImageJ (V1.48, National Institutes of Health, Bethesda, MD, USA) and data of study #3 were analysed with MATLAB (The Mathworks, Natick, MA). Fascicles and aponeuroses were visually identified and tracked. Fascicles were drawn over the path of fascicle fragments or in the same directions of surrounding fragments. The pennation angle was calculated as the angle between the fascicles and the deep aponeurosis of the muscle (study #2), or the average of this angle with both deep

and superficial aponeurosis (study #3). Values were then averaged across fascicles within a muscle to obtain a representative fascicle length and pennation angle.

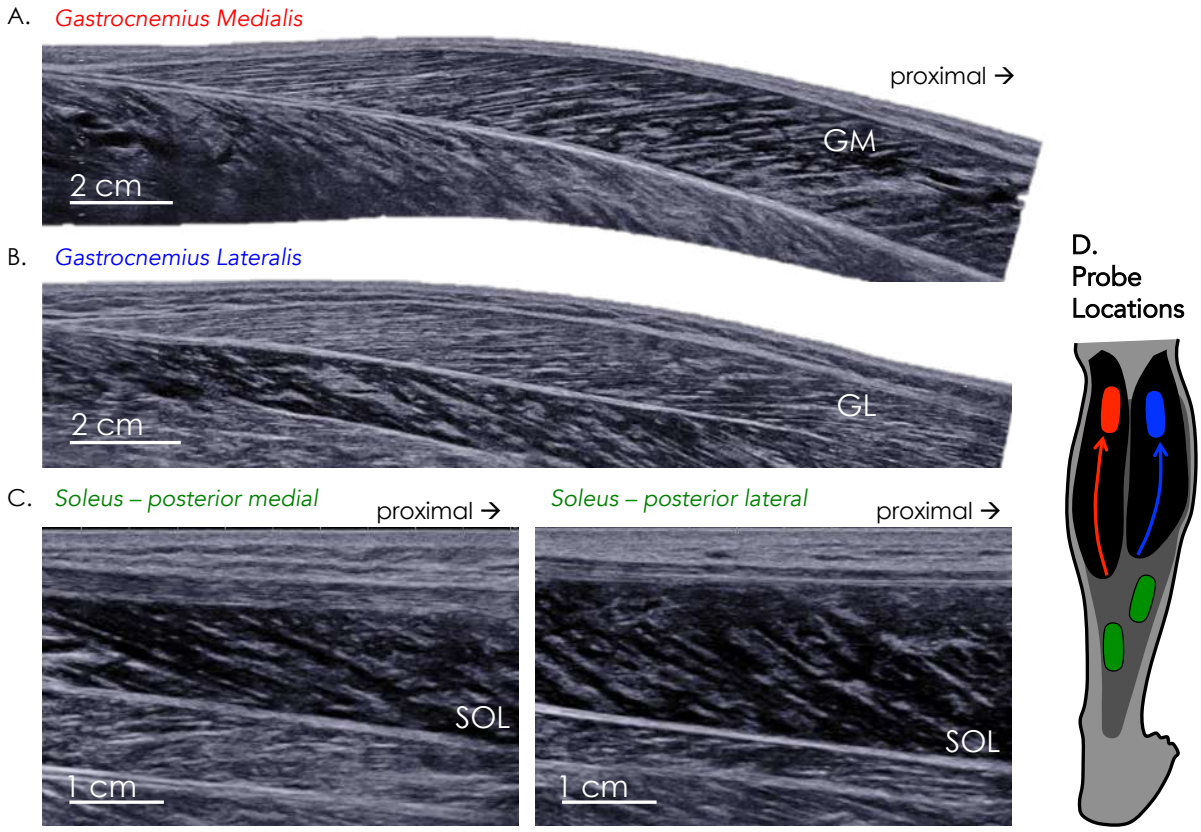

Figure 31. Typical examples of ultrasound images used to calculate fascicle length and pennation angle for *gastrocnemius medialis* (panel A), *gastrocnemius lateralis* (panel B) and *soleus* (panel C). *Note the two locations for the SOL measure: medial (panel C. left) and lateral (panel C. right). The different probe locations are drawn on the panel D.*

4.2. Measure of muscle volume with Magnetic Resonance Imaging

For study #2, volumetric acquisitions of the lower leg (from heel to mid-thigh) were performed using a 3T magnetic resonance imaging scanner (Ingenia, Phillips, The Netherlands) and a three-dimensional e-THRIVE sequence (repetition time: 6.0 ms, echo time: 3.0 ms, field of view: 400×400×199.5 mm, voxel size: 0.70×0.70×3.00 mm, flip angle: 10 deg). Slice thickness was 6 mm without an inter-slice gap. This sequence was chosen to enhance the separation between muscles. Participants were lying in supine position, with their hip and knee fully extended, and the foot held perpendicular to the shank. Magnetic resonance

images were analysed using 3D image analysis software (Mimics, Materialize, Belgium). GM, GL and SOL were segmented manually on each slice, from the distal slice, where the SOL could first be visualized to the most proximal slice, where the GM and GL insertions were visible. As GL and SOL were fused in some slices within the proximal region, we used the visible landmarks on the preceding and subsequent images to assist the segmentation between muscles. Volume of each muscle was calculated by selecting the optimal smoothing option in Mimics. Because of the difficulty to access MRI, an alternative method has been used to measure muscles volumes in study #3.

4.3. Measure of muscle volume with freehand 3D ultrasonography

For study #3, volume of GM, GL, and SOL were estimated using freehand 3-dimensional ultrasound (method detailed in the literature review, Part 1, Section1.2.1). Specifically, multiple 2D ultrasound images of the muscles were combined with 3D motion of the ultrasound probe to reconstruct the muscle in 3D, through the use of Stradwin software (v5.4; Mechanical Engineering, Cambridge University, UK). B-mode ultrasound images (9.5 cm depth) were recorded using a 40-mm linear probe (2–10 MHz; Aixplorer; Supersonic Imagine, Aix-en-Provence, France). Position and orientation of the probe were recorded by using a six-camera optical motion analysis system (Optitrack, Natural Point, USA) to track a rigid cluster of four markers attached to the probe. For this assessment, participants were prone, with the lower leg in a water bath, with the knee angle at 135° and the ankle angle at 90°. The water bath was custom-designed (Figure 32), so that it was possible to image the whole leg (from Achilles insertion on the heel until proximal *gastrocnemii* insertion over the knee) with minimal probe inclination and tissue compression. This is because probe inclination led to artefacts in 3D reconstruction and pressure alters the quality of the scan and reconstruction as well (Barber et al., 2009; Prager et al., 2002). Four to six parallel sweeps were performed, from the knee to the ankle, at a low speed (approximately 15 s per sweep). A gating threshold of 5 mm was set in Stradwin software, which ensured that B-mode images were recorded at least every time that the US probe has moved by 5 mm.

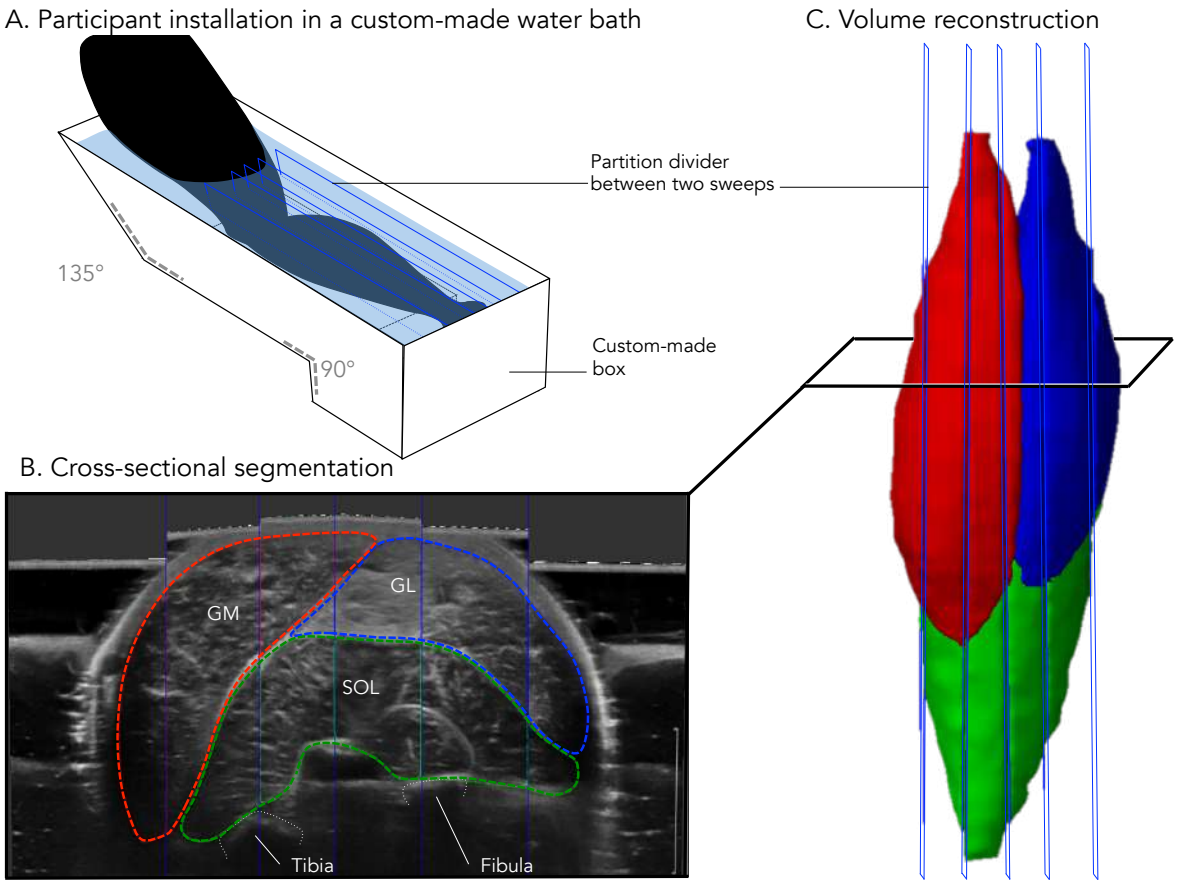

Figure 32. Three-dimension reconstruction of *triceps surae* measured with the freehand 3D ultrasound technique. *Panel A: participants were prone with their leg in a custom-made water bath, with knee and ankle at approximately 135° and 90°, respectively. Panel B: each muscle was segmented manually from the axial slices. The axial slice depicted in this figure is from 33 % of the proximodistal part of the leg. Panel C: 3D-reconstruction of the segmented gastrocnemius medialis (GM, red), gastrocnemius lateralis (GL, blue) and soleus (SOL, green).*

GM, GL, and SOL were segmented manually ~ every 5 slice by the same examiner as for study #2. A second examiner processed the data in order to assess the inter-observer reliability. Similarly to the analysis of MRI images, some anatomical landmarks were identified to keep the delimitation consistent between participants. The most challenging muscle was the SOL, as image quality reduces at greater depths with in the image (Figure 33, panel A). Usually, delimitation started from the distal slice where its half-moon shape could be easily visualized. While moving proximally, the vessel group anterior to its anterior border was used as a landmark. Volume was estimated for each *triceps surae* head using the volume algorithms provided by the Stradwin software (Treece et al., 1999).

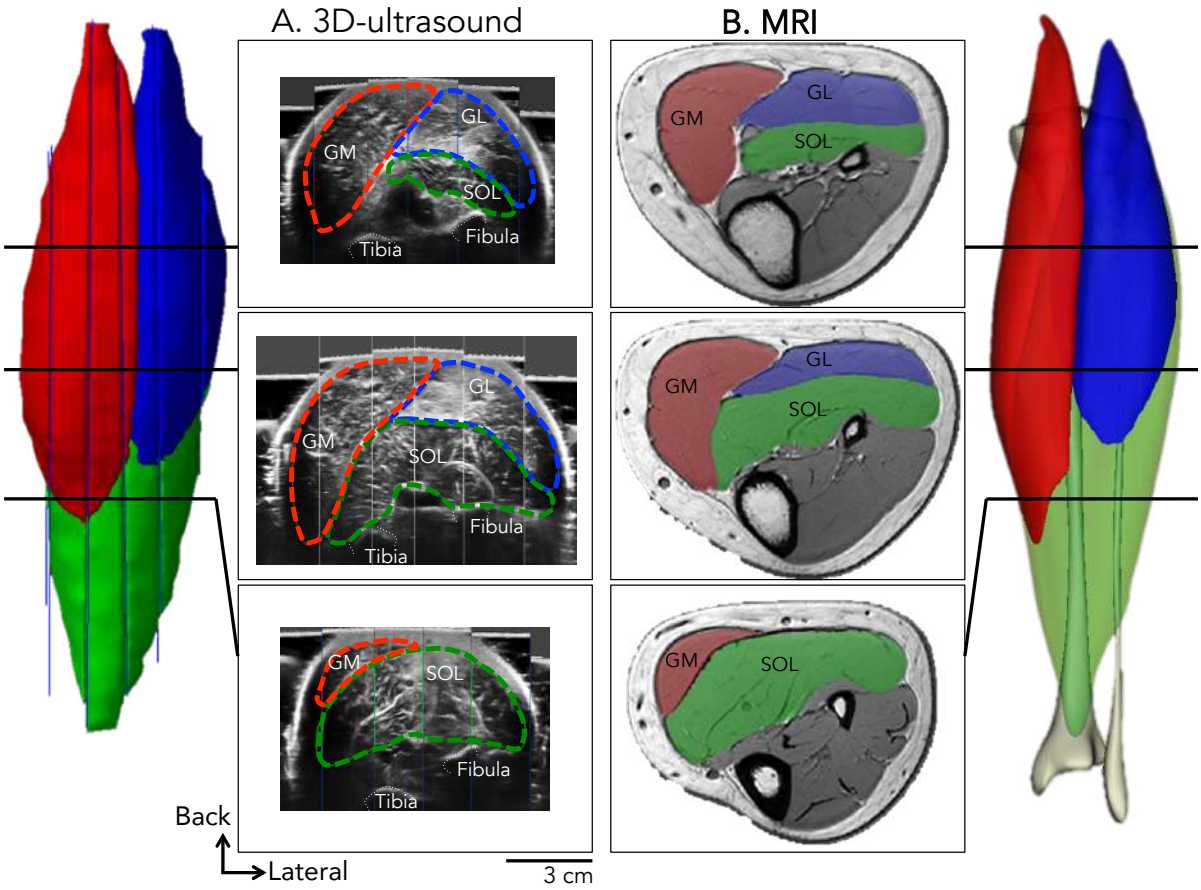

Figure 33. *Triceps surae* volume collected with 3D ultrasound (panel A) and MRI (panel B) on two different participants. *Volume reconstruction of each technique is drawn on the lateral sides. Cross-sectional areas have been extracted at approximately 25, 50 and 75 % of leg length. Note the different aspect of the leg shape: participants were lying front (panel A) and supine (panel B). Cross-sectional areas in panel B have been flipped vertically in order to align views between the two techniques. GM, gastrocnemius medialis; GL, gastrocnemius lateralis; SOL, soleus.*

4.4. Calculation of muscle Physiological Cross-Sectional Area

Muscle PCSAs were calculated by dividing muscle volume by fascicle length (study #3). For study #2, we considered muscle functional PCSAs, which include the cosine of pennation angle (see the literature review, Part 1, Section 1.2.1.a). We calculated ratios of PCSA to quantify the distribution of PCSA among the *triceps surae* group. Ratios were calculated as the PCSA of one muscle divided by the summed PCSA of the *triceps surae* muscles (GM, GL

and SOL). Because we were also interested in *gastrocnemii* distribution, the PCSA ratio of GM (study #2) and GL (study #3) over *gastrocnemii* was also calculated.

5. Tendon behaviour

Myotendinous junctions tracking of GM, GL and SOL were conducted in study #3 during isometric submaximal contractions at 20 and 40 % of MVC. The GM and GL myotendinous junctions were defined as the intersection of the superficial and deep aponeurosis, forming an easily identifiable acute angle (Figure 34). For SOL, the myotendinous junction was defined as the most distal point at which muscle fibers were inserted onto the Achilles tendon (free tendon), as identified within the curved shape of the distal SOL (Figure 34). To account for possible movement of the ultrasound probe during acquisitions, a thin piece of tape was attached to the skin to represent a fixed reference landmark on the B-mode images. Change in each subtendon length was estimated from each myotendinous junction displacement. And each subtendon strain was calculated from each subtendon length change during isometric submaximal contractions, divided by initial subtendon length. The initial tendon length was measured at rest, before contraction, in the same joint configuration than for isometric contractions. Of note, this strain calculation is global and does not provide information about localised regions of strain within the tendon. It is likely that strain is not homogeneously distributed throughout the tendon (Zelik and Franz, 2017).

For this technique to be valid it is important to account for the inevitable ankle rotation that occurs during active isometric plantarflexion tasks (Karamanidis et al., 2005). A small joint rotation (heel lift) during contraction inherently results in an overestimation of the myotendinous junction displacement, as the muscle-tendon unit logically decreases in length (Figure 35). To account for the effect of this joint rotation, the ankle angle was measured and a correction factor was calculated for each participant. To this end, each participant first underwent passive ankle rotations from 2° of dorsiflexion to 15° of plantarflexion (in average), at 1 °/s. During these ankle rotations, ankle angle and myotendinous junction displacements were determined (Figure 35). Of note, EMG was used to check for the absence of muscle activation during these passive plantarflexion motion (Bojsen-Moller et al., 2010).

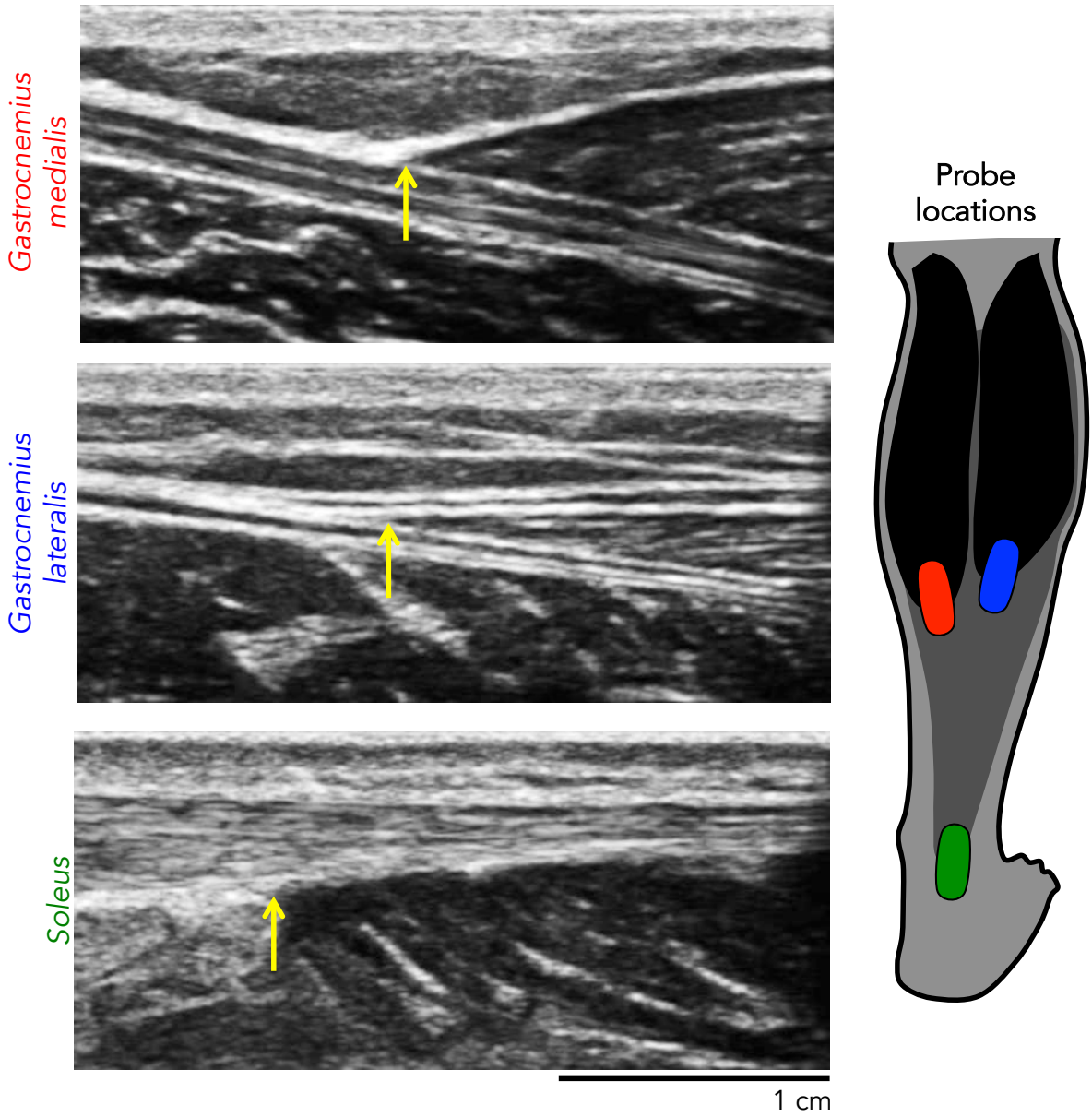

Figure 34. Identification of myotendinous junctions of *gastrocnemius medialis* (top panel), *gastrocnemius lateralis* (middle panel) and *soleus* (bottom panel). *The yellow arrow indicates where were myotendinous junctions determined for each muscle. The right panel shows the probe position for gastrocnemius medialis (red), gastrocnemius lateralis (blue) and soleus (green) myotendinous junction tracking. Images are data extracted from study #3, during submaximal contractions at 40 % of MVC.*

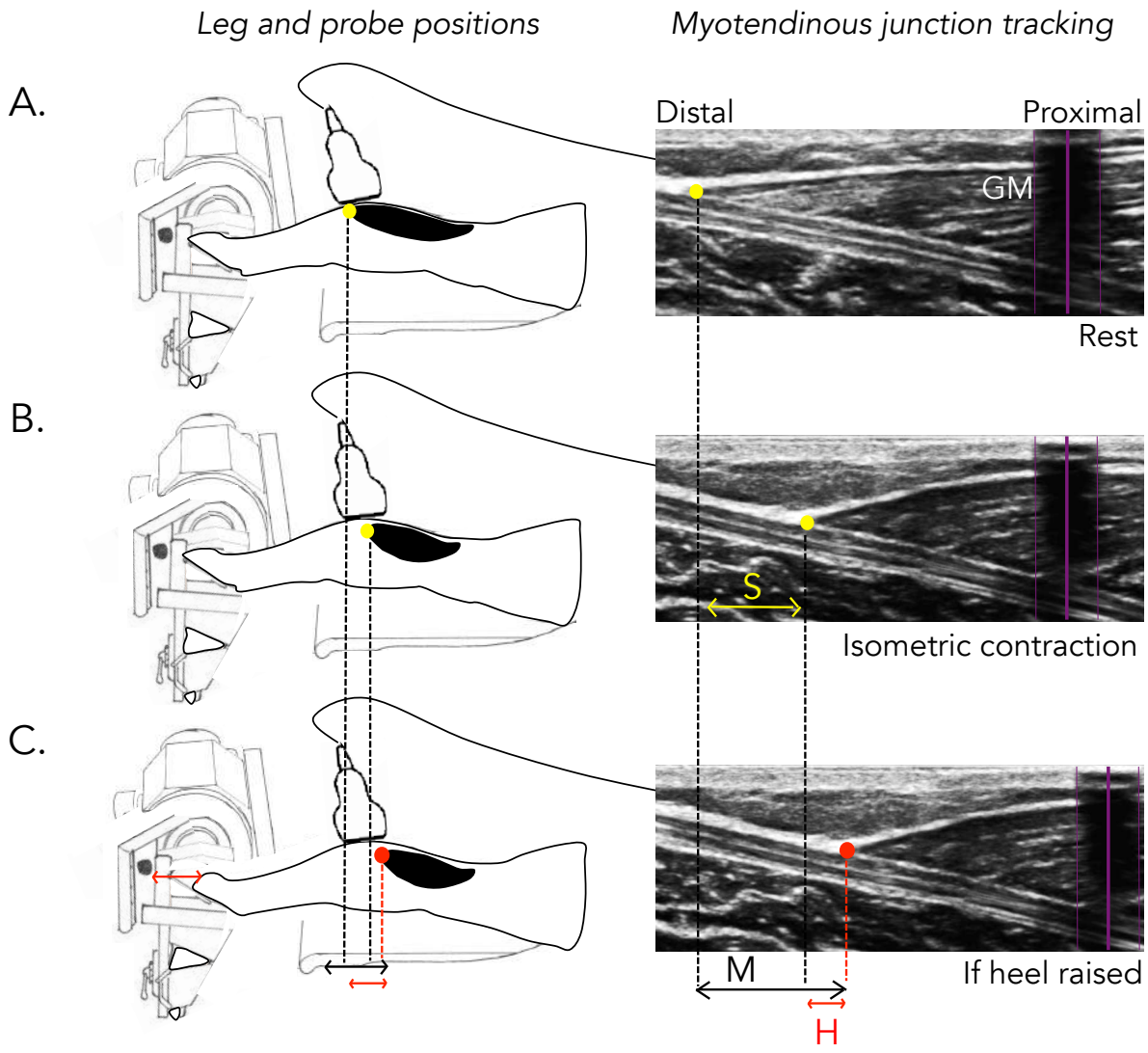

Figure 35. Myotendinous junction tracking from rest (panel A) to isometric submaximal contraction (panel B). *The displacement measured (M) depends on the real displacement due to the muscle shortening S, and also on the displacement due to heel lift (H). The panel C depicts the additional displacement H when the heel has lift during the isometric contraction. H was called the correction factor, and was subtracted to the measured displacement M.*

The longitudinal displacement of the myotendinous junction was tracked manually using a custom-made Matlab script on every five frames (Figure 36). The relationship between ankle angle and myotendinous displacement assessed during passive motions was fitted with a third order polynomial fit. To correct for the displacement of the myotendinous junction due to the ankle rotation that occurred during isometric contractions, the displacement associated with

this change in ankle angle was first identified from the relationship between ankle angle and myotendinous junction displacement assessed during passive motion, and then subtracted from the raw displacement.

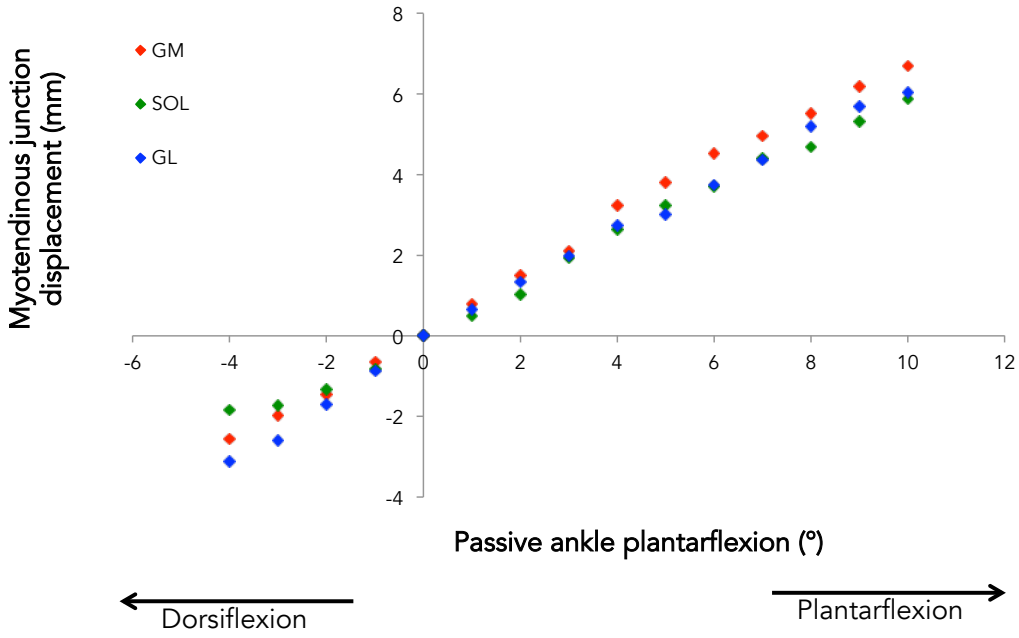

Figure 36. Individual example of the relationship between myotendinous junction displacement of each head of the *triceps surae* and ankle joint angle, during passive stretching on the dynamometer. *For this participant (#12), the range of motion was set from 4° of dorsiflexion until 10° of plantarflexion. At the maximum plantarflexion angle (10°), gastrocnemius medialis (GM), gastrocnemius lateralis (GL) and soleus (SOL) moytendinous junctions moved proximally of 6.7, 6.0 and 5.9 mm respectively, 0 being the position of the myotendinous junction when the ankle is at a right angle (foot perpendicular to the shank). Positive values correspond to plantarflexion; negative values correspond to dorsiflexion.*

6. Force index calculation

6.a. Estimation of individual muscle force

Our experimental approach to estimate the distribution of force among individual muscles relies on a simplified formulation of the well-established Hill-type muscle model (Zajac, 1989). This model predicts muscle force as a function of activation, PCSA, pennation angle, force-length and force-velocity properties. In the absence of non-invasive experimental technique to assess the force-length and force-velocity relationship of individual muscles, we

focused on isometric tasks during which the difference in force produced by synergist muscles is mainly determined by factors other than contraction velocity. Then, the ability for a muscle to produce isometric force directly relates to its length (i.e. the force-length relationship) and therefore the joint angles over which the isometric contraction is performed. In these studies, we chose joint angles to place each of the tested muscles at a ~ similar length relative to their optimal length. As explained in the literature review (Part 1, Session 1.2.2.a), human GM and SOL muscle length-tension curves have been indirectly estimated from torques and fascicle length measures (Hoffman et al., 2012; Maganaris, 2001). These studies reported an optimal angle at approximately 15° of dorsiflexion for the SOL (Maganaris, 2001) and at 19° of dorsiflexion for the GM (with knee extended at 175°; Hoffman et al., 2012). Therefore, we can assume that at an ankle angle of 90° (foot perpendicular to the shank), both GM and the SOL operate in the ascending limb of their force–length relationship. Here, we assumed that GL and GM would also operate optimally at a similar relative length, due to their close anatomy (Szaro et al., 2009), architecture (Maganaris et al., 1998), composition (Johnson et al., 1973), and similar ascending part of their force-length relationships (Maganaris, 2003). As such, we considered that at an ankle angle of 90°, the difference of force production between muscles was minimally affected by difference in length relative to their optimal length. We considered that the difference of force between GM, GL and SOL primarily depended on their activation and functional PCSA. We considered the following index of force F_m for individual muscles:

$$F_m = PCSA \times Act$$

Equation (9)

Where F_m is the muscle force in arbitrary unit (u.a), PCSA is the functional PCSA (i.e. it accounts for pennation angle; in cm^2), and Act is the muscle activation (normalised to the maximum, in %). Note that in study #2, the index of force F_m was multiplied by the specific tension (P_0) of slow fibre type (12 $N.cm^{-2}$; Maganaris et al., 2001) in order to have a dimension of the force index that corresponds to Newtons. Given the size principle of orderly recruitment (Henneman and Oslon, 1965; Henneman et al., 1965), it is likely that small motor units were preferentially recruited below 40 % of MVC. As each head of the *triceps surae* has more than 40 % slow fibres (50.8, 46.8 and 87.7% for GM, GL and SOL, respectively; Johnson et al., 1973), we reasonably assumed that mainly slow fibres were active during the

investigated tasks (submaximal contractions at 20 and 40 % of MVC). Of note, as indices of each muscle were multiplied by the same coefficient (i.e. 12), this did not affect statistical outcome, either for individual force indices nor ratios. Finally, to quantify the distribution of force among the group, muscle contributions were calculated using ratios of force indices. Throughout this work, ratios were calculated as the force index of one muscle divided by the summed force indices of *triceps surae* (GM, GL and SOL). Because we were also interested among *gastrocnemii* distribution, a force ratio of GM (study #2) or GL (study #3) over *gastrocnemii* was also calculated.

Many factors contribute to muscle force. Currently, we have tools to investigate some of these factors, but many of them are not easy, or impossible to measure at the level of individual muscles (e.g. specific tension, force-length relationship). We overcome these limitations by experimental design, where unknown factors play minimal roles. Results and interpretations of this doctoral research are limited to isometric contractions, but are thought to add a great deal to the literature.

PhD EXPERIMENTATIONS

STUDY 1

Do individual differences in the distribution of activation between synergist muscles reflect individual strategies?

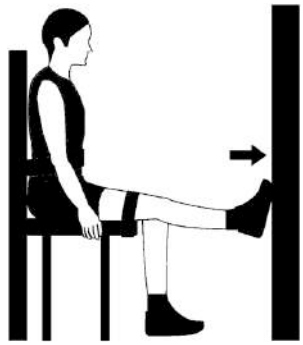

Associated publication:

Crouzier, M., Hug, F., Dorel, S., Deschamps, T., Tucker, K., Lacourpaille, L. (2018).
Do individual differences in the distribution of activation between synergist muscles reflect individual strategies?
Experimental Brain Research, 223 (7): 625 – 635.

ABSTRACT

Individual differences in the distribution of activation between synergist muscles have been reported during a wide variety of tasks. Whether these differences represent actual individual strategies is unknown. The aims of this study were to: (*i*) test the between-day reliability of the distribution of activation between synergist muscles, (*ii*) to determine the robustness of these strategies between tasks, and to (*iii*) describe the inter-individual variability of activation strategies in a large sample size. Eighty-five volunteers performed a series of single-joint isometric tasks with their dominant leg (knee extension and plantarflexion) and locomotor tasks (pedalling and walking). Of these participants, 62 performed a second experimental session that included the isometric tasks. Myoelectrical activity of six lower limb muscles (the three superficial heads of the *quadriceps* and the three heads of the *triceps surae*) was measured using surface EMG and normalised to that measured during MVC. When considering isometric contractions, distribution of normalised EMG amplitude among synergist muscles, considered here as activation strategies, was highly variable between individuals (15.8 % < CV < 42.7 %) and robust across days (0.57 < ICC < 0.82). In addition, individual strategies observed during simple single-joint tasks were correlated with those observed during locomotor tasks [0.37 < r < 0.76 for *quadriceps* (n = 83); 0.30 < r < 0.66 for *triceps surae* (n = 82); all $p < 0.001$]. Our results provide evidence that people who bias their activation to a particular muscle do so during multiple tasks, and that variability results from actual differences in activation strategies.

Key words

Electromyography, Muscle coordination, Pedalling, Gait

Experimental Brain Research
https://doi.org/10.1007/s00221-018-5445-6

RESEARCH ARTICLE

Do individual differences in the distribution of activation between synergist muscles reflect individual strategies?

Marion Crouzier[1] · François Hug[1,2,4] · Sylvain Dorel[1] · Thibault Deschamps[1] · Kylie Tucker[2,3] · Lilian Lacourpaille[1]

Received: 16 May 2018 / Accepted: 24 November 2018

Abstract

Individual differences in the distribution of activation between synergist muscles have been reported during a wide variety of tasks. Whether these differences represent actual individual strategies is unknown. The aims of this study were to: (i) test the between-day reliability of the distribution of activation between synergist muscles, (ii) to determine the robustness of these strategies between tasks, and to (iii) describe the inter-individual variability of activation strategies in a large sample size. Eighty-five volunteers performed a series of single-joint isometric tasks with their dominant leg [knee extension and plantarflexion at 25% of maximal voluntary contraction (MVC)] and locomotor tasks (pedalling and walking). Of these participants, 62 performed a second experimental session that included the isometric tasks. Myoelectrical activity of six lower limb muscles (the three superficial heads of the quadriceps and the three heads of the triceps surae) was measured using surface electromyography (EMG) and normalized to that measured during MVC. When considering isometric contractions, distribution of normalized EMG amplitude among synergist muscles, considered here as activation strategies, was highly variable between individuals ($15.8\% < CV < 42.7\%$) and robust across days ($0.57 < ICC < 0.82$). In addition, individual strategies observed during simple single-joint tasks were correlated with those observed during locomotor tasks [$0.37 < r < 0.76$ for quadriceps ($n = 83$); $0.30 < r < 0.66$ for triceps surae ($n = 82$); all $P < 0.001$]. Our results provide evidence that people who bias their activation to a particular muscle do so during multiple tasks. Even though inter-individual variability of EMG signals has been well described, it is often considered noise which complicates the interpretation of data. This study provides evidence that variability results from actual differences in activation strategies.

Keywords Electromyography · Muscle coordination · Pedalling · Gait

Introduction

Human movement results from the coordination of multiple muscles. Given the redundant nature of our motor control system (Valero-Cuevas et al. 2015), even simplest tasks can be achieved by different muscle activation strategies. This leads to the assumption that each individual uses their own unique coordination strategy (Hug and Tucker 2017).

Surface electromyography (EMG) remains the most common technique used to provide insight into muscle activation strategies. Inter-individual variability of EMG signals has been observed during a wide variety of tasks, from multi-joint tasks [e.g., gait (Ahn et al. 2011; Ivanenko et al. 2002; Winter and Yack 1987); pedalling (De Marchis et al. 2013; Hug et al. 2010)] to simple isometric single-joint tasks [e.g., plantarflexion (Masood et al. 2014) and knee extension (Hug et al. 2015)]. For example, the distribution of activation between the lateral (GL) and medial (GM) head of the gastrocnemius during gait varied greatly between individuals, with seven out of the ten participants activating their GM more than their GL, and the other three participants activating their GM and GL nearly equally (Ahn et al. 2011). Such large individual

✉ Lilian Lacourpaille
lilian.lacourpaille@univ-nantes.fr

1 Faculty of Sport Sciences, Laboratory "Movement, Interactions, Performance" (EA 4334), University of Nantes, 25 bis boulevard Guy Mollet, 44300 Nantes, France

2 School of Health and Rehabilitation Sciences, NHMRC Centre of Clinical Research Excellence in Spinal Pain, Injury and Health, The University of Queensland, Brisbane, Australia

3 School of Biomedical Sciences, The University of Queensland, Brisbane, Australia

4 Institut Universitaire de France (IUF), Paris, France

differences have also been observed during more controlled tasks, such as isometric knee extensions where the number of participants using greater activation of the lateral head of the quadriceps (VL) being almost equal to those using greater activation of the medial head (VM) (Hug et al. 2015). It is important to understand the origin of such inter-individual variability, and the mechanical impact of individual patterns on the soft tissues and joint structures (Alessandro et al. 2018). However, we believe that a necessary first step is to provide evidence that these individual differences in activation reflect the existence of actual individual strategies rather than random variability.

To confidently interpret these inter-individual differences as evidence of individual muscle activation strategies, it is necessary to address the following considerations. First, individual differences in activation strategy should persist over time. Second, they should be robust between tasks. Third, these differences should be reported on a large sample size, previous experiments being typically conducted with fewer than 20–25 participants [12 and 22 healthy controls in Masood et al. (2014) and Hug et al. (2015), respectively].

With these considerations in mind, the aims of this study were: (i) to test the between-day reliability of the distribution of activation between synergist muscles, (ii) to determine the robustness of these strategies between tasks, and (iii) to describe the inter-individual variability of activation strategies in a large sample size. To address these aims, we considered muscle activation strategies as the distribution of normalized EMG amplitude among synergist muscles within two muscle groups from the lower limb (quadriceps and triceps surae muscle groups). We tested the between-day reliability and described activation strategies measured during well-controlled isometric tasks, and compared the activation strategies used during isometric tasks to those used during gait and submaximal pedalling.

Methods

Participants

Eighty-five healthy volunteers (55 males and 30 females; Table 1) participated in this study. Participants had no history of lower leg pain that had limited function within the 2 months prior to testing. All participants were between 18 and 43 years. The ethics committee "CPP Ouest V" approved the study (n°CPP-MIP-010) and all procedures adhered to the Declaration of Helsinki. Participants provided informed written consent. Each participant completed the International Physical Activity Questionnaire [IPAQ; evaluation tool of physical activity (Craig et al. 2003)].

Table 1 Demographic and anthropometric data for the tested population

	Males ($n=55$)	Females ($n=30$)
Age	24.3 ± 5.3	23.4 ± 5.4
Height (cm)	179.9 ± 6.9	165.2 ± 5.6
Body mass (kg)	72.2 ± 7.8	57.0 ± 5.8
MVC knee extension torque (Nm)	282.2 ± 65.0	188.9 ± 36.9
MVC plantarflexion torque (Nm)	161.2 ± 27.8	123.0 ± 18.1
Physical activity (MET-min/week)	5568 ± 4874	4387 ± 2618
Left footed	8 (14.5%)	7 (23.3%)

Maximal Voluntary Contraction (MVC) torque was measured during isometric contractions. Physical activity was estimated using the International Physical Activity Questionnaire (IPAQ; Craig et al. 2003)

Experimental design

The experimental session consisted in a series of single-joint isometric tasks performed with the dominant leg [knee extension and plantarflexion at 25% of maximal voluntary contraction (MVC)] and multi-joint submaximal tasks (pedalling at 150 Watts and walking on a treadmill at 0.83 m/s). These tasks were performed in a randomized order. From the 85 participants, 62 participated in a second experimental session 11 ± 12 days (range 1–58 days) after the first session. This second session included both the submaximal knee extension and plantarflexion tasks and data were used to assess the between-day reliability of the activation strategies during well-controlled tasks. A series of maximal isometric tasks was performed at the beginning of each session for normalization of the surface EMG signal and for determination of the target torque for the submaximal isometric tasks.

Myoelectrical activity

Myoelectrical activity was collected using surface EMG from two muscle groups of the dominant leg: rectus femoris (RF), vastus lateralis (VL), and vastus medialis (VM) for the quadriceps; gastrocnemius medialis (GM), gastrocnemius lateralis (GL), and soleus (SOL) for the triceps surae. For each muscle, a pair of self-adhesive Ag/AgCl electrodes (diameter of the recording area: 5 mm; Kendall Medi-Trace™, Canada) was attached to the skin with an inter-electrode distance of 20 mm (center-to-center) at the site recommended by SENIAM (Hermens et al. 2000). This location was refined using B-mode ultrasound (Aixplorer, Supersonic Imagine, France), such that the electrodes were placed longitudinally with respect to the muscle fascicle alignment (for VM, VL, GM, and GL), and

away from the border of neighbouring muscles. The electrode locations were intentionally not marked on the skin, such that variability of the electrode placement, which is a possible cause of inter-individual variability of EMG signals, would not contribute to the between-individual variability observed in this study. Prior to electrode application, the skin was shaved and cleaned with alcohol. Electrode cables were well secured to the skin with a tubular elastic bandage (tg®fix, Lohmann & Rauscher International, GmbH & Co. KG, Germany) to minimize movement artefacts. EMG signals were band-pass filtered (8–500 Hz) and pre-amplified close to the electrodes (375×) and digitized at a sampling rate of 1000 Hz using an EMG acquisition system (ME6000, Mega Electronics Ltd, Finland).

Experimental protocol

Isometric contractions

Participants performed a series of isometric knee extension and plantarflexion tasks while seating on an isokinetic dynamometer (Con-Trex, CMV AG, Dübendorf, Switzerland) with their hip flexed at 70° (0° = hip fully extended). For the knee extension tasks, the knee was positioned at 80° of flexion (0° = knee fully extended) and the shank was fixed to the dynamometer with inextensible strap. For the plantarflexion task, the knee was fully extended; the ankle was positioned at 0° (the foot perpendicular to the shank). Two inextensible straps were used to immobilize their torso. For each task, participants first performed a standardized warm-up, which included a series of 20 isokinetic contractions with a progressive increase in contraction intensity and 4 submaximal contractions at 60, 70, 80, and 90% of their subjective maximal contraction for 3–4 s, with 1 min rest between each contraction. This warm-up was followed by three maximal isometric voluntary contractions for 3 s, with 90 s rest between each contraction. Then, the experimental task involved matching submaximal target torque set at 25% of MVC during two short (≈ 10–15 s) isometric contractions with 20–30 s rest between each repetition. This target force level was presented on a feedback screen.

Pedalling

The pedalling task was performed on an electronically braked cycloergometer (Excalibur Sport; Lode, Groningen, The Netherlands) equipped with standard cranks (170 mm) and clipless pedals. The saddle height was standardized, such that it was at the same level as the greater trochanter of the participants during standing. Participants were instructed to maintain their seated position throughout the task. After familiarization with the cycloergometer, participants were asked to pedal at 150 W at 80 rpm for 1 min. A Transistor–Transistor Logic (TTL) pulse indicated the top dead center of the right pedal (highest position of the pedal) and was recorded on the EMG acquisition system, such that the crank position and the EMG data were synchronized.

Gait

To minimize perturbations induced by the external environment and to ensure that all the participants adopted the same walking speed, the experiments were conducted on a treadmill (Cardiotread, Cardioline, Trento, Italy). Participants walked barefoot and familiarized with the treadmill before the start of the experimental task, which consisted in walking at 0.83 m/s for 1 min. A force-sensitive resistor (FSR; FSR151AS) was taped under the heel of the dominant leg to detect the onset of the foot contact, i.e., the onset of the stance phase. These signals were recorded on the acquisition system used for EMG, such that the foot pressure and the EMG data were synchronized.

Data analysis

All mechanical and EMG data were processed using MATLAB (The Mathworks, Nathicks, USA). Raw EMG signals were first band-pass filtered (20–495 Hz) with a second-order Butterworth filter and a notch filter at 50 Hz was applied. Then, EMG signals were inspected for noise or artefact. At this stage, data were discarded for isometric plantarflexion (one participant; technical problems), pedalling (one participant; movement artefacts), and gait (two participants; movement artefacts).

Maximal torque and maximal EMG amplitude

Torque signals from the isometric tasks were low-pass filtered at 10 Hz. Maximal MVC torque was determined for both the three maximal knee extensions and the three maximal plantarflexions as the maximal torque measured over a 500-ms time window. To determine the maximal EMG amplitude, the root mean square (RMS) of the EMG signal was calculated over a moving time window of 500 ms and the maximal value was considered as the maximal activation level.

Submaximal EMG amplitude

During the isometric torque-matched tasks performed at 25% of MVC, the RMS EMG amplitude was calculated over 5 s at the middle of the force plateau. These values were averaged between the two contractions, such that one representative value was further considered.

For the pedalling task, the raw EMG signal was first rectified. After excluding the first 20 cycles, we selected the

first 15 consecutives cycles free of any artefacts. Each of these cycles was then interpolated to 200 time points and an ensemble-averaged cycle was obtained. The RMS EMG amplitude was calculated between − 5.5 and 44.4% of cycle, which corresponded to the downstroke phase [340°–160°; (Brochner Nielsen et al. 2017)]. EMG was considered during this phase as it represents the main phase of activity for both the knee extensors and the plantarflexors (Hug and Dorel 2009).

A similar procedure was used for gait, where 15 consecutive strides identified using the foot-sensible resistor sensors (onset of pressure) were ensemble-averaged. As activation of the quadriceps muscles is low during walking at low speed (< 5% of RMS EMG_{max} in our study), it was difficult to distinguish between noise and EMG for some participants. As such, only the muscles from the triceps surae were considered. The RMS EMG amplitude was calculated between 0 and 65% of cycle, which corresponded to the stance phase (Hebenstreit et al. 2015) during which these muscles are active (Schmitz et al. 2009).

For each submaximal task, the EMG amplitude was normalized to that determined during the maximal isometric task. This procedure was important to make between-muscles and between-days comparisons, but did not affect the relationship between tasks assessed from the first experimental session. We considered the activation contribution of each muscle to a given muscle group through the calculation of the activation ratio:

$$\frac{\text{Muscle } (i)}{\text{Muscle Group}} \text{ ratio } (\%) = \frac{\text{RMS EMG muscle } (i)}{\text{RMS EMG Muscle 1} + \text{Muscle 2} + \text{Muscle 3}} \times 100, \quad (1)$$

where (*i*) represents an individual muscle from the synergistic group considered.

For each muscle group, we also considered the activation ratio between the two muscles that share the same function (i.e., VL/VM as monoarticular knee extensors; GM/GL as biarticular plantarflexors).

Statistics

Statistical analyses were performed in Statistica v7.0 (Statsoft, Tulsa, OK, USA). All data are reported as mean ± SD. A Student *t* test was used to compare age and physical activity level between males and females. To test the robustness of the activation strategies during the isometric tasks, the between-day reliability of the EMG data was assessed using the intra-class correlation coefficient (ICC) and the standard error of measurement (SEM) as recommended by Hopkins (2000). ICC values were calculated as a measure of between-day reliability with values less than 0.4, between 0.4 and 0.6, between 0.6 and 0.75, and greater than 0.75 as poor, fair, good, and excellent agreement, respectively (Cicchetti et al. 2006). The inter-individual variability of the distribution of the activation ratios (VL/VM, RF/Quad, VL/Quad, VM/Quad; GM/GL, GM/TS, GL/TS, and SOL/TS) was then assessed using descriptive statistics [standard deviation (SD), coefficient of variation (CV), range, and interquartile range (IQR)]. As the previous studies reported sex difference in activation strategies (Hewett et al. 2005), separate repeated-measures analyses of variance (ANOVA) were performed for each activation ratio to determine the difference between males and females [between subject factor: sex (males vs. females); within-subject factor: task (knee extension or plantarflexion, pedalling, and gait)]. Post hoc analyses were performed using the Bonferroni test. The level of significance was set at $P < 0.05$. To determine the relationship between tasks (isometric tasks, gait, and pedalling), we calculated the Pearson's correlation coefficient. To provide insights into possible explanations for individual differences, we tested the relationship between each activation ratio and potential explanatory factors (physical activity level and MVC torque).

Results

Submaximal isometric tasks

Between-day reliability

Individual examples of raw EMG signals are depicted in Fig. 1. For the isometric knee extensions performed at 25% of MVC, the between-day reliability of the normalized RF, VL, and VM RMS EMG amplitude was fair to good (ICC > 0.50 and SEM < 3.5% of MVC; Table 2). Similarly, the reliability of the activation ratios was fair to good (ICC > 0.57 and SEM < 4.7%; Table 2). Even though the ICC value for RF RMS EMG and VL/VM ratio was interpreted as fair, the SEM values remained relatively low. For the isometric plantarflexions performed at 25% of MVC, the between-day reliability of the normalized GM, GL, and SOL RMS EMG amplitude was good to excellent (ICC > 0.64 and SEM < 3.4% of RMS EMG_{max}; Table 2). Similarly, the reliability of the activation ratios was good to excellent (ICC > 0.65 and SEM < 6.4%; Table 2). This overall fair-to-excellent reliability obtained on 62 participants suggests that activation strategies are robust between days.

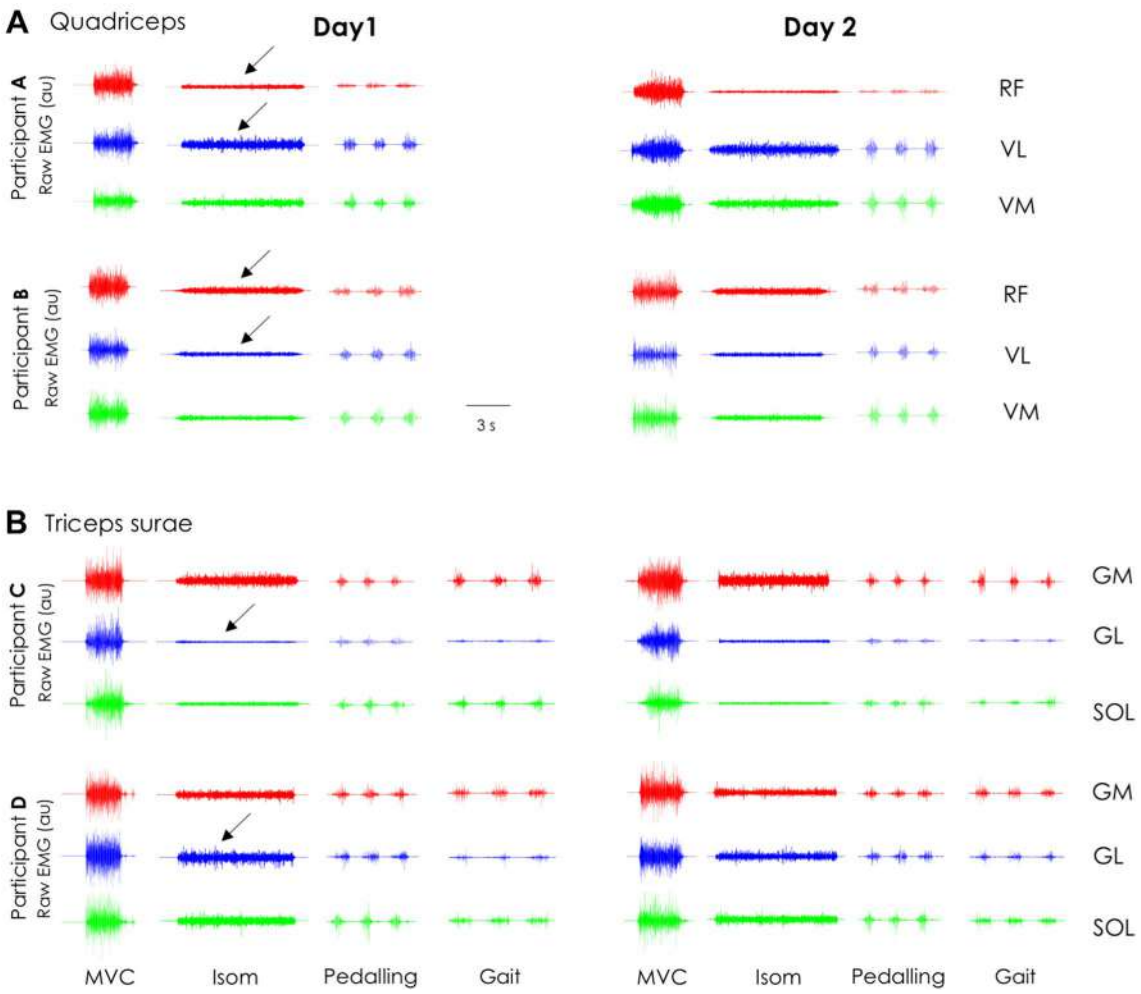

Fig. 1 Individual examples of the raw surface electromyographic signals. Representative raw electromyographic signal (EMG, arbitrary unit) of each head of the quadriceps (panel A: rectus femoris, RF; vastus lateralis, VL; vastus medialis, VM) and triceps surae (panel B: gastrocnemius medialis, GM; gastrocnemius lateralis, GL; soleus, SOL). EMG activity was measured during maximal voluntary contraction (MVC), isometric submaximal contractions performed at 25% of MVC (Isom), pedalling, and gait. Arrows show the inter-individual differences (e.g., Participant A: VL-biased; Participant C: GM-biased); the two columns (Day 1 and Day 2) illustrate the between-day consistencies

Table 2 Between-day reliability of muscle activation (RMS EMG) and activation ratios measured during the submaximal isometric force-matched tasks at 25% of MVC

$n=62$	RF RMS EMG	VL RMS EMG	VM RMS EMG	VL/VM	RF/Quad	VL/Quad	VM/Quad
ICC (90% CI)	0.50 (0.33–0.64)	0.63 (0.48–0.74)	0.62 (0.48–0.74)	0.57 (0.41–0.70)	0.71 (0.58–0.80)	0.61 (0.46–0.73)	0.64 (0.50–0.75)
SEM	3.4	3.5	3.4	4.7	4.4	4.1	3.8
$n=62$	GM RMS EMG	GL RMS EMG	SOL RMS EMG	GM/GL	GM/TS	GL/TS	SOL/TS
ICC (90% CI)	0.73 (0.61–0.81)	0.64 (0.50–0.75)	0.77 (0.67–0.84)	0.73 (0.62–0.81)	0.82 (0.74–0.88)	0.65 (0.50–0.75)	0.74 (0.63–0.82)
SEM	3.4	3.2	3.3	6.4	4.7	5.2	5.5

ICC intra-class coefficient of correlation, *SEM* standard error of measurement (expressed in % of RMS EMG_{max} for RMS EMG values and as % for the ratios), *RF* rectus femoris, *VL* vastus lateralis, *VM* vastus medialis, *Quad* quadriceps, *GM* gastrocnemius medialis, *GL* gastrocnemius lateralis, *SOL* soleus, *TS* triceps surae

Individual differences

Individual differences in activation strategies during the well-controlled single-joint tasks were assessed. During the isometric knee extensions at 25% of MVC, the mean EMG amplitude was 15.0 ± 4.6, 18.3 ± 5.7, and 17.6 ± 5.1% of RMS EMG_{max} for RF, VL, and VM, respectively. The mean ratio of EMG amplitude was 50.8 ± 8.0% (range 32.4–69.9%; IQR = 9.9; CV = 15.8%) for VL/VM, 29.7 ± 7.5% (range 14.9–57.1%; IQR = 9.8; CV = 25.3%) for RF/Quad, 35.8 ± 7.1% (range 21.3–58.2%; IQR = 11.0; CV = 19.8%) for VL/Quad, and 34.5 ± 6.4% (range 15.4–51.0%; IQR = 8.7; CV = 18.5%) for VM/Quad. As indicated by ranges, IQR, and CV, there was large variability between individuals (Fig. 2). For example, when considering the VL/VM ratio, there were an almost equal number of participants demonstrating greater VL RMS EMG than those with greater VM RMS EMG.

During the isometric plantarflexions at 25% of MVC, the mean EMG amplitude was 21.3 ± 6.2, 11.3 ± 5.8, and 18.3 ± 7.0% of RMS EMG_{max} for GM, GL, and SOL, respectively. The mean ratio of EMG amplitude was 66.2 ± 13.1% (range 35.5–89.6%; IQR = 19.2; CV = 19.8%) for GM/GL, 42.3 ± 10.5% (range 9.3–65.3%; IQR = 13.1; CV = 24.7%) for GM/TS, 21.7 ± 9.3% (range 5.0–46.7%; IQR = 14.0; CV = 42.7%) for GL/TS, and 36.0 ± 11.1% (range 16.6–78.9%; IQR = 13.8; CV = 30.8%) for SOL/TS. As observed for the quadriceps muscle group, range, IQR, and CV showed large variability between individuals (Fig. 3). Nine of the 84 participants activated their GL more than GM; the remaining participants activated their GM more than GL, with GM/GL ratios ranging from 50.0 to 89.6%.

There was no significant correlation between any of the activation ratios and MVC torque or IPAQ results (all *r* values < 0.18). This suggests that the activation strategies do not depend on muscle strength or physical activity level.

Relationship between isometric contractions and locomotor tasks

During pedalling, the mean EMG amplitude was 9.1 ± 5.0, 22.7 ± 9.5, and 25.1 ± 10.2% of RMS EMG_{max} for RF, VL, and VM, respectively; and 17.3 ± 5.7, 15.2 ± 6.1, and 19.8 ± 8.6% of RMS EMG_{max} for GM, GL, and SOL, respectively. During gait, the mean EMG amplitude was 14.4 ± 4.4, 7.7 ± 3.0, 14.9 ± 5.7% of RMS EMG_{max} for GM, GL, and SOL, respectively. Mean activation ratios are depicted in Table 3.

When considering the quadriceps muscle heads, there was a main effect of sex only for RF/Quad ($P = 0.003$), which was lower for males than females, regardless of the task. There was a main effect of task for each ratio (all *P* values < 0.0001). There was no significant sex × task interaction (all *P* values > 0.081), except for the VM/Quad activation ratio ($P = 0.041$). When the *post hoc* analysis was performed on VM/Quad, no significant differences

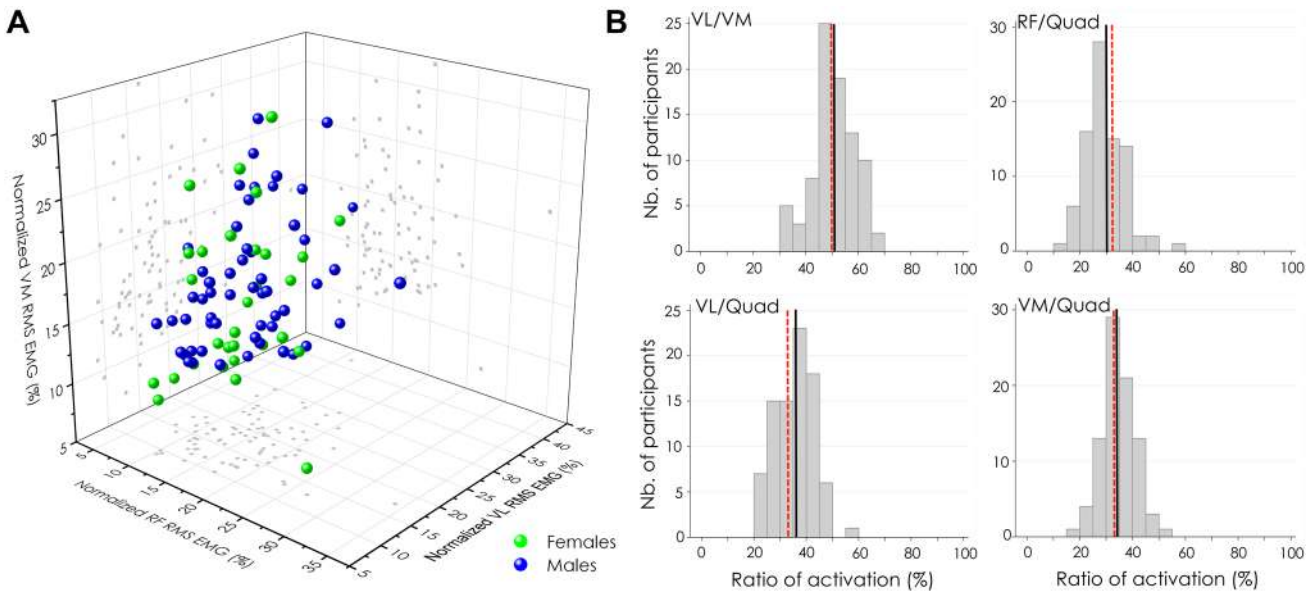

Fig. 2 Variability of activation strategies during the isometric knee extension task. **a** Normalized EMG amplitude for each muscle head. The spread of the dots within this 3-D space confirms that strategies to distribute activation among the synergist muscles are individual-specific. **b** Group distribution of the ratio of activation (RMS EMG). The red vertical line indicates a balanced activation among the synergist muscles (i.e., 50% and 33% when two muscles and three muscles were considered, respectively). The dashed vertical line indicates the mean value. *RF* rectus femoris, *VL* vastus lateralis, *VM* vastus medialis, *Quad* quadriceps

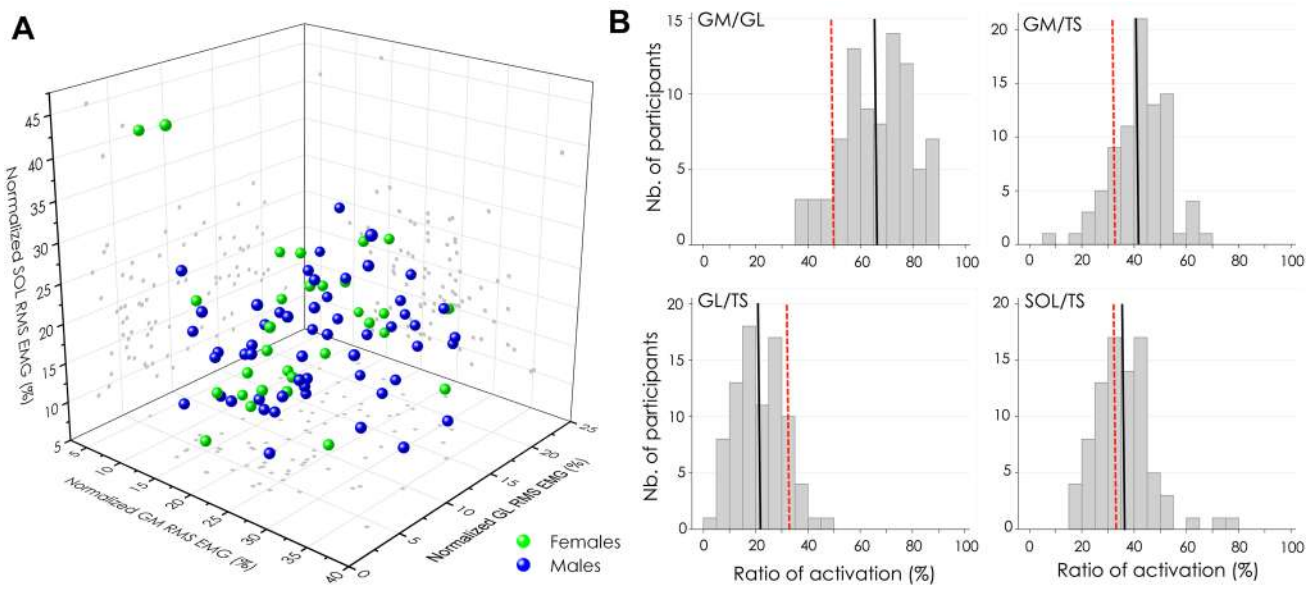

Fig. 3 Variability of activation strategies during the isometric plantarflexion task. **a** Normalized EMG amplitude for each muscle head. The spread of the dots within this 3-D space confirms that strategies to distribute activation among the synergist muscles are individual-specific. **b** Group distribution of the ratio of activation (RMS EMG). The red vertical line indicates a balanced activation among the synergist muscles (i.e., 50% and 33% when two muscles and three muscles were considered, respectively). The dashed vertical line indicates the mean value. *GM* gastrocnemius medialis, *GL* gastrocnemius lateralis, *SOL* soleus, *TS* triceps surae

Table 3 Correlation of the activation ratios between tasks

	VL/VM	RF/Quad	VL/Quad	VM/Quad	GM/GL	GM/TS	GL/TS	SOL/TS
Isom vs. Pedalling	0.76	0.37	0.72	0.60	0.37	0.21	0.41	0.30
Isom vs. Gait					0.55	0.43	0.61	0.43
Pedalling vs. Gait					0.43	0.47	0.47	0.66

All the correlations were significant, with effect sizes ranging from moderate to large, except that of GM/TS between Isom and pedalling ($P = 0.058$)

RF rectus femoris, VL vastus lateralis, *VM* vastus medialis, *Quad* quadriceps, *GM* gastrocnemius medialis, *GL* gastrocnemius lateralis, *SOL* soleus, *TS* triceps surae, *Isom* isometric

were observed between males and females (all P values > 0.225), but significant differences were observed between tasks (all P values < 0.001). For the sake of clarity, all these results are reported in Table 4.

When considering the heads of the *triceps surae*, we observed a main effect of sex for GM/GL ($P = 0.027$) but not for the other ratios (all P values > 0.074). There was a main effect of task for all the ratios (all P values < 0.023). We observed a significant sex × task interaction for GM/GL, GM/TS, and SOL/TS (all P values < 0.03), but not for GL/TS ($P = 0.558$). *Post hoc* analysis showed that neither GM/TS nor SOL/TS were significantly different between males and females, for any of the tasks (all P values > 0.051). However, GM/GL activation ratio was higher for males ($68.8 \pm 11.9\%$) than females ($61.7 \pm 14.1\%$) during isometric plantarflexion ($P = 0.039$), while no difference was found during pedalling ($P = 0.655$) and gait ($P = 1$). For the sake of clarity, all these results are reported in Table 4.

Each ratio of activation measured during pedalling was positively correlated to that measured during the isometric knee extension for quadriceps muscles ($n = 84$; $0.37 < r < 0.76$; all P values < 0.001; Table 3). Similar significant correlations were observed between pedalling and isometric plantarflexion for triceps surae ($n = 83$; $0.30 < r < 0.41$; all P values < 0.001; Table 3), except for GM/TS ($P = 0.058$). Notably, the coefficients of correlation were lower for the triceps surae muscles than for the quadriceps muscles. When considering the triceps surae, each ratio of activation measured during gait was positively correlated to that measured during the isometric plantarflexion ($n = 82$; $0.43 < r < 0.61$; all P values < 0.001; Table 3) or pedalling ($n = 82$; $0.43 < r < 0.66$; all P values < 0.001; Table 3). Overall, it signifies that

Table 4 Between-task comparison of activation strategies

	VL/VM		RF/Quad		VL/Quad		VM/Quad	
	Males	Females	Males	Females	Males	Females	Males	Females
A. Quadriceps								
Isom	51.3 ± 7.1	50.0 ± 9.5	28.6 ± 7.3	31.6 ± 7.6	36.8 ± 6.8	34.1 ± 7.4	34.7 ± 5.5	34.3 ± 7.8
Pedalling	46.9 ± 8.1	48.1 ± 11.2	14.0 ± 7.1	19.1 ± 3.9	40.4 ± 8.2	38.9 ± 9.0	45.6 ± 7.7[a]	42.0 ± 9.7[a]
	Main effect task ($P < 0.001$; Isom > Ped)		Main effect sex ($P = 0.003$; F > M) Main effect task ($P < 0.001$; Isom > Ped)		Main effect task ($P < 0.001$; Isom < Ped)		Sex × task interaction ($P = 0.041$)	
	GM/GL		GM/TS		GL/TS		SOL/TS	
	Males	Females	Males	Females	Males	Females	Males	Females
B. Triceps surae								
Isom	68.8 ± 11.9	61.7 ± 14.1[c]	44.2 ± 8.9	38.8 ± 12.1	20.5 ± 8.6	24.0 ± 10.2	35.3 ± 9.6	37.2 ± 13.4
Pedalling	55.6 ± 8.6[a]	50.7 ± 8.6[a]	34.9 ± 6.5[a]	30.8 ± 6.4[a]	28.1 ± 7.3	30.1 ± 6.9	37.0 ± 8.8	39.1 ± 8.5
Gait	65.8 ± 8.9[b]	65.1 ± 8.1[b]	38.2 ± 6.6[a]	41.2 ± 7.1[b]	20.1 ± 6.3	22.1 ± 5.8	41.7 ± 7.8[a,b]	36.7 ± 7.6
	Sex × task interaction ($P = 0.030$)		Sex × task interaction ($P < 0.001$)		Main effect Task ($P < 0.001$ Ped > Isom and Gait)		Sex × task interaction ($P = 0.003$)	

The distribution of activation among synergist muscles was estimated using the calculation of activation ratio

RF rectus femoris, *VL* vastus lateralis, *VM* vastus medialis, *Quad* quadriceps, *GM* gastrocnemius medialis, *GL* gastrocnemius lateralis, *SOL* soleus, *TS* triceps surae, *Isom* isometric

[a]Different compared to isometric

[b]Different compared to pedalling

[c]Difference between males and females

even though between-tasks differences in activation ratios logically exist at the group level (Table 4), individual-specific strategies are retained between tasks.

Discussion

This study has three main findings. First, the distribution of normalized EMG amplitude among synergist muscles is robust between days, allowing us to consider that it represents an individual muscle activation strategy. Second, these strategies vary greatly between individuals. Third, distribution of EMG amplitude is correlated between tasks, providing evidence that people who bias their activation to a particular muscle do so during multiple motor tasks. Even though inter-individual variability of EMG signals has been well described in the literature, it is often considered noise which complicates the interpretation of data. This study provides evidence that inter-individual variability results from actual differences in activation strategies. It is our contention that consideration of this inter-individual variability is important to expand our knowledge of the role of muscle coordination in the development of musculoskeletal disorders.

Important considerations to interpret individual differences in EMG amplitude

There are three important considerations when interpreting inter-individual differences in EMG amplitude as an evidence of individual-specific motor strategies. The first is to test the consistency of EMG data across days. Our results, obtained from a subgroup of 62 participants, demonstrate a fair-to-good reliability for the quadriceps muscles and a good-to-excellent reliability for the triceps surae muscles. Even though the quadriceps muscles exhibited lower ICC values than the triceps surae muscles, SEM values were similar between muscle groups, which suggest that the lower ICC values were likely explained by the smaller variance of the quadriceps muscles rather than a lower reliability. Despite the overall good reliability, between-day variability inevitably exists. Importantly, this between-day variability may not be (entirely) explained by variability of the activation strategies between days as methodological factors may also affect EMG amplitude [e.g., electrode placement, normalization procedure, and skin impedance; reviewed in Farina et al. (2004)]. In contrast to the previous work (Hug et al. 2015), we intentionally did not mark the electrode locations, such that day-to-day variability of the electrode placement could contribute to a possible difference in the

observed motor behaviour between days. It was important to not exclude this source of between-day variability as electrode placement might explain, at least in part, the inter-individual variability of the EMG signals. It is important to note that other factors such as crosstalk and signal cancellation may affect the relationship between EMG amplitude and muscle activation (Farina et al. 2004). To limit crosstalk, we followed the SENIAM recommendations and we used B-mode ultrasound to place the electrodes away from the muscle borders. To limit the influence of signal cancellation, we normalized the EMG amplitude to that measured during MVC (Keenan et al. 2005).

The second important consideration relates to the interpretation of the distribution of EMG amplitude as a neural strategy. Even though the ratio of VL/VM EMG amplitude observed from the group data ($50.8 \pm 8.0\%$) is in accordance with the recent results suggesting a balanced or common neural drive between these muscles (Martinez Valdes et al. 2018; Laine et al. 2015), it is well understood that EMG amplitude only provides a crude index of neural drive, i.e., the number of motor neuron action potentials (Dideriksen et al. 2011; Enoka and Duchateau 2015). EMG amplitude is more closely related to muscle activation, which relates to the number of muscle fibre action potentials (Dideriksen et al. 2011; Enoka and Duchateau 2015). Note that the relationship between neural drive and muscle activation depends on the size of the motor units, i.e., the number of muscle fibres within each active motor unit. In the absence of a difference in muscle fibre electrical properties between muscles (muscle fibre conduction velocity and size of the motor unit action potentials), between-muscle difference in EMG amplitude can be interpreted as between-muscle difference in activation (Enoka and Duchateau 2015; Farina et al. 2010). First, there is no evidence that fibre conduction velocity differs between synergist muscles during non-fatiguing contractions performed at a low intensity, as were performed in our study. This is because slow-twitch muscle fibres are likely preferentially recruited during such tasks (Henneman et al. 1965). Second, the difference in the size of the motor units action potential, if any, might have been minimized by the normalization procedure (Martinez-Valdes et al. 2018). With these considerations in mind, we interpreted the inter-individual differences in the distribution of normalized EMG amplitude across synergist muscles as differences in muscle activation strategies rather than differences in neural strategies.

Individual-specific muscle activation strategies

The vast majority of studies on muscle coordination report values averaged from a group of individuals, making it impossible to appreciate the individual differences in the activation strategies that inevitably exist. Here, a large inter-individual variability of the activation ratios was observed during the submaximal single-joint tasks (Figs. 2, 3), the magnitude of which exceeded the within-participant variability assessed between two different days. To the best of our knowledge, the significance of inter-individual variability has received a little attention in the literature. Pal et al. (2012) reported a wide range of VL/VM activation ratios in people with patellofemoral pain during gait, but different methodologies for EMG normalization and ratio calculation preclude comparison with our data. Other work reported a similar individual variability in the activation ratios for quadriceps (Hug et al. 2015) or triceps surae muscles (Ahn et al. 2011; Masood et al. 2014), but they were conducted on relatively small sample sizes (between 8 and 22 individuals). The novelty of the present study is to describe these individual differences in a larger sample size ($n = 85$) and to demonstrate the robustness of the distribution of EMG amplitude between muscles across time, allowing us to consider that it represents a true individual-specific activation strategy. Furthermore, even though the distribution of activation was significantly different between some (but not all) tasks, a significant correlation of the activation ratios between tasks was observed. Differences in muscle function imposed by the different mechanical constraints (isometric vs. dynamic contractions) might have involved different neuronal circuits (Kurtzer et al. 2005; Shadmehr 2016), leading to the observed differences between tasks. However, the existence of significant correlation between tasks indicates that a participant who exhibits an activation strategy biased toward a specific muscle will exhibit this strategy regardless of the task (at least within the tasks considered here in). Overall, these results provide strong evidence for the individuality principle (Ting et al. 2015), i.e., individuals exhibit different activation strategies, evidenced here as different distribution of activation across synergist muscles. Importantly, these strategies may evolve as a result of changes within the musculoskeletal systems due to training/disuse (e.g., muscle typology and muscle volume), or the presence of musculoskeletal pain (Hodges and Tucker 2011). The extent to which individual features (or signatures) are retained throughout this adaptation process is unknown.

Despite not being the main outcome of this study, differences in the mean activation ratios were observed between tasks, and between males and females. We believe that the interpretation of these differences requires the consideration of the relative contraction intensity (in percentage of maximal intensity), which may differ between tasks or between males and females during gait and pedalling. Indeed, the distribution of activation logically depends on the contraction intensity, with the contribution of synergist muscles being more balanced at higher contraction intensities that require near-complete or complete activation (Hug et al. 2015; Pincivero and Coelho 2000). However, because differences

in contraction intensity remained of small amplitude, they are unlikely to fully explain the observed between-task and between-sex differences. Note that the sex difference observed for some, but not all, activation ratios is in accordance with the previous studies reporting between-sex difference in activation strategies (Hewett et al. 2005). The origin of these differences remains unclear.

Origin of individual muscle activation strategies

Interestingly, the inter-individual variability of the distribution of EMG amplitude was observed even during well-controlled tasks, such as the single-joint isometric contractions, and the pedalling task. Here, we argue that this consistency provides evidence that they reflect true difference in activation strategies rather than different kinetics/kinematics strategies. Yet, the origin of these individual differences is unknown. They can be discussed in regards to the current motor control theories. The optimal feedback control theory (Todorov 2004) proposed that motor patterns are selected, such that movement costs (e.g., smoothness, activation, jerk, and energy) are constantly minimized. Within this framework, it is possible that each individual optimizes a different cost and/or that optimizing the same cost(s) requires different activation strategies across individuals because of individual characteristics (e.g. anatomy, muscle morphology, muscle moment arm, and neural constraints). An alternative motor control theory, the good-enough theory, proposes that a hierarchy of sensorimotor networks gradually adapt through trial-and-error learning to produce effective movements which are good enough to achieve the task goal (Loeb 2012). It is, therefore, possible that individuals develop different good-enough muscle activation strategies through motor exploration, experience, and training, leading to habitual rather than optimal strategies (De Rugy et al. 2012). Here, we did not find any association between the level of physical activity and the activation strategies. However, the IPAQ questionnaire only evaluates general physical activity. It is possible that past and present experience with specific motor skills (i.e., motor history) might have participated to shape individual strategies. Retrospective studies on large cohorts or longitudinal studies performed at different lifespans are needed to address this question. An alternative explanation of our results is that the distribution of muscle activation, but not that of neural drive differs between participants, as recently suggested from data averaged over a group of participants (Martinez Valdes et al. 2018). In this case, it would mean that individual muscle activation strategies would originate from peripheral features rather than differences in neural drive. Further works with advanced EMG decomposition techniques are needed to unravel the origin of the inter-individual variability of activation strategies as described in the present study.

Consequences of individual muscle activation strategies

Although the origin of the individual differences in muscle activation strategies is unknown, we believe that they may have important functional consequences. First, muscle activation strategies might impact muscle performance. Prilutsky and Zatsiorsky (2002) suggested that fatigue may be minimized by more equal stress distribution (and thus activation) among muscles with similar typology. In other words, if activation is not equally shared between synergist muscles throughout a fatiguing task, fatigue would develop sooner in the most activated muscle, which would, therefore, be the weakest link. As such, Avrillon et al. (2018) reported a significant negative correlation between the imbalance of activation across the hamstring muscles and the time to exhaustion during a submaximal force-matched task, i.e., the larger the imbalance of activation across muscles, the lower the muscle endurance performance.

Second, each individual muscle activation strategy may have specific mechanical effect on the musculoskeletal system (Hug and Tucker 2017). As muscle activation is not systematically adjusted to balance forces between the synergist muscles of differing force-generating capacities, it is likely to lead to a force imbalance between these muscles (Crouzier et al. 2018; Hug et al. 2015). Importantly, the magnitude of this force imbalance may vary greatly between participants. Even though the mechanical effect of this force imbalance on non-muscular structures is unknown, it is possible that some activation strategies put some individuals at more risk of developing musculoskeletal disorders (Hug and Tucker 2017).

Conclusion

Although it is well known that muscle activation can vary between individuals, these differences have been very rarely considered as relevant information to expand our knowledge on motor control. By showing their robustness, our results strongly provide evidence that these differences reflect the existence of individual activation strategies. Further works with advanced EMG decomposition techniques are needed to unravel the origin of the observed inter-individual variability of the activation strategies as described in the present study.

Acknowledgements The authors thank Killian Bouillard and Lois Boucherf (University of Nantes, France) for collecting some data of this study.

Funding This study was supported by a grant from the Région Pays de la Loire (QUETE project, no. 2015-09035). François Hug was

supported by a fellowship from the Institut Universitaire de France (IUF).

Compliance with ethical standards

Conflict of interest The authors have no financial conflicts of interest to disclose.

References

Ahn AN, Kang JK, Quitt MA, Davidson BC, Nguyen CT (2011) Variability of neural activation during walking in humans: short heels and big calves. Biol Lett 7:539–542

Alessandro C, Rellinger BA, Barroso FO, Tresch MC (2018) Adaptation after vastus lateralis denervation in rats demonstrates neural regulation of joint stresses and strain. eLife 7:e38215

Avrillon S, Guilhem G, Barthélémy A, Hug F (2018) Coordination of hamstring is individual specific and is related to motor performance. J Appl Physiol 125(4):1069–1079

Brochner Nielsen NP, Hug F, Guevel A, Fohanno V, Lardy J, Dorel S (2017) Motor adaptations to unilateral quadriceps fatigue during a bilateral pedaling task. Scand J Med Sci Sports 27:1724–1738

Cicchetti D, Bronen R, Spencer S, Haut S, Berg A, Oliver P, Tyrer P (2006) Rating scales, scales of measurement, issues of reliability: resolving some critical issues for clinicians and researchers. J Nerv Ment Dis 194:557–564

Craig CL, Marshall AL, Sjöström M, Bauman AE, CBooth ML, Ainsworth BE, Pratt M, Ekelund U, Yngve A, Sallis JF et al (2003) International physical activity questionnaire: 12 country reliability and validity. Med Sci Sports Exerc 35:1381–1395

Crouzier M, Lacourpaille L, Nordez A, Tucker K, Hug F (2018) Neuromechanical coupling within the human triceps surae and its consequences on individual force sharing strategies. J Exp Biol

De Rugy A, Loeb GE, Carroll TJ (2012) Muscle coordination is habitual rather than optimal. J Neurosci 32:7384–7391

De Marchis C, Schmid M, Bibbo D, Bernabucci I, Conforto S (2013) Inter-individual variability of forces and modular muscle coordination in cycling: a study on untrained subjects. Hum Mov Sci 32:1480–1494

Dideriksen JL, Enoka RM, Farina D (2011) Neuromuscular adjustmens that constrain submaximal EMG amplitude at task failure of sustained isometric contractions. J Appl Physiol 111:485–494

Enoka RM, Duchateau J (2015) Inappropriate interpretation of surface EMG signals and muscle fiber characteristics impedes understanding of the control of neuromuscular function. J Appl Physiol (1985) 119:1516–1518

Farina D, Merletti R, Enoka RM (2004) The extraction of neural strategies from the surface EMG. J Appl Physiol 96:1486–1495

Farina D, Holobar A, Merletti R, Enoka RM (2010) Decoding the neural drive to muscles from the surface electromyogram. Clin Neurophysiol 121:1616–1623

Hebenstreit F, Leibold A, Krinner S, Welsch G, Lochmann M, Eskofier BM (2015) Effect of walking speed on gait sub phase durations. Hum Mov Sci 43:118–124

Henneman E, Somjen C, Carpenter DO (1965) Excitability and inhibitability of motoneurons of different sizes. J Neurophysiol 28:599–620

Hermens HJ, Freriks B, Disselhorst-Klug C, Rau G (2000) Development of recommendations for SEMG sensors and sensor placement procedures. J Electromyogr Kinesiol 10:361–374

Hewett TE, Zazulak BT, Myer GD, Ford KR (2005) A review of electromyographic activation levels, timing differences, and increased anterior cruciate ligament injury incidence in female athletes. Br J Sports Med 39:347–350

Hodges PW, Tucker K (2011) Moving differently in pain: a new theory to explain the adaptation to pain. Pain 152:90–98

Hopkins W (2000) Measures of reliability in sports medicine and science. Sports Med 30:1–15

Hug F, Dorel S (2009) Electromyographic analysis of pedaling: a review. J Electromyogr Kinesiol 19:182–198

Hug F, Tucker K (2017) Muscle coordination and the development of musculoskeletal disorders. Exerc Sport Sci Rev 45:201–208

Hug F, Turpin NA, Guével A, Dorel S (2010) Is interindividual variability of EMG patterns in trained cyclists related to different muscle synergies? J Appl Physiol 108:1727–1736

Hug F, Goupille C, Baum D, Raiteri BJ, Hodges PW, Tucker K (2015) Nature of the coupling between neural drive and force-generating capacity in the human quadriceps muscle. Proc R Soc B 282(1819):20151908

Ivanenko YP, Grasso R, Macellari V, Lacquaniti F (2002) Control of foot trajectory in human locomotion: role of ground contact forces in simulated reduced gravity. J Neurophysiol 87:3070–3089

Keenan KG, Farina D, Maluf KS, Merletti R, Enoka RM (2005) Influence of amplitude cancellation on the stimulated surface electromyogram. J Appl Physiol 98:120–131

Kurtzer I, Herter TM, Scott SH (2005) Random change in cortical load representation suggests distinct control of posture and movement. Nat Neurosci 8:498–504

Laine CM, Martinez-Valdes E, Falla D, Mayer F, Farina D (2015) Motor neuron pools of synergists thigh muscles share most of their synaptic input. J Neurosci 35:12207–12216

Loeb GE (2012) Optimal isn't good enough. Biol Cybern 106:757–765

Martinez Valdes E, Negro F, Falla D, De Nunzio AM, Farina D (2018) Surface EMG amplitude does not identify differences in neural drive to synergistic muscles. J Appl Physiol 124:1071–1079

Masood T, Bojsen-Moller J, Kalliokoski KK, Kirjavainen A, Aarimaa V, Magnusson SP, Finni T (2014) Differential contributions of ankle plantarflexors during submaximal isometric muscle action: a PET and EMG study. J Electromyogr Kinesiol 24:367–374

Pal S, Besier TF, Draper CE, Fredericson M, Gold GE, Beaupre GS, Delp SL (2012) Patellar tilt correlates with vastus lateralis: vastus medialis activation ratio in maltracking patellofemoral pain patients. J Orthop Res 30:927–933

Pincivero DM, Coelho AJ (2000) Activation li earity and parallelism of the superficila quadriceps across the isometric intensity spectrum. Muscle Nerve 23:393–398

Prilutsky BI, Zatsiorsky VM (2002) Optimization-based models of muscle coordination. Exerc Sport Sci Rev 30:32–38

Schmitz A, Silder A, Heiderscheit B, Mahoney J, Thelen DG (2009) Differences in lower-extremity muscular activation during walking between healthy older and young adults. J Electromyogr Kinesiol 19:1085–1091

Shadmehr R (2016) Distinct neural circuits for control of movement vs. holding still. J Neurophysiol 117:1431–1460

Ting LH, Chiel HJ, Trumbower RD, Allen JL, McKay JL, Hackney ME, Kesar TM (2015) Neuromechanical principles underlying movement modularity and their implications for rehabilitation. Neuron 86:38–54

Todorov E (2004) Optimality principles in sensorimotor control. Nat Neurosci 7:907–915

Valero-Cuevas FJ, Cohn BA, Yngvason HF, Lawrence EL (2015) Exploring the high-dimensional structure of muscle redundancy via subject-specific and generic musculoskeletal models. J Biomech 48:2887–2896

Winter DA, Yack HJ (1987) EMG profiles during normal human walking: stride-to-stride and inter-subject variability. Electroencephalogr Clin Neurophysiol 67:402–411

STUDY 2

Neuromechanical coupling in the human *triceps surae* and its consequence on individual force-sharing strategies

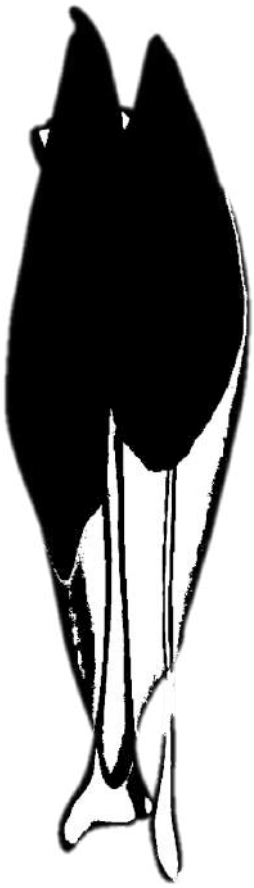

Associated publication:

Crouzier, M., Lacourpaille, L., Nordez, A., Tucker, K., Hug, F. (2018). Neuromechanical coupling in the human *triceps surae* and its consequence on individual force-sharing strategies. *Journal of Experimental Biology*, 221 (pt21).

ABSTRACT

Little is known about the factors that influence the coordination of synergist muscles that act across the same joint, even during single joint isometric tasks. The overall aim of this study was to determine the nature of the relationship between the distribution of activation and the distribution of force-generating capacity among the three heads of the *triceps surae*. Twenty volunteers performed isometric plantarflexions, during which the activation of GM, GL and SOL was estimated using EMG. Functional muscle PCSA was estimated using imaging techniques and was considered as an index of muscle force-generating capacity. The distribution of activation and PCSA among the three muscles varied greatly between participants. A significant positive correlation between the distribution of activation and the distribution of PCSA was observed when considering the two bi-articular muscles at intensities ≤ 50 % of the maximal contraction ($0.51 < r < 0.62$). Specifically, the greater the PCSA of GM compared with GL, the stronger bias of activation to the GM. There was no significant correlation between monoarticular and biarticular muscles. A higher contribution of GM activation compared with GL activation was associated with lower *triceps surae* activation ($-0.66 < r < -0.42$) and metabolic cost ($-0.74 < r < -0.52$) for intensities ≥ 30 % of the maximal contraction. Considered together, an imbalance of force between the three heads was observed, the magnitude of which varied greatly between participants. The origin and consequences of these individual force-sharing strategies remain to be determined.

Key words

Muscle coordination, Calf, Achilles tendon, Activation, Electromyography

© 2018. Published by The Company of Biologists Ltd | Journal of Experimental Biology (2018) 221, jeb187260. doi:10.1242/jeb.187260

RESEARCH ARTICLE

Neuromechanical coupling within the human triceps surae and its consequence on individual force-sharing strategies

Marion Crouzier[1], Lilian Lacourpaille[1], Antoine Nordez[1,2], Kylie Tucker[3] and François Hug[1,4,5,*]

ABSTRACT

Little is known about the factors that influence the coordination of synergist muscles that act across the same joint, even during single-joint isometric tasks. The overall aim of this study was to determine the nature of the relationship between the distribution of activation and the distribution of force-generating capacity among the three heads of the triceps surae [soleus (SOL), gastrocnemius medialis (GM) and gastrocnemius lateralis (GL)]. Twenty volunteers performed isometric plantarflexions, during which the activation of GM, GL and SOL was estimated using electromyography (EMG). Functional muscle physiological cross-sectional area (PCSA) was estimated using imaging techniques and was considered as an index of muscle force-generating capacity. The distribution of activation and PCSA among the three muscles varied greatly between participants. A significant positive correlation between the distribution of activation and the distribution of PCSA was observed when considering the two bi-articular muscles at intensities ≤50% of the maximal contraction ($0.51<r<0.62$). Specifically, the greater the PCSA of GM compared with GL, the stronger bias of activation to the GM. There was no significant correlation between monoarticular and biarticular muscles. A higher contribution of GM activation compared with GL activation was associated with lower triceps surae activation ($-0.66<r<-0.42$) and metabolic cost ($-0.74<r<-0.52$) for intensities ≥30% of the maximal contraction. Considered together, an imbalance of force between the three heads was observed, the magnitude of which varied greatly between participants. The origin and consequences of these individual force-sharing strategies remain to be determined.

KEY WORDS: Muscle coordination, Calf, Achilles tendon, Activation, Electromyography

INTRODUCTION

Coordination at multiple levels, e.g. between muscles within a synergistic group, over one or more joints, and between limbs, is required to achieve the vast majority of movements. With multiple muscles able to act upon the same joint, many different muscle coordination strategies are theoretically possible to achieve the same motor goal (Diedrichsen et al., 2010; Kutch and Valero-Cuevas, 2011). Force sharing among synergistic muscle groups has been studied extensively in animal models as well as with biomechanical models (reviewed in Herzog, 2000, 2017). Even though these works provided substantial insight into muscle coordination strategies, they did not identify the factors that influence the coordination of synergist muscles that act across the same joint, even during simple isometric tasks. Addressing this issue is fundamental to understanding the control of movement, and requires knowledge of the relationship between the activation a muscle receives and its force-generating capacity.

Large inter-individual variability in the distribution of force-generating capacity exists among synergist muscles. For example, the ratio of physiological cross-sectional area (PCSA) between the vastus lateralis (VL) and vastus medialis (VM) measured on 12 human cadavers varied between 47.3 and 68.3% (Farahmand et al., 1998). It is unclear how the nervous system accounts for these individual differences in force-generating capacity. There are several hypotheses. First, activation is equally shared between synergist muscles, in which case the imbalance of force would match the imbalance of force-generating capacity (solution 1, Fig. 1). Second, the force sharing strategy is similar among individuals with either balanced or imbalanced force between synergist muscles. In this latter case, the distribution of activation would vary between individuals (solution 2, Fig. 1). Third, the muscle with the higher force-generating capacity receives greater activation, in which case the overall activation would be reduced but a large imbalance of force would exist [solution 3; supported by some biomechanical models (Crowninshield and Brand, 1981), Fig. 1]. Finally, it is possible that there is no specific coupling between activation and force-generating capacity (solution 4, not shown in the figure).

Hug et al. (2015) reported a large positive correlation between the ratio of muscle activation [quantified using electromyography (EMG)] and the ratio of muscle force-generating capacity (i.e. the muscle PCSA) in two synergist muscles of the thigh (VL and VM). Specifically, individuals with greater force-generating capacity of VL compared with VM exhibited a stronger bias of activation to VL. However, interpretations of this neuromechanical coupling in terms of motor control principles and biomechanical consequences remain unclear. First, it is likely that this coupling contributed to reduce the average activation of the whole muscle group, leading to a lower effort (Fig. 1). However, owing to limitations of measuring activation of the deep vastus intermedius muscle through surface electrodes, this hypothesis has not been tested. Second, the neuromechanical coupling reported by Hug et al. (2015) logically led to a force imbalance between the VM and VL, the magnitude of which varied greatly between participants. However, the quadriceps muscle is not an ideal model to understand the mechanical effect of this force imbalance on the non-muscular structures. This is because a force imbalance between the VL and VM can be counterbalanced at the joint level by different moment arms. In addition, the

[1]University of Nantes, Laboratory 'Movement, Interactions, Performance' (EA 4334), Faculty of Sport Sciences, 44000 Nantes, France. [2]Health and Rehabilitation Research Institute, Faculty of Health and Environmental Sciences, Auckland University of Technology, Auckland, 1010 New Zealand. [3]The University of Queensland, School of Biomedical Sciences, Brisbane, Queensland 4072, Australia. [4]The University of Queensland, NHMRC Centre of Clinical Research Excellence in Spinal Pain, Injury and Health, School of Health and Rehabilitation Sciences, Brisbane, Queensland 4072, Australia. [5]Institut Universitaire de France (IUF), 75231 Paris, France.

*Author for correspondence (francois.hug@univ-nantes.fr)

F.H., 0000-0002-6432-558X

Received 20 June 2018; Accepted 12 September 2018

Journal of Experimental Biology (2018) 221, jeb187260. doi:10.1242/jeb.187260

List of abbreviations

EMG	electromyography
Gas	gastrocnemii
GL	gastrocnemius lateralis
GM	gastrocnemius medialis
MVC	maximal voluntary contraction
PCSA	physiological cross-sectional area
RMS	root mean square
SOL	soleus
TS	triceps surae
VL	vastus lateralis
VM	vastus medialis

difference in PCSA between the VL and VM is moderate. It is unclear how the activation is distributed between synergist muscles with a much larger difference in force-generating capacity. If such a coupling persists, a dramatic imbalance of muscle force would be observed. This imbalance could have important mechanical effects on the soft tissues and joint structures, with either positive (e.g. adaptation in mechanical properties, tissue remains functional) or negative consequences (pathological changes in the tissues).

The human triceps surae is an ideal muscle group to provide insight into the coordination of synergist muscles that act across the same joint. First, activation of each of the three heads of the triceps surae [gastrocnemius medialis (GM), gastrocnemius lateralis (GL) and soleus (SOL)] can be measured using surface EMG. Second, each head is connected to a fascicle bundle of the same tendon, the Achilles tendon (Szaro et al., 2009). As such, an imbalance of force between the three heads is likely to have mechanical effect on the tendon, as suggested in cadaver preparations (Arndt et al., 1999) and from computational modelling (Handsfield et al., 2016). Third, the three heads of the triceps surae have large differences in PCSA; i.e. GM PCSA is 2.1 times larger than that of GL, and SOL PCSA is 2.6 and 5.5 times larger than that of GM and GL, respectively (Albracht et al., 2008). Finally, this muscle group is composed of two

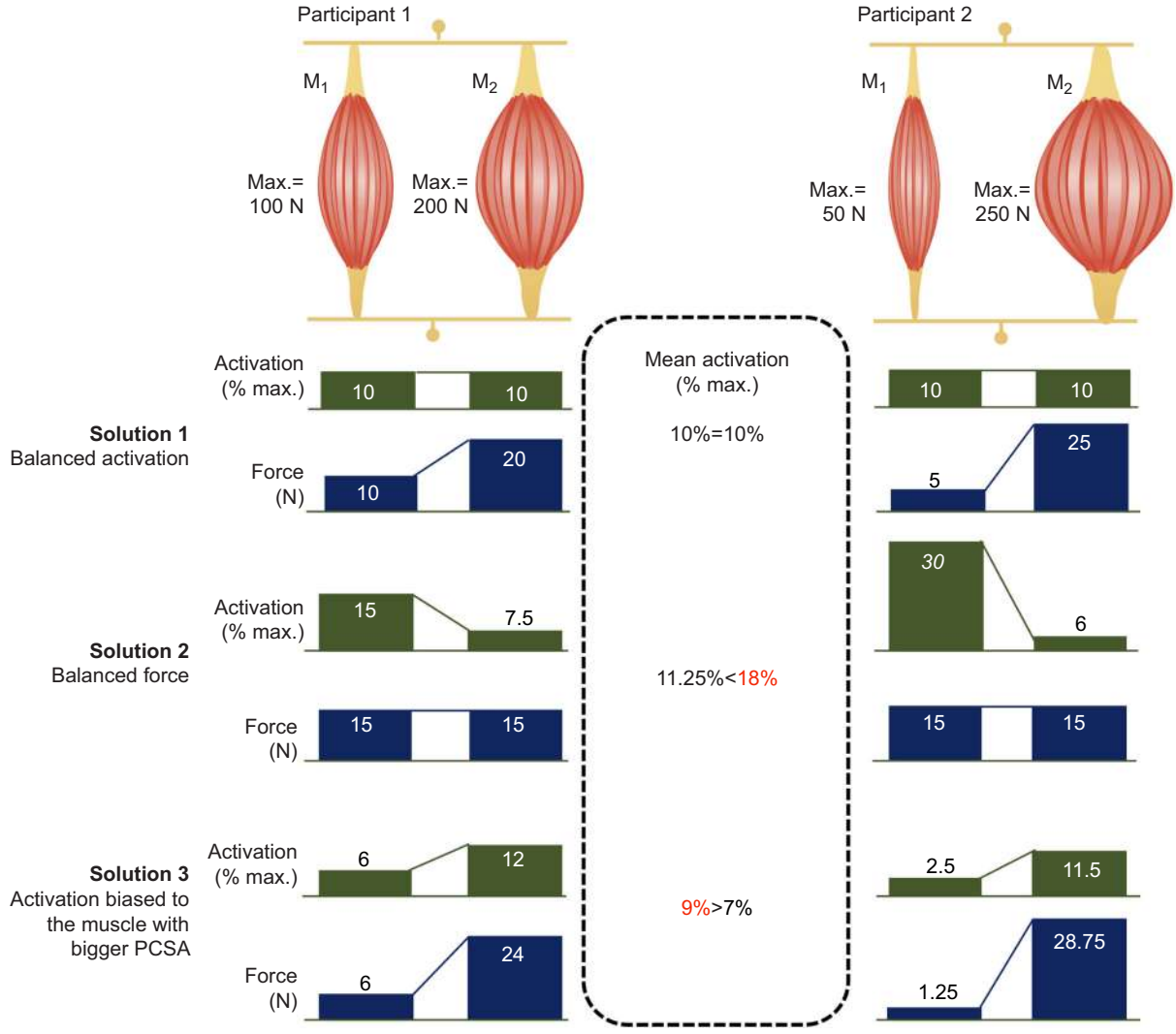

Fig. 1. Illustration to explain how the nervous system could account for individual differences in force-generating capacity between synergist muscles. M1 and M2 are two synergist muscles acting across the same joint(s). In the present case, M1 and M2 can be the gastrocnemius medialis and lateralis. Solution 1: activation is equally shared between synergist muscles, in which case the imbalance of force would match the imbalance of the force-generating capacity. Solution 2: the force-sharing strategy is similar among individuals with either balanced or imbalanced force between synergist muscles. In this latter case, the distribution of activation would vary between individuals. Solution 3: the muscle with the higher force-generating capacity receives greater activation, in which case the overall activation would be reduced but a large imbalance of force would exist. Note that there is a solution 4 (not shown) in which there is no specific coupling between activation and force-generating capacities.

biarticular muscles (GL and GM) and one monoarticular muscle (SOL), providing the opportunity to test whether a similar coupling between the distribution of activation and the distribution of force-generating capacity exists between synergist muscles with different functions.

The overall aim of this study was to determine the relationship between the ratio of activation measured during an isometric submaximal plantarflexion task and the ratio of force-generating capacity between the three heads of the triceps surae. The comparison of the GM and GL enables us to understand the activation distribution of two muscles having identical functions and very different force-generating capacities, while the comparison of SOL and both gastrocnemii (Gas) provides insight into the activation distribution of muscles with different functions. We tested two hypotheses: (1) a positive correlation between GM/Gas activation and GM/Gas PCSA would exist, demonstrating a coupling between the distribution of activation and the distribution of force-generating capacity for the GM and GL (solution 3, Fig. 1) but not for muscles with different functions (SOL and Gas), and (2) this coupling would contribute to reduce the overall activation of the triceps surae and the metabolic cost. Further, we described the inter-individual variability of the force-sharing strategies. Data are discussed in relation to possible mechanical effects on the Achilles tendon.

MATERIALS AND METHODS

Participants

The study was conducted with 20 healthy volunteers (age: 26 ±6 years, height: 173±11 cm, body mass: 64.3±12.4 kg; 10 males and 10 females). Participants had no history of lower leg pain that had limited function or required them to seek intervention from a healthcare professional within the past 6 months. Participants were informed of the methods used before providing written consent. The experimental procedures were approved by the local ethics committee (Rennes Ouest V, CPP-MIP-010) and all procedures adhered to the Declaration of Helsinki.

Protocol

Within a 2-month period, participants attended three sessions: one magnetic resonance imaging session, where images were taken and used to measure muscle volume and tendon moment arm (moment arm data not reported here); and two experimental sessions during which they performed a series of maximal and submaximal isometric plantarflexion tasks while muscle activation was recorded. The two experimental sessions were interspaced by at least 1 day, in order to test the between-day reliability of muscle activation strategies. Measurements of fascicle length and pennation angle needed for functional PCSA estimation were performed following the plantarflexion tasks, during one of the two experimental sessions.

During the experimental sessions, the participants performed isometric plantarflexion tasks lying prone (hip and knee fully extended) on a dynamometer (Con-Trex, CMV AG, Dübendorf, Switzerland). This knee position ensured a contribution of the three heads of the triceps surae to plantarflexion torque. The right foot was fixed to the dynamometer with inextensible straps. After a standardized warm-up, the participants performed five maximal isometric voluntary ankle plantarflexions [maximal voluntary contractions (MVCs)] for 3 s, with 120 s rest in between. Two out of the five MVCs were randomly chosen to test the voluntary activation level using the twitch interpolation technique. This procedure (described in detail below) aimed to determine whether the participants produced true maximal efforts. The submaximal tasks involved: (i) submaximal isometric torque-matched tasks set at 20% of MVC, and (ii) increasing isometric plantarflexion torque linearly from a relaxed state to 70% of MVC over a 10-s period. Each submaximal task was repeated four times (eight contractions in total) in a random order. Feedback of the torque output was displayed to the experimenter and the participant.

Estimation of muscle activation

Surface electromyography

Myoelectrical activity was collected from three muscles of the right leg: GM, GL and SOL. Skin was first shaved and cleaned with alcohol to minimize the skin–electrode impedance and facilitate electrode fixation. For each muscle, a pair of surface Ag/AgCl electrodes (diameter of the recording area: 5 mm; Kendall Medi-Trace^{TM}, Canada) was attached to the skin with a ∼20 mm inter-electrode distance (centre-to-centre). Electrode location was checked with a B-mode ultrasound (v11.0, Aixplorer, Supersonic Imagine, Aix-en-Provence, France) to ensure that they were positioned away from the borders of the neighbouring muscles and aligned with fascicle direction. Electrode cables were well secured to the skin with adhesive tape to minimize movement artefacts. EMG signals were pre-amplified close to the electrodes and digitized at 1000 Hz using an EMG amplifier unit (ME6000, Mega Electronics Ltd, Finland).

Voluntary activation level

For each muscle, the EMG amplitude recorded during submaximal contractions was normalized to that measured during MVCs. It was therefore critical that each participant produced a true maximal contraction. To verify that the plantar flexors were maximally activated, a doublet electrical stimulus (inter-stimulus interval: 10 ms; duration of the stimulus: 1 ms; amplitude: 400 V) was delivered during two of the five MVCs, by a constant current stimulator (DS7AH, Digitimer, UK) through two electrodes. This was delivered to the tibial nerve using the self-adhesive cathode (50 mm diameter), placed over the nerve in the popliteal fossa, and the anode (80×130 mm), placed over the anterior tibial tuberosity. To determine the maximal amplitude of the resting twitch, the output current was incrementally increased (from 0 mA, with an incremental step of 5 mA) until a maximum ankle plantarflexion torque was reached despite an increase in current intensity. To ensure maximal response during testing, a supramaximal stimulus intensity of 120% of the intensity previously determined was used (mean: 127.5±38.6 mA). Participants were informed about the electrical stimulation just prior to these particular contractions. The supramaximal doublet stimulus was delivered during the plateau of the MVC, and within 5 s in the subsequent rest period to elicit superimposed and resting twitches, respectively.

Mechanical and electromyography data analysis

Force and EMG signals were processed using MATLAB (The MathWorks, Natick, MA, USA). Force signals were low-pass filtered at 10 Hz. Then, MVC torque was calculated from the maximal contractions performed without twitch interpolation as the maximal torque over a 300-ms moving average. The percentage of voluntary activation was measured from the torque signal according to the equation of Todd et al. (2004):

$$\text{Voluntary activation} = \left(1 - \frac{\text{Superimposed twitch}}{\text{Resting twitch}}\right) \times 100. \quad (1)$$

Raw EMG signals were first visually inspected for noise or artefact. Among the 440 trials [11 trials (3 MVCs+4 submaximal trials+4 ramp trials)×2 sessions×20 participants], 13 trials (8 submaximal tasks and 5 ramp trials) were excluded because of electrical noise confirmed by a fast Fourier transformation analysis. EMG results were averaged between the remaining trials such that there were no missing data in the statistics. The maximal root mean square EMG (EMG_{RMS}) was calculated from the MVCs performed without twitch interpolation as the maximal EMG_{RMS} value over a 300 ms time window. During the submaximal isometric force-matched tasks, the EMG_{RMS} was calculated over 5 s at the middle of the force plateau. During the ramp tasks, EMG_{RMS} was calculated over 300 ms time windows and linearly interpolated to a torque-scale ranged from 0% to 70% of MVC. For each muscle, these values were normalized to the maximal EMG_{RMS} measured during the MVC ($EMG_{RMS,max}$). The ratio of activation (%) was calculated from these normalized values as follows:

$$\frac{\text{Muscle } i}{\text{Triceps surae}} = \frac{EMG_{RMS,i}}{EMG_{RMS,GM} + EMG_{RMS,GL} + EMG_{RMS,SOL}} \times 100. \quad (2)$$

Note that the GM/Gas ratio (%) was also considered and calculated as follows:

$$\frac{GM}{Gas} = \frac{EMG_{RMS,GM}}{(EMG_{RMS,GM} + EMG_{RMS,GL})} \times 100. \quad (3)$$

Muscle physiological cross-sectional area

Because of the pennated structure of the three muscle heads, the whole component of the force developed by the fibres does not act in the line of action (Haxton, 1944). Therefore, the pennation angle was considered for functional PCSA calculation, as proposed in previous work (Lieber, 2002; Sacks and Roy, 1982). Functional PCSA was calculated as follows:

$$PCSA = \frac{V}{L_f} \times \cos(\theta_p), \quad (4)$$

where V is muscle volume in cm^3, L_f is fascicle length in cm and θ_p is pennation angle in deg. As for EMG (Eqns 2 and 3), the following ratios of PCSA were calculated: GM/Gas, GM/TS, GL/TS and SOL/TS.

Muscle volume

Volumetric acquisitions of the lower leg (from heel to mid-thigh) were performed using a 3T magnetic resonance imaging scanner (Ingenia, Phillips, The Netherlands) using a three-dimensional e-THRIVE sequence (repetition time: 6.0 ms, echo time: 3.0 ms, field of view: 400×400×199.5 mm, voxel size: 0.70×0.70×3.00 mm, flip angle: 10 deg). Slice thickness was 6 mm without an inter-slice gap. This sequence was chosen to enhance the separation between muscles. Two to three volumes were acquired to cover the whole lower leg, with the participants in supine position, lying with their hip and knee fully extended, and the foot held perpendicular to the shank. Magnetic resonance images were analysed using 3D image analysis software (Mimics, Materialise, Belgium). GM, GL and SOL were segmented manually on each slice by an experienced examiner, from the distal slice, where the SOL could first be visualized to the most proximal slice, where the GM and GL insertions were visible. As GL and SOL were fused in some slices within the proximal region, we used the visible landmarks on the preceding and subsequent images to assist the segmentation between muscles. A 3D reconstruction was performed (Mimics; option=optimal; Fig. 2) before the volume of each muscle was calculated.

Muscle fascicle length and pennation angle

An ultrasound scanner (Aixplorer v11.0, Supersonic Imagine, France) coupled with a 50 mm linear probe (4–15 MHz; SuperLinear 15-4, Vermon, Tours, France) was used in panoramic mode to assess the fascicle length of GM, GL and SOL muscles. This mode uses an algorithm that fits a series of images, allowing scanning of entire fascicles within one continuous scan (Hedrick, 2000). The advantage of this method over classical measurements from one B-mode image is that it does not require extrapolating the non-visible part of the fascicle, thus providing a more accurate estimation of muscle fascicle length (Noorkoiv et al., 2010).

To verify the accuracy of the in-built panoramic mode, we performed a pilot study on a bovine sample (approximately 30×10×5 cm). Four needles were inserted through the meat sample. The needle extremities remained visible outside the meat, and a retro-reflective marker (diameter: 10 mm) was attached to each needle extremity (a total of eight markers). The inter-needle distances were determined using an optoelectronic motion capture system composed of four cameras (Flex 13, Optitrack, Natural Point, USA). The inter-needle distances (from midline to midline) were 4.32, 4.85 and 6.75 cm; and the straight distance between the first and fourth needles was 15.16 cm. Three ultrasound panoramic scans were performed; the reliability of the inter-needle distance measured during these three trials was excellent (for all distances, CV<1.3%). The three trials were averaged, and then compared with the distances measured using the motion capture system, to test the accuracy of the measurement. The absolute error percentage was lower than 2.2%.

For the fascicle length and pennation angle measurement protocol, participants were placed in the same position as was used for the experimental tasks, i.e. lying prone, hip and knee fully extended, and the ankle maintained at 0 deg. The proximal and distal insertions and the medial and lateral borders of the GM and GL were located using B-mode ultrasound. A line was drawn on the skin at the middle of the muscle belly from the distal to the proximal insertion following the fascicle path. The US probe was then placed on the line and oriented within the plane of the fascicles. The scan consisted of moving the probe along this line with minimal pressure applied to the skin, to minimize compression of the muscle. Two reconstructed panoramic images were recorded per muscle (Fig. 3). To assess the SOL fascicle length and pennation angle, the US probe was placed over the GL myotendinous junction. This probe location was chosen because fascicles were clearly visible. Although the SOL has a multipennate structure, a recent study investigating the 3D architecture of the whole SOL muscle reported no difference in fascicle length between its four compartments (medial–anterior, lateral–anterior, medial–posterior and lateral–posterior) (Bolsterlee et al., 2018). We therefore considered that our probe location provided fascicle length data that were representative of the whole muscle. As SOL fascicle length was shorter than that of the GM and GL, entire fascicles were measured from two conventional B-mode ultrasound images. For each image, we aimed to measure three fascicles (proximal, mid distance and distal) leading to a total of up to six fascicles analysed per muscle and per operator. Owing to technical problems with some images, an average of 6, 5.5 and 3.9 fascicles were measured for the GM, GL and SOL, respectively. As some fascicles exhibited a small curvature, we used a segmented line with a spline fit to model the fascicles and calculate their length (Fig. 3; ImageJ V1.48, National Institutes of Health, Bethesda, MD,

Journal of Experimental Biology (2018) 221, jeb187260. doi:10.1242/jeb.187260

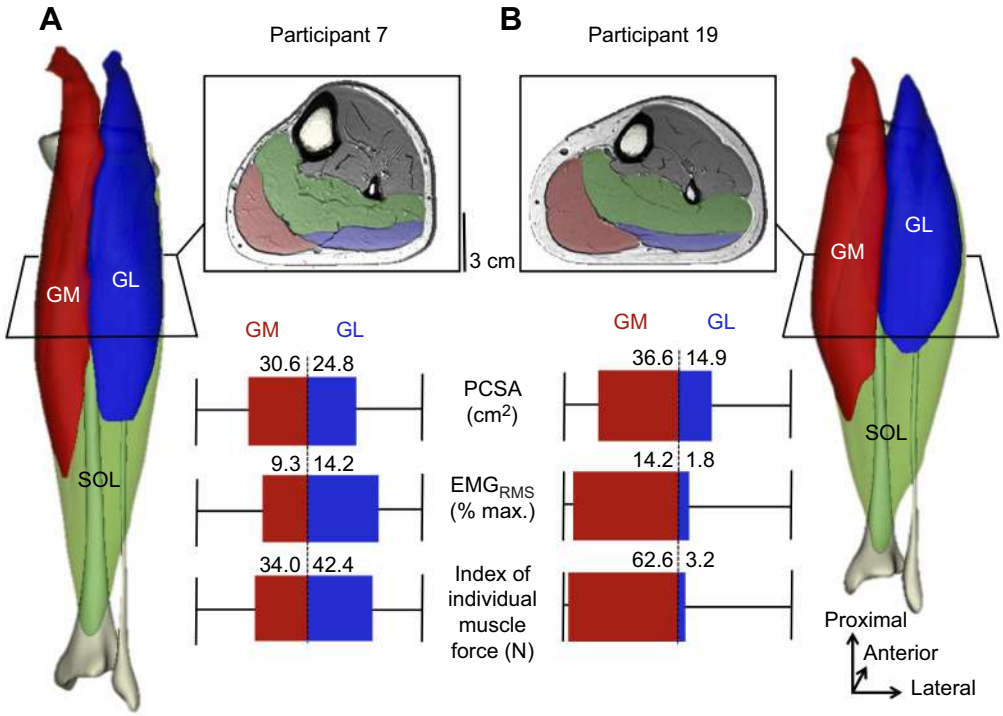

Fig. 2. Individual examples of data from two participants. Each muscle was manually segmented from each axial image, as depicted in the middle-top of the figure. The gastrocnemius medialis [GM (red)], gastrocnemius lateralis [GL (blue)] and soleus [SOL (green)] are shown. Example axial slices are from ~33% of the proximo-distal part of the leg. Muscle volumes were reconstructed in 3D (lateral panels). Then, measures of muscle balance were calculated (middle-bottom panel). (1) Functional physiological cross-sectional area (PCSA) was calculated from muscle volume, fascicle length and pennation angle (measured using panoramic ultrasound images, see Fig. 3). (2) Muscle activation was measured during a submaximal isometric plantarflexion task performed at 20% of the maximal voluntary contraction (EMG_{RMS}; % max.). (3) The index of individual muscle force was calculated by multiplying PCSA, muscle activation and specific tension (based on theoretic values; see Materials and Methods). In the examples here, the GM/Gas index of force was 44.5% for participant 7 (A) and 95.1% for participant 19 (B), which highlights an extreme difference between participants.

USA). The pennation angle was calculated as the angle between the fascicles and the deep aponeurosis of the muscle. Values were then averaged across fascicles within a muscle to obtain a representative fascicle length and pennation angle of the whole muscle.

Estimation of an index of metabolic cost

As indicated above, muscle force is proportional to the PCSA of active muscle fibres. Therefore, muscles with long fibres require a larger active muscle volume to generate a given force (Biewener, 2016). As such, they consume more ATP per unit force generated than muscles with short fibres. In this way, an index of overall metabolic cost was calculated by considering active muscle PCSA and muscle volume of muscle i, as follows:

$$\text{Index of metabolic cost} = \sum_{i=1}^{3} \frac{\text{PCSA}_i \times \text{EMG}_{\text{RMS},i}}{V_i}, \quad (5)$$

where muscles 1 to 3 are the GM, GL and SOL, respectively.

Estimation of an index of individual muscle force

Even though individual muscle force can be measured in freely moving animals using force transducers placed on each subtendon (Herzog et al., 1993; Walmsley et al., 1978), this invasive technique cannot be used in humans. The force produced by a muscle depends on both the activation it receives and several biomechanical factors such as its PCSA, force–length and force–velocity relationships, and specific tension (P_0). Because the force–length and force–velocity relationships remain challenging to estimate *in vivo*, we focused on isometric contractions during which we considered that these relationships played a minor role in the difference of force produced by the synergist muscles. In other words, we considered that the difference of force between the synergist muscles depended mainly on their PCSA, their activation and their specific tension. Therefore, an index of muscle force (N) was calculated for the 20% hold contraction as follows:

$$\text{Index of force} = \text{PCSA} \times \text{EMG}_{\text{RMS,normalized}} \times P_0, \quad (6)$$

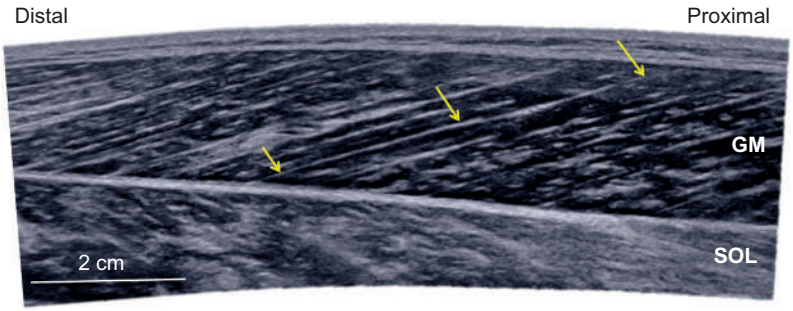

Fig. 3. Individual example of a panoramic ultrasound image for the gastrocnemius medialis (GM) muscle. This image was used to calculate GM fascicle length. The yellow arrows indicate a fascicle. SOL, soleus.

where EMG_{RMS} is expressed as a percentage of the $EMG_{RMS,max}$, PCSA in cm^2 and specific tension in N cm^{-2}. Given the size principle of orderly recruitment (Henneman and Oslon, 1965; Henneman et al., 1965), it is likely that small motor units were preferentially recruited at 20% of MVC. As each head of the triceps surae is composed by more than 20% of slow fibres (50.8, 46.9 and 87.7% for GM, GL and SOL, respectively) (Johnson et al., 1973), we reasonably assumed that only slow fibres were active. We therefore considered values of specific tension reported for slow fibres, i.e. 12 N cm^{-2} (Fitts et al., 1989; Larsson and Moss, 1993). As for EMG and PCSA, the following ratios of force index were calculated: GM/Gas, GM/TS, GL/TS and SOL/TS.

Statistics

Statistical analyses were performed in Statistica v7.0 (Statsoft, Tulsa, OK, USA). Distributions consistently passed the Shapiro–Wilk normality test and all data are reported as means±s.d. To test the robustness of the activation strategies, the between-day reliability of the EMG data was tested using the intra-class correlation coefficient (ICC) and the standard error of measurement (s.e.m.).

Separate repeated-measures ANOVAs were used to determine whether volume, fascicle length, functional PCSA and the PCSA/volume ratio were different between muscles [within-subject factor: muscle (GM, GL and SOL)]. Ratios of muscle activation and ratios of muscle force estimated during the submaximal tasks at 20% of MVC were compared separately with a repeated-measures ANOVA [within-subject factor: ratio (GM/Gas, GM/TS, GL/TS and SOL/TS)]. To test the effect of contraction intensity on the ratio of muscle activation, we performed a repeated-measures ANOVA for each ratio of activation separately (GM/Gas, GM/TS, GL/TS and SOL/TS) [within-subject factor: torque (every 10% from 10 to 70% of MVC)]. When appropriate, *post hoc* analyses were performed using the Bonferroni test.

To test the first hypothesis, we determined the relationship between the ratio of activation and the ratio of PCSA using Pearson's correlation coefficient. We only considered the GM/Gas and the SOL/TS ratios to understand the neuromechanical coupling of two muscles having identical (GM and GL) or different (SOL and Gas) functions. Note that the correlation made with GM/TS and GL/TS ratios would have contained redundant information with the other two ratios. To test the second hypothesis, we used Pearson's correlation coefficient to assess the relationship between ratios of activation and either the normalized EMG amplitude averaged across the three muscles or the index of metabolic cost. The level of significance was set at $P<0.05$.

RESULTS

Muscle activation

Voluntary activation level

The maximal isometric plantarflexion torque measured during the contractions performed without twitch interpolation was 124.0±28.8 Nm. Participants reached a voluntary activation level of 98.4±3.3% (range: 92.1–100%) and 99.1±2.4% (range 95.0–100%) during the first and second sessions, respectively. As such, we considered that the maximal EMG_{RMS} measured during the MVC tasks represented the maximal activation for all of the studied muscles.

Isometric contractions at 20% of MVC

The between-day reliability of the normalized EMG_{RMS} values was excellent (ICC>0.81, SEM<2.8% of $EMG_{RMS,max}$; Table 1). Reliability of the ratio of activation was good to excellent (ICC>0.71, s.e.m.<6.8%; Table 1). Overall, this provides evidence that the coordination strategies were robust between days. Thus, EMG data were averaged between the two sessions for further analysis.

Table 1. Between-day reliability of muscle activation (EMG_{RMS}) and activation ratios measured during the submaximal isometric force-matched tasks at 20% of maximal voluntary contraction (MVC)

	Muscle activation			Activation ratios			
	GM	GL	SOL	GM/Gas	GM/TS	GL/TS	SOL/TS
ICC	0.83	0.84	0.81	0.80	0.81	0.76	0.71
s.e.m. (%)	2.0	1.3	2.8	6.8	5.6	3.5	5.4

ICC, Intra-class coefficient of correlation; s.e.m., standard error of measurement (expressed in % of $EMG_{RMS,max}$ for EMG_{RMS} values and as % for the ratios); GM, gastrocnemius medialis; GL, gastrocnemius lateralis; SOL, soleus; TS, triceps surae. n=20.

The activation ratios during the isometric 20% MVC contractions were: GM/Gas, 65.0±13.2% (range: 37.7–88.7%); GM/TS, 36.3±11.4% (range: 19.1–57.0%); GL/TS, 18.8±6.4% (range: 7.3–31.6%); and SOL/TS, 44.8±8.9% (range: 26.4–61.0%). The GL/TS ratio was lower than both the GM/TS ratio ($P<0.001$) and the SOL/TS ratio ($P<0.001$); there was no difference between the GM/TS and SOL/TS ratios despite the P-value being close to significance ($P=0.06$). Notably, there was a large variability between individuals (Fig. 4).

Isometric ramp contractions

There was a main effect of torque level on both the GL/TS ($P<0.001$) and SOL/TS ($P<0.001$) ratios of activation (Fig. 5). Specifically, the GL/TS ratio measured at 10% of MVC was significantly lower than that measured at 40% of MVC and above (all $P<0.01$). In other words, the relative contribution of the GL increased with contraction intensity. Also, the SOL/TS ratio measured at 10% of MVC was significantly higher than that measured at 50% of MVC and above (all $P<0.02$). This indicates that the contribution of SOL relative to the whole triceps surae decreased with contraction intensity. Together, these results provide evidence that the contribution of GL and SOL tend to be closer to 33% (i.e. balanced activation between the three muscles) as contraction intensity increased. Note that the GM/TS ratio of activation was not affected by contraction intensity (main effect of torque level: $P=0.97$), and contributed ∼33% of the total triceps surae activation throughout the ramp contraction.

Physiological cross-sectional area

There was a main effect of muscle ($P<0.001$) on volume, with SOL volume being systematically larger than that of GM ($P<0.001$) and GL ($P<0.001$). GM volume was also larger than that of GL ($P<0.001$; Table 2). There was a main effect of muscle ($P<0.001$) on fascicle length. Specifically, SOL exhibited a shorter fascicle length than both GM ($P<0.001$) and GL ($P<0.001$). Further, GM fascicle length was shorter than GL fascicle length ($P<0.001$; Table 2). There was a main effect of muscle ($P<0.001$) on pennation angle. Specifically, GL had a smaller pennation angle than both GM ($P<0.001$) and SOL ($P<0.001$). There was no difference between GM and SOL.

Consistent with volume and fascicle length differences, there was a main effect of muscle ($P<0.001$) on functional PCSA (Table 2). SOL PCSA was systematically larger than GM ($P<0.001$) and GL PCSA ($P<0.001$), and GM PCSA was larger than GL PCSA ($P<0.001$). The ratio of PCSA was 68.6±4.6% (range 55.2–74.0%) for GM/Gas, 27.2±4.0% (range 17.9–33.1%) for GM/TS,

Journal of Experimental Biology (2018) 221, jeb187260. doi:10.1242/jeb.187260

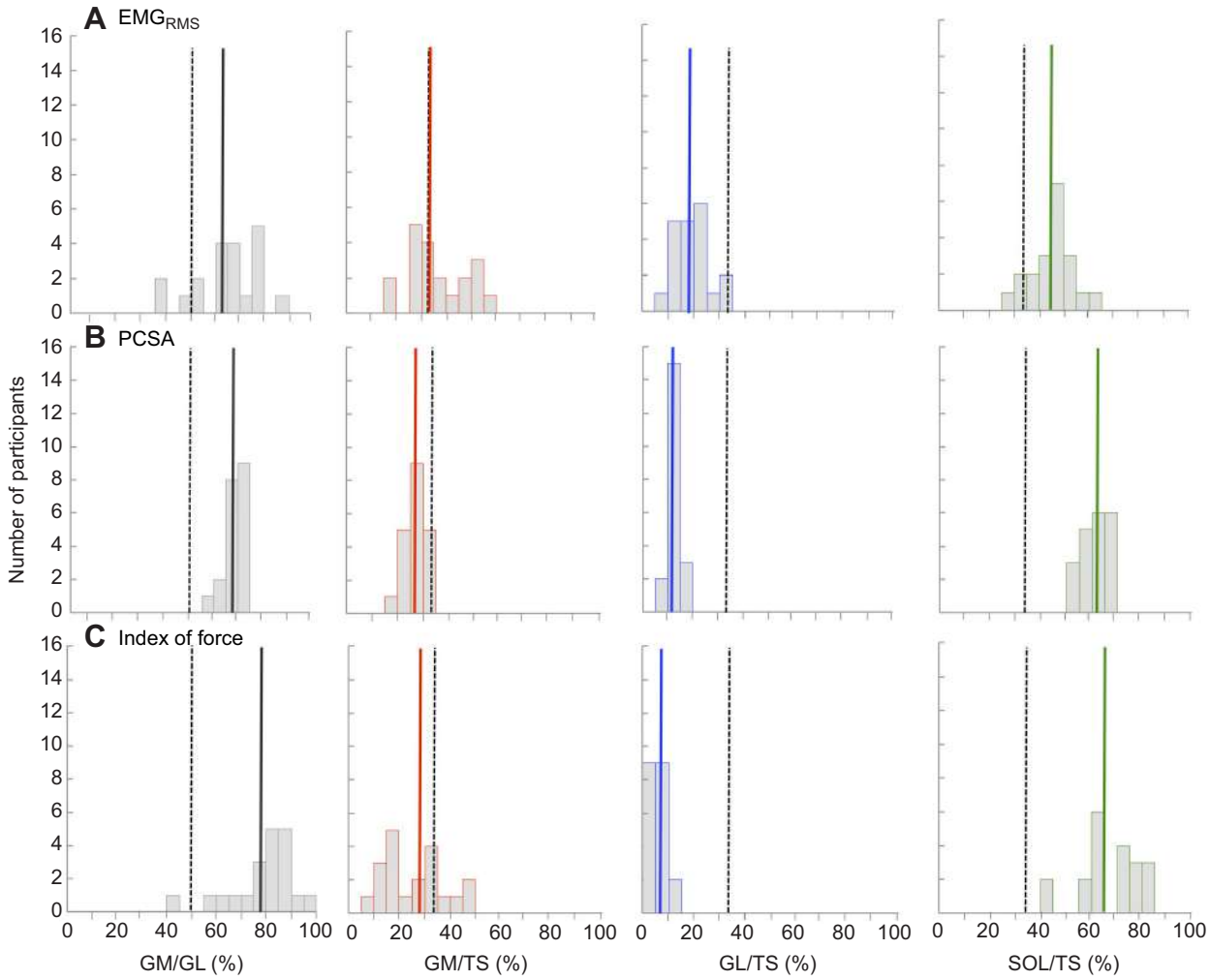

Fig. 4. Group distribution of (A) the ratio of activation (EMG_{RMS}), (B) the ratio of physiological cross-sectional area (PCSA) and (C) the ratio of index of force. Results are from the submaximal contraction performed at 20% of the maximal voluntary contraction. Vertical bold lines depict the mean results reported in the present study, and the dashed lines depict what would be a balanced ratio between synergist muscles (i.e. 50% for GM/Gas and 33.3% for ratios with three muscles considered). GM, gastrocnemius medialis; GL, gastrocnemius lateralis; SOL, soleus. TS, triceps surae. *n*=20.

12.4±2.4% (range 8.8–19.5%) for GL/TS and 60.4±5.2% (range 50.6–68.5%) for SOL/TS. The variability between participants was large (Fig. 5).

Relationship between activation and muscle PCSA

There was a significant positive correlation (r=0.53, P<0.005) between the ratio of GM/Gas activation measured during the force-matched task at 20% of MVC and the ratio of GM/Gas PCSA (Table 3). This indicates that the greater the force-generating capacity of GM compared with GL, the stronger bias of activation to the GM. Significant positive correlations were also observed when considering this activation ratio measured during the ramp contraction at intensities between 10 and 50% of MVC (0.51<r<0.62, all P<0.025; Table 3). No significant correlation was observed at 60 and 70% of MVC when the ratio of GM/Gas activation tended toward 50%. When considering the SOL/TS ratios (activation versus PCSA), there was no significant correlation (all r<0.33, all P>0.05; Table 3).

Consequences of the neuromechanical coupling on overall activation and metabolic cost

To interpret the consequences of the coupling between the ratio of GM/Gas activation and the ratio of GM/Gas PCSA, we first explored the relationship between the ratio of GM/Gas activation and the normalized EMG amplitude averaged across the three muscle heads. We observed a negative significant correlation at 30% of MVC and above (–0.66<r<–0.42, P<0.05; Table 4, Fig. 6). This confirms the hypothesis that the coupling between the distribution of PCSA and the distribution of activation contributes to a reduction of the overall activation of the triceps surae. Interestingly, slightly larger correlations were observed when considering the index of metabolic cost (–0.74<r<–0.52, P<0.05; Table 4, Fig. 6). Fig. 6 depicts a 3D representation of the relationship between GM/Gas activation, contraction intensity and either mean activation [R^2 (linear fit)=0.94; Fig. 6A] or the index of metabolic cost [R^2 (linear fit)=0.93; Fig. 6B]. Note that no significant correlation was observed when considering the ratio of SOL/TS activation (all r<–0.41 for correlations with activation and all r< 0.39 for correlations with the index of metabolic cost).

Inter-individual variability of force-sharing strategies

For the sake of clarity, indexes of force are reported only for the submaximal contraction performed at 20% of MVC. Using Eqn 6, indices of force were 69.0±37.1, 17.3±11.0 and 200.5±103.1 N for the GM, GL and SOL, respectively. The mean ratio of force index was 78.9±12.6%, 26.2±11.8%, 6.0±2.5% and 67.8±11.6% for

Journal of Experimental Biology (2018) 221, jeb187260. doi:10.1242/jeb.187260

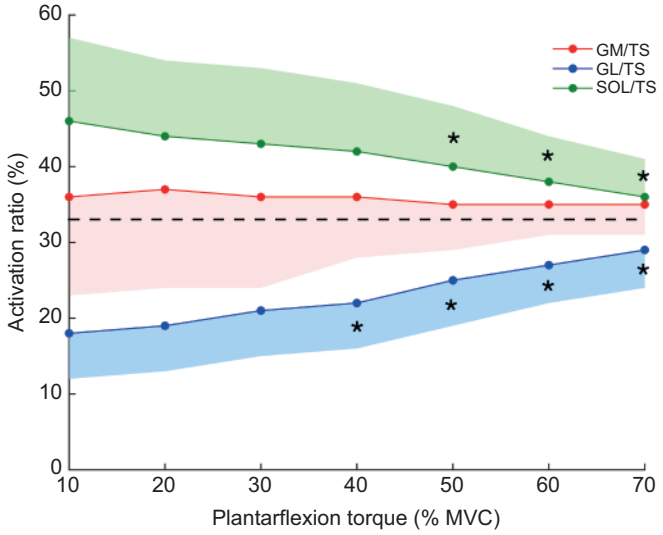

Fig. 5. Ratios of muscle activation as a function of contraction intensity. GM/TS (red), GL/TS (blue) and SOL/TS (green) logically converge to 33% (balanced activation) as contraction intensity increased. MVC, maximal voluntary contraction; GM, gastrocnemius medialis; GL, gastrocnemius lateralis; SOL, soleus; TS, triceps surae. * indicates significant difference compared with 10% of MVC. *n*=20.

GM/Gas, GM/TS, GL/TS and SOL/TS, respectively. The GL/TS force ratio was significantly lower than that for GM/TS ($P<0.001$) and SOL/TS ($P<0.001$). The GM/TS force ratio was significantly lower than that for SOL/TS ($P<0.001$). Very large variability between individuals is highlighted in Fig. 4.

DISCUSSION

This study has several novel findings. First, although there was no significant correlation between the distribution of activation and the distribution of force-generating capacity between monoarticular and biarticular muscles (SOL/TS ratio), a positive correlation was observed when considering the two biarticular muscles that share the same function (GM/Gas ratio). Specifically, the greater the force-generating capacity of the GM compared with the GL, the stronger bias of activation to the GM. Second, a higher ratio of GM/Gas activation was associated with lower triceps surae activation and metabolic cost. Third, there was a significant force imbalance between synergist muscles, the magnitude of which varied greatly between participants. These results provide insight into our understanding of the interplay between the activation a muscle receives and its torque-generating capacity. Also, these observations may have clinical relevance as they provide the impetus to consider individual muscle coordination strategies as an intrinsic risk factor to the development of Achilles tendinopathy.

Distribution of muscle activation

Because of its important role during balance and locomotion, the triceps surae has received much attention in the literature. In the studies that focused on muscle activation, GM and GL muscles are often considered equivalent such that only the GM (Duysens et al., 1991) or GL (Kyrolainen and Komi, 1994) is measured. Further, biomechanical models often consider the GL and GM as a single muscle (Herzog et al., 1991; Winter and Challis, 2008). However, multiple studies provide evidence that activation is not balanced between these muscles, with the vast majority of studies reporting higher activation for the GM than the GL during a wide variety of tasks, e.g. standing (Héroux et al., 2014), calf raises (Fiebert et al., 2000; Riemann et al., 2011) and submaximal isometric plantarflexion (Cresswell et al., 1995; Lacourpaille et al., 2017; McLean and Goudy, 2004). All these results are in line with our results showing on average a two times higher activation of the GM than the GL during the isometric plantarflexion at 20% of MVC. In the present study, the SOL exhibited a slightly greater activation level than both the GM and GL, which is consistent with results from Mademli and Arampatzis (2005), but inconsistent with those of Cresswell et al. (1995) and Masood et al. (2014), all being performed during isometric submaximal tasks but in varying positions. Note that an activation biased toward the SOL muscle, which exhibits both the biggest PCSA and the highest slow-twitch fibre content, may reduce the metabolic cost of the contraction at low contraction intensity, as discussed below. Logically, the imbalance of activation across the GM, GL and SOL tends to disappear at higher contraction levels (70% of MVC during the ramped contraction; Fig. 5), where near-complete activation of all synergists is required. It is important to note that the aforementioned results are derived from group data that are not representative of each individual.

The vast majority of studies on muscle coordination report values averaged from a group of individuals, making it impossible to appreciate the individual differences in the activation strategies that inevitably exist. Here, we report a wide range of activation ratio during a standardized isometric single-joint task. For example, during the 20% of MVC hold contraction, SOL/TS and GM/Gas activation ratios ranged from 26.4% to 61.0% and from 37.7% to 88.7%, respectively. To the best of our knowledge, this inter-individual variability has received little attention. During gait, Ahn et al. (2011) reported large differences in the ratio of activation between the GM and GL, with seven out of the 10 participants activating their GM more than their GL, and the other three

Table 2. Muscle architecture

	GM			GL			SOL		
	Males	Females	Mean	Males	Females	Mean	Males	Females	Mean
Volume (cm^3)	280.7±48.5	218.7±40.6	249.7±53.9*	171.2±22.9	104.2±20.4	137.7±40.3‡	489.4±75.5	350.9±60.8	420.1±97.5*,‡
FL (cm)	5.1±0.8	5.8±0.7	5.4±0.8*	6.2±0.5	6.7±0.9	6.4±0.7‡	3.6±0.9	4.2±0.6	3.9±0.8*,‡
PA (deg)	21.6±3.8	17.3±1.7	19.5±3.6*	13.2±2.7	9.1±1.9	11.2±3.1‡	24.4±7.0	16.3±3.8	20.3±6.9*
PCSA (cm^2)	54.7±11.7	37.5±5.3	46.1±13.2*	27.0±3.3	15.5±2.9	21.3±6.6‡	127.9±25.4	80.3±14.3	104.1±31.6*,‡
PCSA/volume (10^3 cm^{-1})	19.5±3.0	17.4±2.2	18.5±2.8*	15.8±1.2	15.1±1.9	15.5±1.6‡	26.3±4.5	23.1±2.8	24.7±4.0*,‡

Volume, fascicle length (FL), pennation angle (PA), physiological cross-sectional area (PCSA) and the ratio PCSA/volume are reported for males and females separately to facilitate comparison with other works. Statistics are only reported for mean values; *n*=20. GM, gastrocnemius medialis; GL, gastrocnemius lateralis; SOL, soleus.

*Indicates significant difference with GL.

‡Indicates significant difference with GM.

Journal of Experimental Biology (2018) 221, jeb187260. doi:10.1242/jeb.187260

Table 3. Correlation coefficients between the ratio of EMG_{RMS} and the ratio of physiological cross-sectional area (PCSA)

	Activation ratios	
% MVC	GM/Gas	SOL/TS
10	0.59*	0.10
20 hold	0.53*	0.34
20	0.62*	0.11
30	0.61*	0.11
40	0.60*	0.03
50	0.51*	−0.03
60	0.34	−0.26
70	0.20	−0.25

MVC, maximal voluntary contraction; GM, gastrocnemius medialis; GL, gastrocnemius lateralis; SOL, soleus; TS, triceps surae. 20 hold represents the results obtained during the isometric contractions performed separately at 20% of MVC.
*Indicates a significant correlation (P<0.05). n=20.

Table 4. Correlation coefficients between the ratio of EMG_{RMS} and both the mean activation of the triceps surae and the index of overall metabolic cost

% MVC	GM/Gas EMG versus mean TS activation	GM/Gas EMG versus overall metabolic cost
10	−0.12	−0.21
20 hold	−0.21	−0.37
20	−0.30	−0.38
30	−0.42*	−0.52*
40	−0.56*	−0.62*
50	−0.55*	−0.65*
60	−0.59*	−0.74*
70	−0.66*	−0.68*

The ratios of EMG_{RMS} were estimated during the submaximal isometric tasks isometric performed at 20% (20 hold) of the maximal voluntary contraction (MVC) and from 0 to 70% of MVC. Indices of overall metabolic cost were calculated by considering active muscle PCSA and muscle volume. TS, triceps surae.
*Indicates a significant correlation (P<0.05). n=20.

participants activating their GM and GL nearly equally. However, interpretation of the individual differences during gait requires considerations. Because body weight may influence the contraction intensity of the calf muscles during gait and because we report that activation ratios are affected by even small changes in contraction intensity (Fig. 5), it is difficult to determine whether the variability of activation ratios observed during gait is explained by different mechanical demand related to different body weights and/or by actual differences in activation strategies. Activation ratios between the heads of the triceps surae measured during a standardized isometric task have been reported in two previous studies (Masood et al., 2014; McLean and Goudy, 2004). Their results are in line with our observation that large individual differences in activation strategies exist. The novelty of our study among others is to demonstrate the robustness of these activation ratios across time, allowing us to consider that they represent individual-specific strategies. Another novelty of this study is to consider the relationship with the force-generating capacities, and therefore the mechanical consequence of these individual strategies.

Coupling between muscle activation and PCSA

In this study, we considered both muscle activation and functional PCSA to interpret the mechanical consequences of individual differences in muscle activation. The SOL exhibited a much larger PCSA than both the GM (×2.6) and the GL (×5.5). This large PCSA imbalance was a prerequisite for the present study, which aimed to assess the mechanical coupling within a group of synergist muscles with large difference in PCSA. Overall, the PCSA and volume values we estimated are very close to those reported by Albracht et al. (2008) and Fukunaga et al. (1996), respectively. Inspection of data for individual participants revealed large variability of the PCSA distribution among the three heads of the triceps surae, albeit with smaller magnitude than that observed for activation. For example, the GM/Gas and SOL/TS PCSA ratios ranged from 55.2% to 74.0% and from 50.6% to 68.5%, respectively. To our knowledge, this is the first study to report such individual differences for this muscle group.

Our first aim was to determine the nature of the relationship between the ratio of activation and the ratio of functional PCSA (considered as force-generating capacity). We observed a positive correlation between GM/Gas activation and GM/Gas PCSA, indicating that the greater the force-generating capacity of the GM compared with the GL, the stronger bias of activation to the GM. This was observed for the 20% hold plantarflexion and during the ramp contraction from 10 to 50% of MVC (Table 3). This result is in line with previous findings (Hug et al., 2015), showing a similar correlation when considering the lateral and medial heads of the quadriceps.

In the present study, we also considered synergist muscles that share different functions, i.e. monoarticular for SOL and biarticular for GM and GL. When considering data averaged over the whole population, the ratio of SOL/TS activation was higher than both GM/TS and GL/TS activation ratios at low contraction intensities (Fig. 5). This strategy seems particularly economic considering that SOL exhibits the larger PCSA (Table 2) and the larger proportion of type I fibres (Johnson et al., 1973). In addition, its architecture with short fascicles (Table 2) leads to a lower metabolic cost per unit force. Indeed, for two muscles that are both producing the same force, that have the same volume and typology, but different fibre lengths (and PCSA), the muscle with the longer fibre lengths has a greater metabolic cost (for a review, see Biewener, 2016). However, this association between muscle activation and muscle architecture observed at the group level, from averaged data, could not explain the inter-individual variability in activation strategies. Indeed, we found no correlation between SOL/TS ratio activation and SOL/TS force-generating capacity at any of the contraction intensities. For the sake of clarity, we did not report the results for the SOL/GM and SOL/GL ratios, but it is important to note that considering these ratios did not change the outcome, i.e. there was no significant correlation between distribution of activation and distribution of PCSA ($-0.20<r<0.31$). Although we cannot rule out that this absence of significant correlation is explained by methodological considerations, as discussed below, we believe that difference in function between the SOL and the gastrocnemii might explain this result. Indeed, activation of biarticular muscles depends on moment demands at two joints (Prilutsky, 2000), making it complicated to comply at the same time with neuromechanical coupling and the constraints of the task. In other words, the distribution of activation between the monoarticular SOL muscle and the biarticular gastrocnemii muscles cannot be only determined by the difference of force-generating capacity between the SOL and the gastrocnemii, but also need to consider the task constraints, which depend on actions at both the ankle and knee joints. This is in accordance with previous results showing a partial uncoupling of SOL and gastrocnemii activity in response to altered torque and velocity during pedalling in humans (Wakeling and Horn, 2009), during paw shakes in cats (Smith et al., 1980) or during locomotion in cats

Journal of Experimental Biology (2018) 221, jeb187260. doi:10.1242/jeb.187260

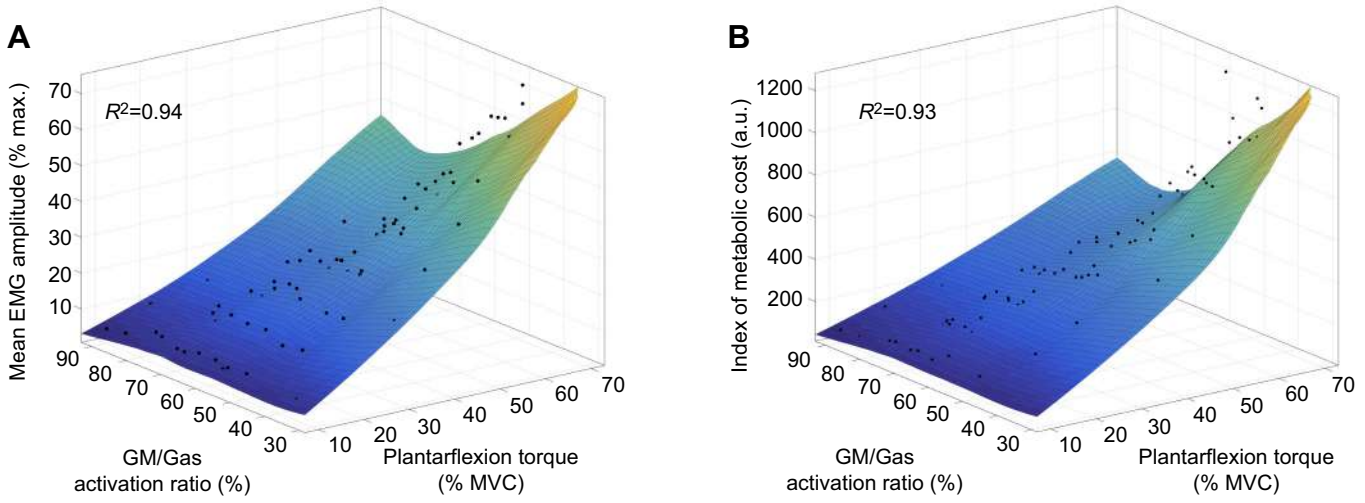

Fig. 6. Three-dimensional representation of the relationship between GM/Gas activation, contraction intensity and relationship between either (A) mean activation or (B) the index of metabolic cost. *n*=20.

(Walmsley et al., 1978). In the latter study, SOL force remained constant across speeds (from 0.6 to 3.0 m s^{-1}) while GM force increased with speed. As hypothesized for respiratory muscles (De Troyer et al., 2005), the distribution of muscle PCSA would be optimized to muscle function. As such, for muscles with multiple functions, PCSA might be optimized more for one function than another. The GM and GL muscles, involved in both plantarflexion and knee flexion, might have their PCSA set to knee flexion, such that knee flexion torque is maximized, while SOL might have its PCSA set to plantarflexion.

The absence of correlation when considering the distribution of activation and the distribution of PCSA between the SOL and the gastrocnemii might also be explained by the large difference in force-generating capacity, especially between the SOL and the GL. In the case of a positive coupling between activation and PCSA, large imbalances of force would be produced between these synergist muscles. These imbalances could ultimately have negative consequences for the Achilles tendon.

Benefits of the coupling between GM/Gas activation and GM/Gas PCSA

As presented in Fig. 1, a positive correlation between the distribution of force-generating capacity and the distribution of activation should lead to an overall lower activation, and thus a lower effort. This was partially confirmed by the negative correlation between the ratio of GM/Gas activation and the averaged normalized EMG amplitude observed during the ramp contraction at 30% of MVC and above (Table 4, Fig. 6). The lack of correlation at lower intensities (10 and 20% of MVC) could be explained by the contribution of other non-recorded plantarflexor muscles, which might have a greater relative contribution at these low intensities. For example, even though the participants were instructed to avoid compensatory strategies to produce plantarflexion torque, it remains possible that they used toe flexion at low intensities. Finally, it is also possible that the lack of significant correlation is explained by the relatively small sample size.

Similar results, with slightly larger coefficients of correlation (Table 4), were obtained when considering an overall index of metabolic cost calculated from the ratio PCSA/muscle volume and the relative muscle activation (Eqn 5). Because this index does not consider important parameters such as muscle typology, it represents only a crude estimate of metabolic cost. Despite this, we believe that the significant correlation between this index and the ratio of GM/Gas activation provides preliminary evidence that the GM/Gas activation strategy contributes to reduce the overall metabolic cost of the task.

It is important to note that in the triceps surae configuration, the muscle with the shortest fascicle length (SOL) is also the one with the biggest volume, and that the muscle with the longest fascicle length has the smallest volume (GL). This naturally results in the best combination to produce force: the muscle capable of producing the highest amount of force (with the biggest PCSA) is also the one with the most economic metabolic cost (smallest PCSA/volume ratio because of its smallest fascicle length; for a review, see Biewener, 2016). This can, at least in part, explain the relationship between the index of metabolic cost and the ratio of GM/Gas activation, and the higher ratio of SOL/TS activation observed at the group level.

Overall, these results align particularly well with theoretical models (Crowninshield and Brand, 1981; Dul et al., 1984). For example, Crowninshield and Brand (1981) proposed that individual muscle forces are selected such that the sum of muscle stresses cubed is minimized. Considering the linear relationship often reported between EMG amplitude and muscle force during isometric contractions, it is reasonable to consider that the mean activation that we calculated represents an index of the mean muscle stress. If we considered the cubed sum of normalized EMG amplitude instead of the sum, similar negative correlations with the ratio of GM/Gas activation were observed. Even though the model proposed by Crowninshield and Brand (1981) also predicted a positive correlation between SOL/TS PCSA and SOL/TS stress (or EMG), this was not confirmed by our experimental study. Another model proposed by Dul et al. (1984) considered that force-sharing strategy is chosen such that fatigue is minimized. Their model included information about the fibre type content in addition of muscle force-generating capacity. This approach echoes fairly well with the greater SOL/TS activation ratio observed at low intensity at the group level. In the absence of measurements of muscle fibre content, it is impossible to determine whether the model proposed by Dul et al. (1984) would predict well the wide range of individual strategies that we observed. Although these models may be relevant for well-controlled isometric tasks, it is important to acknowledge

that results obtained from direct measurement of muscle force during dynamic tasks in animals did not fit adequately with predictions made with the aforementioned models (Herzog and Leonard, 1991). Indeed, none of these models can predict the change in force-sharing observed with changes in the mechanical constraints of the task (GL and SOL in the cat: Herzog and Leonard, 1991; GM and SOL in the cat: Walmsley et al., 1978; GM and SOL in the cat: Whiting et al., 1984).

Individual force-sharing strategies and their functional consequences

These results have important implication for the understanding of individual force-sharing strategies. Importantly, for the force to be balanced across the three heads of the triceps surae, the muscle(s) with the lower force-generating capacity should be driven more. However, such a negative correlation was not observed, either for SOL/TS or GM/Gas. This finding provides evidence of an imbalance of force between the three heads, which varies considerably between participants (Fig. 4). Even though the inter-individual variability of force-sharing strategies has received little attention in the literature, such a large inter-individual variability can be inferred from experimental data measured in animals using force transducers. For example, the ratio of gastrocnemius/SOL peak force measured in five cats during downhill walking varied between 41.5% and 61.0% (data calculated from table 2 in Herzog et al., 1993). This force imbalance might have an important mechanical effect on the distal tendon (Achilles tendon) that is composed of three compartments, or fascicle bundles, that originate from each of the three heads of the triceps surae (Cummins and Anson, 1946; Szaro et al., 2009). The load distribution between Achilles subtendons is likely to be determined, at least in part, by the individual force-sharing strategy (Arndt et al., 1998; Bojsen-Møller and Magnusson, 2015; Kinugasa et al., 2013), with some strategies having the potential to induce suboptimal loading. For example, a direct relationship between individual muscle contributions and force distribution across the Achilles tendon has been demonstrated on cadaver preparations (Arndt et al., 1999).

Despite it being tempting to conclude that the large individual differences in force-sharing strategies that we report directly translate to individual differences in Achilles subtendon loading, intermuscular force transmission between the heads of the triceps surae may result in a redistribution of force between the Achilles subtendons, as recently suggested (Maas and Finni, 2018). It is also possible that every subtendon exhibits different mechanical properties (related to their elastic modulus, cross-sectional area, length) and that these properties vary between individuals. As such an imbalance of muscle force would not directly impose an imbalance of strain distribution between the subtendons. In this way, recent studies performed in rats (Finni et al., 2017) and humans (Pekala et al., 2017) have highlighted different mechanical properties between the three subtendons, with large differences between individuals (Pekala et al., 2017). Finally, the twisted structure of the Achilles tendon might also participate in reducing differences in strains between the subtendons (Edama et al., 2015).

As proposed in the literature, the distribution of loads and strains within the Achilles tendon could be involved in the development of Achilles pathology such as tendinopathy (Bojsen-Møller and Magnusson, 2015; Kannus, 1997). The present study provides evidence for individual-specific force-sharing strategies. Although it is possible that a subgroup of individuals exhibiting a specific profile of force-sharing strategy is more at risk of developing Achilles tendinopathy, it remains to be demonstrated.

Methodological considerations

There are multiple methodological limitations that require consideration. First, muscle activation was indirectly assessed using surface EMG. In order to minimize crosstalk and to ensure similar electrode location between participants, we used a standardized procedure. Specifically, we determined anatomical landmarks and we used B-mode ultrasound to check the appropriate location of the surface electrodes, away from the border of neighbouring muscles. Despite these precautions, we cannot exclude the possibility that part of the individual differences in EMG amplitudes may originate from slightly different placement of the electrodes relative to an individual's anatomy. However, the good between-day reliability of the EMG data (Table 1) provides some evidence that small changes in electrode location did not significantly alter the results. Second, for between-muscle and between-participant comparisons, it was important to normalize the RMS EMG values measured during the submaximal tasks to those measured during MVC. For this normalization procedure to be correct, we ensured that participants reached the maximal voluntary activation level during the MVC task. Results showing voluntary activation close to 100% make us confident that the normalization procedure was appropriate. Third, we focused on an isometric task because between-muscle difference in torque-generating capacity during a dynamic task requires knowledge of various mechanical factors that are difficult to estimate for each individual *in vivo* (e.g. force–velocity and force–length relationships, change in moment arm as a function of joint angles). We therefore considered the differences in PCSA between synergist muscles as representative of differences in force-generating capacity. However, it is important to note that the PCSA values are sensitive to the joint angle tested. In addition, results cannot be extrapolated to dynamic contractions where activation/force-sharing strategies may be affected by the mechanical constraints of the task (Smith et al., 1980; Wakeling and Horn, 2009). Future research might provide further insights into neuromechanical coupling during dynamic tasks by informing muscle modelling (e.g. Dick et al., 2017) with experimental data (e.g. PCSA, moment arms). Finally, testing was performed with the ankle in the neutral position (0 deg), where we assumed that the three heads of the triceps surae are at a similar muscle length relative to their optimal length. This assumption seems reasonable for GM and GL because their anatomy (Szaro et al., 2009), architecture (Maganaris et al., 1998), composition (Johnson et al., 1973) and ascending parts of their force–length relationships (Maganaris, 2003) are very similar. The comparison between gastrocnemii and the SOL is less straightforward as their composition, anatomy and function differ. However, at 0 deg, gastrocnemii and the SOL both operate in the ascending limb and plateau region of the force–length relationship, with an optimal angle at approximately 15 deg of dorsiflexion for the SOL (Maganaris, 2001) and at 19 deg of dorsiflexion for the GM (Hoffman et al., 2012). Therefore, it seems reasonable to assume that the force imbalance between synergist muscles that we estimated is minimally affected by difference in the operating ranges of the muscles over the force–length relationship.

Conclusions

This study provides insight into the neuromechanical coupling that exists within synergist muscles during an isometric contraction. An important result lies in the consequences of the activation strategies on the imbalance of the force production between synergist muscles, and the high between-individual variability. This large individual variability in the force-sharing strategy raises the question of its

impact on the Achilles tendon. Further studies are required to investigate whether the individual coordination strategies could constitute an intrinsic risk factor to the development of Achilles tendon disorders.

Competing interests
The authors declare no competing or financial interests.

Author contributions
Conceptualization: M.C., L.L., A.N., K.T., F.H.; Methodology: M.C., L.L., A.N., F.H.; Software: M.C., L.L., F.H.; Investigation: M.C., L.L.; Resources: F.H.; Data curation: M.C., F.H.; Writing - original draft: M.C., K.T., F.H.; Writing - review & editing: M.C., L.L., A.N., K.T., F.H.; Supervision: L.L., K.T., F.H.; Project administration: L.L., F.H.; Funding acquisition: F.H.

Funding
This study was supported by a grant from the Région Pays de la Loire (QUETE project, no. 2015-09035). M.C. was supported by a scholarship from the French ministry of higher education and research. F.H. was supported by a fellowship from the Institut Universitaire de France (IUF) and a travel grant from the International French Society of Biomechanics.

Data availability
Data are available from the Dryad Digital Repository (Crouzier et al., 2018): https://doi.org/10.5061/dryad.68jc53n.

References
Ahn, A. N., Kang, J. K., Quitt, M. A., Davidson, B. C. and Nguyen, C. T. (2011). Variability of neural activation during walking in humans: short heels and big calves. *Biol. Lett.* **7**, 539-542.
Albracht, K., Arampatzis, A. and Baltzopoulos, V. (2008). Assessment of muscle volume and physiological cross-sectional area of the human triceps surae muscle *in vivo*. *J. Biomech.* **41**, 2211-2218.
Arndt, A. N., Komi, P. V., Brüggemann, G.-P. and Lukkariniemi, J. (1998). Individual muscle contributions to the *in vivo* Achilles tendon force. *Clin. Biomech.* **13**, 532-541.
Arndt, A., Brüggemann, G.-P., Koebke, J. and Segesser, B. (1999). Asymmetrical loading of the human triceps surae – I. Mediolateral force differences in the Achilles tendon. *Foot Ankle Int.* **20**, 444- 449.
Biewener, A. A. (2016). Locomotion an an emergent property of muscle contractile dynamics. *J. Exp. Biol.* **219**, 285-294.
Bojsen-Møller, J. and Magnusson, S. P. (2015). Heterogeneous loading of the human Achilles tendon *in vivo*. *Exerc. Sport Sci. Rev.* **43**, 190-197.
Bolsterlee, B., Finni, T., D'Souza, A., Eguchi, J., Clarke, E. C. and Herbert, R. D. (2018). Three-dimensional architecture of the whole human soleus muscle *in vivo*. *Peer J* **6**, e4610.
Cresswell, A., Löscher, W. and Thorstensson, A. (1995). Influence of gastrocnemius muscle length on triceps surae torque development and electromyographic activity in man. *Exp. Brain Res.* **105**, 283-290.
Crouzier, M., Lacourpaille, L., Nordez, A., Tucker, K. and Hug, F. (2018) Data from: Neuromechanical coupling within the human triceps surae and its consequence on individual force sharing strategies. Dryad Digital Repository. https://doi.org/10.5061/dryad.68jc53n
Crowninshield, R. D. and Brand, R. A. (1981). A physiologically based criterion of muscle force prediction in locomotion. *J. Biomech.* **14**, 793-802.
Cummins, E. J. and Anson, B. J. (1946). The structure of the calcaneal tendon (of Achilles) in relation to orthopedic surgery, with additional observations on the plantaris muscle. *Surg. Gynecol. Obstet.* **83**, 107-116.
De Troyer, A., Kirkwood, P. A. and Wilson, T. A. (2005). Respiratory action of the intercostal muscles. *Physiol. Rev.* **85**, 717-756.
Dick, T. J. M., Biewener, A. A. and Wakeling, J. M. (2017). Comparison of human gastrocnemius forces predicted by Hill-type muscle models and estimated from ultrasound images. *J. Exp. Biol.* **220**, 1643- 1653.
Diedrichsen, J., Shadmehr, R. and Ivry, R. (2010). The coordination of movement: optimal feedback control and beyond. *Trends Cogn. Sci.* **14**, 31-39.
Dul, J., Johnson, G. E., Shiavi, R. and Townsen, M. A. (1984). Muscular synergism – II. A minimum-fatigue criterion for load sharing between synergistic muscles. *J. Biomech.* **17**, 675-684.
Duysens, J., Tax, A. A. M., van der Doelen, B., Trippel, M. and Dietz, V. (1991). Selective activation of human soleus or gastrocnemius in reflex responses during walking and running. *Exp. Brain Res.* **87**, 193-204.
Edama, M., Kubo, M., Onishi, H., Takabayashi, T., Inai, T., Yokoyama, E., Hiroshi, W., Satoshi, N. and Kageyama, I. (2015). The twisted structure of the human Achilles tendon. *Scand. J. Med. Sci. Sports* **25**, e497-e503.
Farahmand, F., Senavongse, W. and Amis, A. A. (1998). Quantitative study of the quadriceps muscles and trochlear groove geometry related to instability of the patellofemoral joint. *J. Orthop. Res.* **16**, 136-143.
Fiebert, I. M., Spielholz, N. I., Applegate, B., Crabtree, F. G., Martin, L. A. and Parker, K. L. (2000). A comparison of iEMG activity between the medial and lateral heads of the gastrocnemius muscle during partial weight bearing plantarflexion contractions at varying loads. *Isokinet. Exerc. Sci.* **8**, 65-72.
Finni, T., Bernabei, M., Baan, G. C., Noort, W., Tijs, C. and Maas, H. (2017). Non-uniform displacement and strain between the soleus and gastrocnemius subtendons of rat Achilles tendon. *Scand. J. Med. Sci. Sports* **28**, 1009-1017.
Fitts, R. H., Costill, D. L. and Gardetto, P. R. (1989). Effect of swim exercise training on human muscle fiber function. *J. Appl. Physiol.* **66**, 465-475.
Fukunaga, T., Roy, R. R., Shellock, F. G., Hodgson, J. A. and Edgerton, V. R. (1996). Specific tension of human plantar flexors and dorsiflexors. *J. Appl. Physiol.*, 158-165.
Handsfield, G. G., Inouye, J. M., Slane, L. C., Thelen, D. G., Miller, G. W. and Blemker, S. S. (2016). A 3D model of the Achilles tendon to determine the mechanisms underlying nonuniform tendon displacements. *J. Biomech.* **51**, 17-25.
Haxton, H. A. (1944). Absolute muscle force in the ankle flexors in man. *J. Physiol.* **103**, 267-273.
Hedrick, W. R. (2000). Extended field of view real-time ultrasound. *J. Diagn. Med. Sonogr.* **16**, 103-107.
Henneman, E. and Oslon, C. B. (1965). Relations between structure and function in the design of skeletal muscles. *J. Neurophysiol.* **28**, 581-598.
Henneman, E., Somjen, C. and Carpenter, D. O. (1965). Excitability and inhibitability of motoneurons of different sizes. *J. Neurophysiol.* **28**, 599-620.
Héroux, M. E., Dakin, C. J., Luu, B. L., Inglis, J. T. and Blouin, J. S. (2014). Absence of lateral gastrocnemius activity and differential motor unit behavior in soleus and medial gastrocnemius during standing balance. *J. Appl. Physiol.* **116**, 140-148.
Herzog, W. (2000). Muscle properties and coordination during voluntary movement. *J. Sports Sci.* **18**, 141-152.
Herzog, W. (2017). Skeletal muscle mechanics: questions, problems and possible solutions. *J. Neuroeng. Rehabil.* **14**, 98.
Herzog, W. and Leonard, T. R. (1991). Validation of optimization models that estimate the forces exerted by synergistic muscles. *J. Biomech.* **24**, 31-39.
Herzog, W., Read, L. J. and Keurs, H. (1991). Experimental determination of force-length relations of intact human gastrocnemius muscles. *Clin. Biomech.* **6**, 230-238.
Herzog, W., Leonard, T. R. and Guimaraes, C. S. (1993). Forces in gastrocnemius, soleus, and plantaris tendons of the freely moving cat. *J. Biomech.* **26**, 945 - 953.
Hoffman, B. W., Lichtwark, G. A., Carroll, T. J. and Cresswell, A. G. (2012). A comparison of two Hill-type skeletal muscle models on the construction of medial gastrocnemius length-tension curves in humans in vivo. *J. Appl. Physiol.* **113**, 90-96.
Hug, F., Goupille, C., Baum, D., Raiteri, B. J., Hodges, P. W. and Tucker, K. (2015). Nature of the coupling between neural drive and force-generating capacity in the human quadriceps muscle. *Proc. R. Soc. B* **28**2, 20151908.
Johnson, M. A., Polgar, D., Weightman, D. and Appleton, D. (1973). Data on the distribution of fibre types in thirty-six human muscles an autopsy study. *J. Neurol. Sci.* **18**, 111-129.
Kannus, P. (1997). Etiology and pathophysiology of chronic tendon disorders in sports. *Scand. J. Med. Sci. Sports* **7**, 78-85.
Kinugasa, R., Oda, T., Komatsu, T., Edgerton, V. R. and Sinha, S. (2013). Interaponeurosis shear strain modulates behavior of myotendinous junction of the human triceps surae. *Physiol. Rep.* **1**, e00147.
Kutch, J. J. and Valero-Cuevas, F. J. (2011). Muscle redundancy does not imply robustness to muscle dysfunction. *J. Biomech.* **44**, 1264-1270.
Kyrolainen, H. and Komi, P. V. (1994). Stretch reflex responses following mechanical stimulation in power- and endurance-trained athletes. *Int. J. Sports Med.* **15**, 290-294.
Lacourpaille, L., Nordez, A. and Hug, F. (2017). The nervous system does not compensate for an acute change in the balance of passive force between synergist muscles. *J. Exp. Biol.* **220**, 3455-3463.
Larsson, L. and Moss, R. L. (1993). Maximum velocity of shortening in relation to myosin isoform composition in single fibres from human skeletal muscles. *J. Physiol.* **472**, 595-614.
Lieber, R. L. (2002). Skeletal muscle structure, function and plasticity: the physiological basis of rehabilitation. Baltimore: Lippincott Williams & Wilkins.
Maas, H. and Finni, T. (2018). Mechanical coupling between muscle-tendon units reduces peak stresses. *Exerc. Sport Sci. Rev.* **46**, 26-33.
Mademli, L. and Arampatzis, A. (2005). Behaviour of the human gastrocnemius muscle architecture during submaximal isometric fatigue. *Eur. J. Appl. Physiol.* **94**, 611-617.
Maganaris, C. N. (2001). Force-length characteristics of in vivo human skeletal muscle. *Acta Physiol. Scand.* **172**, 279-285.
Maganaris, C. N. (2003). Force-length characteristics of the in vivo human gastrocnemius muscle. *Clin. Anat.* **16**, 215-223.

Maganaris, C. N., Baltzopoulos, V. and Sargeant, A. J. (1998). In vivo measurements of the triceps surae complex architecture in man- implications for muscle function. *J. Physiol.* **512**, 603-614.
Masood, T., Bojsen-Moller, J., Kalliokoski, K. K., Kirjavainen, A., Aarimaa, V., Magnusson, S. P. and Finni, T. (2014). Differential contributions of ankle plantarflexors during submaximal isometric muscle action: a PET and EMG study. *J. Electromyogr. Kinesiol.* **24**, 367-374.
McLean, L. and Goudy, N. (2004). Neuromuscular response to sustained low-level muscle activation: within- and between-synergist substitution in the triceps surae muscles. *Eur. J. Appl. Physiol.* **91**, 204-216.
Noorkoiv, M., Stavnsbo, A., Aagaard, P. and Blazevich, A. J. (2010). In vivo assessment of muscle fascicle length by extended field-of-view ultrasonography. *J. Appl. Physiol.* **109**, 1974-1979.
Pekala, P. A., Henry, B. M., Ochala, A., Kopacz, P., Taton, G., Mlyniec, A., Walocha, J. A. and Tomaszewski, K. A. (2017). The twisted structure of the Achilles tendon unraveled- A detailed quantitative and qualitative anatomical investigation. *Scand. J. Med. Sci. Sports* 1-11.
Prilutsky, B. (2000). Coordination of one-joint and two-joint muscles. *Motor Control* **4**, 1-44.
Riemann, B. L., Limbaugh, G. K., Eitner, J. D. and LeFavi, R. G. (2011). Medial and lateral gastrocnemius activation differences during heel-raise exercise with three different foot positions. *J. Strength Conditionong Res.* **25**, 634- 639.
Sacks, R. D. and Roy, R. R. (1982). Architecture of the hind limb muscles of cats – functional significance. *J. Morphol.* **195**, 173-185.
Smith, J. L., Betts, B., Edgerton, V. R. and Zernicke, R. F. (1980). Rapid ankle extension during paw shakes: selective recruitment of fast ankle extensors. *J. Neurophysiol.* **43**, 612-620.
Szaro, P., Witkowski, G., Smigielski, R., Krajewski, P. and Ciszek, B. (2009). Fascicles of the adult human Achilles tendon – an anatomical study. *Ann. Anat.* **191**, 586-593.
Todd, G., Taylor, J. L. and Gandevia, S. C. (2004). Reproducible measurement of voluntary activation of human elbow flexors with motor cortical stimulation. *J. Appl. Physiol.* **97**, 236-242.
Wakeling, J. M. and Horn, T. (2009). Neuromechanics of muscle synergies during cycling. *J. Neurophysiol.* **101**, 843-854.
Walmsley, B., Hodgson, J. A. and Burke, R. E. (1978). Forces produced by Medial gastrocnemius and Soleus muscles during locomotion in freely moving cats. *J. Neurophysiol.* **41**, 1203-1216.
Whiting, W. C., Robert, J. C., Roy, R. R. and Edgerton, V. R. (1984). A technique for estimating mechanical work of individual muscles in the cat during treadmill locomotion. *J. Biomech.* **19**, 685-694.
Winter, S. L. and Challis, J. H. (2008). Reconstruction of the human gastrocnemius force–length curve *in vivo* – Part 2 – experimental results. *J. Appl. Biomech.* **24**, 207-214.

STUDY 3

Force-sharing within the *triceps surae*: an Achilles heel in Achilles tendinopathy

Associated publication:

Crouzier, M., Tucker, K., Lacourpaille, L., Doguet, V., Fayet, G., Dauty, M., Hug, F (2018).
Force-sharing within the *triceps surae*: an Achilles heel in Achilles tendinopathy.
Medicine & Science in Sports & Exercise, 52 (5): 1236.

ABSTRACT

The primary aim of this study was to determine whether the distribution of force between the three heads of the *triceps surae* differs between people with Achilles tendinopathy and controls. The secondary aim was to determine the effect of this force distribution on subtendon strain. Data were collected for 21 participants with Achilles tendinopathy and 21, case-wise paired, asymptomatic controls. Ultrasonography was used to measure muscle volume, fascicle length, pennation angle and subtendon length at rest. Muscle activation was estimated using surface EMG during maximal and submaximal isometric plantarflexion tasks. The product of normalised activation, PCSA, and the cosine of the pennation angle was considered as an index of individual muscle force. Displacement of the distal myotendinous junction of each muscle was measured during the submaximal contractions. The contribution of the GL to the overall *triceps surae* PCSA and activation was 8.5 % ($p = 0.047$) and 24.7 % lower (main effect group $p = 0.009$) in people with Achilles tendinopathy than in the controls, respectively. Consequently, GL contributed approximately 28 % less (main effect group $p = 0.025$) to the *triceps surae* force in people with Achilles tendinopathy. The contribution of GM and SOL was not different between groups. Subtendon strain was not different between groups ($p = 0.835$). These results provide evidence for a difference in force-sharing strategy within the *triceps surae* in people with Achilles tendinopathy compared with the controls.

Key words

Muscle coordination, Gastrocnemius, Physiological cross-sectional area, Electromyography, Musculoskeletal disorder

Force-sharing within the Triceps Surae: An Achilles Heel in Achilles Tendinopathy

MARION CROUZIER[1], KYLIE TUCKER[2,3], LILIAN LACOURPAILLE[1], VALENTIN DOGUET[1], GUILLEMETTE FAYET[4], MARC DAUTY[5], and FRANÇOIS HUG[1,3,6]

[1]Nantes University, Movement, Interactions, Performance, MIP, Nantes, FRANCE; [2]The University of Queensland, School of Biomedical Sciences, Brisbane, AUSTRALIA; [3]The University of Queensland, NHMRC Centre of Clinical Research Excellence in Spinal Pain, Injury and Health, School of Health and Rehabilitation Sciences, Brisbane, AUSTRALIA; [4]CHU Nantes, Clinical Neurophysiology Department, Nantes, FRANCE; [5]CHU Nantes, Physical Medicine and Rehabilitation Department, Nantes, FRANCE; and [6]Institut Universitaire de France (IUF), Paris, FRANCE

ABSTRACT

CROUZIER, M., K. TUCKER, L. LACOURPAILLE, V. DOGUET, G. FAYET, M. DAUTY, and F. HUG. Force-sharing within the Triceps Surae: An Achilles Heel in Achilles Tendinopathy. *Med. Sci. Sports Exerc.*, Vol. 52, No. 5, pp. 1076–1087, 2020. **Purpose:** The primary aim of this study was to determine whether the distribution of force between the three heads of the triceps surae differs between people with Achilles tendinopathy and controls. We also aimed to determine the effect of this force distribution on subtendon strain. **Methods:** Data were collected for 21 participants with Achilles tendinopathy and 21, case-wise paired, asymptomatic controls. Ultrasonography was used to measure muscle volume, fascicle length, pennation angle and subtendon length at rest. Muscle activation was estimated using surface electromyography during maximal and submaximal isometric plantarflexion tasks. The product of normalized activation, physiological cross-sectional area, and the cosine of the pennation angle was considered as an index of individual muscle force. Displacement of the distal myotendinous junction of each muscle was measured during the submaximal contractions. **Results:** The contribution of the gastrocnemius lateralis to the overall triceps surae physiological cross-sectional area and activation was 8.5% ($P = 0.047$, $d = 0.75$) and 24.7% lower (main effect group $P = 0.009$, $d = 0.67$) in people with Achilles tendinopathy than in the controls, respectively. Consequently, gastrocnemius lateralis contributed approximately 28% less (main effect group $P = 0.025$, $d = 0.62$) of the triceps surae force in people with Achilles tendinopathy. The contribution of gastrocnemius medialis and soleus was not different between groups. Subtendon strain was not different between groups ($P = 0.835$). **Conclusions:** These results provide evidence for a difference in force-sharing strategy within the triceps surae in people with Achilles tendinopathy compared with the controls. Whether this altered strategy is a cause or a consequence of Achilles tendinopathy should be explored further. **Key Words:** MUSCLE COORDINATION, GASTROCNEMIUS, PHYSIOLOGICAL CROSS-SECTIONAL AREA, ELECTROMYOGRAPHY, MUSCULOSKELETAL DISORDER

Achilles tendinopathy is associated with localized pain during activities that load the tendon. As such, Achilles tendinopathy is associated with lower exercise tolerance, impaired function, and reduced quality of life. The lifetime incidence of Achilles tendinopathy is approximately 1 in every two long-term middle- and long-distance runners (1), and symptoms may last for many years (2). The etiology of this disease is poorly understood. New approaches are required to understand the mechanisms that underlie the development of Achilles tendinopathy, its persistence, and resolution.

Address for correspondence: François Hug, Ph.D., University of Nantes, Laboratory « Movement, Interactions, Performance » (EA 4334), 25 bis Boulevard Guy Mollet, BP 72206, 44322 Nantes Cedex 3, France; E-mail: francois.hug@univ-nantes.fr.

Submitted for publication August 2019.
Accepted for publication November 2019.

0195-9131/20/5205-1076/0
MEDICINE & SCIENCE IN SPORTS & EXERCISE®

DOI: 10.1249/MSS.0000000000002229

The Achilles tendon is the largest tendon in the body and links the triceps surae (TS) to the calcaneus. Its architecture is complex, as it is composed of three subtendons (or three main fascicle bundles), that each arises from gastrocnemius medialis (GM), gastrocnemius lateralis (GL), and soleus (SOL). Together, the subtendons exhibit a twisted structure, the degree of which varies between individuals (3). Nonuniform displacements within the Achilles tendon have been observed using ultrasound imaging during isometric contractions (4) and passive stretching (5). Nonuniform displacements are consistent with a nonuniform distribution of load within the tendon as suggested by *in vivo* (6) and *in vitro* studies (7). In addition, shear force at the interface of tendon fascicles has been evidenced by measuring Lubricin concentration, a protein whose expression is stimulated by shear force (8). Nonoptimal distribution of load and/or the amount of shear forces between subtendons have been hypothesized to contribute to the development of Achilles tendinopathy (8,9). Using a modeling approach, Handsfield et al. (10) suggested that the nonuniform distribution of load or strain within the Achilles tendon is mainly determined by the distribution of force among the heads of the TS. This link between the distribution of load within the Achilles tendon

APPLIED SCIENCES

and the distribution of force among individual muscles has also been suggested by indirect *in vivo* measurement (4). Together, these works suggest that the distribution of muscle force might be involved in the development of Achilles tendinopathy; but this remains to be tested.

Muscle coordination relates to the distribution of force among individual muscles (or force-sharing strategy) to produce a motor task (11). As there is no noninvasive experimental technique that can measure the force produced by individual muscles *in vivo*, it is not possible to directly determine the role of muscle coordination strategies in the development of musculoskeletal disorders, including Achilles tendinopathy. Recently, we published a series of studies that considered the product of muscle activation, pennation angle and muscle physiological cross-sectional area (PCSA) as an index of the force produced by individual muscles during isometric contractions (12–14).

The primary aim of this exploratory study was to determine whether the distribution of force between the heads of the TS differs in people with Achilles tendinopathy compared with controls. We hypothesized that people with Achilles tendinopathy would exhibit a different force distribution between the heads of the TS during submaximal isometric tasks. In the case that a difference in force sharing strategy was observed between our groups, we further aimed to determine whether particular force-sharing strategies in people with Achilles tendinopathy were associated with recovery of symptoms over a 6-month follow-up period. Our secondary aim was to determine the effect of this force distribution on subtendons' strain.

MATERIALS AND METHODS

Participants

The study was conducted with 45 volunteers who were recruited by local advertisement (Table 1), that is, 23 participants with Achilles tendinopathy and 22 controls. First, all participants were directed to an online questionnaire to determine if they were likely eligible to participate. Then, the eligible participants with Achilles tendinopathy attended a physical screening conducted by a physiotherapist to verify whether they met the following inclusion criteria: (i) between 18 and 45 yr old, (ii) self-reported pain within the Achilles tendon within the last week, rated at least 3 on an 11-point scale from 0 (no pain) to 10 (unbearable pain), (iii) increased pain when walking or running slowly, and (iv) pain duration of at least 3 wk. Pain on palpation of the tendon was used to confirm the location of sensitivity. The exclusion criteria for both groups were: (i) pain/injury within the lower limbs within the previous 6 months (except in the Achilles tendon for people with Achilles tendinopathy), (ii) corticosteroids injection in the lower limb within the previous 6 months, and (iii) a history of lower limb surgery. To provide validated information about Achilles tendon pain and disability, all participants completed the Victorian Institute of Sport Assessment—Achilles questionnaire (VISA-A) (15). Physical activity level was estimated using the International Physical Activity Questionnaire (IPAQ) [evaluation tool of physical activity (16)] and the type of physical activity was investigated with questions on disciplines that were practiced regularly. Recruitment of control participants was targeted to match between group by type and volume of physical activity, and then by age, height, and body mass (all within ±15%).

Two participants with Achilles tendinopathy and one healthy control were excluded for technical reasons that are explained further below. Therefore, data were reported for 21 participants in each group. Table 1 provides the demographic characteristics of these participants. Within each group, 18 of the 21 participants practiced running 2 h 36 min ± 2 h 18 min·wk^{-1}. Four participants with Achilles tendinopathy had bilateral Achilles tendinopathy, in which case, the side with the highest level of pain just prior to data collection was chosen for data collection. Five of the participants with Achilles tendinopathy had insertional tendinopathy, and 16 had midportion tendinopathy, as determined by the physiotherapist during palpation. The average duration of Achilles tendinopathy symptoms was 3.6 ± 2.7 months. Ten of 21 participants with tendinopathy had their dominant side measured as this was their painful (or more painful) side at the time of testing. The side considered for the control group was chosen to match with dominance of the tested side of their paired-Achilles tendinopathy participant. This resulted in that the proportions of dominant (48%) and nondominant sides tested (52%) were similar in the two groups. All participants were informed of the protocol and methods used before providing written informed consent. The experimental procedures were approved by the local ethics committee (Rennes Ouest V-CPP-MIP-010), and all procedures adhered to the declaration of Helsinki.

Experimental Protocol

Participants attended one laboratory session. First, ultrasound images were taken at rest and used to estimate muscle volume,

TABLE 1. Demographic and injury characteristics.

	Control Group (n = 21)	Achilles Tendinopathy Group (n = 21)	P
Age (yr)	35.1 ± 7.7	36.2 ± 8.3	0.660
Height (cm)	177.5 ± 7.8	175.9 ± 8.0	0.525
Body mass (kg)	71.8 ± 10.5	72.7 ± 8.7	0.763
BMI (kg·m^{-2})	22.7 ± 2.4	23.4 ± 1.5	0.251
Physical activity (MET·min·wk^{-1})	4601 ± 1983	3903 ± 2105	0.275
Gender [females/males]	3/18	3/18	–
VISA-A (24 = severe Achilles tendinopathy; 100 = healthy)	99.8 ± 0.5	65.6 ± 15.2[a]	<0.001

Participants were paired-matched by type and volume of physical activity, age, height, and body mass.
[a]Significant difference between groups.
BMI, body mass index.

muscle fascicle length, tendon length, and tendon thickness. Second, participants underwent six passive plantarflexion motions during which the displacement of each myotendinous junction was measured using B-mode ultrasound. Third, after a standardized familiarization with the plantarflexion task and a standardized warm-up, the participants performed four maximal isometric voluntary ankle plantarflexion tasks (MVC) for 3 s each, with 120 s rest in between. Then, submaximal isometric tasks involved matching target torques of 20% and 40% of MVC. Six 8-s trials were performed at both intensities, leading to 12 submaximal contractions with at least 20 s of rest in between. Feedback of the target and torque output was provided using visual feedback displayed on a monitor. Both muscle activation and myotendinous junction displacement were measured during these submaximal contractions.

During all of the aforementioned measurements, except the ultrasound estimation of muscle volume (knee at 135° of flexion), the participants were lying prone on an isokinetic ergometer (Con-Trex; CMV AG, Dübendorf, Switzerland) with hip and knee fully extended, and with the ankle angle set at 0° (shank perpendicular to the foot). Their foot was fixed with rigid straps, and an electronic goniometer (Penny and Giles twin-axis, Biometrics Ltd, UK) was placed along the distal fibula and the lateral part of the fifth metatarsal to measure small changes in ankle angle that inevitably occur during plantarflexion. Participants were asked to mention any feeling of pain throughout the experimentation.

Six months after this laboratory session, participants with Achilles tendinopathy were contacted by email, and asked to complete the VISA-A and IPAQ questionnaires, and they were asked whether they had received treatment for their Achilles tendinopathy. Twenty of the 21 included participants responded at 6.8 ± 0.5 months after data collection. The participants were considered to have recovered if their VISA score had improved by at least 20 points (17).

Muscle Architecture

Muscle volume. Volume of GM, GL, and SOL were estimated using freehand 3-dimensional (D) ultrasound. Specifically, multiple 2D ultrasound images of the muscles were combined with 3D motion of the ultrasound probe to reconstruct the muscle in 3D (Stradwin v5.4; Mechanical Engineering, Cambridge University, UK). B-mode ultrasound images (9.5 cm depth) were recorded using a 40-mm linear probe (2–10 MHz; Aixplorer; Supersonic Imagine, Aix-en-Provence, France). Position and orientation of the probe were recorded by using a six-camera optical motion analysis system (Optitrack, Natural Point, USA) to track a rigid cluster of four markers attached to the probe. For this assessment, participants were prone, with their lower leg in a custom-made water bath, with knee and ankle angle at approximately 135° and 0°, respectively (Fig. 1). Four to six parallel sweeps were performed from the knee to the ankle at a low speed leading to approximately 15 s per sweep. A gating threshold of 5 mm was set in Stradwin, which ensured that B-mode images were recorded every time that the ultrasound probe has moved by 5 mm. The B-mode ultrasound images of GM, GL, and SOL were then segmented manually by two examiners. Volume was estimated for each muscle head using the calculation provided by the Stradwin software (Fig. 1).

Muscle fascicle length and pennation angle. The ultrasound scanner coupled with a 50-mm linear probe (4–15 MHz; Aixplorer, Supersonic Imagine, Aix-en-Provence, France) was used in panoramic mode to estimate the fascicle length and the pennation angle of GM and GL, as further detailed elsewhere (14). Three images were recorded for each muscle. As SOL has short muscle fascicles, conventional B-mode ultrasound images were used for this muscle. The ultrasound probe was placed on SOL medially and laterally, below the GM and GL myotendinous junctions, respectively.

Ultrasound images were analyzed using MATLAB (The Mathworks, Natick, MA), where fascicles and aponeuroses were visually identified and tracked. Fascicles were drawn over the path of fascicle fragments or in the same directions of surrounding fragments. We aimed to measure the length and pennation angle of three fascicles per image (one each from the proximal, mid and distal regions), resulting in up to nine fascicles for each muscle. As some fascicles exhibited small curvatures, we used segmented lines. The pennation angle was considered as the average of the acute angles between the fascicle, and both the superficial and deep aponeurosis, respectively. For each muscle, values from the measured fascicles were averaged to get a representative fascicle length and pennation angle of the entire muscle. After visual inspection for image quality, 41 images out of the 504 images (3 trials- 4 locations × 42 participants) were excluded from the analysis because the fascicles were not adequately within the plane of the image. This resulted in an average number of 8.6 ± 1.5 (GM), 8.0 ± 1.6 (GL), and 15.9 ± 1.6 (SOL) fascicles per participant, with a minimum of three.

Muscle physiological cross-sectional area. Muscle PCSA was estimated as follows:

$$\mathrm{PCSA} = \frac{\text{muscle volume}}{\text{fascicle length}} \quad [1]$$

with muscle volume in cubic centimeters, fascicle length in centimeters, PCSA in square centimeters.

The ratios of PCSA were calculated as follows:

$$\frac{\text{muscle } (i)}{\text{triceps surae (TS)}}(\%) = \frac{\text{PCSA muscle } (i)}{(\text{PCSA GM} + \text{GL} + \text{SOL})} \times 100 \quad [2]$$

The ratio of GL PCSA over the sum of GL and GM PCSA (GL/Gas) was also considered.

Anatomical Tendon Features

To measure the thickness of the tendon, the linear ultrasound probe (4–15 MHz; Aixplorer; Supersonic Imagine, Aix-en-Provence, France) was aligned with tendon fascicles in the longitudinal plane and positioned such that both the anterior and the posterior boundaries of the Achilles tendon were visible. The probe was placed 1 cm proximally to the calcaneal attachment.

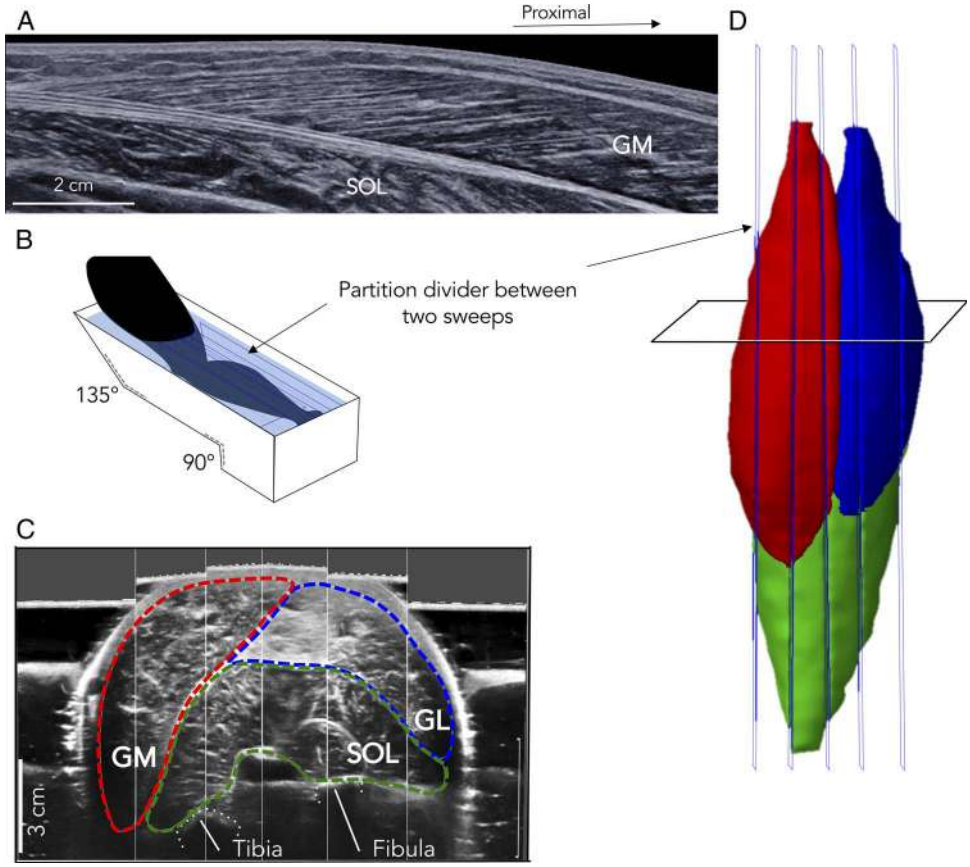

FIGURE 1—Muscle architectural measurements. The fascicle length was assessed using panoramic ultrasound images (panel A). An example of the GM muscle is shown on this figure. Three-dimension reconstruction of TS was realized with the freehand 3D ultrasound technique. Participants were prone, with their lower leg in a custom-made water bath, with knee and ankle angle at approximately 135° and 0°, respectively (panel B). Each muscle was segmented manually from the axial slices (panel C). The axial slice depicted in this figure is from ~33% of the proximodistal part of the leg. The 3D reconstruction of the segmented GM (*red*), GL (*blue*), and SOL (*green*) is shown on panel D.

The thickness of the tendon was calculated as the maximum perpendicular distance between the anterior and the posterior tendon boundary over the free tendon.

The length of each subtendon was estimated by measuring the distance between the insertion of the Achilles tendon on proximal part of the calcaneus and the distal myotendinous junction of each muscle as identified using B-mode ultrasound.

Muscle Activation

Maximal voluntary activation level. It was very important for each participant to produce a true maximal contraction during their MVC trials because the amplitude of the EMG signal recorded during submaximal contractions was normalized to that measured during MVC. To determine if the plantarflexors were activated maximally, a constant current stimulator (DS7AH; Digitimer, UK) delivered a doublet electrical stimulus (interstimulus interval: 10 ms; duration: 1 ms; amplitude: 400 V) to the tibial nerve during two of the four MVCs. For this stimulation, a self-adhesive cathode (50 mm diameter) was placed on the skin that lay directly over the tibial nerve, in the popliteal fossa, and the anode (80 × 130 mm) was placed on the skin over the *anterior tibialis* tuberosity. While the participants were at rest, the output current was increased incrementally (from 10 mA, with incremental steps of 10 mA) until a maximum plantarflexion torque was reached despite an increase in current intensity. We used 120% of this intensity for the rest of the protocol (mean intensity used: 103.4 ± 36.9 mA). The supramaximal doublet stimulus was delivered during the plateau of the MVC, and within 5 s in the subsequent rest period to elicit superimposed and resting twitches, respectively. Participants were informed about the electrical stimulation prior to these contractions.

Torque signals were sampled at 1000 Hz (Labchart V8; ADInstruments, Dunedin, New Zealand) and low-pass filtered at 10 Hz using a second-order Butterworth filter. Then, MVC torque was calculated from the maximal contractions as the maximal torque over a 300-ms time window. Note that for the trials with twitch interpolation, only the torque signal before the superimposed twitch was considered. The percentage of voluntary activation was calculated as previously described by Place et al. (18).

Of the 45 participants who were recruited, one participant with Achilles tendinopathy was unable to reach a maximal voluntary activation level >50%. This participant's data were not considered, and no paired control was recruited. The

demographic information for this participant is not included in Table 1.

Surface electromyography. Myoelectrical activity was collected via surface EMG from GM, GL, and SOL. First, the skin was shaved and cleaned with alcohol and wireless surface electrodes (Trigno Flex; Delsys, Boston, MA) were attached to the skin with double-sided tape. For each *gastrocnemii*, the electrode was placed on the middle line of the muscle belly at its two third distal. For SOL, two electrodes were placed below GM and GL myotendinous junctions, to record the two portions of the posterior part of SOL. As there was no difference in normalized EMG amplitude between these two regions, data from these two electrodes were averaged. Electrode location was checked with B-mode ultrasound to ensure that they were positioned away from the borders of the neighboring muscles and aligned with the direction of the fascicles. The EMG signals were band-pass filtered (10–850 Hz) and digitized at a sampling rate of 2000 Hz (Trigno; Delsys), and they were recorded on the same acquisition system that was used for the torque signal (Labchart V8; ADInstruments).

Raw EMG signals were inspected for electrical noise and movement artifacts. Because of noise or artifacts, 24 trials (11 MVC and 13 submaximal tasks) among the 672 trials (16 trials [4 MVC +12 submaximal trials] × 42 participants) were excluded. Because all MVC trials of a participant with Achilles tendinopathy had to be excluded, this participant and their matched control were excluded from all analyses. For the MVC trials, the root mean square of the EMG signal (RMS EMG) was calculated over a moving time window of 300 ms with 99% overlap. The resulting highest value over the four contractions was considered as the maximal RMS EMG value for further analysis. For the submaximal isometric force-matched tasks at 20% and 40% of MVC, the RMS EMG was calculated over 5 s at the middle of the force plateau and normalized to that determined during the maximal isometric contractions. As for PCSA, the following ratios of normalized RMS EMG were calculated: GL/Gas, GM/TS, GL/TS, and SOL/TS (equation 2).

Index of Individual Muscle Force

We considered that the difference of force produced by synergist muscles during isometric plantarflexion tasks depends mainly on their difference in activation and PCSA. To consider the component of the force acting in the line of action of the muscle, we also considered the pennation angle of the fascicles. An index of force was, therefore, calculated as follows (14):

$$\text{index of force} = \text{PCSA} \times \cos(\text{pennation angle}) \times \text{normalized RMS EMG} \quad [3]$$

Where normalized RMS EMG is expressed as a percentage of maximal RMS EMG, PCSA in square centimeters and pennation angle in degrees. As was done for EMG and PCSA, the following force ratios were calculated: GL/Gas, GM/TS, GL/TS, and SOL/TS (equation 2).

Myotendinous Junction Displacement

Displacement of the myotendinous junction of each muscle (GM, GL, or SOL) was measured using a 50-mm US linear probe (4–15 MHz) at a frame rate of 53 Hz. The GM and GL myotendinous junctions were defined as the intersection of the superficial and deep aponeurosis, forming an easily identifiable acute angle (Fig. 2). For SOL, the myotendinous junction was defined as the most distal point at which muscle fibers were inserted onto the Achilles tendon (free tendon), as identified within the curved shape of the distal SOL (Fig. 2). To account for possible movement of the ultrasound probe during acquisitions, a thin piece of tape was attached to the skin to represent a fixed reference landmark on the B-mode images (Fig. 2).

The displacements of the myotendinous junction of each muscle were measured during the submaximal isometric contractions at each target torque, that is, 20% and 40% of MVC. Note that a small joint rotation (heel lift) inevitably occurs during isometric plantarflexion tasks, which result in an overestimation of the myotendinous junction displacement, as the muscle–tendon unit logically decreases in length. To account for the effect of this joint rotation, the ankle angle was measured and a correction factor was calculated for every participant. To this end, each participant first underwent passive ankle rotations from 2° of dorsiflexion to 15° of plantarflexion at $1°{\cdot}s^{-1}$. During these ankle rotations, ankle angle and myotendinous junction displacements were measured using the electrogoniometer and B-mode ultrasound, respectively. Two trials were conducted for each muscle in a randomized order, resulting in six passive trials. EMG was used to check for the absence of muscle activation during the passive plantarflexion motion. In cases in which muscle activity was detected visually, the trials were repeated.

The longitudinal displacement of the myotendinous junction was tracked manually using a custom-made Matlab script on every five frames. First, the relationship between ankle angle and myotendinous displacement assessed during passive motions was fitted with a third-order polynomial fit. When the two ultrasound videos used for tracking a myotendinous junction were judged to be of high quality, they were both kept and results were averaged (73.4% of the cases). If both ultrasound videos were not judged to be of high quality, only the video with the highest quality was kept (22.8% of the cases). For the remaining 3.8% of the cases, both trials were excluded. Therefore, data are reported for 19 pairs (38 participants). To correct for the displacement of the myotendinous junction due to the ankle rotation that occurred during isometric contractions, the displacement associated with this change in ankle angle was first identified from the relationship between ankle angle and myotendinous junction displacement assessed during passive motion, and then subtracted from the raw displacement. Only the corrected values are reported herein. For each subtendon (GM, GL, and SOL) and each level of submaximal contraction (20% and 40% of MVC), tendon strain was calculated by dividing the corrected displacement of the myotendinous junction by the resting length of the subtendon.

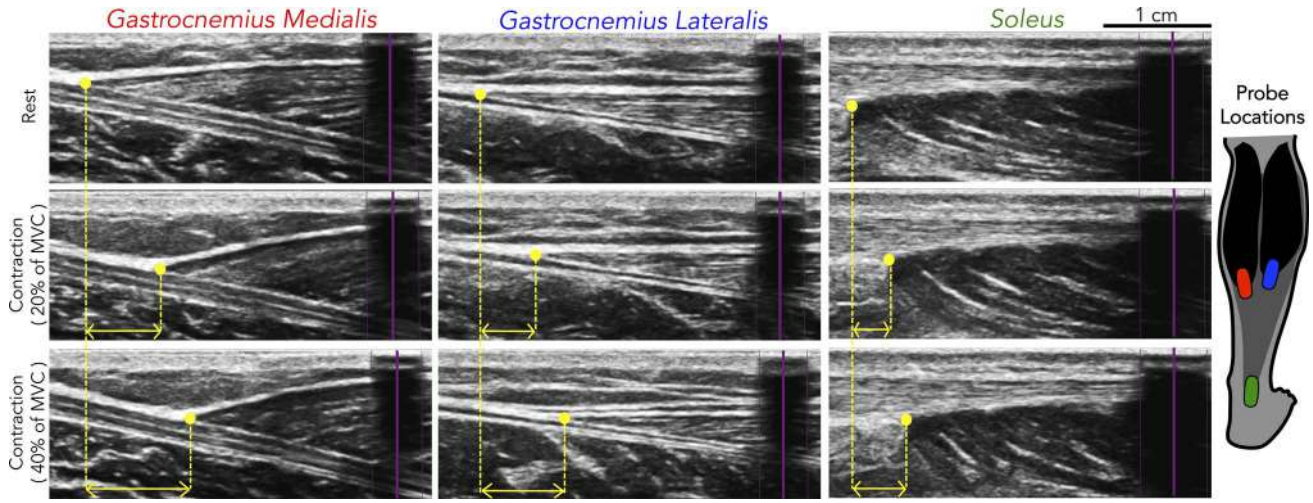

FIGURE 2—Typical example of ultrasound images used for the tracking of the myotendinous junction. Ultrasound images are depicted for the relaxed state (top images) and the two contraction intensities (20% and 40% of MVC). The myotendinous junction is shown by the yellow dot. Each myotendinous junction was tracked manually using a custom-made program. A hypoechoic tape was used as a reference landmark, and it is visible as the *large black strip* (highlighted in purple, within each of the ultrasound images). The *double yellow arrow* represents the displacement of the myotendinous junction of each muscle. The location of the ultrasound probe placement relative to the calf is shown in the right image.

Statistics

A skewness and kurtosis test was used to test for a normal distribution (Stata v12.0; StataCorp LP, Lakeway). If distributions did not pass the normality test, data were transformed as recommended by the software ("ladder" option). Specifically, all of the indices of individual muscle force were transformed using a square root function. The GL/Gas EMG and force ratios and the SOL/TS force ratio were squared. To test the interrater reliability of the volume measurement, muscle segmentation was performed by a second examiner and data were compared using the intraclass correlation coefficient (ICC) and the SEM. All data are reported as mean ± standard deviation.

Statistical analyses were performed in Statistica v7.0 (Statsoft, Tulsa, OK). Tendon thickness, demographic, and injury characteristics were compared between groups using unpaired *t* tests. Subtendon length, muscle volume, muscle fascicle length, pennation angle, and muscle PCSA were compared between groups using a two-way repeated-measures ANOVA (within subject factor: muscle [GM, GL and SOL]; between-subject factor: group [control and Achilles tendinopathy]). Each ratio of PCSA (GL/Gas, GM/TS, GL/TS, and SOL/TS) was compared between groups using unpaired t tests. To test our main hypothesis, each ratio of activation and index of force was compared between groups with a two-way repeated-measures ANOVA (within subject factor: intensity [20% and 40% of MVC]; between-subject factor: group [control and Achilles tendinopathy]). To determine whether people with Achilles tendinopathy exhibited different muscle activation, muscle force and subtendon strain than the controls, we used a three-way repeated-measures ANOVA (within subject factors: muscle or subtendon [GM, GL, and SOL] and intensity [20% and 40% of MVC]; between-subject factor: group [control and Achilles tendinopathy]). When appropriate, *post hoc* analyses were performed using Fisher's LSD test. To test the association between recovery in people with Achilles tendinopathy at 6 months and particular force-sharing strategies, we compared the force ratios between people who recovered and people who did not recover using an unpaired *t*-test. We tested the relationship between ratios, duration of symptoms, and severity of the pathology (VISA-A score) using Pearson's correlation.

The level of significance was set at $P \leq 0.05$. The Cohen's *d* values (the standard deviation of the control group was used as the standardizer) were calculated for the primary outcomes and reported as measures of effect size, with 0.20, 0.50, and 0.80 as small, medium, and large effects, respectively.

RESULTS

Anatomical Tendon Features

The thickness of the Achilles tendon was greater in participants with Achilles tendinopathy (6.7 ± 1.4 mm) than in the controls (5.7 ± 1.2 mm; $P = 0.018$, $d = 0.81$). When considering the length of each subtendon, there was a main effect of muscle ($P < 0.001$, Table 2). Specifically, SOL subtendon (5.5 ± 1.8 cm) was shorter than both GM subtendon (18.9 ± 2.3 cm; $P < 0.001$, $d = 2.08$) and GL subtendon (21.0 ± 1.9 cm; $P < 0.001$, $d = 2.07$). In addition, the GM subtendon was shorter than GL subtendon ($P < 0.001$, $d = 0.80$). On this measure, there was neither a main effect of group ($P = 0.564$) nor an interaction between muscle and group ($P = 0.603$).

Muscle Architecture

The ICC values calculated for GM, GL, and SOL volume were excellent (all ICC > 0.94). The SEM values were lower than 14.7 cm^3 (SOL). For further analysis, only values from the most experienced operator have been considered. There was a main effect of muscle on volume ($P < 0.001$, Table 2), with SOL being larger than both GM ($P < 0.001$, $d = 1.72$) and GL ($P < 0.001$, $d = 1.83$). Gastrocnemius medialis was also

TABLE 2. Muscle and tendon measurements.

		Controls			Achilles Tendinopathy		
		GM	GL	SOL	GM	GL	SOL
Muscle architecture (n = 21 and 21)							
Volume (cm^3)		244.2 ± 41.9	154.6 ± 32.6	451.0 ± 57.7	232.8 ± 38.5	145.4 ± 28.9	424.9 ± 71.9
Fascicle length (cm)		5.9 ± 0.7	6.7 ± 0.8	4.0 ± 0.7	5.5 ± 0.7	6.6 ± 0.9	3.4 ± 0.5
Pennation angle (°)		17.7 ± 1.6	13.4 ± 2.3	22.6 ± 3.7	18.4 ± 2.1	13.2 ± 2.0	24.8 ± 4.2
PCSA (cm^2)		41.8 ± 6.6	23.2 ± 5.0	115.4 ± 24.1	42.5 ± 5.8	22.1 ± 4.1	124.5 ± 21.4
Muscle activation (n = 21 and 21)							
	% MVC						
RMS EMG (% MVC)	20	13.5 ± 5.8	8.0 ± 4.1	16.6 ± 4.8	16.9 ± 6.1	**6.0 ± 3.3**[a]	17.4 ± 6.3
	40	27.1 ± 5.2	23.3 ± 8.6	25.7 ± 7.3	29.1 ± 6.7	**18.7 ± 8.5**[a]	30.5 ± 12.1
Muscle force (n = 21 and 21)							
Index of force (au)	20	5.4 ± 2.6	1.9 ± 1.3	17.6 ± 6.3	6.9 ± 2.9	1.3 ± 0.8	19.7 ± 8.3
	40	10.7 ± 2.5	5.3 ± 2.5	27.3 ± 10.2	11.8 ± 3.3	4.1 ± 2.2	34.7 ± 15.5[b]
Subtendon characteristics (n = 19 and 19)							
Length (cm)		18.5 ± 2.4	20.7 ± 2.0	5.5 ± 2.1	19.2 ± 2.2	21.3 ± 1.8	5.5 ± 1.6
MTJ displacement (cm)	20	0.54 ± 0.21	0.43 ± 0.12	0.46 ± 0.16	0.56 ± 0.19	0.46 ± 0.18	0.42 ± 0.17
	40	0.92 ± 0.29	0.68 ± 0.26	0.61 ± 0.28	0.90 ± 0.29	0.74 ± 0.23	0.62 ± 0.23
Strain (%)	20	2.9 ± 1.0	2.1 ± 0.7	9.1 ± 3.5	2.9 ± 1.0	2.2 ± 0.8	8.3 ± 4.0
	40	5.0 ± 2.0	3.3 ± 1.3	11.9 ± 5.7	4.7 ± 1.5	3.5 ± 1.1	12.4 ± 6.3

Data are reported for the Control and Achilles tendinopathy groups.
Note that significant interactions are not shown within the table.
[a](bold cells) Significant main effect of group.
[b]Significant difference between groups. Note that significant interactions are not shown within the table.

larger than GL ($P < 0.001$, $d = 1.51$). However, there was neither a significant interaction between muscle and group ($P = 0.353$) nor a main effect of group ($P = 0.230$) on this measure.

A significant main effect of muscle was observed for both fascicle length and pennation angle (both $P < 0.001$; Table 2). Soleus exhibited shorter fascicles and greater pennation angle than both GM (both $P < 0.001$, both $d > 1.52$) and GL (both $P < 0.001$, both $d > 1.88$). Gastrocnemius medialis had shorter fascicle length and greater pennation angle than GL (both $P < 0.001$, both $d > 1.16$). There was no significant main effect of group for fascicle length ($P = 0.059$) or pennation angle ($P = 0.172$). In addition, there was no significant interaction between muscle and group ($P = 0.118$ for fascicle length or $P = 0.051$ for pennation angle). Of note, the P value for the pennation angle was close to being significant.

When considering muscle PCSA (Table 2), there was a main effect of muscle ($P < 0.001$). Specifically, SOL PCSA was larger than both GM ($P < 0.001$, $d = 1.89$) and GL PCSA ($P < 0.001$, $d = 1.96$). The GM PCSA was also larger than GL PCSA ($P < 0.001$, $d = 1.76$). There was neither a main effect of group ($P = 0.352$) nor a significant interaction between muscle and group ($P = 0.120$). When considering the whole TS, that is, the sum of GM, GL, and SOL PCSA, there was no significant difference between groups (180.5 ± 32.2 and 189.1 ± 26.9 cm^2 for the Control and Achilles tendinopathy groups, respectively; $P = 0.352$).

When considering the ratios of PCSA, a between-group difference was observed for GL/TS, which was approximately 8.5% lower in participants with Achilles tendinopathy than controls ($P = 0.047$, $d = 0.75$) (Table 3). No difference was observed between groups for GM/TS PCSA ($P = 0.292$, $d = 0.29$) and SOL/TS PCSA ($P = 0.071$, $d = 0.54$).

Muscle Activation

Voluntary activation level. None of the patients reported pain in the Achilles tendon region during data collection. The maximal isometric plantarflexion torque was not different between groups (controls, 143.5 ± 24.7 N·m and Achilles tendinopathy, 136.1 ± 31.5 N·m; $P = 0.403$, $d = 0.30$). Participants reached a voluntary activation level close to 100%, with no difference between groups (controls, 97.4% ± 6.7% and Achilles tendinopathy, 97.9% ± 4.8%; $P = 0.798$, $d = 0.07$). Thus, we considered that the maximal RMS EMG amplitude measured during the MVC tasks represented the maximal activation for all muscles, in all participants.

Submaximal isometric contractions. When considering the normalized EMG RMS values, we observed a significant main effect of muscle ($P < 0.001$, Table 2), a significant main effect of intensity ($P < 0.001$) and an interaction between muscle and group ($P = 0.049$). However, there was no significant interaction between muscle, intensity, and group ($P = 0.067$). For

TABLE 3. Ratios of PCSA, muscle activation, and indexes of force.

		Controls				Achilles Tendinopathy			
	% MVC	GL/Gas	GM/TS	GL/TS	SOL/TS	GL/Gas	GM/TS	GL/TS	SOL/TS
PCSA (%)		35.6 ± 3.5	23.4 ± 2.9	12.9 ± 1.4	63.7 ± 3.6	34.2 ± 4.4	22.6 ± 2.5	11.8 ± 2.0[b]	65.6 ± 3.2
Activation (%)	20	38.6 ± 17.9	34.9 ± 13.5	20.8 ± 8.6	44.3 ± 13.4	**27.0 ± 14.1**[a]	41.6 ± 13.1	**15.1 ± 8.7**[a]	43.4 ± 14.0
	40	45.2 ± 9.3	36.1 ± 6.7	30.0 ± 7.2	33.8 ± 7.9	**38.0 ± 13.4**[a]	38.4 ± 11.0	**23.4 ± 9.1**[a]	38.2 ± 11.5
Force index (%)	20	27.7 ± 18.6	22.7 ± 10.8	7.5 ± 3.9	69.8 ± 11.7	**17.9 ± 12.5**[a]	26.0 ± 11.6	**5.3 ± 4.0**[a]	68.7 ± 12.8
	40	32.0 ± 9.1	25.9 ± 6.4	12.1 ± 3.9	62.0 ± 8.4	**26.0 ± 12.7**[a]	25.6 ± 10.4	**8.8 ± 5.1**[a]	65.6 ± 12.4

Data are reported for the control and Achilles tendinopathy groups.
Note that significant interactions are not shown within the table.
[a](bold cells) A significant main effect of group.
[b]Significant difference between groups.

the sake of clarity, we only report below the between-group differences, which are related to the main aims of this study. *Post hoc* showed that regardless the contraction intensity, GL RMS EMG was approximately 22.8% lower in the people with Achilles tendinopathy than controls ($P = 0.043$, $d = 0.33$). There was no between-group difference for GM ($P = 0.094$, $d = 0.31$) and SOL ($P = 0.083$, $d = 0.37$).

Activation ratios were calculated to represent the distribution of activation within TS (Table 3). There was a main effect of intensity on GL/Gas, GL/TS, and SOL/TS EMG ratios (all $P < 0.001$) but this was not the case for GM/TS EMG ratio ($P = 0.585$). There was no significant interaction between intensity and group (all $P > 0.132$); however, we observed a main effect of group for both GL/Gas ($P = 0.011$, $d = 0.76$) and GL/TS EMG ratios ($P = 0.009$, $d = 0.67$). Specifically, GL/Gas and GL/TS EMG ratio were lower in people with Achilles tendinopathy than in the controls (Table 3).

Distribution of Muscle Force

When considering the index of force values, we observed significant main effects of muscle ($P < 0.001$), and intensity ($P < 0.001$), an interaction between muscle and intensity ($P = 0.018$) and between muscle intensity and group ($P = 0.042$). Again, we only report below the between-group differences. At 40% of MVC, SOL index of force was approximately 27.0% higher in people with Achilles tendinopathy than controls ($P = 0.039$, $d = 0.65$). There were no other between-group differences (all P values >0.251).

Force ratios were calculated to represent the distribution of force within TS (Fig. 3; Table 3). There was no interaction between group and intensity for any of the ratios (all $P > 0.095$); however, there was a main effect of group for both GL/Gas ($P = 0.025$, $d = 0.67$) and GL/TS force ratios ($P = 0.023$, $d = 0.62$). Specifically, regardless the intensity, GL/Gas and GL/TS ratios were 11.2% and 28.5% lower, respectively, in people with Achilles tendinopathy compared with the controls. When considering the Achilles tendinopathy group, there were no significant correlations between either GL/Gas or GL/TS force ratios and the duration of symptoms (both r values <0.16, $P > 0.2$). Similarly, no significant correlation was observed between these force ratios and the VISA-A scores (both r values <0.11, $P > 0.2$).

Six months after the collection of the original data, 11 participants reported a clinically significant improvement in their symptoms (VISA-A increased by 33.3 ± 14.9 points) and 9 others did not (VISA-A increase by 4.3 ± 6.2 points). The comparison of the GL/TS force ratio at 20% of MVC of these

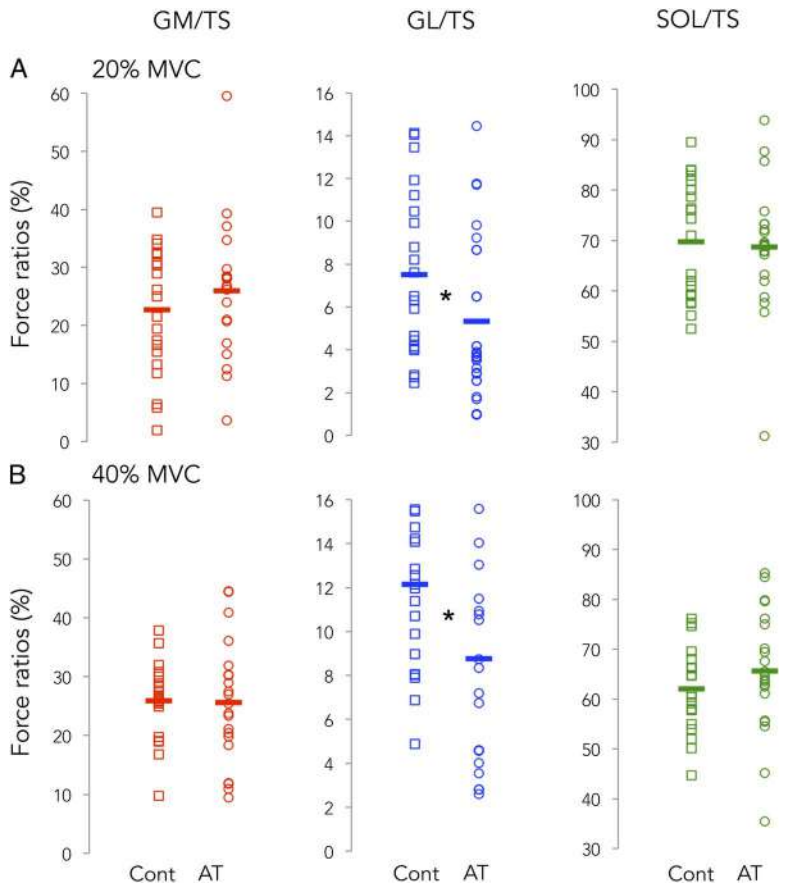

FIGURE 3—Individual and mean data for each muscle force ratio. Data are presented for both the control (*open squares*) and Achilles tendinopathy (*open circles*) groups during 20% of MVC (A) and 40% of MVC (B) contractions. Note the different *y*-axis scales for each panel. Indexes of force are calculated as the product of activation, pennation angle, and physiological cross-sectional area. *Statistical difference between the Control and Achilles tendinopathy group data ($P < 0.05$).

two subgroups indicated that people who did not recover had a smaller GL/TS force ratio (4.0% ± 2.5%) than people who recovered (7.1% ± 4.6%; $P = 0.087$). Note that the effect size was large ($d = 0.84$), but the difference was not significant. There were no differences for any other force ratio at 20% of MVC with all P values > 0.171. No between-group differences were found when considering the higher contraction intensity, that is, 40% of MVC (all $P > 0.158$).

Myotendinous Junction Displacement and Subtendon Strain

Displacement of each myotendinous junction (GM, GL, and SOL) was measured to estimate the change in each subtendon length during contraction. The ankle joint increased by 2.5° ± 1.5° (i.e., more plantarflexed) and by 5.4° ± 2.0° during the isometric contractions at 20% and 40% of MVC, respectively.

There were main effects of muscle ($P < 0.001$), intensity ($P < 0.001$), and a significant interaction between muscle and intensity ($P < 0.001$) on myotendinous junction displacement (Table 2). Specifically, at both 20% and 40% of MVC, GM myotendinous junction displacement was larger than that of both GL (for both intensities $P < 0.001$; $d = 0.48$ and 0.63 at 20% and 40% of MVC, respectively) and SOL (for both intensities $P < 0.001$; $d = 0.49$ and 0.85 at 20% and 40% of MVC, respectively). Although there was no difference between GL and SOL at 20% of MVC ($P = 0.652$, $d = 0.05$), GL myotendinous displacement was larger than that of SOL at 40% of MVC ($P < 0.001$; $d = 0.30$). However, there was neither a main effect of group ($P = 0.530$) nor an interaction between muscle and group ($P = 0.980$), indicating that the displacement of the myotendinous junctions did not differ between groups.

When considering the myotendinous displacement normalized to resting tendon length (tendon strain), there was a main effect of subtendon ($P < 0.001$), intensity ($P < 0.001$), and a significant interaction between intensity and subtendon ($P < 0.001$). Specifically, at 20% of MVC, the strain of both GM and GL subtendons was smaller than that of SOL subtendon (both $P < 0.001$ and both $d > 1.46$), with no difference between GM and GL ($P = 0.165$, $d = 0.72$). At 40% of MVC, both GM and GL subtendons strain was less than that of SOL subtendon (both $P < 0.001$ and $d > 1.37$), but GM subtendon had a higher strain than GL subtendon ($P < 0.001$; $d = 0.74$). There was neither a main effect of group ($P = 0.835$) nor an interaction between subtendon and group ($P = 0.746$).

DISCUSSION

The aim of this study was to determine whether the force distribution between the heads of the TS (muscle coordination) differs in people with Achilles tendinopathy compared with controls. We observed a different force distribution between the two populations with the GL muscle contributing significantly less to the overall submaximal isometric plantarflexion force in people with Achilles tendinopathy compared with the controls. This difference is explained by both a lower relative GL PCSA and GL activation in people with Achilles tendinopathy. Despite this altered force distribution in people with Achilles tendinopathy, the displacement of the myotendinous junctions did not differ between the populations during the submaximal isometric contractions. This is the first study to identify a difference in force distribution between muscles of the TS in people with Achilles tendinopathy compared with controls, which, moreover, might be associated with the potential for recovery. Additional work is needed to understand the role of this altered coordination strategy in the development or persistence of Achilles tendinopathy.

Muscle force-generating capacities. The maximal plantarflexion torque measured during the maximal contractions was not different between our two groups, which aligns with some (19,20) but not all previous studies (21,22). To the best of our knowledge, the current study is the first to use the twitch interpolation technique to verify that the voluntary activation was maximal in both participants with Achilles tendinopathy and controls. The inability to reach maximal voluntary contraction (as observed in one excluded participant with Achilles tendinopathy) might explain why some studies observed a lower maximal plantarflexion torque in people with Achilles tendinopathy. Another explanation for these discrepancies might be the characteristics of the task with most previous studies reporting a lower overall maximal force in people with Achilles tendinopathy for data collected during dynamic tasks (which contrasts with our isometric plantarflexion tasks). O'Neillet al. (21) reported a lower peak torque in people with Achilles tendinopathy than controls during dynamic maximal tasks performed at various knee positions. As large between-group differences were observed regardless of the position of the knee, they concluded that the monoarticular SOL had the greatest impact on the lower torques observed.

In our study, we considered the difference in PCSA as being representative of the difference in force-generating capacity between muscles. When considering the ratio of PCSA, we observed no between-group differences for GM/TS and SOL/TS PCSA but a significantly 8.5% lower GL/TS PCSA in people with Achilles tendinopathy. To the best of our knowledge, our study is the first to estimate PCSA of each head of the TS in people with Achilles tendinopathy. One study compared muscle volume between the affected and nonaffected limbs in people with Achilles tendinopathy (23) and reported differences, which aligned with our findings. Specifically, they reported a 14% smaller GL volume in the affected limb compared with the nonaffected limb.

Muscle activation. The between-day reliability of the distribution of normalized EMG amplitude among the heads of the TS has been demonstrated in a previous study (24), suggesting that it represents a robust individual strategy. Previous studies have estimated the activation of the TS muscles in people with Achilles tendinopathy during walking (25), running (26), isometric plantarflexion tasks (22), and dynamic plantarflexion tasks (27,28). However, these studies used different normalization procedures and reported different activation parameters

(e.g., onset/offset timings and EMG amplitude), which makes it difficult to directly compare their results with our results. Using a protocol similar to the protocol used in the present study, Masood and colleagues (22) observed greater EMG amplitude of the SOL in the symptomatic legs of people with Achilles tendinopathy compared with healthy controls. Even though we reported no significant difference in SOL EMG amplitude between the two groups, we observed a 27.0% higher SOL force in people with Achilles tendinopathy than controls at 40% of MVC. This is likely explained by both a larger, albeit nonsignificant, SOL activation and SOL PCSA in participants with Achilles tendinopathy than controls (Table 2). Most notably, we observed both a lower normalized GL EMG amplitude and a lower GL/TS activation ratio providing evidence of a lower GL contribution to the overall activation in people with Achilles tendinopathy. Even though the amplitude of the difference was only moderate (effect size: $d = 0.67$), it is consistent with the smaller relative GL/TS PCSA, which strengthens the likelihood that these outcomes are relevant.

Force-sharing strategies. Even though the distribution of force among the heads of the TS has been regarded as a potential contributor to Achilles tendon problems (9,11,21), this has never been investigated experimentally. This may be because there is no noninvasive technique to measure individual muscle force, leading to indirect approaches that rely on either experimental measures, biomechanical models, or both. As proposed in previous works (12–14), we considered that the difference of force produced between synergist muscles during isometric contractions is mainly due to their difference in muscle activation and PCSA. Therefore, we assumed that the three heads of the TS operated at a similar relative length of their optimal length, which seems reasonable considering the similar anatomy and function of GM and GL and previous works suggesting similar optimal angles for GM (19° of dorsiflexion (29)] and SOL [15° of dorsiflexion (30)]). We also assumed that specific tension would not impact the outcome because tasks were conducted at submaximal intensities, for which mainly slow twitch fibers are likely recruited for the three muscles in both groups.

Using the aforementioned approach, we observed a lower contribution of GL force to overall TS force, regardless the intensity of the contraction. We contend that this provides strong evidence that people with Achilles tendinopathy use a different force-sharing strategy during this simple isometric plantarflexion task. Even though we did not study higher contraction intensities, it is very likely that such differences would be also observed at higher force levels. This is because as intensity increases, the difference between individual muscles relies more on PCSA than activation differences as activation of all the muscles logically converge toward 100% (14).

Impact of altered force sharing strategies on Achilles tendon mechanical behavior. To provide a better understanding of the mechanical effect of the force sharing strategies on the Achilles tendon behavior, we assessed the displacement of each of the three myotendinous junctions using ultrasound imaging. Of note, inevitable ankle rotation was observed during the submaximal isometric plantarflexion tasks. As detailed in Materials and Methods, we applied a correction factor to account for this rotation. As the correction factors were not different between groups, it is unlikely that this ankle rotation influenced our main outcomes.

The tendon strain measured in the control group at 40% of MVC for GM (5.0% ± 2.0%) was either higher [2.2%, Finni et al. (31)] or similar [4.5%, Wolfram (32)] to values reported in previous studies for the same muscle at close contraction intensity. It is noteworthy that only a few studies have investigated both GM and GL, and those that have done so have reported either a similar strain (33,34) or a larger strain for GM than GL (32). Consistent with Wolfram (32), we report a larger strain for GM than GL. This difference observed in both controls and participants with Achilles tendinopathy might be explained by the combination of both a shorter GM tendon length and a larger GM force index compared with GL.

Despite our evidence that the contribution of GL to the overall TS force was lower in participants with Achilles tendinopathy, we did not observe any between-group difference in the myotendinous junction displacement or the tendon strain for any subtendon. Three reasons may explain this result. First, even though a degree of independence between the subtendons has been suggested (35), it is likely that the transmission of lateral force occurs between the subtendons (36). A different degree of force transmission between the populations may obscure the differences in force distribution. Second, the strain experienced by a subtendon depends on both muscle force and its mechanical properties. As tendons remodel over time and adapt to the forces they are subjected to, it is possible that the mechanical properties of the GL subtendon changed as a result of long-term lower contribution of the GL muscle to the TS force in our Achilles tendinopathy group. This proposition is consistent with an emerging body of literature that suggests lower stiffness of the Achilles tendon in people with Achilles tendinopathy (37). However, these studies used elastography, which cannot distinguish between the Achilles subtendons. Therefore, we do not know whether the lower stiffness that has been observed is specific to the GL subtendon or generalized to all of the subtendons. Third, it is possible that the contraction intensities (20% and 40% of MVC) were too low to identify between-group differences. As mentioned above, large force differences between muscles are expected at higher intensities when these differences are closely related to the differences in PCSA. Thus, it is likely that different muscle force distribution between populations would lead to different Achilles tendon behavior at higher levels of contraction. It is consistent with previous studies that reported a larger GM subtendon strain in people with Achilles tendinopathy during maximal contractions (19).

Clinical relevance. The lower contribution of GL to the overall TS force observed in people with Achilles tendinopathy is supported by a lower contribution of both PCSA and activation. As muscle PCSA and activation are estimated using different techniques, we are confident that the observed differences

are biomechanically relevant. However, our experimental design does not allow us to determine whether altered force-sharing strategies are the cause or the consequence of the pathology. Overall, the clinical relevance of this difference must be further explored.

It is important to note that the effect size of the between-group differences in GL/TS force is only moderate. This can be explained by the interindividual variability that exists, especially among people with Achilles tendinopathy, with the GL/TS force ratio ranging from 2.6% to 20.2% at 40% of MVC (Fig. 3). If we consider altered force-sharing as a cause of Achilles tendinopathy, this high interindividual variability might be explained by the well-known multifactorial etiology of Achilles tendinopathy, with altered force-sharing being present only in a subgroup of individuals. An alternative explanation is that altered force-sharing is a consequence of Achilles tendinopathy, in which case, we may expect a correlation between the duration of the symptom and the GL/TS force ratio. However, such a correlation was not found ($r = 0.17$ and -0.05 at 20% and 40% of MVC, respectively).

Interestingly, a previous study has provided evidence that eccentric training can change activation ratios within the TS group in healthy people (34). In addition, Masood and coworkers (38) observed a significant increase in GL activation during isometric plantarflexion tasks in people with Achilles tendinopathy after a 12-wk training program. Of note, no change in either GM or SOL activation was observed with training. As their participants had significant relief from their symptoms after the rehabilitation program, this result does provide support for a relationship between the contribution of the GL muscle to plantarflexion force and Achilles tendinopathy symptoms. This potentially echoes the observation we made that people whose symptoms improved over a 6-month period, tended to have higher GL/TS force ratio at the time of the original testing. However, it should be confirmed on a larger sample size. Of note, in our study, an improvement in the symptoms was neither associated with a change in physical activity level (as assessed by comparing IPAQ before the study and 6 months later), nor associated with a healthcare intervention.

Because the estimation of muscle force during a dynamic task relies on indirect information, such as the force length and force velocity relationship, we chose to study a more controlled task. Then, it remains unclear if the lower contribution of the GL force would also be observed during a dynamic task.

CONCLUSIONS

We observed different muscle coordination strategies between the two populations, with the GL muscle in people with Achilles tendinopathy contributing significantly less to the overall submaximal isometric TS force than for controls. Further investigations are needed to unravel the biomechanical consequences of altered muscle coordination strategies on the Achilles tendon and to determine whether altered coordination is the cause or consequence of the pathology. Consideration of muscle coordination during dynamic tasks would provide further insights, but it would require the use of a different approach that combines experimental data with musculoskeletal modeling.

M. C. is supported by a scholarship from the French Ministry of Higher Education and research and a research grant from the *Société Française de Physiothérapie*. F. H. is supported by a fellowship from the *Institut Universitaire de France* (IUF) and a travel grant from the Société de Biomécanique. Support was received from the French Ministry of Sport (17-R-04) and the Agence Nationale pour la Recherche (ANR-19-CE17-002-01, COMMODE project).

The results of the study are presented clearly, honestly, and without fabrication, falsification, or inappropriate data manipulation. The results of the present study do not constitute endorsement by ACSM.

Data are available as supplemental material at https://doi.org/10.6084/m9.figshare.10116158.

REFERENCES

1. Kujala UM, Sarna S, Kaprio J. Cumulative incidence of Achilles tendon rupture and tendinopathy in male former elite athletes. *Clin J Sport Med*. 2005;15:133–5.
2. de Jonge S, de Vos RJ, Van Schie HT, Verhaar JA, Weir A, Tol JL. One-year follow-up of a randomised controlled trial on added splinting to eccentric exercises in chronic midportion Achilles tendinopathy. *Br J Sports Med*. 2010;44(9):673–7.
3. Szaro P, Witkowski G, Smigielski R, Krajewski P, Ciszek B. Fascicles of the adult human Achilles tendon—an anatomical study. *Ann Anat*. 2009;191(6):586–93.
4. Clark WH, Franz JR. Do triceps surae muscle dynamics govern non-uniform Achilles tendon deformations? *PeerJ*. 2018;6:e5182.
5. Arndt A, Bengtsson AS, Peolsson M, Thorstensson A, Movin T. Non-uniform displacement within the Achilles tendon during passive ankle joint motion. *Knee Surg Sports Traumatol Arthrosc*. 2012;20(9):1868–74.
6. Arndt AN, Komi PV, Brüggemann G-P, Lukkariniemi J. Individual muscle contributions to the in vivo Achilles tendon force. *Clin Biomech (Bristol, Avon)*. 1998;13(7):532–41.
7. Arndt A, Brüggemann G-P, Koebke J, Segesser B. Asymmetrical loading of the human triceps surae—I. Mediolateral force differences in the Achilles tendon. *Foot Ankle Int*. 1999;20:444–9.
8. Sun YL, Wei Z, Zhao C, et al. Lubricin in human Achilles tendon: the evidence of intratendinous sliding motion and shear force in Achilles tendon. *J Orthop Res*. 2015;33(6):932–7.
9. Bojsen-Moller J, Magnusson SP. Heterogeneous loading of the human Achilles tendon in vivo. *Exerc Sport Sci Rev*. 2015;43(4):190–7.
10. Handsfield GG, Inouye JM, Slane LC, Thelen DG, Miller GW, Blemker SS. A 3D model of the Achilles tendon to determine the mechanisms underlying nonuniform tendon displacements. *J Biomech*. 2017;51:17–25.
11. Hug F, Tucker K. Muscle coordination and the development of musculoskeletal disorders. *Exerc Sport Sci Rev*. 2017;45(4):201–8.
12. Hug F, Goupille C, Baum D, Raiteri BJ, Hodges PW, Tucker K. Nature of the coupling between neural drive and force-generating capacity in the human quadriceps muscle. *Proc Biol Sci*. 2015;282(1819). pii: 20151908.
13. Avrillon S, Guilhem G, Barthelemy A, Hug F. Coordination of hamstrings is individual specific and is related to motor performance. *J Appl Physiol (1985)*. 2018;125(4):1069–79.
14. Crouzier M, Lacourpaille L, Nordez A, Tucker K, Hug F. Neuromechanical coupling within the human triceps surae and its consequence on individual force-sharing strategies. *J Exp Biol*. 2018;221(Pt 21). pii: jeb187260.

15. Robinson JM, Cook JL, Purdam CR, et al. The VISA-A questionnaire: a valid and reliable index of the clinical severity of Achilles tendinopathy. *Br J Sports Med*. 2001;35:335–41.
16. Craig CL, Marshall AL, Sjöström M, et al. International physical activity questionnaire: 12 country reliability and validity. *Med Sci Sports Exerc*. 2003;35(8):1381–95.
17. Tumilty S, Munn J, Abbott JH, McDonough S, Hurley DA, Baxter GD. Laser therapy in the treatment of Achilles tendinopathy: a pilot study. *Photomed Laser Surg*. 2008;26(1):25–30.
18. Place N, Maffiuletti NA, Martin A, Lepers R. Assessment of the reliability of central and peripheral fatigue after sustained maximal voluntary contraction of the quadriceps muscle. *Muscle Nerve*. 2007; 35(4):486–95.
19. Child S, Bryant AL, Clark RA, Crossley KM. Mechanical properties of the Achilles tendon aponeurosis are altered in athletes with Achilles tendinopathy. *Am J Sports Med*. 2010;38(9):1885–93.
20. Arya S, Kulig K. Tendinopathy alters mechanical and material properties of the Achilles tendon. *J Appl Physiol (1985)*. 2010;108(3): 670–5.
21. O'Neill S, Barry S, Watson P. Plantarflexor strength and endurance deficits associated with mid-portion Achilles tendinopathy: the role of soleus. *Phys Ther Sport*. 2019;37:69–76.
22. Masood T, Kalliokoski K, Bojsen-Møller J, Magnusson SP, Finni T. Plantarflexor muscle function in healthy and chronic Achilles tendon pain subjects evaluated by the use of EMG and PET imaging. *Clin Biomech (Bristol, Avon)*. 2014;29(5):564–70.
23. DiLiberto FE, Nawoczenski DA, Tome J, Tan RK, DiGiovanni BF. Changes in muscle morphology following gastrocnemius recession for Achilles tendinopathy: a prospective cohort imaging study. *Foot Ankle Spec*. 2019;1938640019857805.
24. Crouzier M, Hug F, Dorel S, Deschamps T, Tucker K, Lacourpaille L. Do individual differences in the distribution of activation between synergist muscles reflect individual strategies? *Exp Brain Res*. 2019; 237(3):625–35.
25. Baur H, Divert C, Hirschmüller A, Müller S, Belli A, Mayer F. Analysis of gait differences in healthy runners and runners with chronic Achilles tendon complaints. *Isokinetics Exerc Sci*. 2004;12:111–6.
26. Wyndow N, Cowan SM, Wrigley TV, Crossley KM. Triceps surae activation is altered in male runners with Achilles tendinopathy. *J Electromyogr Kinesiol*. 2013;23(1):166–72.
27. Reid D, McNair PJ, Johnson S, Potts G, Witvrouw E, Mahieu N. Electromyographic analysis of an eccentric calf muscle exercise in persons with and without Achilles tendinopathy. *Phys Ther Sport*. 2012;13(3):150–5.
28. Yu J. Comparison of lower limb muscle activity during eccentric and concentric exercises in runners with Achilles tendinopathy. *J Phys Ther Sci*. 2014;26(9):1351–3.
29. Hoffman BW, Lichtwark GA, Carroll TJ, Cresswell AG. A comparison of two Hill-type skeletal muscle models on the construction of medial gastrocnemius length-tension curves in humans in vivo. *J Appl Physiol*. 2012;113(1):90–6.
30. Maganaris CN. Force-length characteristics of in vivo human skeletal muscle. *Acta Physiol Scand*. 2001;172:279–85.
31. Finni T, Hodgson JA, Lai AM, Edgerton VR, Sinha S. Nonuniform strain of human soleus aponeurosis-tendon complex during submaximal voluntary contractions in vivo. *J Appl Physiol (1985)*. 2003; 95(2):829–37.
32. Wolfram S. *Differential Behaviour of the Medial and Lateral Heads of Gastrocnemius during Plantarflexion: The Effect of Calcaneal Inversion and Eversion*. UK: Manchester Metropolitan University; 2017. 161 p.
33. Morrison SM, Dick TJ, Wakeling JM. Structural and mechanical properties of the human Achilles tendon: sex and strength effects. *J Biomech*. 2015;48(12):3530–3.
34. Obst SJ, Newsham-West R, Barrett RS. Changes in Achilles tendon mechanical properties following eccentric heel drop exercise are specific to the free tendon. *Scand J Med Sci Sports*. 2016;26(4): 421–31.
35. Edama M, Kubo M, Onishi H, et al. The twisted structure of the human Achilles tendon. *Scand J Med Sci Sports*. 2015;25(5): e497–503.
36. Finni T, Cronin NJ, Mayfield D, Lichtwark GA, Cresswell AG. Effects of muscle activation on shear between human soleus and gastrocnemius muscles. *Scand J Med Sci Sports*. 2017;27(1):26–34.
37. Coombes BK, Tucker K, Vicenzino B, et al. Achilles and patellar tendinopathy display opposite changes in elastic properties: a shear wave elastography study. *Scand J Med Sci Sports*. 2018;28(3):1201–8.
38. Masood T, Kalliokoski K, Magnusson SP, Bojsen-Moller J, Finni T. Effects of 12-wk eccentric calf muscle training on muscle-tendon glucose uptake and SEMG in patients with chronic Achilles tendon pain. *J Appl Physiol (1985)*. 2014;117(2):105–11.

GENERAL DISCUSSION

In this thesis, we investigated muscle coordination among the *triceps surae* muscles during isometric contractions, in people with no significant history of lower limb pain and injury, and people with Achilles tendinopathy. Our experimental approach to estimate muscle force combined the evaluation of muscle structural features and muscle activation. The first two studies provided insight into the distribution of activation during isometric and dynamic tasks (**study #1**) and the distribution of muscle force during isometric tasks (**study #2**) in pain-free populations. **Study #3** compared muscle coordination between people with and without Achilles tendinopathy during isometric tasks.

Results from this doctoral research were threefold. First, the distribution of normalised EMG amplitude among synergist muscles was robust between days, was correlated between tasks (i.e. isometric, walking, cycling), and varied greatly between individuals. Second, we demonstrated that there is a positive significant correlation between the distribution of PCSA and the distribution of activation during submaximal isometric plantarflexion tasks (under 50 % of MVC) when considering *gastrocnemii*. This is important as GM and GL share the same function. The large inter-individual variability in the distribution of force among GM, GL and SOL muscles was noteworthy. Third, the distribution of force among *triceps surae* differed in people with Achilles tendinopathy compared with controls, with GL contributing less to the *triceps surae* force.

The results from these studies are discussed in the following four sections: 1) the methodological considerations of our experimental approach to estimate individual muscle force, 2) the distribution of PCSA, activation and force among the *triceps surae*, 3) the impact of muscle coordination on the Achilles subtendons mechanical behaviour and 4) the clinical relevance of current findings.

1. Methodological considerations of the estimation of muscle force

In this work, studies #2 and #3 estimated the distribution of muscle force within the *triceps surae*, at both maximal and submaximal levels. Maximal force-generating capacity of each individual head was estimated with the calculation of PCSA. Considered together, muscle activation and PCSA were used to calculate individual muscle force indices during submaximal contraction. Our approach relies on a number of assumptions, which each needs some considerations that are discussed below.

1.1. Maximal isometric force: PCSA

An important aspect of our approach is to consider PCSA as an index of the maximal muscle force-generating capacity. The *in vivo* estimation of PCSA involved measurements of volume, fascicle length and pennation angle.

Methods used for volume calculation were different between studies #2 and #3. Because of the difficulty to access MRI, which was only available for study #2, we used an alternative method called freehand 3D-ultrasonography to measure muscle volumes in study #3. The validity of freehand 3D-ultrasonography when compared to MRI, and inter-day reliability of this technique to determine muscle volumes, have been previously reported (Barber et al., 2009). Nonetheless, to ensure the validity of our setup, we ran a pilot study on 6 participants who participated in study #2 to compare the volume obtain using freehand 3D US with MRI. Percentages of difference between the two techniques were 2.4 ± 2.0, 3.5 ± 1.7 and 3.6 ± 2.3 % for GM, GL and SOL volumes, respectively. Muscle volumes measured in the current work, either with MRI or freehand 3D-ultrasonography, were consistent with those reported in the literature. We reported muscle volumes of 247 ± 48, 146 ± 37 and 436 ± 80 cm^3 for GM, GL and SOL respectively (studies #2 and #3 averaged), while our review of the literature led to muscle volume of approximately 260, 139 and 441 cm^3, for GM, GL and SOL respectively (averaged data of studies reported in the Table 1 in the literature review, Part 2, Section 1.2).

To measure fascicle length, both protocols in studies #2 and #3 involved panoramic images for GM and GL, and conventional B-mode images for SOL. On average, we found GM, GL and SOL fascicle lengths of about 5.9 ± 0.7, 6.7 ± 0.8 and 4.0 ± 0.7 cm, respectively. These values are close to the mean values reported in the literature measured at similar joint angles (i.e. ~ 5.2 cm for GM, ~ 5.8 cm for GL, and ~ 3.9 cm for SOL, see Table 1 in the literature review, Part 2, Section 1.2). The technique of diffusion tensor imaging with anatomically constrained tractography, that has been developed recently (Bolsterlee et al., 2019), allows the estimation of a high number of fascicles within a muscle. Subsequently, this technique is more representative of the global muscle architecture (e.g. 2450, 1597 and 1826 fascicles could be measured for GM, GL and the posterior part of SOL respectively; Bolsterlee et al., 2019). With this technique, fascicle lengths were estimated to be 6.1, 6.8 and 4.8 cm for GM, GL and the posterior part of SOL, respectively (Bolsterlee et al., 2019). Of note, these values

remain within the range reported in our studies. Even if their values are slightly higher, it is important to note that Bolsterlee et al. (2019) measured fascicle lengths at different joint angles (ankle at 70° and knee at ~ 162°; compared to 90° and 180° in our studies #2 and #3) and for different proportion of men and women (50 % men in their study; compared to 70 % men in our studies #2 and #3 considered together). Overall, as long as variations are similar between muscles, it is unlikely that this would have impacted the force distribution we observed.

As a result, the PCSA measured in the current work (41.8 ± 6.6, 23.2 ± 5.0 and 115.4 ± 24.1 cm^2, for GM, GL and SOL respectively) were in accordance with mean values from the literature: ~ 49, ~ 27 and ~ 120 cm^2 for GM, GL and SOL, respectively (from Table 1 in the literature review, Part 2, Section 1.2). We considered PCSA as the indicator for the maximal force-generating capacity of the muscle, but it is important to note that PCSA is inherently dependent on muscle architecture, hence fascicle length and pennation angle. During an isometric contraction, muscle architecture is itself dependent on (*i*) the joint angle chosen for the isometric contraction, as it determines muscle length and inherently fascicle lengths and (*ii*) the intensity of contraction, as fascicles shorten with increase in contraction intensity. Considerations concerning the joint configuration are discussed in the next section (1.2.2). Architecture changes with contraction intensity were documented for the *quadriceps*. PCSA estimated from fascicle length measured during MVC and PCSA estimated from fascicle length measured at rest were similarly associated with the maximal torque (r = 0.53 and 0.52, respectively). This implies that resting measurements of muscle size, as conducted in our studies, were suitable for determining the relationship between muscle PCSA and maximal force (Massey et al., 2015).

1.2. Submaximal isometric force: indices of force

Many parameters contribute to the production of muscle force (Rohrle et al., 2019). To investigate the distribution of force among a muscle group, the current work aimed (*i*) to identify all relevant factors that could contribute to muscle force with respect to the experimental tasks considered, and (*ii*) to measure each of these factors for each individual muscle and individual participant. The main limitation we faced is the impossibility to determine parameters such as specific tension, force-length, force-velocity relationships for each head *in vivo*. We overcame this drawback by setting an experimental design that limits involvement of these factors. In other words, by performing submaximal isometric

contractions, a simplified approach of Hill-model could be used. Our approach is similar to studies that quantified maximal individual muscle force by weighting the overall force to each muscle, based on their relative PCSA (Lieber and Boakes, 1988; Morse et al., 2007; Narici et al., 1992; Trezise et al., 2016). In our experimental design, the additional consideration of muscle activation provides insight on force distribution at low submaximal intensities. Considerations related to this experimental design are discussed below.

1.2.1. Specific tension

The maximal force-generating capacity of a muscle depends on its PCSA and specific tension. However, in the current thesis, the experimental approach to estimate individual force that a muscle develops did not account for specific tension. This is because there is currently no technique to measure *in vivo* specific tension of individual muscles. Even if muscle biopsy could indicate muscle fibre-type composition, specific tension could at best be crudely approximated from this measure, as the relationship between specific tension at the fibre and muscle level is still obscure (see the literature review, Part 1, Section 1.2.1.b). Moreover, we contend that if we knew individual muscles fibre-type composition, their consideration would not have modified the main outcomes of this work. This is because we compared muscles at submaximal intensities, where slow type fibres are preferentially recruited. This is due to the *size principle* of orderly recruitment of motor units (Henneman and Oslon, 1965; Henneman et al., 1965). Therefore, we assumed that slow type fibres were preferentially recruited to perform the low submaximal tasks, which potentially limits the influence of specific tension on the estimation of the differences in force produced by the three heads of the *triceps surae*.

1.2.2. Impact of the force-length relationship

In our studies, plantarflexion tasks were performed with the knee fully extended and the ankle at 90° of plantarflexion (foot perpendicular to the shank). At these angles we considered that the three heads of the *triceps surae* are at a similar muscle length relative to their optimal length. This is supported by studies that estimated an optimal angle at approximately 15° of dorsiflexion for the SOL (Maganaris, 2001), and at 19° of dorsiflexion for the GM (when the knee is extended at 175°; Hoffman et al., 2012). No such studies were conducted on GL, but it was shown that the force-length relationships of the two *gastrocnemii* have similar relative shape (Maganaris, 2003). Hence, we assumed that GL was also at a similar muscle length relative to its optimal length. As a result, we assumed that the chosen joint configuration was

appropriate to reduce the impact of difference in the operating ranges of the muscles (over their force–length relationship) on the estimation of force-sharing strategies.

1.2.3. Isometric contractions

Findings of the present work provide the first impetus supporting that a high imbalance of force exists. Studying isometric contractions was the first step towards *in vivo* quantification of force, but force-sharing could change depending on the task. Herzog (1998) showed that the force-sharing among the cat *triceps surae* encompasses the entire possible range; from large SOL forces and zero gastrocnemii forces during still standing, to large *gastrocnemii* forces and no SOL forces during high-frequently paw shakes. Walmsley et al. (1978) demonstrated that the peak force of *medial gastrocnemius* (2.5 N) is ~ 40 % of the peak force of SOL during slow cat walking (6.3 N); it is ~ 79 % (4.6 N) of the peak force of SOL during fast cat walking (6.3 N). These data were reported from the same animal, demonstrating variability within animal between tasks, but variability between cats was not reported. From the seven cats involved in their study, it is unclear if the cat that bias force to GM during walking slow is the cat that bias force to GM during walking fast. In our context, we could wonder whether people who bias their force toward a specific muscle during isometric contractions also bias their force toward this specific muscle during walking. During dynamic task, muscle force still depend on maximum force capacity and activation, but additionally on its force–length and force–velocity relationships (Zajac, 1989). Although architectural parameters that determine maximal muscles force-generating capacity will remain the same, muscle activation could be distributed differently between isometric and dynamic task. To this purpose, in study #1, we characterized the distribution of muscle activation in the *quadriceps* and *triceps surae* groups during isometric contractions, during walking and pedaling. We found that distribution of muscle activation was correlated between isometric contractions and these two dynamic tasks. For example, there were significant positive correlations between walking and isometric submaximal contractions for GM/TS, GL/TS and SOL/TS activation ratio (all $r > 0.43$; $n = 85$; Figure 37). These results provided evidence that people who bias their activation to a particular muscle during isometric contractions do so during other motor tasks, at least within the tasks and muscle groups considered here in. Of note, such results on the distribution of cannot be extrapolated to the distribution of force as we may speculate that dynamic properties could impact the distribution of force differently between individuals. However, it is unlikely that these properties fully counteract the inter-individual differences in the distribution of activation and force-generating capacity that we

observed.

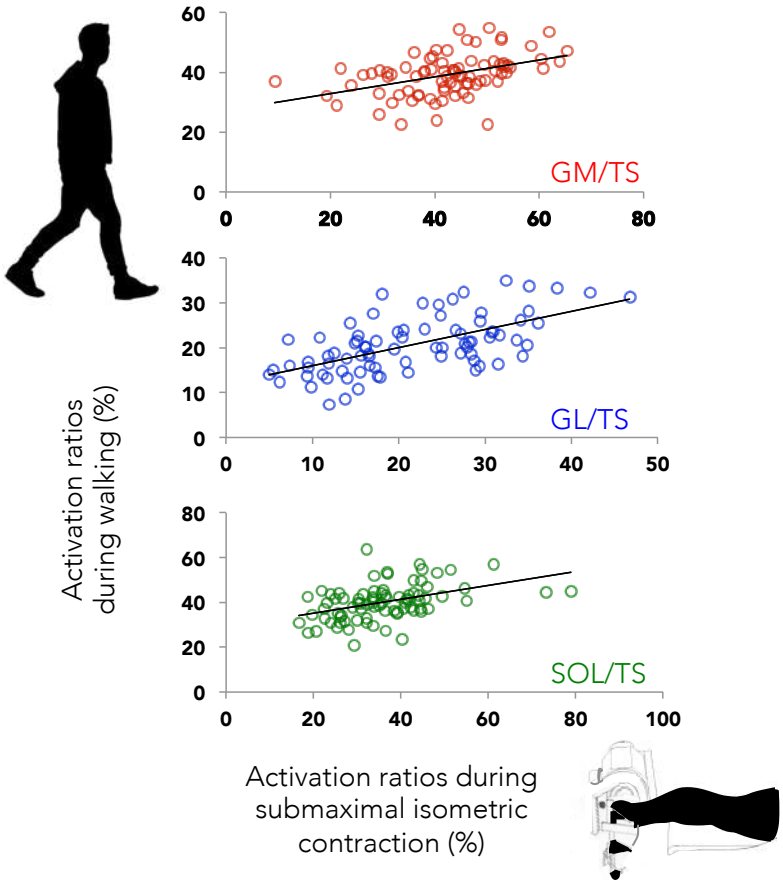

Figure 37. Correlation between activation ratios calculated during walking and isometric submaximal contraction at 25 % of MVC, from study #1. *GM/TS, GL/TS and SOL/TS ratios had respective r values of 0.43, 0.61 and 0.43 (n = 85 participants). GM, gastrocnemius medialis; GL, gastrocnemius lateralis; SOL, soleus; TS, triceps surae.*

1.3. Toward the estimation of muscle force in dynamic condition

The two most important architectural parameters of muscles are PCSA (proportional to maximum muscle force) and fascicle length (proportional to maximum muscle velocity; Lieber and Friden, 2000). Hence depending on their architectural features, muscles are intrinsically designed for a specific function. In the human body, it is not uncommon to find synergist muscles with very different architecture. It is thought to be more efficient, in terms of muscle mass, to have multiple highly specialized muscles than a single "*super-muscle*" that

can accomplish the task of multiple muscles (Lieber and Friden, 2000). Lieber and Friden (2000) demonstrated this with the example of two wrist extensors (*extensor carpi radialis brevis* and *extensor carpi radialis longus*). Together, these muscles combine properties to (*i*) produce a maximum tetanic tension (based on the sum of their PCSAs) of 250.9 N and (*ii*) produce a maximum angular velocity (based on the length of the *extensor carpi radialis longus* fibers) of ~ 2800 °.s^{-1}. For a single muscle to combine these properties (fiber length of 76 mm and a CSA of 4.2 cm^2), the "*super-muscle*" would weight 30 % greater than the sum of the two muscle masses. Similarly, a heterogeneous distribution of properties is observed in the *triceps surae* group. The muscle with the shortest fascicle length (~ 4 cm; SOL) also exhibits the biggest volume (~ 440 cm^3), and the muscle with the longest fascicle length (~ 6.6 cm; GL) has the smallest volume (~ 140 cm^3; Figure 38).

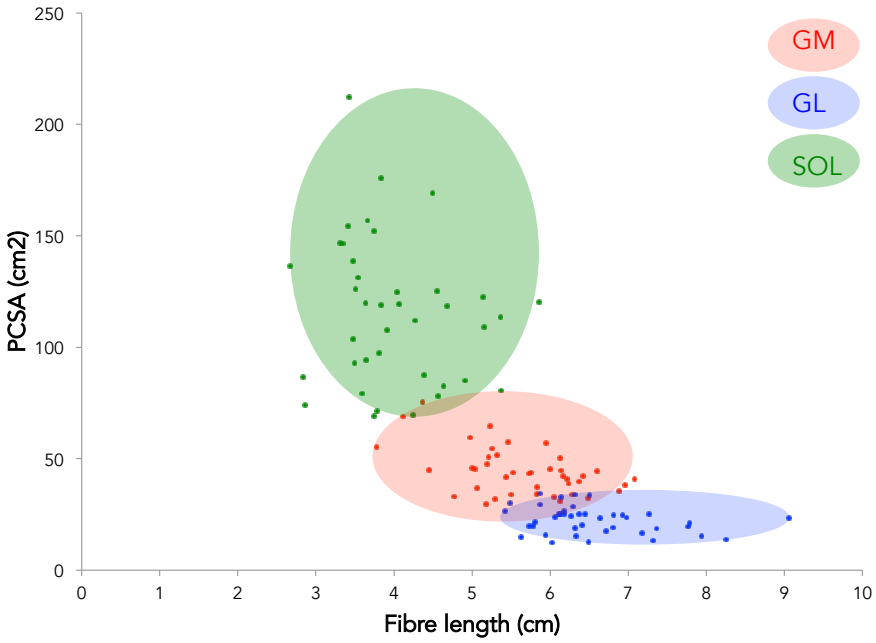

Figure 38. Scattergraph of the fiber length and physiological cross-sectional area (PCSA) of muscles in the *triceps surae* muscle (from study #2 and #3, control group only; n = 41). *This graph illustrates the relative specific functions of gastrocnemius medialis (GM), gastrocnemius lateralis (GL) and soleus (SOL). The high SOL PCSA makes it specialized for high forces. The long fibres of GL makes it specialized for high shortening velocity capacity.*

Hence, from their architecture, we know that *triceps surae* heads are intrinsically designed for different functions (Lieber and Friden, 2000): SOL has better force-generating capacity (larger volume) whereas GL has better velocity-generating capacity (longer fibers). For this

reason, we might hypothesize a "re" distribution of force during dynamic tasks. During isometric contractions, SOL is acting with the greatest advantage and our data (studies #2 and #3) supported that SOL contributed the greatest to the force generation (~ 75 % of the *triceps surae* force). During high velocity contractions, we may expect that GL will contribute to a higher extent (Figure 39).

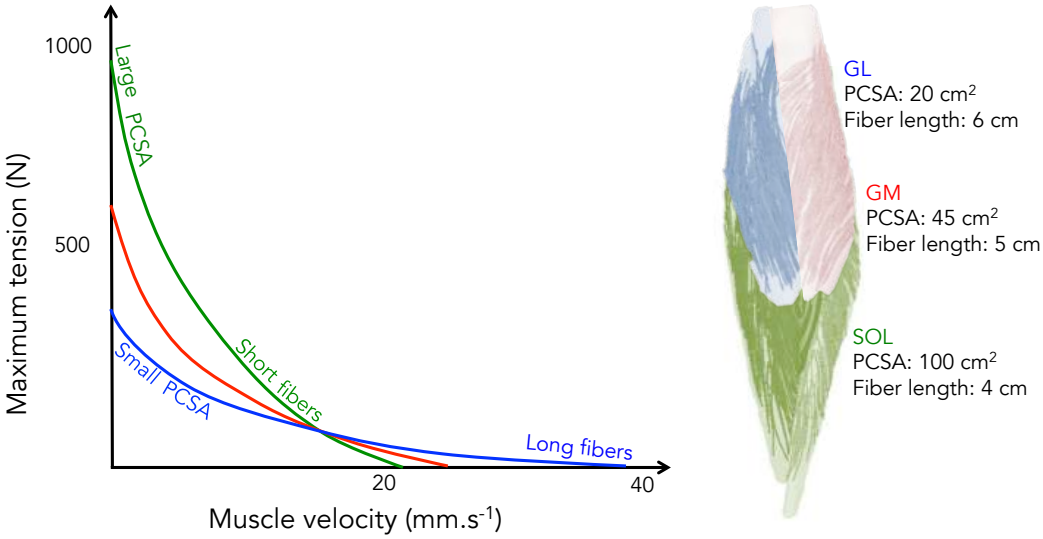

Figure 39. Comparison of isotonic force-velocity properties among *triceps surae* muscles. *Hypothetical arrangement of force-velocity relationship in triceps surae muscles: gastrocnemius lateralis (GL) combines the smallest physiological cross-sectional area (PCSA) and longest fibers, soleus (SOL) combines the biggest PCSA and the shortest fibers, and gastrocnemius medialis (GM) presents in between characteristics. Their relative intrinsic shape is speculative. Inspired from Lieber and Friden (2000). The 3D reconstruction of triceps surae (right) is from Bolsterlee et al. (2019).*

The estimation of force-sharing during dynamic contractions is challenged by the need to know the force-length and force-velocity relationships for each individual muscle. In 2017, Dick et al. (2017) performed a study where they compared human *gastrocnemii* forces predicted by Hill-type models with the forces estimated from *in vivo* measures during pedalling. Specifically, predicted forces from a Hill-type model were driven by individual-specific measures of muscle activation, ultrasound-based measures of muscle fascicle length, velocities and pennation angles. Estimated forces were ultrasound-based from tendon length changes and stiffness estimates. Their results revealed that Hill-type muscle models predicted well *gastrocnemii* forces, when compared to estimated forces (via ultrasound measures). As depicted in Figure 40, during pedalling, the normalised GL force was higher than GM. Of

note, (*i*) some parameters involved in Hill-type predicted forces had to be estimated from literature and taken from non-human data (e.g. the normalised active force-length relationship, the specific tension), and (*ii*) the forces used to test the model are themselves estimated from ultrasound measures (i.e. they are non-direct measures). As such, data interpretation must be mindful of these limits, but the acquirement of experimental data sets, as done in the aforementioned work (Dick et al., 2017), are necessary and useful for testing and improving models. They constitute strong basis for a better understanding of muscle force-sharing during dynamic contractions in humans *in vivo*.

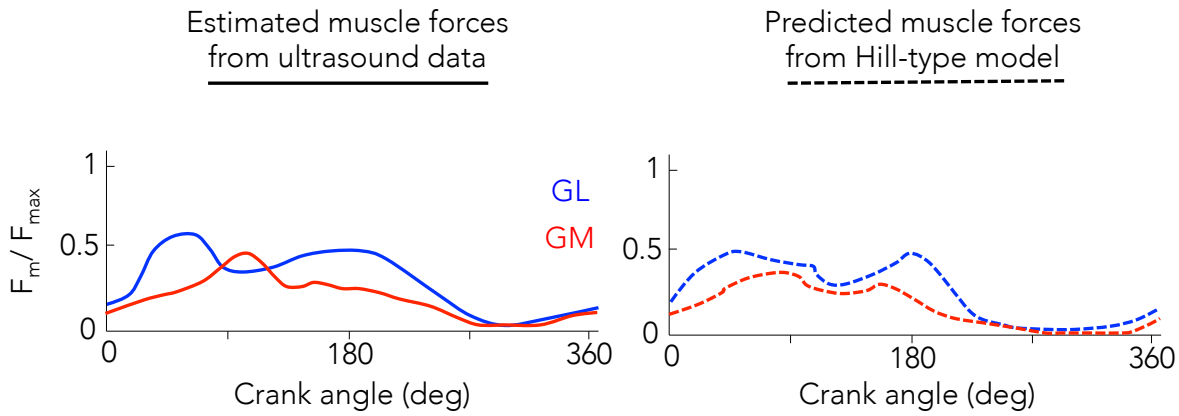

Figure 40. Time-varying force profiles for *gastrocnemius lateralis* (GL) and *gastrocnemius medialis* (GM) during pedalling (cadence: 100 rotations per minute, crank torque: 26 N.m). *Data are represented for one participant, adapted from the study of Dick et al. (2017). Estimated forces are represented in full lines, predicted forces from the Hill-type model are in dotted lines. Muscle forces (F_m) are normalised to the maximum isometric maximal force (F_{max}) of either GL or GM.*

2. Distribution of PCSA, activation, and force among *triceps surae*

2.1. Distribution of PCSA among the *triceps surae*

2.1.1. Synthesis of studies #2 and #3

In this work, two studies (#2 and #3) quantified muscle force-generating capacities through the calculation of PCSA. Results were not different between the two studies (Figure 41), despite differences in the methods used for volume estimation (MRI and freehand 3D-ultrasonography), and were in accordance with the data from the literature (as detailed above in Section 1.1).

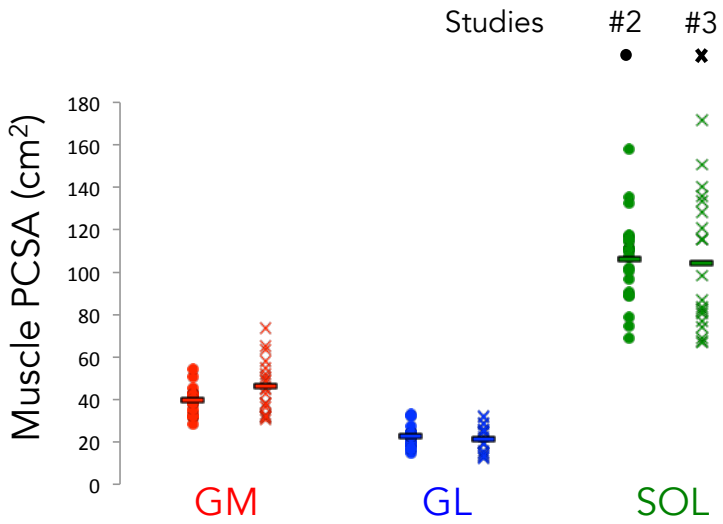

Figure 41. Synthesis for *triceps surae* physiological cross-sectional area (PCSA) data of studies #2 (circles) and #3 (crosses). *Studies #2 and #3 yielded similar results. In average for the two studies, GM, GL and SOL PCSA were 42.9, 21.9 and 105.2 cm^2, which represent gastrocnemius medialis (GM), gastrocnemius lateralis (GL) and soleus (SOL) contributions of 25, 13 and 6 2% of the total triceps surae PCSA.*

2.1.2. Inter-individual variability

Inspection of individual data revealed large variability of the PCSA distribution between participants among the three heads of the *triceps surae*, albeit with smaller magnitude than that observed for activation (see Section 2.2 below). For example (from study #2), the GM/Gas and SOL/TS PCSA ratios ranged from 55.2 % to 74.0 % and from 50.6 % to 68.5 %, respectively. To our knowledge, this was the first study to report such individual differences for this muscle group. The consequences of such variability are discussed below (Section 2.3.2).

2.2. Distribution of activation among a group of synergist muscles

This doctoral work provides two important findings regarding the distribution of muscle activation. First, we demonstrated the robustness of activation ratios across time, (studies #1 and #2). Second, we showed that activation ratios vary greatly between individuals (studies #1, #2 and #3). Together, these results provide the first impetus that activation ratios represent individual-specific strategies.

2.2.1. Synthesis of studies #1, #2 and #3 for isometric plantarflexion tasks

In the three studies of this thesis, we measured *triceps surae* muscle activation during isometric submaximal plantarflexion tasks in healthy populations [n = 85, 20 and 21 in studies #1, #2 and #3 (control group only), respectively]. Protocols presented subtle differences. First, studies #2 and #3 investigated muscle activation while participants were lying prone; hip and knee extended, ankle at 90° of plantarflexion. In constrast, study #1 investigated muscle activation as participants were sitting; hip at 80° of flexion, knee extended, ankle at 90° of plantarflexion. Second, the intensity of submaximal plantarflexion tasks was 20 % of MVC in studies #2 and #3; and 25 % of MVC in study #1. Overall, our studies confirmed that activation is not equally distributed between *triceps surae* muscles. On average from the three studies, we found a two times higher normalised activation of the GM (~ 18 %) than the GL (~ 9 %) during the isometric plantarflexion at 20 and 25 % of MVC. The GM/Gas activation ratio was not different between studies (all p values > 0.18). This result is consistent with the vast majority of previous studies, which also reported higher activation for the GM than the GL during a wide variety of tasks, e.g. standing (Heroux et al., 2014), calf raises (Fiebert et al., 2000; Riemann et al., 2011) and submaximal isometric plantarflexion (Cresswell et al., 1995; Lacourpaille et al., 2017; McLean and Goudy, 2004). GM/TS, GL/TS and SOL/TS activation ratios were not different between studies #2 and #3 (that investigated the same intensities of contraction in the same position), but differences were found when comparing study #1 (25 % at MVC) with studies #2 and #3 (20 % of MVC). Specifically, in studies #2 and #3, GM/TS activation ratio was lower ($p = 0.003$), GL/TS activation ratio was not different ($p = 0.257$), and SOL/TS activation ratio was higher ($p < 0.001$) compared to study #1 (Figure 42). This is because in studies #2 and #3, SOL exhibited a slightly greater activation level (~ 16 %) than both the GM (~ 13 %) and GL (~ 7 %), which is consistent with previous results (Mademli and Arampatzis, 2005). In study #1, it was GM that exhibited a slightly greater activation level (~ 21 %) than the SOL (~ 18 %) and GL (~ 11 %), and this is also consistent with previous results (Cresswell et al., 1995; Masood et al., 2014a). The consistent lower activation of GL we observed in such tasks (isometric submaximal plantarflexions) is in agreement within the literature (all aforementioned studies). The inconsistencies regarding GM and SOL relative activation presented both throughout the three current studies and within the literature, which eventually could be explained by participant positioning (e.g. lying *vs* sitting), are unclear and should be further explored.

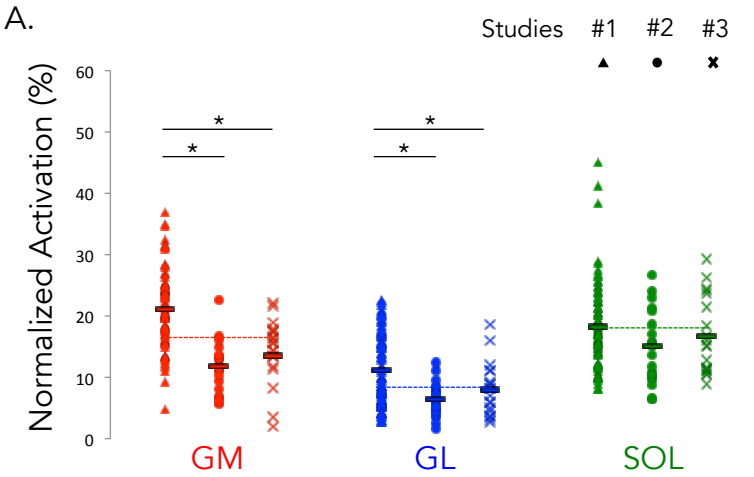

B.

Activation Ratios	GM/TS (%)	GL/TS (%)	SOL/TS (%)
▲	42.2 ± 10.7	21.7 ± 9.4	36.1 ± 11.0
●	36.3 ± 11.4 $	18.8 ± 6.4 $	44.8 ± 8.9 $
✖	35.0 ± 13.6 $	20.7 ± 8.5 $	44.3 ± 13.4 $

Figure 42. Synthesis of data from *triceps surae* activation, for studies #1 (triangles) #2 (circles) and #3 (crosses; control group only) during submaximal isometric contractions. *For study #1 data were collected at 25 % of MVC while studies #2 and #3 data were collected at 20 % of MVC. Panel A: data distribution for individual muscle activation: gastrocnemius medialis (GM, red), gastrocnemius lateralis (GL, blue) and soleus (SOL, green). Flat black contoured hyphens are averages for each study; dotted lines represent averages for the three studies merged. Panel B: table of activation ratios for each study. TS, triceps surae. *, activation different from study #1. $, ratio different from study #1.*

2.2.2. Between-day reliability

In this work, studies #1 and #2 quantified the between-day reliability of the distribution of activation. Our results, obtained from a subgroup of 62 (study #1) and 20 participants (study #2), demonstrated a fair-to-good reliability for the *quadriceps* muscles (study #1) and a good-to-excellent reliability for the *triceps surae* muscles (studies #1 and #2). Even though the *quadriceps* muscles exhibited lower ICC values (ICC > 0.57) than the *triceps surae* muscles (ICC > 0.65), SEM values were similar between muscle groups (SEM < 4.7 % and < 6.4 % for *quadriceps* and *triceps surae* respectively). As such, the lower ICC values of *quadriceps* muscles are likely explained by the smaller variance between individuals for *quadriceps* activation rather than a lower reliability. The reliability of distribution of activation over-time

observed here for *quadriceps* and *triceps surae* muscles are consistent with similar investigation for the hamstring (ICC > 0.57, SEM < 5.6%; Avrillon et al., 2018). Despite the overall good reliability, between-day variability inevitably exists. This between-day variability may not be (entirely) explained by variability of the activation strategies between days as methodological factors may also affect EMG amplitude (e.g. capacity of the individual to fully contract their muscle during MVCs; reviewed in Farina et al., 2004b)].

2.2.3. Inter-individual variability

The vast majority of studies on muscle coordination reported values averaged from a group of individuals, making it impossible to appreciate the individual differences in the activation strategies. In our three studies, we report a wide range of activation ratios during a standardized isometric single-joint task (see the large data spread in Figure 42). For example in study #2, during the submaximal contraction at 20 % of MVC, SOL/TS and GM/Gas activation ratios ranged from 26.4 % to 61.0 % and from 37.7 % to 88.7 %, respectively. The significance of inter-individual variability has received little attention in the literature. In a study that investigated activation ratios between the heads of the *triceps surae* during gait, Ahn et al. (2011) reported that among a group of 10 participants, seven activated their GM more than their GL while the other three participants activated their GM and GL nearly equally. Their results are in line with our observation that inter-individual differences in activation strategies exist. Other works, conducted on other muscle groups (e.g. *quadriceps*) and/or during different tasks also observed inter-individual variability in the activation ratios (De Marchis et al., 2013; Hug et al., 2015a; Hug et al., 2010; Ivanenko et al., 2002; Winter and Yack, 1987). However, these experiments were performed on relatively small sample size (typically less than 20 participants). The novelty of study #1 was to describe these individual differences in a much larger sample size (n = 85). The large inter-individual variability and their robustness over time supported that there are individual muscle activation strategies. The uniqueness of these muscle activation strategies has now also been supported using a machine learning approach (Hug et al., 2019). In their study, Hug et al. (2019) used an algorithm to identify participants from activation data collected on 8 lower-limb muscles of 80 participants during walking and cycling, on two different days. For the classification, data from day 2 were tested using the classifier, which had been trained on data from day 1. The activation profiles were assigned to the corresponding individuals with a classification rate of up to 91 %, which demonstrates the uniqueness of participant's muscle activation patterns.

The origin of these individual differences is still unknown. In study #2, we investigated the role of the muscle PCSA, the main peripheral factor related to the maximal muscle force-generating capacity. Synergist muscles sometimes have large differences in size and morphology. This may be accounted by the nervous central system and explain, at least in part, the observed distributions of activation.

2.3. The neuro-mechanical coupling

2.3.1. Neuro-mechanical coupling in one-joint and two-joint muscles

Bi-articular gastrocnemii. The control of joint torques generated by the human body is complex, and there is an ultimate interaction between neural (the neural drive to muscles) and mechanical factors for each muscle (Mogk et al., 2009). Mechanical factors combine properties such as muscle architecture (e.g. PCSA), dynamics (e.g. force-length relationship) or biomechanical features (e.g. moment arm). There could be a relationship between these neural and mechanical factors. For example, the distribution of muscle activation and the distribution of PCSA between synergist muscles could be positively correlated (case 3 on Figure 16 in the literature review, Part 1; 2.1.3) or negatively correlated (case 2 on Figure 16 on the literature review, Part 1; 2.1.3; Mogk et al., 2009). A neuro-mechanical positive coupling has already been identified in a hand muscle. The EMG contribution of *first dorsal interosseous* during voluntary index finger flexion was compared in two thumb postures. When the thumb position allowed the *first dorsal interosseous* to have a greater capacity (~ 50 % greater) to produce torque about the metacarpophalangeal joint, the relative activation toward *first dorsal interosseous* was ~ 28 % greater (Hudson et al., 2009). Similarly, an investigation of thigh muscles (VM and VL) showed that ratios of activation and ratios of PCSA were positively correlated (Hug et al., 2015a). Specifically, the greater the force-generating capacity of the VL compared with the VM, the stronger bias of activation to the VL (Figure 43).

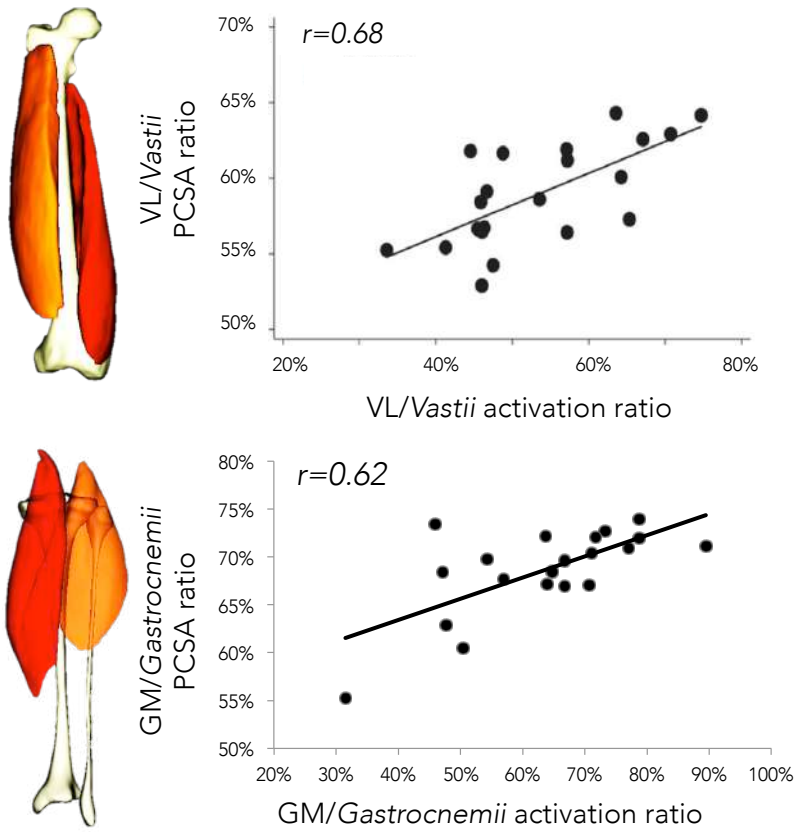

Figure 43. Relationship between distribution of muscle activation and distribution of physiological cross-sectional area (PCSA). *There is a significant positive correlation among vastii (panel A; from Hug et al., 2015) and gastrocnemii (panel B; current work study #2). GM, gastrocnemius medialis; VL, vastus lateralis.*

In study #2, we observed a similar positive correlation between GM/Gas activation ratio and GM/Gas PCSA ratio, indicating that the greater the force-generating capacity of the GM compared with the GL, the stronger bias of activation to the GM (Figure 43). This was observed for submaximal contractions that were performed under 50 % of MVC ($0.51 < r < 0.62$; all $p < 0.025$; study #2). Of note, with data from study #3 (at 20 and 40 % of MVC), similar results were found, i.e. a significant correlation between GM/Gas activation ratio and GM/Gas PCSA ratio (both $r > 0.47$). In study #2, no correlation was observed at 60 and 70 % of MVC, which was expected as the ratio of GM/Gas activation logically tends towards 50 % (when all muscles activation get closer to their maximum, i.e. 100 % of MVC). To investigate the role of the *triceps surae* biomechanical advantage (i.e. its moment arm) in the observed neuro-mechanical coupling among *gastrocnemii*, Achilles tendon moment arm was measured

from MRIs of participants of the study #2 (19 participants; one had to be excluded because of low MRI quality for the sagittal images taken purposely for moment arm calculation). Moment arms were calculated using the centre of rotation method (Fath et al., 2010; Maganaris, 2004), as the perpendicular distance from the line of action of the *triceps surae* to the centre of the ankle rotation. We observed a significant negative correlation between the moment arm of the Achilles tendon and the GM/Gas force ratio (from 30 % to 70 % of MVC, all $r > 0.43$). This indicates that individuals with a short moment arm exhibit a larger imbalance of activation toward the GM. A similar relationship has been previously reported between indirect measures of Achilles moment arm and the activation ratio of GM/Gas measured during gait (Ahn et al., 2011). Further research is needed to unravel the origin of this relationship.

Bi-articular gastrocnemii and mono-articular SOL. When investigating the neuro-mechanical coupling for synergist muscles that share different functions, i.e. mono-articular for SOL and bi-articular for GM and GL, we did not found any significant correlation. Indeed, SOL/TS activation ratio did not correlate with SOL/TS PCSA ratio at any of the contraction intensities (all $r < 0.34$ in study #2). This was also the case with data from study #3 ($r < 0.22$). For the sake of clarity within the specific studies, we did not report the results for the SOL/GM and SOL/GL ratios there. However, it is important to note that there was no significant correlation between distribution of activation and distribution of PCSA ($-0.20 < r < 0.31$; data from study #2). The difference in function between the SOL and the *gastrocnemii* might explain the absence of correlation for SOL/TS activation and PCSA ratios. Indeed, activation of bi-articular muscles depends on moment demands at two joints (Prilutsky, 2000), which may make it more complicated to comply at the same time with neuro-mechanical coupling and the constraints of the task. In other words, the distribution of activation between the mono-articular SOL muscle and the bi-articular *gastrocnemii* muscles cannot be solely determined by the difference in the distribution of force-generating capacity between the SOL and the *gastrocnemii*, but also need to consider the task constraints, which depend on actions at both the ankle and knee joints. This is in accordance with previous results showing an uncoupling of SOL and *gastrocnemii* activity in response to altered torque and velocity during pedaling in humans (Wakeling and Horn, 2009), during paw shakes in cats (Smith et al., 1980) or during locomotion in cats (Walmsley et al., 1978). Finally, it is possible that the human body takes into account more than muscle features (e.g. PCSA, moment arm) or muscle function (e.g. actions at different joints) to distribute activation

among a group of synergists. Indeed, this neuro-mechanical coupling was not observed among the group of hamstrings (*semi-tendinosous*, *semi-membranosous* and *biceps femoris*), even if the three muscles cross the same joints (Avrillon et al., 2018). The hamstring group presents a very high heterogeneity of force-generating capacities between the three heads (semi-tendinosous PCSA is 41 and 44% lower than biceps femoris and semi-menbranosous respectively; Avrillon et al., 2018). In this case, a coupling between ratios of PCSA and ratios of activation would have had strong (and potentially negative) consequences for the non-muscular structures that surround the hamstring muscles.

2.3.2. Consequences of the neuro-mechanical coupling

Task performance. It was hypothesized that the existence of a neuro-mechanical coupling as observed in study #2 would lead to an overall lower activation. For example, take the simulation presented on the literature review (Figure 16' below). For a given force (30 N in the example), in the case where muscles **activations** are balanced, the overall activation was 10 %. In the case where muscles **forces** are balanced, the overall activation was 18 %. Finally in the case of a neuro-mechanical coupling, the overall activation was 7 %. To interpret the consequences of the coupling between the ratio of GM/Gas activation and the ratio of GM/Gas PCSA with our experimental data, we explored the relationship between the ratio of GM/Gas activation and the normalised EMG amplitude averaged across the three muscle heads (the overall *triceps surae* activation). We observed a negative significant correlation at 30 % of MVC and above ($-0.66 < r < -0.42$; $p < 0.05$; data from study #2). This confirmed the hypothesis that the coupling between the distribution of PCSA and the distribution of activation between *gastrocnemii* contributes to a reduction of the overall activation of the *triceps surae* (in comparison to cases where activations, or forces, are balanced).

Furthermore, as the higher ratio of GM/Gas activation is associated with lower *triceps surae* activation, the neuro-mechanical coupling is thought to reduce the metabolic cost of the task. This is because metabolic cost of force generation is based on active muscle volume and muscle architecture (Biewener, 2016). Longitudinal muscle force is proportional to the cross-sectional area of active muscle fibers. Therefore, muscles with long fibers require a larger active muscle volume to generate a given force (Biewener, 2016). As such, they consume more ATP per unit force generated than muscles with short fibers (Figure 44). We calculated an index of metabolic cost, representative of the active volume of the *triceps surae*, from the relative muscle activation (i.e. normalised EMG times PCSA) divided by the volume. This

index was negatively correlated with the ratio of GM/Gas activation (–0.74 < r < –0.52; p < 0.05). It is important to note that this metabolic cost index does not consider important parameters such as muscle typology and represents only a crude estimate of metabolic cost. Despite this, the significant correlation between this index and the ratio of GM/Gas activation provides preliminary evidence that the GM/Gas activation strategy contributes to reduce the overall metabolic cost of the task.

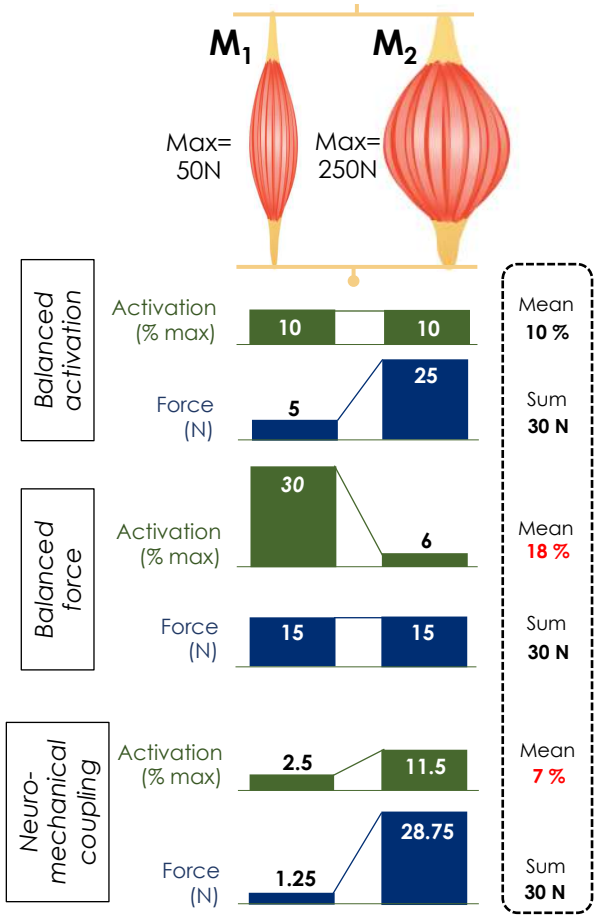

Figure 16'. Mean activation for the different scenarios (balanced activation, balanced force, neuro-mechanical coupling). *Here, M1 and M2 are two hypothetical synergist muscles. For example, they could be gastrocnemius lateralis and gastrocnemius medialis, respectively.*

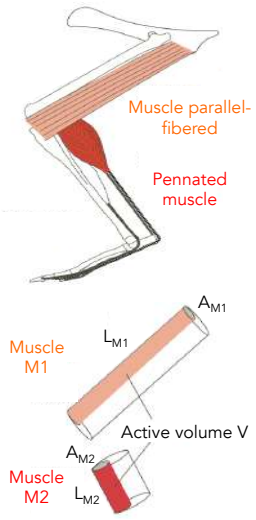

Figure 44. Comparison of parallel (M1) versus pennated-fibered (M2) muscles in relation to functional properties. *Cost of force generation is related to active muscle volume (V), defined as the volume of muscle activated to generate a given force. If we assume that muscle force generation is proportional to the cross-sectional area A of activated fibres, longer-fibered muscles require a larger volume V of activated muscle to generate a given force. Here, muscle M1 and M2 generate similar forces ($A_{M1} = A_{M2}$), but fascicle length of muscle M1 is three times greater than muscle M2 ($L_{M1} = 3\ L_{M2}$). Consequently, muscle M1 consumes roughly threefold more energy to produce a given force compared with muscle M2 ($V_{M1} = 3\ V_{M2}$). From Biewener (2016).*

Non-muscular structures loading. As muscles attach to the skeleton via tendons, the distribution of forces among synergist muscles may impact joint and/or tendon loading. Muscle activation and muscle PCSA both contribute to muscle force. Hence, the coupling of distribution of PCSA and distribution of activation between two muscles exacerbates the force imbalance. If we take the example of the knee, the observed neuro-mechanical coupling between VL and VM (see Figure 43 above) led to a VL/*Vastii* force ratio of 61 % during submaximal isometric contractions at 20 % of MVC (Hug et al., 2015), with values ranging from 38 to 84 %. Strong imbalance between medio-lateral forces that act on the patella (mainly produced by these two muscles) might cause aberrant contact stresses within the knee due to patellar loading or displacement and lead to pathology. For this reason, it has been suggested that the central nervous system may also aim at regulating stresses within joints (rather than reducing metabolic cost only, for example). This is supported by investigations on rats reporting adaptations of the balance of activation between VL and VM after denervation of one of the two muscles (Figure 45; Alessandro et al., 2018) or the attachment of a spring that pulled the patella laterally (Figure 45; Barroso et al., 2019). The stronger co-variation between VM and VL activation, than with the third monoarticular muscle (*vastus intermedius*), or with the biarticular *rectus femoris* observed in rats (Alessandro et al., 2020) was interpreted as another observation to support the regulation of stress within patellofemoral joint (Figure 45). Although both neural and biomechanical factors are important factors to estimate the distribution of muscle *forces* that act on the patella, it is

important to note that it is the distribution of muscle *torques* that would quantify the best the impact on the patella. In other words, if VM and VL have different moment arms, it is not impossible that their respective moment arms compensate for their differences of force. Further investigations are needed to unravel such questions.

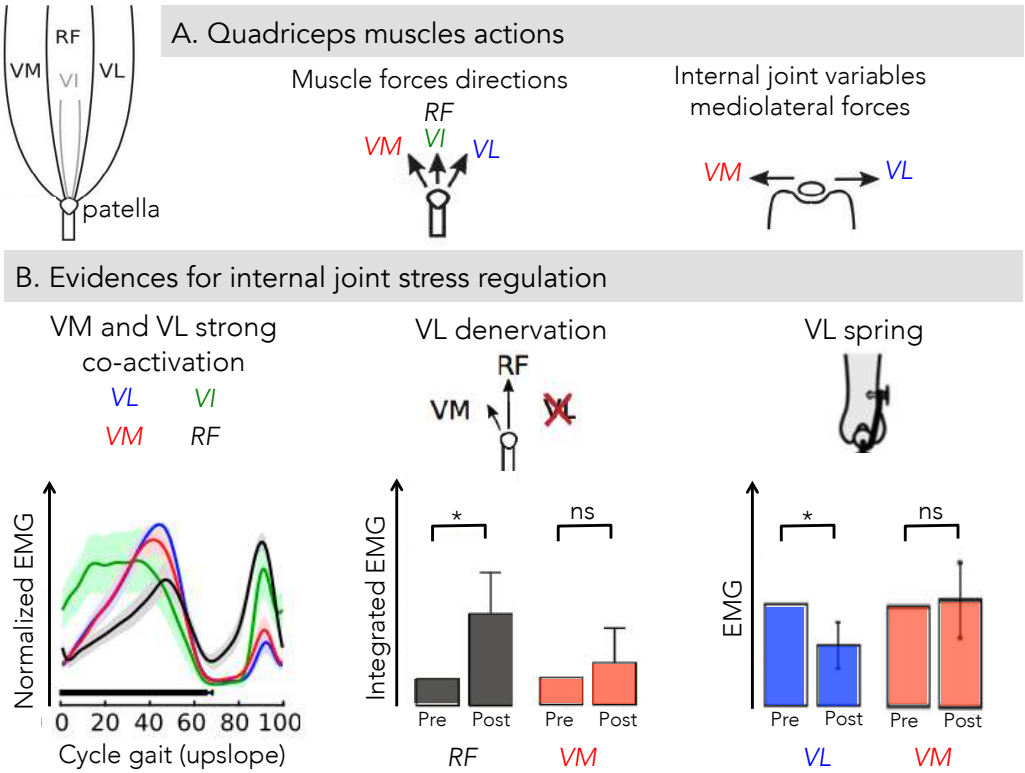

Figure 45. Quadriceps actions and activations. *Panel A: quadriceps muscles attach to the patella. Besides knee extension, vastus medialis (VM) and vastus lateralis (VL) also produce opposite mediolateral forces on the patella, while rectus femoris (RF) and vastus intermedius (VI) have minimal effect on mediolateral patellar forces. Panel B: stride-averaged activity of VM and VL are strongly coordinated across task conditions. After VL denervation, the preferentially increase in RF activation rather than an increase in VM activation (during gait) supports a neural regulation for internal joint stresses. After attaching a lateral spring, the decrease in VL activation and unaffected VM activation (during gait) is consistent with an increase net medial muscular force on the patella to compensate for the imposed lateral force by the spring. Adapted from Alessandro et al. (2020); Alessandro et al. (2018); Barroso et al. (2019).*

For the purpose of this study, even if GM, GL and SOL share their distal insertion through the Achilles, it may not be entirely true to assume that they have similar moment arms. Considering potential differences between GM, GL and SOL moment arms may be required

to more accurately estimate the **torque**-sharing. In this work, we were interested in the **force**-sharing, where moment arms do not contribute, as it is the distribution of force that impact tendon behaviour, and tendon health. Thus, we think that the absence of moment arm consideration did not impact our results. It was hypothesized (study #3) that some specific distributions of force could relate to tendinopathy.

2.4. Distribution of force among *triceps surae* in people with Achilles tendinopathy

2.4.1. Maximal isometric force

In study #3, the plantarflexion peak torque measured during the MVC was not different between controls and people with Achilles tendinopathy. This aligns with some (Arya and Kulig, 2010; Child et al., 2010) but not all previous studies (Masood et al., 2014b; O'Neill et al., 2019). To the best of our knowledge, study #3 is the first to use the twitch interpolation technique to verify that the voluntary activation was maximal in participants with Achilles tendinopathy. The inability to reach maximal voluntary contraction (as observed in one excluded participant with Achilles tendinopathy) might explain why some studies observed a lower maximal plantarflexion torque in people with Achilles tendinopathy. Another explanation for these discrepancies might be the characteristics of the task with most previous studies reporting a lower overall maximal force for data collected during dynamic tasks (which contrasts with our isometric plantarflexion tasks). O'Neill et al. (2019) reported a lower peak torque in people with Achilles tendinopathy than controls during dynamic maximal plantarflexion tasks (concentric and eccentric), at varying knee positions. As large between-group differences for torque production were observed regardless of the position of the knee, it suggested that the mono-articular SOL had the greatest impact on the lower torques observed (O'Neill et al., 2019). It is true that theoretically, the knee extended position allows both the *gastrocnemii* and soleus to work more efficiently, whilst the knee flexed position mechanically disadvantages the *gastrocnemii*, thereby testing soleus force production more specifically. However, flexing the knee does not completely isolate SOL force. We know that muscle forces do not simply sum with each other's, as supposed by the 20 % loss of each individual force capacity during agonistic muscle contraction, compared with when simulated in isolation (de Brito Fontana et al., 2020). Moreover, using the knee position to test specifically some *triceps surae* heads cannot give insight into the interplay between *gastrocnemii*.

In our study, we considered the difference in PCSA as being representative of the difference in force-generating capacity between muscles. When considering the ratio of PCSA, we observed no between-group differences for GM/TS and SOL/TS PCSA but a significantly 8.5 % lower GL/TS PCSA in people with Achilles tendinopathy. To the best of our knowledge, our study is the first to estimate PCSA of each head of the *triceps surae* in people with Achilles tendinopathy. One study compared muscle volume between the affected and non-affected limbs in people with Achilles tendinopathy (Di Liberto et al., 2019) and reported differences, which align with our findings. Specifically, authors report a 14 % smaller GL volume in the affected limb compared to the non-affected limb. If the neuro-mechanical coupling between *gastrocnemii* also exists in people with Achilles tendinopathy, the smaller GL contribution to PCSA may potentially be associated with a lower GL contribution to activation.

2.4.2. Muscle activation

Previous studies have estimated the activation of the *triceps surae* muscles in people with Achilles tendinopathy during walking (Baur et al., 2004), running (Wyndow et al., 2013), isometric plantarflexion tasks (Masood et al., 2014b), and dynamic plantarflexion tasks (Reid et al., 2012; Yu, 2014). However, these studies used different normalisation procedures and reported different activation parameters (e.g. onset/offset timings and EMG amplitude), which makes difficult to directly compare their results with our results. Using a protocol similar to the protocol used in the present study, Masood et al. (2014b) observed greater normalised EMG amplitude of the SOL in the symptomatic legs (~ 37 % of maximal EMG amplitude) of people with Achilles tendinopathy compared to healthy controls (~ 25 % of maximal EMG amplitude). Even though we reported no significant difference in SOL EMG amplitude between the two groups, we observed a 27 % higher SOL force index in people with Achilles tendinopathy than controls at 40 % of MVC. This is likely explained by larger, albeit non-significant, SOL activation (+ 18 %) and SOL PCSA (+ 8 %) in participants with Achilles tendinopathy than controls. Most notably, we observed both a lower GL activation (- 19.7 %) and a lower GL/TS activation (- 22.0 %) ratios providing evidence of a lower GL contribution to the overall activation in people with Achilles tendinopathy. Even though the amplitude of the difference was only moderate (effect size: d = 0.67), it is consistent with the smaller relative GL/TS PCSA (- 8.5 %; discussed in detail below, Section 2.4.4), which strengthens the likelihood that these outcomes are relevant.

2.4.3. Force-sharing

The aim of study #3 was to determine whether the force distribution between the heads of the *triceps surae* differs in people with Achilles tendinopathy compared with controls. We observed a different force distribution between the two populations with the GL muscle contributing significantly less to the overall submaximal isometric plantarflexion force in people with Achilles tendinopathy compared to the controls. This difference was explained by both a lower GL/Gas ratios of activation (of 22.0 %) and PCSA (of 8.5 %) in the Achilles tendinopathy group, and reinforces the existence of a neuro-mechanical coupling between *gastrocnemii* in people with Achilles tendinopathy (described in the next Section 2.4.4). Importantly, PCSA and activation were investigated through 3D-ultrasonography and surface EMG, respectively, which are two unrelated methods. This makes us confident about the existence of an altered coordination in patients with Achilles tendinopathy instead of methodological bias/artefact. We contend that this provides strong evidence that people with Achilles tendinopathy use a different force-sharing strategy during this simple isometric plantarflexion task. Even though we did not study contraction intensities higher than 40 % of MVC, it is very likely that such differences would be also observed at higher force levels. This is because, as intensity increases, the difference between individual muscles relies more on PCSA than activation differences as activation of all the muscles logically converge toward 100 %.

2.4.4. Neuro-mechanical coupling in the presence of Achilles tendinopathy

In the Achilles tendinopathy group, there was a significant correlation between GL/Gas activation and PCSA ratio ($r = 0.49$ and 0.54 at 20 and 40 % of MVC, respectively). Hence, neuro-mechanical coupling exists among *gastrocnemii* in those with Achilles tendinopathy (Figure 46). The Achilles tendinopathy cohort had both lower GL/Gas PCSA and lower GL/Gas activation, creating a group of people with a particular force production strategy (i.e. lower GL contribution).

Study #3 was the first to identify a difference in force distribution between muscles of the *triceps surae* in people with Achilles tendinopathy compared to controls. In this study, we also aimed to investigate the mechanical effect of force distribution on the Achilles tendon by measuring each subtendon strain during contractions. Because the load distribution between Achilles subtendons is influenced, at least in part, by the individual force-sharing strategy (Arndt et al., 1998; Bojsen-Moller and Magnusson, 2015; Kinugasa et al., 2013), some

strategies may have the potential to induce suboptimal loading.

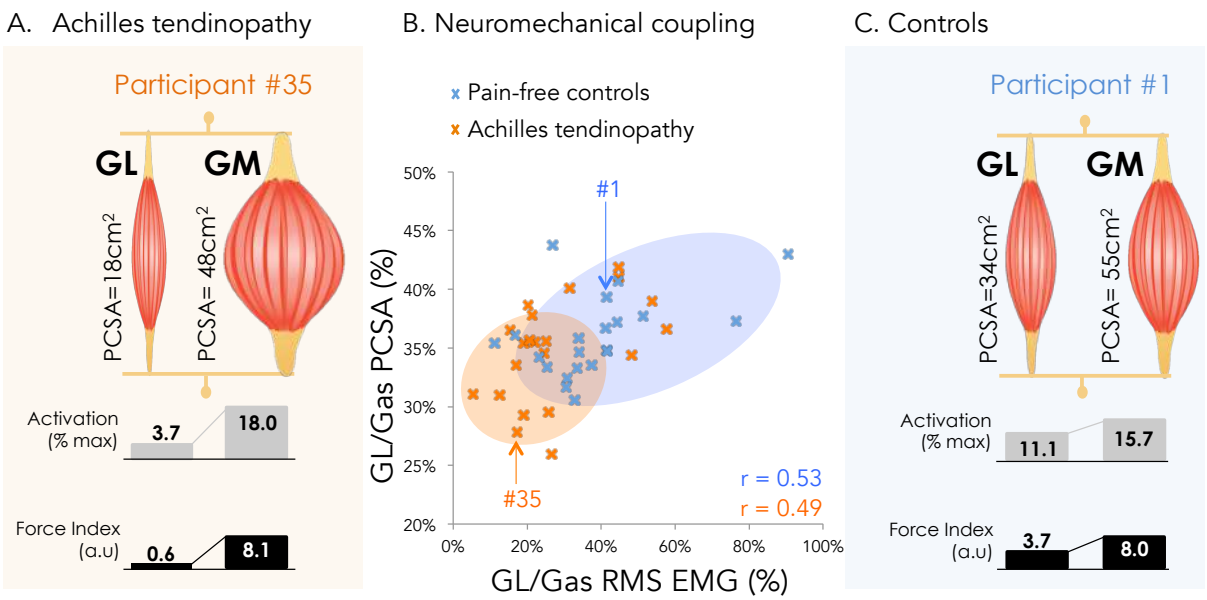

Figure 46. Relationship between GL/Gas ratios of muscle activation and muscle physiological cross-sectional area (PCSA) for study #3 in the Achilles tendinopathy (orange) and control group (blue), at 20 % of MVC. *People with Achilles tendinopathy tend to be situated at the lowest part of the relationship (i.e. lower GL/TS activation and PCSA ratios). Panel A and C: examples for typical participants (#1 and #35). GM, gastrocnemius medialis; GL, gastrocnemius lateralis; Gas, gastrocnemii.*

3. Impact of muscle coordination on Achilles tendon mechanical behaviour

There is some evidence that the displacements of the Achilles subtendons are related to the force distribution among the heads of the *triceps surae* (as explained in the literature review, Part 2; 3.2; Arndt et al., 1999; Handsfield et al., 2017; Maas et al., 2020). In study #3, we found that the contribution of GL to the overall *triceps surae* force was lower in participants with Achilles tendinopathy. Despite this, we did not observe any between-group difference in the myotendinous junction displacement or the tendon strain, for any subtendon (Figure 47).

Three reasons may explain this absence of difference between groups: 1) contraction intensity, 2) subtendon interactions and 3) subtendon mechanical properties. Each of them is discussed below.

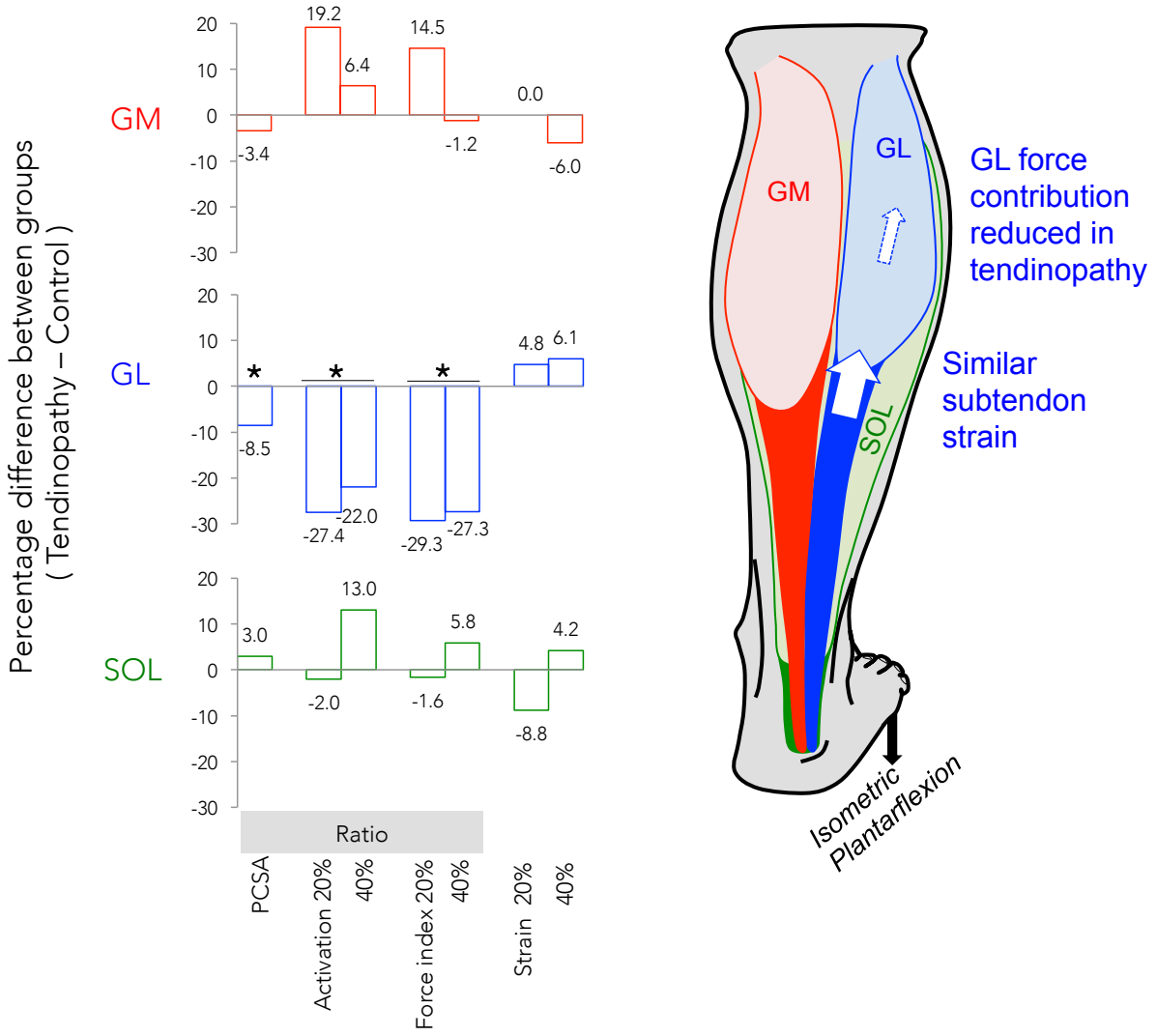

Figure 47. Summary of results, presented as the difference between Achilles tendinopathy minus the Control group. *Ratios of GL/TS for physiological cross-sectional area (PCSA), activation and force were lower in people with Achilles tendinopathy. No between-group difference was found for any subtendon strain. GM, gastrocnemius medialis; GL, gastrocnemius lateralis; SOL, soleus; TS, triceps surae. *, $p < 0.05$.*

3.1. Contraction intensity

Heterogeneous deformations between Achilles subtendons may depend on the level of contraction. Larger differences of absolute force produced between muscles are expected at higher intensities when these differences are closely related to the differences in PCSA. Thus, it is possible that different muscle force distribution between populations would have led to

different Achilles tendon behaviour at higher levels of contraction. In this way, two previous studies reported a larger GM subtendon strain in people with Achilles tendinopathy compared to controls during maximal contractions (Arya and Kulig, 2010; Child et al., 2010). As these two studies did not investigate GL and SOL subtendons, it is not known if and how the global Achilles tendon was heterogeneously affected (e.g. between subtendons differences) in Achilles tendinopathy.

3.2. Interactions between subtendons

Lateral force transmission exists between muscle-subtendon units (Maas and Finni, 2018). The lateral force transmission is described at two levels: at the muscle bellies interface and between the Achilles subtendons (Figure 48). Lateral force transmission has been demonstrated within the *triceps surae* muscle group *in vivo* in humans during passive movements (Ates et al., 2018) and active movements, using selective electrical stimulation on GL muscle to quantify its impact on SOL muscle (Finni et al., 2017b). Muscle activation reduced relative displacement between SOL and GL in the flexed knee position (Finni et al., 2017b). It was hypothesized that the stiffening of the connective tissue structures between SOL and GL increase the magnitude of myofascial force transmission. An alternative explanation was that the mechanical interaction between GL and SOL happened more distally: a shortening of GL elongates the GL subtendon, which pulls the SOL subtendon, thereby bringing the SOL myotendinous junction proximally and shortening SOL muscle. In this later case, the force transmission happened at the tendon level. The amount of interaction between muscle-subtendon units could range from non-existent to complete. In the first case, there is a perfect independency, and each muscle-subtendon unit act as an independent force generator (Figure 48; left part). In other words, the joint moment exerted by two muscles should equal the sum of each muscle individual joint moment (Maas and Finni, 2018). Conversely, the Achilles tendon behaves as a unit, i.e. there is a total transmission of force directly to adjacent muscle-tendon units and the Achilles tendon acts as a common spring. The Figure 48 (right part) illustrates the existence of this mechanical link, the amount of which is unknown, but there is an assumption of *at least a little*. Of note, *gastrocnemii* are represented together on the Figure 48, however, as demonstrated in this thesis, it is our contention that similar questions exist concerning GM and GL interactions, and their effect on the Achilles tendon.

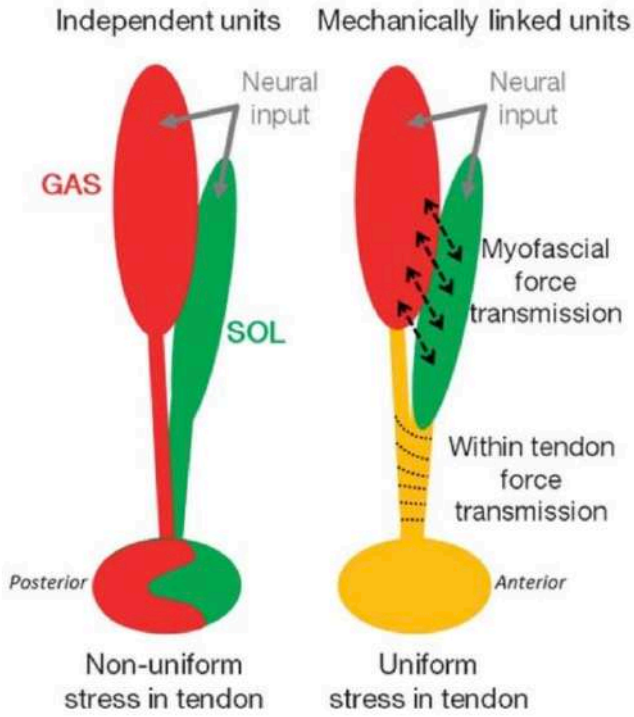

Figure 48. Sagittal view of a schematic illustration for the existence of lateral force transmission. *Left: if the muscle-tendon units of the triceps surae are mechanically independent of each others, all force produced by the muscle fibers will be transmitted exclusively via the respective subtendon within the Achilles tendon. There is no stress distribution; on the drawing the colours indicate different stresses between muscle-tendon units. Right: if the muscle-tendon units are mechanically linked to each other's, force produced by the muscle fibres can be distributed among all units. From Maas and Finni (2018).*

In study #3, a different degree of lateral force transmission between the populations may have obscured the differences in muscle force distribution we observed. Lateral force transmission may be enhanced, or reduced, in a pathological condition, where the properties of connective tissue linkages have been altered (Maas and Sandercock, 2010). In tendinopathy, the natural biochemical composition of the collagenous matrix of the tendon is compromised (de Mos et al., 2007). It is unknown how lateral cross-linkages between the subtendons are affected, and if tendinopathy increases or decreases subtendons interaction. Of note, it is possible that the mechanical interaction between subtendons may have impacted muscle coordination. The "*tendon-up*" theory argues that reduced inter-fascicle sliding at the Achilles tendon level could unfavourably couple GM, GL and SOL behaviour at the muscle level (Clark and Franz, 2019). In the case of aging for example, the more uniform Achilles subtendon tissue displacement that results from increased inter-fascicle adhesion, is thought to precede and

impact the contractile behaviour of *gastrocnemii* in relation to SOL muscle (Clark and Franz, 2018). Albeit highly speculative, one may postulate that if subtendon #A is more strongly attached to subtendon #B; the contractile behaviour of muscle #A could be impeded by stronger resistance and change on the long term. Recently, a study investigated the displacements between Achilles tendon layers at the midportion of people with Achilles tendinopathy (Couppe et al., 2020). They reported a strong tendency ($p = 0.054$) for reduced displacement between deep and superficial Achilles tendon parts (0.5 mm), compared to the contralateral asymptomatic side (1 mm), suggesting stronger mechanical dependency between subtendons in the presence of tendinopathy.

3.3. Achilles subtendon properties

3.3.1. Subtendon properties in pain-free individuals

The strain experienced by a subtendon depends on its mechanical properties (e.g. stiffness and elasticity). Take the example of stiffness, which characterizes the relationship between tendon force and tendon deformation. If two tendons with different stiffness are subjected to a similar force (e.g. 400 N), the stiffer subtendon will strain less than the other. Stiffness is often calculated as the slope of the relationship between the force applied to the tendon (measured from dynamometry and moment-arm data) and its elongation (measured with ultrasound). Achilles tendon elongation can be measured from different anatomical landmarks due to Achilles tendon compartmentalization. For example, some studies estimated stiffness from GM subtendon elongation (e.g. Arya and Kulig, 2010; Lichtwark and Wilson, 2005; Maganaris, 2002; Muraoka et al., 2004), from SOL subtendon elongation (Magnusson et al., 2003), from the two *gastrocnemii* subtendons elongation (Morrison et al., 2015), or from each GM, GL and SOL subtendons elongation (Obst et al., 2016). Importantly, stiffness is then estimated as the slope of the relationship between force and elongation, sometimes considering the overall plantarflexion force (i.e. produced by the sum of GM, GL and SOL muscles). All together, the three heads of the *triceps surae* inherently produce more force than one head alone, which inherently biases the reported stiffness for a particular subtendon. To address this limit, some studies have weighted the investigated muscle contribution to force according to its PCSA proportion among the *triceps surae* (e.g. 18% for GM; Mahieu et al., 2008; Morrissey et al., 2011). Yet, in the absence of tools to quantify individual muscle force, the accurate measure of individual subtendon stiffness remains not possible.

Currently, there are some reasons to assume that the three Achilles subtendons do not have identical mechanical properties in healthy individuals. This is because each subtendon has a different CSA and length (Morrison et al., 2015; Pekala et al., 2017); they each are constraints to different force amounts from their respective head (current work); and they may have different molecular compositions (Corben et al., 2017). Corben et al. (2017) dissected and isolated the three subtendons, from 5 cadavers (> 69 years old; fresh-frozen cadavers), then performed mechanical testing to failure, and determined the molecular content, for each subtendon. As this work has been presented at a meeting (*British Society for Matrix Biology Autumn 2017*), and are still unpublished, the results are very briefly reported. The conference abstract reports that SOL subtendon force at failure (1362 ± 406 N) was higher than both gastrocnemii (force at failure uncommunicated). However, SOL stiffness was not higher than that observed for either *gastrocnemii*. Stress at failure, elastic modulus and hysteresis were lower for SOL than GM and GL subtendons, although these were not significantly different. Water content was higher for SOL subtendon (69 %) than both GM (63 %) and GL (63 %) subtendons. The elastic moduli varied widely (up to 72 %) between the subtendons of individuals, but it was unclear if this represented between subtendons (within individual) or between individuals (within subtendon) variability. This study was conducted on a small number of older individuals. To our knowledge, no similar evaluation has been conducted on larger sample of younger populations. Further investigation of subtendon properties could provide meaningful insight for a clearer understanding of the pathogenesis and/or the recovery of Achilles tendinopathy. With the consideration they require (explained in the previous paragraph), estimations of Achilles subtendon properties *in vivo* suggested specific impact from different type of trainings. For example, after an eccentric training ≥ 6 weeks, the most widely used contraction modality in rehabilitation, GM subtendon stiffness reduced (Foure et al., 2013; Morrissey et al., 2011), while it did not after a concentric training (Morrissey et al., 2011). Other authors observed that immediate change in mechanical properties (strain) following eccentric exercises were rather specific to the SOL subtendon (Obst et al., 2016).

3.3.2. Subtendon properties in Achilles tendinopathy

There is an emerging body of literature that suggests lower stiffness of the Achilles tendon in people with Achilles tendinopathy (Arya and Kulig, 2010; Coombes et al., 2018). However, studies that used elastography, e.g. Coombes et al. (2018), could not distinguish properties

between the Achilles subtendons. This is because we cannot individualize subtendons on ultrasound images. Arya and Kulig (2010) estimated Achilles tendon stiffness from the overall plantarflexion force and GM subtendon deformation only, which cannot completely represent the Achilles tendon behaviour (i.e. GL and SOL subtendons behaviour were unknown). Therefore, we do not know whether the lower stiffness that has been observed is specific to a particular subtendon or generalized to all of the subtendons. To our knowledge, study #3 was the first to investigate strain within the three Achilles subtendons in people with Achilles tendinopathy. Despite our evidence that the contribution of GL to the overall *triceps surae* force was lower in participants with Achilles tendinopathy, we did not observe any between-group differences in the GL myotendinous junction displacement or subtendon strain. A possible explanation is that tendons remodel over time and adapt to the forces they are subjected to (Bohm et al., 2015). Hence, it is possible that the mechanical properties of the GL subtendon changed as a result of the long-term lower contribution of the GL muscle to the *triceps surae* force in our Achilles tendinopathy group. We calculated indices of subtendon stiffness from the slope of the relationship between muscle force indices and individual subtendons displacement from 20 to 40 % of MVC (Figure 49). This simulation did not reveal any difference between groups for any subtendon stiffness (group by muscle interaction $p = 0.25$). However, regardless of the group, GM and GL subtendon stiffness (which was similar; $p = 0.70$) was lower than SOL subtendon stiffness (both $p < 0.001$). This preliminary analysis could not explain the absence of difference in GL subtendon behaviour between groups, which may still be obscured by subtendon interaction, as discussed above. Further investigations are needed. Usually, tendons stiffness's estimation *in vivo* is conducted at higher intensity levels (> 50% of MVC; Seynnes et al., 2015), but such data were not collected in the current study. As the slope was slightly lower for Achilles tendinopathy sufferers (Figure 49), we could expect that the difference between groups would get bigger with increase intensity of contraction.

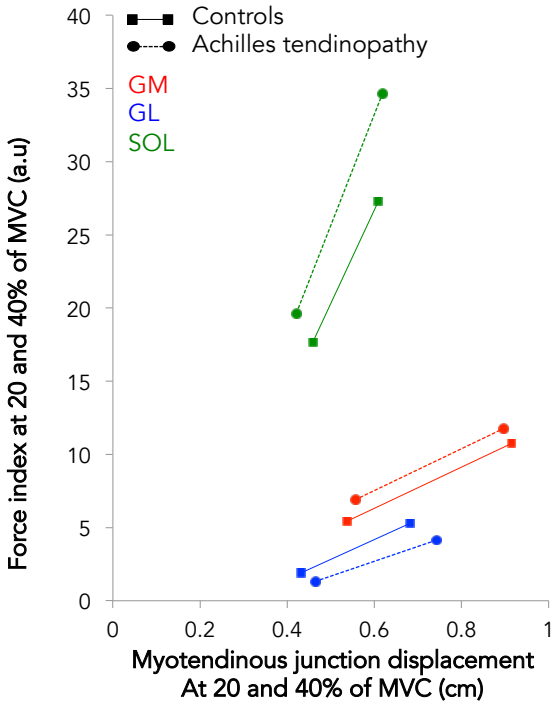

Figure 49. Individual subtendon stiffness. *Stiffness for each subtendon is given by the slope of the relationship between force and tendon deformation. There was no difference between groups, but a clear difference between gastrocnemii (low slope) and soleus (SOL) subtendon (high slope) stiffness's (muscle effect; $p < 0.001$). GM, gastrocnemius medialis; GL, gastrocnemius lateralis; MVC, maximum voluntary contraction.*

4. Clinical relevance of the current findings

4.1. Muscle coordination – the egg or the chicken?

We found a lower contribution of GL muscle to the overall *triceps surae* force in people with Achilles tendinopathy compared to controls. Our experimental design does not allow us to determine whether altered force-sharing strategies are the cause or the consequence of Achilles tendinopathy.

It is important to note that the effect size of the between-group differences in GL/TS force was only moderate. This can be explained by the inter-individual variability that exists, especially among people with Achilles tendinopathy. For example, the GL/TS force ratio, from those with Achilles tendinopathy, ranged from 2.6 % to 20.2 % at 40 % of MVC. If we consider altered force-sharing as a cause of Achilles tendinopathy, this high inter-individual variability might be explained by the well-known multi-factorial etiology of Achilles

tendinopathy, with altered force-sharing being present only in a "subgroup" of individuals among the Achilles tendinopathy group of study #3. An alternative explanation is that altered force-sharing is a consequence of Achilles tendinopathy. In this case, we may expect a correlation between the duration of the symptoms and the GL/TS force ratio. However, such a correlation was not found in the results from study #3 ($r = 0.17$ and $- 0.05$ at 20 % and 40 % of MVC, respectively).

In addition, force distribution might be associated with the potential for recovery. Six months after the collection of the original data in study #3, 11 participants reported a clinically improvement in their symptoms (VISA-A increased by 33.3 ± 14.9 points) and 9 others did not (VISA-A increased by 4.3 + 6.2 points; Tumilty et al., 2008). The comparison of the GL/TS force ratio at 20 % of MVC of these two subgroups indicated that there was a tendency for people who did not recover to have a smaller GL/TS force ratio (4.0 ± 2.5 %) than people who recovered (7.1 ± 4.6 %, $p = 0.087$). Note that the effect size was large ($d = 0.84$) but the difference was not significant. Additional works (e.g. prospective studies) are needed to understand the role of this altered coordination strategy in the development or persistence of Achilles tendinopathy. If altered *triceps surae* force-sharing was a risk factor for Achilles tendinopathy, one can imagine that muscle force investigation could predict future tendinopathy. In this case, exercise-based on load redistribution could be conducted in **prevention** and try to limit the emergence of the disorder. If altered *triceps surae* force-sharing was a negative consequence of Achilles tendinopathy, similar exercise-based on load redistribution would be conducted in **rehabilitation**, once symptoms are present, to prevent further development of the disorder.

4.2. Perspectives for rehabilitation

In study #3, we showed a lower GL contribution to *triceps surae* force as produced during isometric tasks. It remains unclear if the lower contribution of the GL force also exists during dynamic tasks. This constitutes the main limit for the applications of this work. Dynamic tasks are more representative of the way we move in our everyday lives. Moreover, Achilles tendinopathy mostly affect runners, which provides evidence that the repetitive dynamic plantarflexions that occur during running may play an important role. Hence the *triceps surae* sharing of force occurring during dynamic motions is of further interest. In our studies #3, we

assessed isometric tasks, where GL is not expected to be a major contributor, and this was confirmed by the force ratios (GL produced ~ 7 % of the *triceps surae* force at 20% of MVC). It is possible that isometric contractions were not the most likely to evidence a GL weakness, as this muscle is designed for velocity (long fibres and small PCSA), thus should contribute to a higher extent during a dynamic task (i.e. when there is movement velocity) compared to an isometric tasks. In this way, a greater contribution of GL has been observed during cycling in humans *in vivo*, relative to GM (note that SOL was not assessed, as discussed previously in section 1.3; Dick et al., 2017). A deficit of GL force in people with Achilles tendinopathy may be "easier to evidence" in dynamic conditions, when GL is expected to contribute more.

Currently, response to the conservative treatment are heterogeneous (Maffulli et al., 2004). Not all individuals with Achilles tendinopathy are responsive to treatment, and symptoms may last for years for some patients (de Jonge et al., 2010). It is possible that the exercise-based conservative treatment will suit some more than others patients. For example, conservative exercise-based rehabilitation programs may be efficient only with patients who present with an altered muscle force-sharing strategy. Although results from this work needs further exploration (i.e. dynamic tasks) to confirm that the question on the role of force-sharing should be pursued, it raises the question whether it is possible to change muscle coordination in the *triceps surae*. Any technique that impacts the biomechanical or neurophysiological characteristics of muscle force production could affect muscle coordination.

4.2.1. Effect of foot position on the distribution of activation

There is some evidence toward both the ability and the inability to change the distribution of activation (acutely or on the long term), depending on the group of synergist muscles. For example, VM and VL in humans were shown to share the majority of the drive they receive (> 60% of the input; Laine et al., 2015; Negro et al., 2016). This explains why their activations may be difficult to dissociate. However, the opposite (i.e. a modification of distribution of activation among synergist muscles) has been shown for other muscle groups, by changing the limbs' position. For example, active foot positioning changed the activation ratio between medial and lateral hamstrings during exercises such as one-leg deadlift or prone leg curl (Beuchat and Maffiuletti, 2019; Lynn and Costigan, 2009). Or, the *first dorsal interosseous* activation increased relatively to the long flexor muscles activation, when *first*

dorsal interosseous moment arm was increased (i.e. by changing thumb position to acutely change its moment arm; Hudson et al., 2009). Some muscle parameters, such as mechanical advantage (e.g. moment arm), are likely to be accounted for by the central nervous system. For the *triceps surae* muscle group, four studies observed that changing the position of the foot (toes-in versus toes-out) during plantarflexion could alter the ratio of GL/Gas activation (unpublished data from our group; Cibulka et al., 2017; Marcori et al., 2017; Riemann et al., 2011). Specifically, compared to toes-out or neutral foot position, placing toes-in generated an increase in GL/Gas activation ratio during heel raises (Figure 51). Although GM and GL share the same two main functions (plantarflexion and knee flexion), there is some direct evidence that GM and GL may produce different (Lee and Piazza, 2008), or even opposite (Vieira et al., 2013) ankle torques in the frontal plane. GM and GL both insert on the calcaneus through the common Achilles tendon, but their moment arms in the frontal plane (inversion – eversion) may differ. Hence, foot position (toes-in and toes-out) may change their mechanical advantage by changing their relative moment-arms. It is also possible that foot position, by changing their relative function in the frontal plane, results in a facilitatory-inhibitory interplay between GM and GL, as it was suggested to explain similar change of activation distribution observed in hamstrings with foot rotation (Beuchat and Maffiuletti, 2019). Another explanation is that the foot rotation changes the relative length of GM and GL (i.e. shortening the GL and lengthening the GM force-length relationship, or vice-versa), placing the two muscles on different portions of their respective force-length relationships. These hypotheses are obscured by the Achilles tendon twist, which moreover is highly variable between individuals (Pekala et al., 2017). Interestingly, it was found that after a 9-week training program of calf raise, the foot position influenced the magnitude of increase of relative *gastrocnemii* thickness (Nunes et al., 2020). Specifically, toes-out induced greater gains on GM, whereas toes-in potentiated GL growth (Figure 51). Even if such results need further investigation (on *gastrocnemii* volume and PCSA, rather than on simple muscle thickness), together these studies (Cibulka et al., 2017; Marcori et al., 2017; Nunes et al., 2020; Riemann et al., 2011) suggest that foot position affect the distribution of activation and the distribution of muscle hypertrophy in a similar way. Specifically, toes-in would increase the force contribution of GL, relatively to GM.

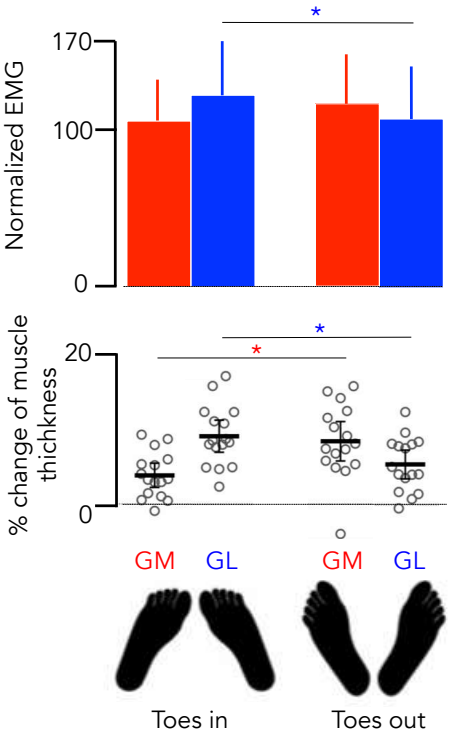

Figure 51. Toes-in and toes-out effect on the relative activation and hypertrophy of *gastrocnemius lateralis* (GL) compared to *gastrocnemius medialis* (GM). *During the concentric phase of heel raises, GL is activated significantly higher with toes-in than toes-out ($p = 0.014$). After a 9-week training with toes-in or toes-out, there are greater gains on GL or GM thickness respectively. *, $p < 0.05$. Adapted from Nunes et al. (2020); Riemann et al. (2011).*

4.2.2. Effect of eccentric training on the distribution of activation

A previous study has provided evidence that eccentric training can change activation ratios within the *triceps surae* group in healthy people (Obst et al., 2016). Eccentric contractions are the most widely used modality of contraction in exercise-based rehabilitations programs for tendinopathy, as pioneered by (Stanish et al., 1986) and followed-up by (Alfredson et al., 1998). In support of this treatment modality, a study investigated the distribution of activation in the *triceps surae* in people with Achilles tendinopathy, before and after a 12-week training program (Masood et al., 2014c). Muscle activation was collected during isometric contractions at 30 % of MVC. Post program, there was a significant increase in GL activation in people with Achilles tendinopathy (Figure 52). Of note, no change in either GM or SOL activation was observed with training. As their participants had significant relief from their symptoms after the rehabilitation program, this result does provide further support for a relationship between the contribution of the GL muscle to plantarflexion force and Achilles tendinopathy symptoms. It is possible that the process through which eccentric muscle calf training improves Achilles tendinopathy is a redistribution of muscle activations (and potentially muscle forces) among the *triceps surae*.

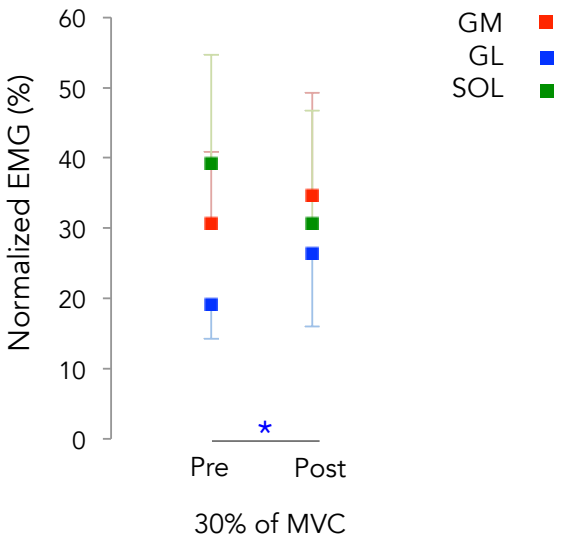

Figure 52. Effect of eccentric exercises on the distribution of activation within *triceps surae*. *Data collected on people with Achilles tendon pain, during isometric contractions at 30 % of MVC, pre and post 12-week eccentric calf muscle training. EMG, electromyography; MVC, maximal voluntary contraction; GM, gastrocnemius medialis; GL, gastrocnemius lateralis; SOL, soleus. Adapted from Masood et al. (2014c).*

5. General conclusion and perspectives

Through an approach that combines muscle activation, volume, and architecture, this doctoral research provided a deeper understanding of coordination between the three heads of the *triceps surae*, in both health and disease.

First, this thesis expanded the fundamental knowledge on motor control. The evidence of muscle activation robustness over time demonstrated that the large differences between individuals reflected true individual activation strategies. Shortly after the publication of study #1, it was demonstrated that these activation strategies could even be considered as activation *signatures* (Hug et al., 2019). Even if further works are needed to unravel the origin and consequences of the individual-specific activation strategies, our study #2 showed that peripheral factors are involved in the choices made by the central nervous system, when considering muscles sharing similar functions. This was demonstrated by the neuro-mechanical coupling that exists within *gastrocnemii* muscles during isometric contractions. Other parameters could be important (e.g. moment arm), and should be considered for further investigations. Overall, this work showed that among the *triceps surae*, there was a high

imbalance between forces produced by each GM, GL and SOL. Furthermore, muscle coordination strategies demonstrated high variability between individuals.

The second important result lies in the health-related aspects of muscle coordination. We demonstrated different *triceps surae* coordination strategies for people with Achilles tendinopathy, compared to healthy controls. The GL muscle contributed significantly less to the overall submaximal isometric *triceps surae* force for people with Achilles tendinopathy than for controls, matched with age, body-mass index and level and type of physical activity. Further investigations are needed to investigate muscle coordination during dynamic tasks, which would require the use of a different approach that combines experimental data with musculoskeletal modeling. Additionally, more investigations are needed to unravel whether altered coordination is the cause or the consequence of Achilles tendinopathy. In the future, this could contribute to improve rehabilitation exercise effectiveness. For example, people identified in the need of balancing force among *triceps surae* could follow specific programs designed for it.

REFERENCES

Adkins, A. N., Franks, P. W. and Murray, W. M. (2017). Demonstration of extended field-of-view ultrasound's potential to increase the pool of muscles for which in vivo fascicle length is measurable. *J Biomech* **63**, 179-185.

Agur, A. M., Ng-Thow-Hing, V., Ball, K. A., Fiume, E. and McKee, N. H. (2003). Documentation and three-dimensional modelling of human soleus muscle architecture. *Clin Anat* **16**, 285-93.

Ahmad, Z., Parkar, A., Shepherd, J. and Rushton, N. (2019). Revolving doors of tendinopathy: definition, pathogenesis and treatment. *Postgrad Med J*.

Ahn, A. N., Kang, J. K., Quitt, M. A., Davidson, B. C. and Nguyen, C. T. (2011). Variability of neural activation during walking in humans: short heels and big calves. *Biology Letters* **7**, 539-42.

Albracht, K., Arampatzis, A. and Baltzopoulos, V. (2008). Assessment of muscle volume and physiological cross-sectional area of the human triceps surae muscle in vivo. *J Biomech* **41**, 2211-2218.

Alessandro, C., Barroso, F. O., Prashara, A., Tentler, D. P., Yeh, H. Y. and Tresch, M. C. (2020). Coordination amongst quadriceps muscles suggests neural regulation of internal joint stresses, not simplification of task performance. *Proc Natl Acad Sci U S A* **117**, 8135-8142.

Alessandro, C., Rellinger, B. A., Barroso, F. O. and Tresch, M. C. (2018). Adaptation after vastus lateralis denervation in rats demonstrates neural regulation of joint stresses and strain. *eLife*.

Alfredson, H. (2010). Eccentric Calf Muscle Training - The Story. *Sportverl Sportschad* **24**, 188-189.

Alfredson, H., Pietilä, T., Jonsson, P. and Lorentzon, R. (1998). Heavy-load eccentric calf muscle training for the treatment of chronic Achilles tendinosis. *American Journal of Sports Medicine* **26**, 360-366.

Ando, R., Nosaka, K., Tomita, A., Watanabe, K., Blazevich, A. J. and Akima, H. (2017). Vastus intermedius vs vastus lateralis fascicle behaviors during maximal concentric and eccentric contractions. *Scand J Med Sci Sports*.

Arampatzis, A., Mademli, L., De Monte, G. and Walsh, M. (2007). Changes in fascicle length from rest to maximal voluntary contraction affect the assessment of voluntary activation. *J Biomech* **40**, 3193-200.

Arndt, A., Bengtsson, A. S., Peolsson, M., Thorstensson, A. and Movin, T. (2012). Non-uniform displacement within the Achilles tendon during passive ankle joint motion. *Knee Surg Sports Traumatol Arthrosc* **20**, 1868-74.

Arndt, A., Brüggemann, G.-P., Koebke, J. and Segesser, B. (1999). Asymmetrical Loading of the Human Triceps Surae- I. Mediolateral Force Differences in the Achilles Tendon. *Foot & ankle international* **20**, 444- 449.

Arndt, A. N., Komi, P. V., Brüggemann, G.-P. and Lukkariniemi, J. (1998). Individual muscle contributions to the in vivo achilles tendon force. *Clinical Biomechanics* **13**, 532 - 541.

Arnoczky, S. P., Lavagnino, M. and Egerbacher, M. (2007). The mechanobiological aetiopathogenesis of tendinopathy: is it the over-stimulation or the under-stimulation of tendon cells? *Int J Exp Pathol* **88**, 217-26.

Arya, S. and Kulig, K. (2010). Tendinopathy alters mechanical and material properties of the Achilles tendon. *J Appl Physiol (1985)* **108**, 670-5.

Ates, F., Andrade, R., Freitas, S. R., Hug, F., Lacourpaille, L., Gross, R., Yucesoy, C. A. and Nordez, A. (2018). Passive stiffness of monoarticular lower leg muscles is influenced by knee joint angle. *Eur J Appl Physiol*.

Avrillon, S., Guilhem, G., Barthelemy, A. and Hug, F. (2018). Coordination of hamstrings is individual specific and is related to motor performance. *J Appl Physiol (1985)* **125**, 1069-1079.

Baldry, P. E. and Thompson, J. W. (2005). Cahpter 18 - Pain in the lower limb. In *Acupuncture, Trigger Points and Musculoskeletal Pain*, (ed. C. Livingstone).

Barber, L., Barrett, R. and Lichtwark, G. (2009). Validation of a freehand 3D ultrasound system for morphological measures of the medial gastrocnemius muscle. *J Biomech* **42**, 1313-9.

Barden, J. M., Balyk, R., Raso, V. J., Moreau, M. and Bagnall, K. (2005). Atypical shoulder muscle activation in multidirectional instability. *Clin Neurophysiol* **116**, 1846-57.

Barroso, F. O., Alessandro, C. and Tresch, M. C. (2019). Adaptation of muscle activation after patellar loading demonstrates neural control of joint variables. *Sci Rep* **9**, 20370.

Basmajian, J. V. and De Luca, C. J. (1985). Muscles alive: their functions revealed by electromyography: Baltimore: Williams & Wilkins.

Baur, H., Divert, C., Hirschmüller, A., Müller, S., Belli, A. and Mayer, F. (2004). Analysis of gait differences in healthy runners and runners with chronic Achilles tendon complaints. *Isokinetics and Exercise Science* **12**, 111 -116.

Benjamin, M., Kaiser, E. and Milz, S. (2008). Structure-function relationships in tendons: a review. *J Anat* **212**, 211-28.

Bernstein, N. A. (1967). The co-ordination and regulation of movements: Oxford: Pergamon Press.

Beuchat, A. and Maffiuletti, N. A. (2019). Foot rotation influences the activity of medial and lateral hamstrings during conventional rehabilitation exercises in patients following anterior cruciate ligament reconstruction. *Phys Ther Sport* **39**, 69-75.

Beyer, R., Kongsgaard, M., Hougs Kjaer, B., Ohlenschlaeger, T., Kjaer, M. and Magnusson, S. P. (2015). Heavy Slow Resistance Versus Eccentric Training as Treatment for Achilles Tendinopathy: A Randomized Controlled Trial. *Am J Sports Med* **43**, 1704-11.

Biewener, A. A. (2016). Locomotion as an emergent property of muscle contractile dynamics. *Journal of Experimental Biology* **219**, 285 - 294.

Biewener, A. A. and Corning, W. R. (2001). Dynamics of mallard (anas platyrhynchos) gastrocnemius function during swimming versus terrestrial locomotion. *Journal of Experimental Biology* **204**, 1745-1756.

Blazevich, A. J., Gill, N. D. and Zhou, S. (2006). Intra- and intermuscular variation in human quadriceps femoris architecture assessed in vivo. *J Anat* **209**, 289-310.

Bley, B. and Abid, W. (2015). Imaging of Tendinopathy: A Physician's Perspective. *J Orthop Sports Phys Ther* **45**, 826-8.

Bogaerts, S., Desmet, H., Slagmolen, P. and Peers, K. (2016). Strain mapping in the Achilles tendon - A systematic review. *J Biomech* **49**, 1411-1419.

Bohm, S., Mersmann, F. and Arampatzis, A. (2015). Human tendon adaptation in response to mechanical loading: a systematic review and meta-analysis of exercise intervention studies on healthy adults. *Sports Med Open* **1**, 7.

Bojsen-Moller, J. and Magnusson, S. (2019). Mechanical properties, physiological behavior and function of aponeurosis and tendon. *Journal of Applied Physiology* **126**, 1800-1807.

Bojsen-Moller, J. and Magnusson, S. P. (2015). Heterogeneous Loading of the Human Achilles Tendon In Vivo. *Exerc Sport Sci Rev* **43**, 190-7.

Bojsen-Moller, J., Schwartz, S., Kalliokoski, K. K., Finni, T. and Magnusson, S. P. (2010). Intermuscular force transmission between human plantarflexor muscles in vivo. *J Appl Physiol* **109**, 1608-18.

Bolsterlee, B., D'Souza, A. and Herbert, R. D. (2019). Reliability and robustness of muscle architecture measurements obtained using diffusion tensor imaging with anatomically constrained tractography. *J Biomech* **86**, 71-78.

Bolsterlee, B., Finni, T., D'Souza, A., Eguchi, J., Clarke, E. C. and Herbert, R. D. (2018). Three-dimensional architecture of the whole human soleus muscle in vivo. *Peer J*.

Bolsterlee, B., Gandevia, S. C. and Herbert, R. D. (2016). Ultrasound imaging of the human medial gastrocnemius muscle: how to orient the transducer so that muscle fascicles lie in the image plane. *J Biomech* **49**, 1002-1008.

Bottinelli, R., Canepari, M., Pellegrino, M. A. and Reggiani, M. (1996). Force-velocity properties of human skeletal muscle fibres: myosin heavy chain isoform and temperature dependence. *J Physiol* **495**, 573-586.

Bottinelli, R., Pellegrino, M. A., Canepari, M., Rossi, D. and Reggiani, M. (1999). Specific contributions of various muscle fibre types to human muscle performance: an in vitro study. *Journal of Electromyography and Kinesiology* **9**, 87-95.

Bottinelli, R. and Reggiani, M. (2000). Human skeletal muscle fibres: molecular and functional diversity. *Progress in Biophysics & molecular biology* **73**, 195-262.

Boucher, J. P., King, M. A., Lefebvre, R. and Pépin, A. (2005). Quadriceps femoris muscle activity in patellofemoral pain syndrome. *American Journal of Sports Medicine* **20**, 527-532.

Buchanan, T. S. (1995). Evidence that maximum muscle stress is not a constant: differences in specific tension in elbow flexors and extensors. *Med Eng Phys* **17**, 529-536.

Bull, A. M., Reilly, P., Wallace, A. L., Amis, A. A. and Emery, R. J. (2005). A novel technique to measure active tendon forces: application to the subscapularis tendon. *Knee Surg Sports Traumatol Arthrosc* **13**, 145-50.

Burke, R. E. and Tsairis, P. (1973). Anatomy and innervation ratios in motor units of cats gastrocnemius. *J Physiol* **234**, 749-765.

Campanini, I., Merlo, A., Degola, P., Merletti, R., Vezzosi, G. and Farina, D. (2007). Effect of electrode location on EMG signal envelope in leg muscles during gait. *J Electromyogr Kinesiol* **17**, 515-26.

Cardoso, T. B., Pizzari, T., Kinsella, R., Hope, D. and Cook, J. L. (2019). Current trends in tendinopathy management. *Best Pract Res Clin Rheumatol* **33**, 122-140.

Ceravolo, M. L., Gaida, J. E. and Keegan, R. J. (2018). Quality-of-Life in Achilles Tendinopathy: An Exploratory Study. *Clin J Sport Med* **00**.

Child, S., Bryant, A. L., Clark, R. A. and Crossley, K. M. (2010). Mechanical properties of the achilles tendon aponeurosis are altered in athletes with achilles tendinopathy. *Am J Sports Med* **38**, 1885-93.

Cibulka, M., Wenthe, A., Boyle, Z., Callier, D., Schwerdt, A., Jarman, D. and Strube, M. J. (2017). Variation in medial and lateral gastrocnemius muscle activity with foot position. *International Journal of Sports Physical Therapy* **12**.

Clark, W. H. and Franz, J. R. (2018). Do triceps surae muscle dynamics govern non-uniform Achilles tendon deformations? *PeerJ* **6**, e5182.

Clark, W. H. and Franz, J. R. (2019). Triceps surae muscle-subtendon interaction differs between young and older adults. *Connect Tissue Res*, 1-10.

Close, R. I. (1972). Dynamic properties of mammalian skeletal muscles. *Physiological reviews* **52**, 129 - 197.

Cook, J. L. and Purdam, C. R. (2008). Is tendon pathology a continuum? A pathology model to explain the clinical presentation of load-induced tendinopathy. *Br J Sports Med* **43**, 409-16.

Cook, J. L., Rio, E., Purdam, C. R. and Docking, S. I. (2016). Revisiting the continuum model of tendon pathology: what is its merit in clinical practice and research? *Br J Sports Med* **50**, 1187-91.

Cook, J. L. and Screen, H. R. (2018). Tendon pathology: Have we missed the first step in the development of pathology? *J Appl Physiol (1985)*.

Coombes, B. K., Tucker, K., Vicenzino, B., Vuvan, V., Mellor, R., Heales, L., Nordez, A. and Hug, F. (2018). Achilles and patellar tendinopathy display opposite changes in elastic properties: A shear wave elastography study. *Scand J Med Sci Sports* **28**, 1201-1208.

Corben, D., Notou, M., Screen, H. and Birch, H. (2017). Do the sub-bundles within the Achilles tendon originating from distinct muscle bellies differ in structural and mechanical properties? In *Automn Meeting of the British-Society-for-Matrix-Biology*. Queen Mary Univ, Mile End Campus, London, England.

Couppe, C., Svensson, R., Josefsen, C. O., Kjeldgaard, E. and Magnusson, S. P. (2020). Ultrasound speckle tracking of Achilles tendon in individuals with unilateral tendinopathy: a pilot study. *Eur J Appl Physiol* **120**, 579-589.

Cowan, S. M., Bennell, K. L., Hodges, P. W., Crossley, K. M. and McConnell, J. (2001). Delayed onset of electromyographic activity of vastus medialis obliquus relative to vastus lateralis in subjects with patellofemoral pain syndrome. *Arch Phys Med Rehabil* **82**, 183-9.

Cresswell, A., Löscher, W. and Thorstensson, A. (1995). Influence of gastrocnemius muscle length on triceps surae torque development and electromyographic activity in man. *Exp Brain Res* **105**, 283 - 290.

Cronin, N. J., Peltonen, J., Ishikawa, M., Komi, P. V., Avela, J., Sinkjaer, T. and Voigt, M. (2008). Effects of contraction intensity on muscle fascicle and stretch reflex behavior in the human triceps surae. *J Appl Physiol* **105**, 226-32.

Crowninshield, R. D. and Brand, R. A. (1981). A physiologically based criterion of muscle force prediction in locomotion. *Journal of Biomechanics* **14**, 793 - 802.

Cummins, E. J. and Anson, B. J. (1946). The structure of the calcaneal tendon (of Achilles) in relation to orthopedic surgery, with additional observations on the plantaris muscle. *Surg Gynecol Obstet* **83**, 107 - 116.

D'Addona, A., Maffulli, N., Formisano, S. and Rosa, D. (2017). Inflammation in tendinopathy. *Surgeon* **15**, 297-302.

Dakin, S. G., Newton, J., Martinez, F. O., Hedley, R., Gwilym, S., Jones, N., Reid, H. A. B., Wood, S., Wells, G., Appleton, L. et al. (2018). Chronic inflammation is a feature of Achilles tendinopathy and rupture. *Br J Sports Med* **52**, 359-367.

Dalmau-Pastor, M., Fargues-Polo, B., Jr., Casanova-Martinez, D., Jr., Vega, J. and Golano, P. (2014). Anatomy of the triceps surae: a pictorial essay. *Foot Ankle Clin* **19**, 603-35.

Davies, G. J. and Dickoff-Hoffman, S. (1993). Neuromuscular testing and rehabilitation of the shoulder complex. *Journal of Orthopaedic & Sports Physical Therapy* **18**, 449-458.

de Brito Fontana, H., de Campos, D., Sawatsky, A., Han, S. W. and Herzog, W. (2020). Why do muscles lose torque potential when activated within their agonistic group? *J Exp Biol* **223**.

de Brito Fontana, H., Roesler, H. and Herzog, W. (2014). In vivo vastus lateralis force-velocity relationship at the fascicle and muscle tendon unit level. *J Electromyogr Kinesiol* **24**, 934-40.

de Jonge, S., de Vos, R. J., Van Schie, H. T., Verhaar, J. A., Weir, A. and Tol, J. L. (2010). One-year follow-up of a randomised controlled trial on added splinting to eccentric exercises in chronic midportion Achilles tendinopathy. *Br J Sports Med* **44**, 673-7.

de Jonge, S., van den Berg, C., de Vos, R. J., van der Heide, H. J., Weir, A., Verhaar, J. A., Bierma-Zeinstra, S. M. and Tol, J. L. (2011). Incidence of midportion Achilles tendinopathy in the general population. *Br J Sports Med* **45**, 1026-8.

De Luca, C. J. (1968). Myoelectric analysis of isometric contractions of the human biceps brachii. Canada: New Brunswick.

De Luca, C. J. (1979). Physiology and Mathematic of Myoelectric Signals. *IEEE Transacions on biomedical engineering* **26**, 313-325.

De Marchis, C., Schmid, M., Bibbo, D., Bernabucci, I. and Conforto, S. (2013). Inter-individual variability of forces and modular muscle coordination in cycling: a study on untrained subjects. *Human movement science* **32**, 1480 - 1494.

de Mos, M., van El, B., DeGroot, J., Jahr, H., van Schie, H. T., van Arkel, E. R., Tol, H., Heijboer, R., van Osch, G. J. and Verhaar, J. A. (2007). Achilles tendinosis: changes in biochemical composition and collagen turnover rate. *Am J Sports Med* **35**, 1549-56.

Dean, B. J., Gettings, P., Dakin, S. G. and Carr, A. J. (2016). Are inflammatory cells increased in painful human tendinopathy? A systematic review. *Br J Sports Med* **50**, 216-20.

Dennerlein, J. T., Diao, E., Mote, C. D. and Rempel, D. M. (1998). Tensions of the flexor digitorum superficialis are higher than a current model predicts. *J Biomech* **31**, 295-301.

Desmedt, J. E. and Godaux, E. (1977). Ballistic contractions in man: characteristic recruitment pattern of single motor units of the tibialis anterior muscle. *J Physiol* **264**, 673-693.

Di Liberto, F., Nawoczenski, D. A., Tome, J., Tan, R. K. and DiGiovanni, B. F. (2019). Changes in Muscle Morphology Following Gastrocnemius Recession for Achilles tendinopathy: a propsective cohort imaging. *Foot Ankle Spec*.

Dick, T. J. M., Biewener, A. A. and Wakeling, J. M. (2017). Comparison of human gastrocnemius forces predicted by Hill-type muscle models and estimated from ultrasound images. *Journal of Experimental Biology* **220**, 1643- 1653.

Dideriksen, J. L., Enoka, R. M. and Farina, D. (2011). Neuromuscular adjustmens that constrain submaximal EMG amplitude at task failure of sustained isometric contractions. *Journal of Applied Physiology* **111**, 485-494.

Dideriksen, K., Boesen, A. P., Reitelseder, S., Couppe, C., Svensson, R., Schjerling, P., Magnusson, S. P., Holm, L. and Kjaer, M. (2017). Tendon collagen synthesis declines with immobilization in elderly humans: no effect of anti-inflammatory medication. *J Appl Physiol (1985)* **122**, 273-282.

Diedrichsen, J., Shadmehr, R. and Ivry, R. (2010). The coordination of movement: optimal feedback control and beyond. *Trends in Cognitive Sciences*.

Divani, K., Chan, O., Padhiar, N., Twycross-Lewis, R., Maffulli, N., Crisp, T. and Morrissey, D. (2010). Site of maximum neovascularisation correlates with the site of pain in recalcitrant mid-tendon Achilles tendinopathy. *Man Ther* **15**, 463-8.

Docking, S. I., Ooi, C. C. and Connell, D. (2015). Tendinopathy: Is Imaging Telling Us the Entire Story? *J Orthop Sports Phys Ther* **45**, 842-52.

Docking, S. I., Rio, E., Cook, J., Carey, D. and Fortington, L. (2019). Quantification of Achilles and patellar tendon structure on imaging does not enhance ability to predict self-reported symptoms beyond grey-scale ultrasound and previous history. *J Sci Med Sport* **22**, 145-150.

Doral, M. N., Alam, M., Bozkurt, M., Turhan, E., Atay, O. A., Donmez, G. and Maffulli, N. (2010). Functional anatomy of the Achilles tendon. *Knee Surg Sports Traumatol Arthrosc* **18**, 638-43.

Dul, J., Johnson, G. E., Shiavi, R. and Townsen, M. A. (1984). Muscular Synergism II. A minimum fatigue criterion for load sharing between synergistic muscles. *Journal of Biomechanics* **17**, 675 - 684.

Edama, M., Kubo, M., Onishi, H., Takabayashi, T., Inai, T., Yokoyama, E., Hiroshi, W., Satoshi, N. and Kageyama, I. (2015). The twisted structure of the human Achilles tendon. *Scand J Med Sci Sports* **25**, e497-503.

Edgerton, V. R., J.L., S. and Simpson, D. R. (1975). Muscle fibre type populations of human leg muscles. *Histochemical Journal* **7**, 259-266.

Egger, A. C. and Berkowitz, M. J. (2017). Achilles tendon injuries. *Curr Rev Musculoskelet Med* **10**, 72-80.

Engstrom, C. M., Loeb, G. E., Reid, J. G., Forrest, W. J. and Avruch, L. (1991). Morphometry of the human thigh muscles. A comparison between anatomical sections and computer tomographic and magnetic resonance images. *J Anat* **176**, 139-156.

Enoka, R. M. and Duchateau, J. (2015). Inappropriate interpretation of surface EMG signals and muscle fiber characteristics impedes understanding of the control of neuromuscular function. *J Appl Physiol (1985)* **119**, 1516-8.

Enoka, R. M. and Duchateau, J. (2019). Chapter 7 - Muscle Function: strength, speed and fatigability. In *Muscle and Exercise Physiology*, pp. 129-157: Academic Press.

Enoka, R. M. and Fuglevand, A. J. (2001). Motor unit physiology: some unresolved issues. *Muscle & Nerve* **24**, 4-17.

Erdemir, A., McLean, L., Herzog, W. and van den Bogert, A. J. (2007). Model-based estimation of muscle forces exerted during movements. *Clinical Biomechanics* **22**, 131 - 154.

Erskine, R. M., Jones, D. A., Maffulli, N., Williams, A. G., Stewart, C. E. and Degens, H. (2011). What causes in vivo muscle specific tension to increase following resistance training? *Exp Physiol* **96**, 145-55.

Erskine, R. M., Jones, D. A., Maganaris, C. and Degens, H. (2009). In vivo specific tension of the human quadriceps femoris muscle. *Eur J Appl Physiol* **106**, 827-838.

Fahlström, M., Lorentzon, R. and Alfredson, H. (2002). Painful conditions in the Achilles tendon region in elite badminton players. *Am J Sports Med* **30**, 51-54.

Farina, D., Holobar, A., Merletti, R. and Enoka, R. M. (2010). Decoding the neural drive to muscles from the surface electromyogram. *Clin Neurophysiol* **121**, 1616-23.

Farina, D., Merletti, R. and Enoka, R. M. (2004a). The extraction of neural strategies from the surface EMG. *J Appl Physiol* **96**, 1486-95.

Farina, D., Merletti, R. and Enoka, R. M. (2014). The extraction of neural strategies from the surface EMG: an update. *J Appl Physiol (1985)* **117**, 1215-30.

Farina, D., Merletti, R., Indino, B. and Graven-Nielsen, T. (2004b). Surface EMG crosstalk evaluated from experimental recordings and simulated signals. Reflections on crosstalk interpretation, quantification and reduction. *Methods Inf Med* **43**, 30-5.

Farina, D., Merletti, R., Indino, B., Nazzaro, M. and Pozzo, M. (2002). Surface EMG crosstalk between knee extensors muscles: experimental and model results. *Muscle & Nerve* **26**, 681-695.

Farina, D., Negro, F., Muceli, S. and Enoka, R. M. (2016). Principles of Motor Unit Physiology Evolve With Advances in Technology. *Physiology (Bethesda)* **31**, 83-94.

Farris, D. J., Trewartha, G., McGuigan, M. P. and Lichtwark, G. A. (2013). Differential strain patterns of the human Achilles tendon determined in vivo with freehand three-dimensional ultrasound imaging. *J Exp Biol* **216**, 594-600.

Fath, F., Blazevich, A. J., Waugh, C. M., Miller, S. C. and Korff, T. (2010). Direct comparison of in vivo Achilles tendon moment arms obtained from ultrasound and MR scans. *J Appl Physiol* **109**, 1644-1652.

Feilmeier, M. (2017). Noninsertional Achilles Tendinopathy Pathologic Background and Clinical Examination. *Clin Podiatr Med Surg* **34**, 129-136.

Feinstein, B., Lindegard, B., Nyman, E. and Wohlfart, G. (1955). Morphologic studies of motor units in normal human muscles. *Acta anat* **23**, 127-142.

Fiebert, I. M., Spielholz, N. I., Applegate, B., Crabtree, F. G., Martin, L. A. and Parker, K. L. (2000). A comparison of iEMG activity between the medial and lateral heads of the gastrocnemius muscle during partial weight bearing plantarflexion contractions at varying loads. *Isokinetics and Exercise Science* **8**, 65 - 72.

Fink, R. H., Stephenson, D. G. and Williams, D. A. (1990). Physiological properties of skinned fibres from neural and dystrophic (Duchenne) human muscle activated by Ca2+ and Sr2+. *J Physiol Lond* **420**, 337-353.

Finni, T., Bernabei, M., Baan, G. C., Noort, W., Tijs, C. and Maas, H. (2017a). Non-uniform displacement and strain between the soleus and gastrocnemius subtendons of rat Achilles tendon. *Scand J Med Sci Sports* **00**, 1-9.

Finni, T., Cronin, N. J., Mayfield, D., Lichtwark, G. A. and Cresswell, A. G. (2017b). Effects of muscle activation on shear between human soleus and gastrocnemius muscles. *Scand J Med Sci Sports* **27**, 26-34.

Finni, T., Komi, P. V. and Lepola, V. (2000). In vivo human triceps surae and quadriceps femoris muscle function in squat jump and counter movement jump. *Eur J Appl Physiol* **83**, 416-426.

Finni, T., Komi, P. V. and Lukkariniemi, J. (1998). Achilles tendon loading during walking: application of a novel optic fiber technique. *Eur J Appl Physiol Occup Physiol* **77**, 289-91.

Fitts, R. H., Costill, D. L. and Gardetto, P. R. (1989). Effect of swim exercise training on human muscle fiber fonction. *Journal of Applied Physiology* **66**, 465 - 475.

Foure, A., Nordez, A. and Cornu, C. (2013). Effects of eccentric training on mechanical properties of the plantar flexor muscle-tendon complex. *J Appl Physiol (1985)* **114**, 523-37.

Fukunaga, T. (1992). Physiological Cross-Sectional Area of Human Leg Muscles Based on Magnetic Resonance Imaging. *Journal of orthopaedic research* **10**, 926-934.

Fukunaga, T., Roy, R. R., Shellock, F. G., Hodgson, J. A. and Edgerton, V. R. (1996). Specific tension of human plantar flexors and dorsiflexors. *Journal of Applied Physiology*, 158 - 165.

Gans, C. and Gaunt, A. S. (1991). Muscle architecture in relation to function. *J Biomech* **24**, 53-65.

Ginn, K., Eastburn, G. and Lee, M. (1993). Evaluation of a buckle force transducer for measuring tissue tension. *Australian Journal of Physiotherapy* **39**, 31-38.

Gollnick, P. D., Sjödin, B., Karlsson, J., Jansson, E. and Saltin, B. (1974). Human soleus muscle: a comparison of fibre composition and enzyme activities with other leg muscles. *Pflugers Arch* **348**.

Grabiner, M. D., Koh, T. J. and Draganich, L. F. (1994). Neuromechanics of the patellofemoral joint. *Medicine & Science in Sports & Exercise* **26**, 10-21.

Green, H. J., Daub, B., Houston, M. E., Thomson, J. A., Fraser, I. and Ranney, D. (1981). Human vastus lateralis and gastrocnemius muscles. *Journal of the neurological Sciences* **52**, 201-210.

Hahs, D. W. and Stiles, R. N. (1989). Buckle muscle tension transducer: what does it measure? . *J Biomech* **22**, 165-166.

Hall, W. C. (2004). Movement and its central control. In *Neuroscience - third edition*. USA: Sinauer Associates, Inc.

Handsfield, G. G., Inouye, J. M., Slane, L. C., Thelen, D. G., Miller, G. W. and Blemker, S. S. (2017). A 3D model of the Achilles tendon to determine the mechanisms underlying nonuniform tendon displacements. *J Biomech* **51**, 17-25.

Handsfield, G. G., Meyer, C. H., Hart, M. H., Abel, M. F. and Blemker, S. S. (2014). Relationships of 35 lower limb muscles to height and body mass quantified using MRI. *J Biomech* **47**.

Handsfield, G. G., Slane, L. C. and Screen, H. R. C. (2016). Nomenclature of the tendon hierarchy: An overview of inconsistent terminology and a proposed size-based naming scheme with terminology for multi-muscle tendons. *J Biomech* **49**, 3122-3124.

Harridge, S. D., Bottinelli, R., Canepari, M., Pellegrino, M. A., Reggiani, M., Esbjornsson, M., Balsom, P. D. and Saltin, B. (1998). Sprint training, in vitro and in vivo muscle function, and myosin heavy chain expression. *J Appl Physiol* **84**.

Harridge, S. D. R., Bottinelli, R., Canepari, M., Pellegrino, M. A., Reggiani, M., Esbjornsson, M. and Saltin, B. (1996). Whole-muscle and single-fibre contractile properties and myosin heavy chain isoforms in humans. *Eur J Physiol* **432**, 913-920.

Haxton, H. A. (1944). Absolute muscle force in the ankle flexors of man. *J Physiol* **103**, 267-273.

Heckman, C. J. and Enoka, R. M. (2012). Motor unit. *Compr Physiol* **2**, 2629-82.

Henneman, E. (1957). Relation between size of neurons and their susceptibility to discharge. *Science* **126**.

Henneman, E. and Oslon, C. B. (1965). Relations between structure and function in the design of skeletal muscles. *Journal of Neurophysiology* **28**, 581 - 598.

Henneman, E., Somjen, C. and Carpenter, D. O. (1965). Excitability and inhibitability of motoneurons of different sizes. *Journal of Neurophysiology* **28**, 599-620.

Hermens, J. H., Freriks, B., Disselhorst-Klug, C. and Rau, G. (2000). Development of recommendations for SEMG sensors and sensor placement procedures. *Journal of Electromyography and Kinesiology* **10**, 361-374.

Heroux, M. E., Dakin, C. J., Luu, B. L., Inglis, J. T. and Blouin, J. S. (2014). Absence of lateral gastrocnemius activity and differential motor unit behavior in soleus and medial gastrocnemius during standing balance. *J Appl Physiol (1985)* **116**, 140-8.

Heroux, M. E., Stubbs, P. W. and Herbert, R. D. (2016). Behavior of human gastrocnemius muscle fascicles during ramped submaximal isometric contractions. *Physiol Rep* **4**.

Herzog, W. (1987). Individual muscle force estimations using a non-linear optimal design. *Journal of Neuroscience Methods* **21**, 167-179.

Herzog, W. (1996). Force-sharing among synergistics muscles: theoretical considerations and experimental approaches. *Exerc Sport Sci Rev* **24**, 173-202.

Herzog, W. (1998). Force-sharing among the primary cat ankle muscles. *European Journal of Morphology* **36**, 280-287.

Herzog, W. (2000). Muscle properties and coordination during voluntary movement. *Journal of Sports Sciences* **18**, 141-152.

Herzog, W. (2017). Skeletal muscle mechanics: questions, problems and possible solutions. *Journal of NeuroEngineering and Rehabilitation* **14**.

Hodgson, J. A., Finni, T., Lai, A. M., Edgerton, V. R. and Sinha, S. (2006). Influence of structure on the tissue dynamics of the human soleus muscle observed in MRI studies during isometric contractions. *J Morphol* **267**, 584-601.

Hoffman, B. W., Lichtwark, G. A., Carroll, T. J. and Cresswell, A. G. (2012). A comparison of two Hill-type skeletal muscle models on the construction of medial gastrocnemius length-tension curves in humans in vivo. *J Appl Physiol* **113**, 90-6.

Hudson, A. L., Taylor, J. L., Gandevia, S. C. and Butler, J. E. (2009). Coupling between mechanical and neural behaviour in the human first dorsal interosseous muscle. *J Physiol* **587**, 917-25.

Hug, F. (2011). Can muscle coordination be precisely studied by surface electromyography? *J Electromyogr Kinesiol* **21**, 1-12.

Hug, F., Goupille, C., Baum, D., Raiteri, B. J., Hodges, P. W. and Tucker, K. (2015a). Nature of the coupling between neural drive and force-generating capacity in the human quadriceps muscle. *Proc R Soc B* **282**.

Hug, F., Hodges, P. W. and Tucker, K. (2015b). Muscle force cannot be directly inferred from muscle activation: illustrated by the proposed imbalance of force between the vastus medialis and vastus lateralis in people with patellofemoral pain. *J Orthop Sports Phys Ther* **45**, 360-5.

Hug, F. and Tucker, K. (2017). Muscle Coordination and the Development of Musculoskeletal Disorders. *Exerc Sport Sci Rev* **45**, 201-208.

Hug, F., Turpin, N. A., Guével, A. and Dorel, S. (2010). Is interindividual variability of EMG patterns in trained cyclists related to different muscle synergies? *Journal of Applied Physiology* **108**, 1727-36.

Hug, F., Vogel, C., Tucker, K., Dorel, S., Deschamps, T., Le Carpentier, E. and Lacourpaille, L. (2019). Individuals have unique muscle activation signatures as revealed during gait and pedaling. *J Appl Physiol (1985)* **127**, 1165-1174.

Hutchison, A. M., Evans, R., Bodger, O., Pallister, I., Topliss, C., Williams, P., Vannet, N., Morris, V. and Beard, D. (2013). What is the best clinical test for Achilles tendinopathy? *Foot Ankle Surg* **19**, 112-7.

Huxley, A. F. (1957). Muscle structure and theories of contraction. *Prog Biophys Biophys Chem* **7**, 255-318.

Iannotti, J. P. and Parker, R. (2013). Spine and Lower limb. In *The Netter collection of Medical Illustrations: Musculoskeletal System, 2nd Edition*, (ed. W. B. S. C. Ltd).

Infantolino, B. W. and Challis, J. H. (2010). Architectural properties of the first dorsal interosseous muscle. *J Anat* **216**, 463-9.

Ivanenko, Y. P., Grasso, R., Macellari, V. and Lacquaniti, F. (2002). Control of foot trajectory in human locomotion: role of ground contact forces in simulated reduced gravity. *Journal of Neurophysiology* **87**.

Jarvinen, T. A., Kannus, P., Maffulli, N. and Khan, K. M. (2005). Achilles tendon disorders: etiology and epidemiology. *Foot Ankle Clin* **10**, 255-66.

Johannsen, F., Jensen, S. and Wetke, E. (2018). 10-year follow-up after standardised treatment for Achilles tendinopathy. *BMJ Open Sport Exerc Med* **4**, e000415.

Johansson, C. (1986). Injuries in elite orienteers. *American Journal of Sports Medicine* **14**, 410-415.

Johnson, M. A., Polgar, D., Weightman, D. and Appleton, D. (1973). Data on the Distribution of Fibre Types in Thirty-six Human Muscles An Autopsy Study. *Journal of the neurological Sciences* **18**, 111 - 129.

Karamanidis, K., Stafilidis, S., DeMonte, G., Morey-Klapsing, G., Bruggemann, G. P. and Arampatzis, A. (2005). Inevitable joint angular rotation affects muscle architecture during isometric contraction. *J Electromyogr Kinesiol* **15**, 608-16.

Karst, G. and Willet, G. M. (1995). Onset timing of electromyographic activity in the vastus medialis oblique and vastus lateralis muscles in subjects with and without patellofemoral pain syndrome. *Phys Ther* **75**, 813-823.

Kawakami, Y., Ichinoise, Y. and Fukunaga, T. (1998). Architectural and functional features of human triceps surae muscles during contraction. *J Appl Physiol*, 398-404.

Kawakami, Y., Nakazawa, K., Fujimoto, T., Nozaki, D., Miyamasa, M. and Fukunaga, T. (1994). Specific tension of elbow flexor and extensor muscles based on magnetic resonance imaging. *Eur J Appl Physiol* **68**, 139-147.

Keenan, K. G., Farina, D., Maluf, K. S., Merletti, R. and Enoka, R. M. (2005). Influence of amplitude cancellation on the stimulated surface electromyogram. *Journal of Applied Physiology* **98**, 120-31.

Khan, K. M., Cook, J. L., Kannus, P., Maffulli, N. and Bonar, S. F. (2002). Time to abandon the "tendinitis" myth. *Biritish of Medicine Journal* **324**, 626-627.

Kinugasa, R., Kawakami, Y. and Fukunaga, T. (2005). Muscle activation and its distribution within human triceps surae muscles. *J Appl Physiol* **99**, 1149-56.

Kinugasa, R., Oda, T., Komatsu, T., Edgerton, V. R. and Sinha, S. (2013). Interaponeurosis shear strain modulates behavior of myotendinous junction of the human triceps surae. *Physiol Rep* **1**.

Komi, P. (1990). Relevance of in vivo force measurements to human biomechanics. *J Biomech* **23**, 23-24.

Korstanje, J. W., Selles, R. W., Stam, H. J., Hovius, S. E. and Bosch, J. G. (2010). Development and validation of ultrasound speckle tracking to quantify tendon displacement. *J Biomech* **43**, 1373-9.

Kudron, C., Carlson, M. J., Meron, A., Sridhar, B. and Brakke Holman, R. (2019). Using Ultrasound Measurement of the Achilles Tendon in Asymptomatic Runners to Assist in Predicting Tendinopathy. *J Ultrasound Med*.

Kujala, U. M., Sarna, S. and Kaprio, J. (2005). Cumulative incidence of Achilles tendon rupture and tendinopathy in male former elite athletes. *Clin J Sport Med* **15**, 133-135.

Kutch, J. J. and Valero-Cuevas, F. J. (2011). Muscle redundancy does not imply robustness to muscle dysfunction. *J Biomech* **44**, 1264-1270.

Kwah, L. K., Pinto, R. Z., Diong, J. and Herbert, R. D. (2013). Reliability and validity of ultrasound measurements of muscle fascicle length and pennation in humans: a systematic review. *J Appl Physiol* **114**, 761-9.

Lacourpaille, L., Nordez, A. and Hug, F. (2017). The nervous system does not compensate for an acute change in the balance of passive force between synergist muscles. *J Exp Biol* **220**, 3455-3463.

Laine, C. M., Martinez-Valdes, E., Falla, D., Mayer, F. and Farina, D. (2015). Motor Neuron Pools of Synergistic Thigh Muscles Share Most of Their Synaptic Input. *J Neurosci* **35**, 12207-16.

Laprade, J., Culham, E. and Brouwer, B. (1998). Comparison of five isometric exercises in the recruitment of the vastus medialis oblique in persons with and without patellofemoral pain syndrome. *Journal of Orthopaedic & Sports Physical Therapy* **27**, 197-204.

Larsson, L. and Moss, R. L. (1993). Maximum velocity of shortening in relation to myosin isoform composition in single fibres from human skeletal msucles. *J Physiol* **472**.

Lavagnino, M., Wall, M. E., Little, D., Banes, A. J., Guilak, F. and Arnoczky, S. P. (2015). Tendon mechanobiology: Current knowledge and future research opportunities. *J Orthop Res* **33**, 813-22.

Lee, S. S. and Piazza, S. J. (2008). Inversion-eversion moment arms of gastrocnemius and tibialis anterior measured in vivo. *J Biomech* **41**, 3366-70.

Lemay, M. A., Bhowmik-Stoker, M., McConnell, G. C. and Grill, W. M. (2007). Role of biomechanics and muscle activation strategy in the production of endpoint force patterns in the cat hindlimb. *J Biomech* **40**, 3679-87.

Lichtwark, G. (2017). Ultrasound Technology for Examining the Mechanics of the Muscle, Tendon, and Ligament. 1-20.

Lichtwark, G. A. and Wilson, A. M. (2005). In vivo mechanical properties of the human Achilles tendon during one-legged hopping. *J Exp Biol* **208**, 4715-25.

Lieber, R. L. (2002). Skeletal muscle structure, function and plasticity: the physiological basis of rehabilitation.

Lieber, R. L. and Boakes, J. L. (1988). Muscle force and moment arm contributions to torque production in frog hindlimb. *American Journal of Physiology - Cell Physiology* **254**, C769 - C772.

Lieber, R. L. and Friden, J. (2000). Functional and clinical significance of skeletal muscle architecture. *Muscle & Nerve* **23**, 1647 - 1666.

Lieberthal, K., Paterson, K. L., Cook, J., Kiss, Z., Girdwood, M. and Bradshaw, E. J. (2019). Prevalence and factors associated with asymptomatic Achilles tendon pathology in male distance runners. *Phys Ther Sport* **39**, 64-68.

Lloyd, D. G. and Besier, T. F. (2003). An EMG-driven musculoskeletal model to estimate muscle forces and knee joint moments in vivo. *Journal of Biomechanics* **36**, 765-776.

Luden, N., Minchev, K., Hayes, E., Louis, E., Trappe, T. and Trappe, S. (2008). Human vastus lateralis and soleus muscles display divergent cellular contractile properties. *Am J Physiol Regul Integr Comp Physiol* **295**, R1593-8.

Lynn, S. K. and Costigan, P. A. (2009). Changes in the medial-lateral hamstring activation ratio with foot rotation during lower limb exercise. *J Electromyogr Kinesiol* **19**, e197-205.

Maas, H. and Finni, T. (2018). Mechanical Coupling Between Muscle-Tendon Units Reduces Peak Stresses. *Exerc Sport Sci Rev* **46**, 26-33.

Maas, H., Noort, W., Baan, G. C. and Finni, T. (2020). Non-uniformity of displacement and strain within the Achilles tendon is affected by joint angle configuration and differential muscle loading. *J Biomech* **101**, 109634.

Maas, H. and Sandercock, T. G. (2010). Force transmission between synergistic skeletal muscles through connective tissue linkages. *J Biomed Biotechnol* **2010**, 575672.

Mademli, L. and Arampatzis, A. (2005). Behaviour of the human gastrocnemius muscle architecture during submaximal isometric fatigue. *Eur J Appl Physiol* **94**, 611-617.

Maffulli, N., Khan, K. and Puddu, G. (1998). Overuse Tendon Conditions- Time to Change a Confusing Terminology. *The Journal of Arthroscopic and Related Surgery* **14**, 840 - 843.

Maffulli, N., Longo, U. G., Kadakia, A. and Spiezia, F. (2019). Achilles tendinopathy. *Foot Ankle Surg*.

Maffulli, N., Sharma, P. and Luscombe, K. (2004). Achilles tendinopathy: aetiology and management. *Journal of the royal society of medecine* **97**, 472 - 476.

Maffulli, N., Wong, J. and Almekinders, L. C. (2003). Types and epidemiology of tendinopathy. *Clinics in Sports Medicine* **22**, 675-692.

Maganaris, C. N. (2001). Force-length characteristics of in vivo human skeletal muscle. *Acta Physiol Scand* **172**, 279 - 285.

Maganaris, C. N. (2002). Tensile properties of in vivo human tendinous tissue.

Maganaris, C. N. (2003). Force-length characteristics of the in vivo human gastrocnemius muscle. *Clin Anat* **16**, 215-23.

Maganaris, C. N. (2004). Imaging-based estimates of moment arm length in intact human muscle-tendons. *Eur J Appl Physiol* **91**, 130-139.

Maganaris, C. N., Baltzopoulos, V., Ball, D. and Sargeant, A. J. (2001). In vivo specific tension of human skeletal muscle. *J Appl Physiol* **90**, 865-872.

Maganaris, C. N., Baltzopoulos, V. and Sargeant, A. J. (1998). In vivo measurements of the triceps surae complex architecture in man- implications for muscle function. *Journal of Physiology* **512**, 603 - 614.

Magnusson, S., Hansen, P., Aagaard, P., Brond, J., Dyhre-Poulsen, J., Bojsen-Moller, J. and Kjaer, M. (2003). Differential strain patterns of the human gastrocnemiusaponeurosis and free tendon, in vivo. *Acta Physiologica Scandinavica* **177**, 185 - 195.

Magnusson, S. P., Langberg, H. and Kjaer, M. (2010). The pathogenesis of tendinopathy: balancing the response to loading. *Nat Rev Rheumatol* **6**, 262-8.

Mahieu, N. N., McNair, P., Cools, A., D'Haen, C., Vandermeulen, K. and Witvrouw, E. (2008). Effect of eccentric training on the plantar flexor muscle-tendon tissue properties. *Med Sci Sports Exerc* **40**, 117-23.

Marchetta, E., Rastelli, F., Chiavaroli, S., Tresoldi, D., Cadioli, M., Falini, A., Rizzo, G. and Lafortuna, C. L. (2012). Image-based measutement of muscles parameters for the assessment of specific tension in elbow flexors. In *GNB*. Rome, Italy.

Marcori, A. J., Moura, T. B. M. A. and Okazaki, V. H. A. (2017). Gastrocnemius muscle activation during plantar flexion with different feet positioning in physically active young men. *Isokinetics and Exercise Science* **25**, 121-125.

Martin, D. C., Medri, M. K., Chow, R. S., Leekam, R. N., Agur, A. M. and McKee, N. H. (2001). Comparing human skeletal muscle architectural parameters of cadavers with in vivo ultrasonographic measurements. *J Anat* **199**, 429-434.

Martin, J. A., Brandon, S. C. E., Keuler, E. M., Hermus, J. R., Ehlers, A. C., Segalman, D. J., Allen, M. S. and Thelen, D. G. (2018a). Gauging force by tapping tendons. *Nat Commun* **9**, 1592.

Martin, R. L., Chimenti, R., Cuddeford, T., Houck, J., Matheson, J. W., McDonough, C. M., Paulseth, S., Wukich, D. K. and Carcia, C. R. (2018b). Achilles Pain, Stiffness, and Muscle Power Deficits: Midportion Achilles Tendinopathy Revision 2018. *J Orthop Sports Phys Ther* **48**, A1-A38.

Martinez-Valdes, E., Negro, F., Falla, D., De Nunzio, A. M. and Farina, D. (2018). Surface electromyographic amplitude does not identify differences in neural drive to synergistic muscles. *J Appl Physiol (1985)* **124**, 1071-1079.

Masci, L., Spang, C., van Schie, H. T. and Alfredson, H. (2016). How to diagnose plantaris tendon involvement in midportion Achilles tendinopathy - clinical and imaging findings. *BMC Musculoskelet Disord* **17**, 97.

Masood, T., Bojsen-Moller, J., Kalliokoski, K. K., Kirjavainen, A., Aarimaa, V., Magnusson, S. P. and Finni, T. (2014a). Differential contributions of ankle plantarflexors during submaximal isometric muscle action: a PET and EMG study. *J Electromyogr Kinesiol* **24**, 367-374.

Masood, T., Kalliokoski, K., Bojsen-Moller, J., Magnusson, S. P. and Finni, T. (2014b). Plantarflexor muscle function in healthy and chronic Achilles tendon pain subjects evaluated by the use of EMG and PET imaging. *Clin Biomech (Bristol, Avon)* **29**, 564-70.

Masood, T., Kalliokoski, K., Magnusson, S. P., Bojsen-Moller, J. and Finni, T. (2014c). Effects of 12-wk eccentric calf muscle training on muscle-tendon glucose uptake and SEMG in patients with chronic Achilles tendon pain. *J Appl Physiol (1985)* **117**, 105-11.

Massey, G., Evangelidis, P. and Folland, J. (2015). Influence of contractile force on the architecture and morphology of the quadriceps femoris. *Exp Physiol* **100**, 1342-51.

Mc Auliffe, S., Synott, A., Casey, H., Mc Creesh, K., Purtill, H. and O'Sullivan, K. (2017). Beyond the tendon: Experiences and perceptions of people with persistent Achilles tendinopathy. *Musculoskelet Sci Pract* **29**, 108-114.

McAuliffe, S., Creesh, K. M., O'Sullivan, K., Purtill, H. and Culloty, F. (2017). Can ultrasound imaging predict the development of Achilles and Patellar tendinopathy? A systematic review and meta-analysis. *British Journal of Sports Medicine* **51**, 1516-1523.

McLean, L. and Goudy, N. (2004). Neuromuscular response to sustained low-level muscle activation: within- and between-synergist substitution in the triceps surae muscles. *Eur J Appl Physiol* **91**, 204-16.

Merletti, R., Rainoldi, A. and Farina, D. (2001). Surface electromyography for noninvasive characterization of muscle. *Exerc Sport Sci Rev* **29**, 20-25.

Mesin, L., Merletti, R. and Rainoldi, A. (2009). Surface EMG: the issue of electrode location. *Journal of Electromyography and Kinesiology* **19**, 719-726.

Milgrom, C., Finestone, A., Zin, D., Mandel, D. and Novack, V. (2003). Cold weather training: a risk factor for Achilles paratendinitis among recruits. *Foot and Ankle international* **24**, 398-401.

Millar, N. L., Murrell, G. A. and McInnes, I. B. (2017). Inflammatory mechanisms in tendinopathy - towards translation. *Nat Rev Rheumatol* **13**, 110-122.

Millar, N. L., Murrell, G. A. C. and Kirwan, P. (2019). Time to put down the scalpel? The role of surgery in tendinopathy. *Br J Sports Med*.

Miller, B. F., Olesen, J. L., Hansen, M., Dossing, S., Crameri, R. M., Welling, R. J., Langberg, H., Flyvbjerg, A., Kjaer, M., Babraj, J. A. et al. (2005). Coordinated collagen and muscle protein synthesis in human patella tendon and quadriceps muscle after exercise. *J Physiol* **567**, 1021-33.

Milner Brown, H. S., Stein, R. B. and Yemm, R. (1973). The orderly recruitment of human motor units during voluntary isometric contractions. *J Physiol* **230**, 359-370.

Mitsiopoulos, N., Baugmartner, R. N., Heymsfield, S. B., Lyons, W., Gallacher, D. and Ross, R. (1998). Cadaver validation of skeletal muscle measurement by magnetic resonance imaging and computerized tomography. *Journal of Applied Physiology* **85**, 115-22.

Mogk, J. P., Goehler, C. M., Hu, X. and Riley, Z. A. (2009). Should the neural-mechanical behaviour of a muscle be coupled or co-vary? *J Physiol* **587**, 3065-6.

Morrison, S. M., Dick, T. J. and Wakeling, J. M. (2015). Structural and mechanical properties of the human Achilles tendon: Sex and strength effects. *J Biomech* **48**, 3530-3.

Morrissey, D., Roskilly, A., Twycross-Lewis, R., Isinkaye, T., Screen, H., Woledge, R. and Bader, D. (2011). The effect of eccentric and concentric calf muscle training on Achilles tendon stiffness. *Clinical Rehabilitations* **25**, 238-247.

Morse, C. I., Thom, J. M., Birch, K. M. and Narici, M. V. (2004). Changes in triceps surae muscle architecture with sarcopenia. *Acta Physiol Scand* **183**, 291-298.

Morse, C. I., Thom, J. M., Reeves, N. D., Birch, K. M. and Narici, M. V. (2005). In vivo physiological cross-sectional area and specific force are reduced in the gastrocnemius of elderly men. *J Appl Physiol* **99**, 1050-1055.

Morse, C. I., Tolfrey, K., Thom, J. M., Vassilopoulos, V., Maganaris, C. N. and Narici, M. V. (2007). Gastrocnemius muscle specific force in boys and men. *J Appl Physiol* **104**, 469-474.

Mosca, M. J., Rashid, M. S., Snelling, S. J., Kirtley, S., Carr, A. J. and Dakin, S. G. (2018). Trends in the theory that inflammation plays a causal role in tendinopathy: a systematic review and quantitative analysis of published reviews. *BMJ Open Sport Exerc Med* **4**, e000332.

Moss, C. L. (1992). Comparison of the histochemical and contractile properties of human triceps surae. *Medical & Biological Engineering & Computing*, 600-604.

Mota, J. A., Gerstner, G. R. and Giuliani, H. K. (2019). Motor unit properties of rapid force development during explosive contractions. *J Physiol* **597**, 2335-2336.

Muramatsu, T., Muroaka, T., Kawakami, Y., Shibayama, A. and Fukunaga, T. (2002). In vivo determination of fascicle curvature in contracting human skeletal muscles. *J Appl Physiol* **92**, 129-134.

Muraoka, T., Muramatsu, T., Fukunaga, T. and Kanehisa, H. (2004). Geometric and elastic properties of in vivo human Achilles tendon in young adults. *Cells Tissues Organs* **178**, 197-203.

Murphy, M., Rio, E., Debenham, J., Docking, S., Travers, M. and Gibson, W. (2018a). Evaluating the Progress of Mid-Portion Achilles Tendinopathy during Rehabilitation: A Review of Outcome Measures for Muscle Structure and Function, Tendon Structure, and Neural and Pain Associated Mechanisms. *International Journal of Sports Physical Therapy* **13**, 537-551.

Murphy, M., Travers, M. and Gibson, W. (2018b). Is heavy eccentric calf training superior to wait-and-see, sham rehabilitation, traditional physiotherapy and other exercise interventions for pain and function in mid-portion Achilles tendinopathy? *Syst Rev* **7**, 58.

Murray, M. P., Baldwin, J. M., Gardner, K. L., Sepic, S. B. and Downs, W. J. (1977). Maximum isometric knee flexor and extensort muscle contractions: normal patterns of torque versus time. *Phys Ther* **57**, 637-643.

Narici, M., Franchi, M. and Maganaris, C. (2016). Muscle structural assembly and functional consequences. *J Exp Biol* **219**, 276-84.

Narici, M., Landoni, L. and Minetti, A. E. (1992). Assessment of human knee extensor muscles stress from in vivo physiological cross-sectional area and strength measurements. *Eur J Appl Physiol* **65**, 438-444.

Narici, M. V., Binzoni, T., Hiltbrand, E., Fasel, J., Terrier, F. and Cerretelli, P. (1996). In vivo human gastrocnemius architecture with changing joint angle at rest and during graded isometric contraction. *Journal of Physiology* **496**, 287-297.

Negro, F., Yavuz, U. S. and Farina, D. (2016). The human motor neuron pools receive a dominant slow-varying common synaptic input. *J Physiol* **594**, 5491-505.

Neyroud, D., Vallotton, A., Millet, G. Y., Kayser, B. and Place, N. (2014). The effect of muscle fatigue on stimulus intensity requirements for central and peripheral fatigue quantification. *Eur J Appl Physiol* **114**, 205-15.

Noorkoiv, M., Stavnsbo, A., Aagaard, P. and Blazevich, A. J. (2010). In vivo assessment of muscle fascicle length by extended field-of-view ultrasonography. *J Appl Physiol* **109**, 1974-1979.

Nunes, J. P., Costa, B. D., Kassiano, W., Kunevaliki, G., Castro-e-Souza, P., Rodacki, A. L. F., Fortes, L. S. and Cyrino, E. S. (2020). Different foot positioning during calf training to induce portion-specific gastrocnemius muscle hypertrophy. *Journal of Strength and Conditionong Research* **25**, 634-9.

O'Neill, S. (2016). A biomechanical approach to Achilles tendinopathy management. In *Health Sciences*: University of Leicester.

O'Neill, S., Barry, S. and Watson, P. (2019). Plantarflexor strength and endurance deficits associated with mid-portion Achilles tendinopathy: The role of soleus. *Phys Ther Sport* **37**, 69-76.

O'Neill, S., Watson, P. and Barry, S. (2016). A delphy study of risk factors for Achilles tendinopathy - opinions of world tendon experts. *International Journal of Sports Physical Therapy* **11**, 684-697.

Obst, S. J., Newsham-West, R. and Barrett, R. S. (2016). Changes in Achilles tendon mechanical properties following eccentric heel drop exercise are specific to the free tendon. *Scand J Med Sci Sports* **26**, 421-31.

Olewnik, L., Wysiadecki, G., Polguj, M. and Topol, M. (2017). Anatomic study suggests that the morphology of the plantaris tendon may be related to Achilles tendonitis. *Surg Radiol Anat* **39**, 69-75.

Owings, T. M. and Grabiner, M. D. (2002). Motor control of the vastus medialis oblique and vastus lateralis muscles is disrupted during eccentric contractions in subjects with patellofemoral pain. *American Journal of Sports Medicine* **30**, 483-487.

Paavola, M., Kannus, P., Paakkala, T., Pasanen, M. and Järvinen, M. (2000). Long-term prognosis of patients with Achilles tendinopathy. *Am J Sports Med* **23**, 634-642.

Pang, B. S. F. and Ying, M. (2006). Sonographic measurement of Achilles tendons in asymptomatic subjects. *J Ultrasound Med* **25**, 1291-1296.

Parente, V., D'Antona, G., Adami, R., Miotti, D., Capodaglio, P., De Vito, G. and Bottinelli, R. (2008). Long-term resistance training improves force and unloaded shortening velocity of single muscle fibres of elderly women. *Eur J Appl Physiol* **104**, 885-93.

Parsons, F. G. (1894). On the morphology of the tendo-Achillis. *J Anar Physiol* **28**, 414-418.

Pekala, P. A., Henry, B. M., Ochala, A., Kopacz, P., Taton, G., Mlyniec, A., Walocha, J. A. and Tomaszewski, K. A. (2017). The twisted structure of the Achilles tendon unraveled- A detailed quantitative and qualitative anatomical investigation. *Scand J Med Sci Sports*, 1-11.

Pertuzon, E. (1972). Relation force-longueur isométrique du muscle humain en contraction maximale.

Powell, P. L., Roy, R. R., Kanim, P., Bello, M. A. and Edgerton, V. R. (1984). Predictability of skeletal muscle tension from architectural determinations in guinea pig hindlimbs. *J Appl Physiol Respir Environ Physiol* **57**, 1715-21.

Powers, C. M., Landel, R. and Perry, J. (1996). Timing and intensity of vastus muscle activity during functional activities in subjects with and without patellofemoral pain. *Phys Ther* **76**, 946-955.

Prager, R., Gee, A., Treece, G. and Berman, L. (2002). Freehand 3D ultrasound without voxels: volume measurement and visualisation using the Stradx system. *Ultrasonics* **40**, 109-115.

Prilutsky, B. (2000). Coordination of one-joint and two-joint muscles. *Motor Control* **4**, 1 - 44.

Prilutsky, B. and Zatsiorsky, M. (2002). Optimization-based models of muscle coordination. *Exerc Sport Sci Rev* **30**, 32-38.

Rajaratnam, B. S., Goh, J. C. and Kumar, P. V. (2013). Control strategies to re-establish glenohumeral stability after shoulder injury. *Sports Science, Medicine & Rehabilitation* **5**.

Ravary, B., Pourcelot, P., Bortolussi, C., Konieczka, S. and Crevier-Denoix, N. (2004). Strain and force transducers used in human and veterinary tendon and ligament biomechanical studies. *Clin Biomech (Bristol, Avon)* **19**, 433-47.

Rees, J. D., Stride, M. and Scott, A. (2014). Tendons--time to revisit inflammation. *Br J Sports Med* **48**, 1553-7.

Reid, D., McNair, P. J., Johnson, S., Potts, G., Witvrouw, E. and Mahieu, N. (2012). Electromyographic analysis of an eccentric calf muscle exercise in persons with and without Achilles tendinopathy. *Phys Ther Sport* **13**, 150-5.

Rice, C. L., Cunningham, D. A., Taylor, A. W. and Paterson, D. H. (1988). Comparison of the histochemical and contractile properties of human triceps surae. *Eur J Appl Physiol* **58**, 165-170.

Riemann, B. L., Limbaugh, G. K., Eitner, J. D. and LeFavi, R. G. (2011). Medial and lateral gastrocnemius activation differences during heel-raise exercise with three different foot positions. *Journal of Strength and Conditionong Research* **25**, 634- 639.

Rio, E., Kidgell, D., Purdam, C., Gaida, J., Moseley, G. L., Pearce, A. J. and Cook, J. (2015). Isometric exercise induces analgesia and reduces inhibition in patellar tendinopathy. *Br J Sports Med* **49**, 1277-83.

Rio, E., Moseley, L., Purdam, C., Samiric, T., Kidgell, D., Pearce, A. J., Jaberzadeh, S. and Cook, J. (2014). The pain of tendinopathy: physiological or pathophysiological? *Sports Med* **44**, 9-23.

Robinson, J. M., Cook, J. L., Purdam, C. R., Visentini, P. J., Ross, J., Maffulli, N., Taunton, J. E. and Khan, K. M. (2001). The VISA-A questionnaire: a valid and reliable index of the clinical severity of Achilles tendinopathy. *British Journal of Sports Medicine* **35**, 335-341.

Rohrle, O., Yavuz, U. S., Klotz, T., Negro, F. and Heidlauf, T. (2019). Multiscale modeling of the neuromuscular system: Coupling neurophysiology and skeletal muscle mechanics. *Wiley Interdiscip Rev Syst Biol Med* **11**, e1457.

Rowe, V., Hemmings, S., Barton, C. J., Malliaras, P., Maffulli, N. and Morrissey, D. (2012). Conservative Management of Midportion Achilles Tendinopathy. *Sports Med* **42**, 941-967.

Sale, D., Quinlan, J., Marsh, E., McComas, J. and Belanger, A. Y. (1982). Influence of joint position on ankle plantarflexion in humans. *J Physiol* **52**, 1636-1642.

Sancho, I., Morrissey, D., Willy, R. W., Barton, C. and Malliaras, P. (2019). Education and exercise supplemented by a pain-guided hopping intervention for male recreational runners with midportion Achilles tendinopathy: A single cohort feasibility study. *Phys Ther Sport* **40**, 107-116.

Schuind, F., Garcia-Elias, M., Cooney, W. P. and An, K. N. (1992). Flexor tendon forces: in vivo measurements. *Journal of Hand Surgery* **17A**, 291-298.

Scott, A., Backman, L. J. and Speed, C. (2015). Tendinopathy: Update on Pathophysiology. *J Orthop Sports Phys Ther* **45**, 833-41.

Scott, A., Docking, S., Vicenzino, B., Alfredson, H., Murphy, R. J., Carr, A. J., Zwerver, J., Lundgreen, K., Finlay, O., Pollock, N. et al. (2013). Sports and exercise-related tendinopathies: a review of selected topical issues by participants of the second International Scientific Tendinopathy Symposium (ISTS) Vancouver 2012. *Br J Sports Med* **47**, 536-44.

Scott, A., Squier, K., Alfredson, H., Bahr, R., Cook, J. L., Coombes, B., de Vos, R. J., Fu, S. N., Grimaldi, A., Lewis, J. S. et al. (2019). ICON 2019: International Scientific Tendinopathy Symposium Consensus: Clinical Terminology. *Br J Sports Med*.

Secher, N. H., Rube, N. and Secher, O. (1982). Effect of tubocurarine on human soleus and gastrocnemius muscles. *Acta anaesth scand* **26**.

Seynnes, O. R., Bojsen-Moller, J., Albracht, K., Arndt, A., Cronin, N. J., Finni, T. and Magnusson, S. P. (2015). Ultrasound-based testing of tendon mechanical properties: a critical evaluation. *J Appl Physiol (1985)* **118**, 133-41.

Sharir, A. and Zelzer, E. (2011). Tendon homeostasis: the right pull. *Curr Biol* **21**, R472.

Shim, V. B., Handsfield, G. G., Fernandez, J. W., Lloyd, D. G. and Besier, T. F. (2018). Combining in silico and in vitro experiments to characterize the role of fascicle twist in the Achilles tendon. *Sci Rep* **8**, 13856.

Siebert, T., Leichsenring, K., Rode, C., Wick, C., Stutzig, N., Schubert, H., Blickhan, R. and Bol, M. (2015). Three-Dimensional Muscle Architecture and Comprehensive Dynamic Properties of Rabbit Gastrocnemius, Plantaris and Soleus: Input for Simulation Studies. *PLoS One* **10**, e0130985.

Simpson, C. L., Kim, B. D., Bourcet, M. R., Jones, G. R. and Jakobi, J. M. (2016). Stretch training induces unequal adaptation in muscle fascicles and thickness in medial and lateral gastrocnemii. *Scand J Med Sci Sports*.

Slane, L. C. and Thelen, D. G. (2014). Non-uniform displacements within the Achilles tendon observed during passive and eccentric loading. *J Biomech* **47**, 2831-5.

Smith, J. L., Betts, B., Edgerton, V. R. and Zernicke, R. F. (1980). Rapid ankle extension during paw shakes: selective recruitment of fast ankle extensors. *Journal of Neurophysiology* **43**.

Spiesz, E. M., Thorpe, C. T., Chaudhry, S., Riley, G. P., Birch, H. L., Clegg, P. D. and Screen, H. R. (2015). Tendon extracellular matrix damage, degradation and inflammation in response to in vitro overload exercise. *J Orthop Res* **33**, 889-97.

Spina, D. C. (2007). The plantaris muscle: anatomy, injury, imaging and treatment. *J Can Chiropr Assoc* **51**, 158 - 165.

Standring, S., Borley, N. R. and Gray, H. (2008). Gray's Anatomy: The anatomical bases of clinical practice, (ed. E. C. Livingstone/Elsevier).

Stanish, W. D., Rubinovich, R. M. and Curwin, S. (1986). Eccentric exercise in chronic tendinitis. *Clin Orthop Relat Res* **208**, 65-8.

Stenroth, L., Peltonen, J., Cronin, N. J., Sipila, S. and Finni, T. (2012). Age-related differences in Achilles tendon properties and triceps surae muscle architecture in vivo. *J Appl Physiol* **113**, 1537-44.

Stienen, G. J. M., Kiers, J. L., Bottinelli, R. and Reggiani, M. (1996). Myofibrillar ATPase activity in skinned human skeletal muscle fibres: fibre type and temperature dependence. *J Physiol* **493**, 299-307.

Strojnik, V. and Komi, P. V. (1998). Neuromuscular fatigue after maximal stretch shortening cycle exercise. *J Appl Physiol* **84**, 344-350.

Sun, Y., Berger, E. J., Zhao, C., An, K. N., Amadio, P. C. and Jay, G. (2006). Mapping lubricin in canine musculoskeletal tissues. *Connect Tissue Res* **47**, 215-21.

Sun, Y. L., Wei, Z., Zhao, C., Jay, G. D., Schmid, T. M., Amadio, P. C. and An, K. N. (2015). Lubricin in human achilles tendon: The evidence of intratendinous sliding motion and shear force in achilles tendon. *J Orthop Res* **33**, 932-7.

Szaro, P., Witkowski, G., Smigielski, R., Krajewski, P. and Ciszek, B. (2009). Fascicles of the adult human Achilles tendon - An anatomical study. *Ann Anat* **191**, 586-593.

Taylor, W. (2005). Musculoskeletal pain in the adult New Zealand population: prevalence and impact. *New Zealand Medical Journal* **118**.

Thorpe, C. T., Birch, H. L., Clegg, P. D. and Screen, H. R. (2013). The role of the non-collagenous matrix in tendon function. *Int J Exp Pathol* **94**, 248-59.

Thorpe, C. T., Karunaseelan, K. J., Ng Chieng Hin, J., Riley, G. P., Birch, H. L., Clegg, P. D. and Screen, H. R. (2016a). Distribution of proteins within different compartments of tendon varies according to tendon type. *J Anat* **229**, 450-8.

Thorpe, C. T., Peffers, M. J., Simpson, D., Halliwell, E., Screen, H. R. and Clegg, P. D. (2016b). Anatomical heterogeneity of tendon: Fascicular and interfascicular tendon compartments have distinct proteomic composition. *Sci Rep* **6**, 20455.

Thorpe, C. T. and Screen, H. R. (2016). Tendon Structure and Composition. In *Metabolic Influences on Risk for Tendon Disorders. Advances in Experimental Medicine and Biology*, vol. 920 eds. P. Ackermann and D. Hart): Springer, Cham.

Todd, G., Taylor, J. L. and Gandevia, S. C. (2004). Reproducible measurement of voluntary activation of human elbow flexors with motor cortical stimulation. *J Appl Physiol* **97**, 236-242.

Trappe, S., Williamson, D., Godard, M., Porter, D., Rowden, G. and Costill, D. (2000). Effect of resistance training on single muscle fiber contractile function in older men. *J Appl Physiol* **89**, 143-152.

Trezise, J., Collier, N. and Blazevich, A. J. (2016). Anatomical and neuromuscular variables strongly predict maximum knee extension torque in healthy men. *Eur J Appl Physiol* **116**, 1159-77.

Tucker, K., Butler, J., Graven-Nielsen, T., Riek, S. and Hodges, P. (2009). Motor unit recruitment strategies are altered during deep-tissue pain. *J Neurosci* **29**, 10820-10826.

Tumilty, S., Munn, J., Abbott, J. H., McDonough, S., Hurley, D. A. and Baxter, G. D. (2008). Laser therapy in the treatment of achilles tendinopathy: a pilot study. *Photomed Laser Surg* **26**, 25-30.

van der Plas, A., de Jonge, S., de Vos, R. J., van der Heide, H. J., Verhaar, J. A., Weir, A. and Tol, J. L. (2012). A 5-year follow-up study of Alfredson's heel-drop exercise programme in chronic midportion Achilles tendinopathy. *Br J Sports Med* **46**, 214-8.

van der Vlist, A. C., Breda, S. J., Oei, E. H. G., Verhaar, J. A. N. and de Vos, R. J. (2019). Clinical risk factors for Achilles tendinopathy: a systematic review. *Br J Sports Med*.

Van Gils, B. S., Steed, R. H. and Page, J. C. (1996). Torsion of the Human Achilles Tendon. *Journal of Foot and Ankle Surgery* **35**, 41-48.

van Vugt, J. P. P. and van Dijk, J. G. (2001). A convenient method to reduce crosstalk in surface EMG. *Clinical physiology* **112**, 538-592.

Vieira, T. M., Minetto, M. A., Hodson-Tole, E. F. and Botter, A. (2013). How much does the human medial gastrocnemius muscle contribute to ankle torques outside the sagittal plane? *Hum Mov Sci* **32**, 753-67.

Wakeling, J. M. and Horn, T. (2009). Neuromechanics of Muscle Synergies During Cycling. *Journal of Neurophysiology* **101**, 843 - 854.

Walmsley, B., Hodgson, J. A. and Burke, R. E. (1978). Forces produced by Medial gastrocnemius and Soleus muscles during locomotion in freely moving cats. *Journal of Neurophysiology* **41**, 1203 - 1216.

Ward, S. R., Eng, C. M., Smallwood, L. H. and Lieber, R. L. (2008). Are Current Measurements of Lower Extremity Muscle Architecture Accurate? *Clinical orthopaedics and related research* **467**, 1074-1082.

Waugh, C. M., Blazevich, A. J., Fath, F. and Korff, T. (2012). Age-related changes in mechanical properties of the Achilles tendon. *J Anat* **220**, 144-55.

Wickiewicz, T. L., Roy, R. R., Powell, P. L., Perrine, J. J. and Edgerton, V. R. (1984). Muscle architecture and force-velocity relationships in humans. *J Appl Physiol Respir Environ Exerc Physiol* **57**, 435-443.

Widrick, J. J., Stelzer, J. E., Shoepe, T. C. and Garner, D. P. (2002). Functional properties of human muscle fibres after short-term resistance exercise training. *Am J Physiol Regulatory Integrative Comp Physiol* **283**.

Wiegel, P., Centner, C. and Kurz, A. (2019). How motor unit recruitment speed and discharge rates determine the rate of force development. *J Physiol* **597**, 2331-2332.

Wilkie, D. R. (1950). The relation between force and velocity in human muscle. *J Physiol* **110**, 249-280.

Winter, D. A. and Yack, H. J. (1987). EMG profiles during normal human walking: stride-to-stride and inter-subject variability. *Electroencephalography and clinical Neurophysiology* **67**, 402-411.

Wolfram, S. (2017). Differential behaviour of the medial and lateral heads of gastrocnemius during plantarflexion: the effect of calcaneal inversion and eversion. In *Department of exercise and sport science*, vol. Thesis, pp. 161. UK: Manchester Metropolitan University.

Wolfram, S., Hodson-Tole, E. F., Morse, C. I., Winwood, K. L. and McEwan, I. M. (2020). Elongation differences between the sub-tendons of gastrocnemius medialis and lateralis during plantarflexion in different frontal plane position of the foot. *Gait Posture* **75**, 149-154.

Woodley, S. J. and Mercer, S. R. (2005). Hamstring muscles: architecture and innervation. *Cells Tissues Organs* **179**, 125-41.

Wyndow, N., Cowan, S., Wrigley, T. V. and Crossley, K. (2010). Neuromotor Control of the Lower Limb in Achilles Tendinopathy *Sports Med* **40**, 715-727.

Wyndow, N., Cowan, S. M., Wrigley, T. V. and Crossley, K. M. (2013). Triceps surae activation is altered in male runners with Achilles tendinopathy. *J Electromyogr Kinesiol* **23**, 166-72.

Yu, J. (2014). Comparison of Lower Limb Muscle Activity during Eccentric and Concentric Exercises in Runners with Achilles Tendinopathy. *Journal of Physical Therapy Sciences* **26**, 1351 - 1353.

Zajac, F. E. (1989). Muscle and tendon: properties, models, scaling, and application to biomechanics and motor control. *Critical Reviews in Biomedical Engineering* **17**, 359-410.

Zelik, K. E. and Franz, J. R. (2017). It's positive to be negative: Achilles tendon work loops during human locomotion. *PLoS One* **12**, e0179976.

Zhao, G., Zhang, J., Nie, D., Zhou, Y., Li, F., Onishi, K., Billiar, T. and Wang, J. H. (2019). HMGB1 mediates the development of tendinopathy due to mechanical overloading. *PLoS One* **14**, e0222369.

UNIVERSITE BRETAGNE LOIRE
EDUCATION
LANGAGES, INTERACTIONS
COGNITION, CLINIQUE

UNIVERSITÉ DE NANTES

Titre: Coordination musculaire et pathologies musculo-squelettiques, *étude de la tendinopathie d'Achille*

Mots clefs: Electromyographie, Surface de section physiologique transversale, Force musculaire, *Triceps sural*, Tendon d'Achille

Résumé: Le tendon d'Achille est composé de trois sous-tendons qui proviennent chacun d'un chef du *triceps surae*: *gastrocnemius medialis*, *gastrocnemius lateralis,* et *soleus*. Une distribution non optimale de la contrainte imposée au tendon d'Achille contribuerait au développement de la tendinopathie d'Achille. D'autre part, la distribution des contraintes sur le tendon d'Achille est en partie déterminée par la distribution de la force entre les chefs des *triceps surae*. L'objectif général de cette thèse était d'étudier le rôle de la coordination musculaire (définie comme la distribution de force entre les muscles) dans le développement d'une tendinopathie d'Achille.

Les forces musculaires de chaque muscle ont été estimées à partir de l'activation, du volume et de l'architecture musculaires. Les résultats ont montré que (*i*) la distribution de l'activation musculaire dans le *triceps surae* est robuste dans le temps, et varie considérablement d'un individu à l'autre; (*ii*) il existe une corrélation positive significative entre la distribution de la surface de section transversale physiologique et la distribution de l'activation au sein des *gastrocnemii*; (*iii*) le *gastrocnemius lateralis* contribue significativement moins à la force totale produite par le *triceps sural* chez les personnes atteintes de tendinopathie d'Achille par rapport aux contrôles. L'altération de la coordination musculaire pourrait être une cause, comme elle pourrait être une conséquence de la tendinopathie d'Achille.

Title: Muscle coordination and musculoskeletal disorders, *investigation of Achilles tendinopathy*

Keywords: Electromyography, Physiological cross-sectional area, Muscle force, *Triceps surae*, Achilles tendon

Abstract: The Achilles tendon is made of three *subtendons* that each arises from a different head of the *triceps surae*: *gastrocnemius medialis, gastrocnemius lateralis* and *soleus*. Non-optimal distribution of load within Achilles tendon would contribute to the development of Achilles tendinopathy. Moreover, there is evidence that the distribution of load or strain within the Achilles tendon is partly determined by the distribution of force among the heads of the *triceps surae*. The overall aim of this thesis was to provide a deeper understanding of the role of muscle coordination (i.e. the distribution of force among muscles) on the development of Achilles tendinopathy.

Individual muscle forces were estimated from muscle activation, volume and architecture. Results showed that (*i*) the distribution of activation among *triceps surae* is robust between days, and varies greatly between individuals; (*ii*) there is a significant positive correlation between the distribution of physiological cross-sectional area and the distribution of activation among *gastrocnemii*; (*iii*) muscle coordination among the *triceps surae* differs in people with Achilles tendinopathy compared with controls, with the *gastrocnemius lateralis* contributing significantly less to total *triceps surae* force in people with Achilles tendinopathy. Whether this altered strategy is a cause or a consequence of Achilles tendinopathy should be further explored.